GREEN ROOIBOS NUTRACEUTICAL: OPTIMISATION OF HOT WATER EXTRACTION AND SPRAY-DRYING BY QUALITY-BY-DESIGN METHODOLOGY

Neil Miller

Thesis presented in partial fulfilment of the requirements for the degree of
Master of Science in Food Science

Department of Food Science
Faculty of AgriSciences
Stellenbosch University

Supervisor: Prof. E. Joubert
Co-supervisor: Prof. D. de Beer

December 2016

DECLARATION

By submitting this thesis/dissertation electronically, I declare that the entirety of the work contained therein is my own, original work, that I am the sole author thereof (save to the extent explicitly otherwise stated), that reproduction and publication thereof by Stellenbosch University will not infringe any third party rights and that I have not previously in its entirety or in part submitted it for obtaining any qualification.

Date: December 2016

ABSTRACT

Unfermented *Aspalathus linearis*, otherwise known as green rooibos (GR), contains high levels of aspalathin, a potent *C*-glucosyl dihydrochalcone antioxidant with antidiabetic bioactivity, unique to rooibos. Inherent variation in the phenolic composition of rooibos is likely to cause significant variability in the aspalathin content of different GR production batches and thus also the batch-to-batch quality of a nutraceutical green rooibos extract (GRE). The aim of this study was to optimise hot water extraction and spray-drying for the production of a shelf-stable GRE. A quality-by-design (QbD) approach was applied, entailing a preliminary risk assessment step, one-factor-at-a-time analysis, and analyses according to a central composite design (CCD) to determine the effects of process parameters on responses. Response surface methodology (RSM) was applied to identify suitable control spaces, i.e. ranges of process input factors in which optimal responses, i.e. product quality, could be expected. Significant variation in aspalathin content of different GR production batches (n = 47; 2.5–4.5%) was demonstrated. The CCD for extraction included three independent variables: extraction time (10–40 min), extraction temperature (41–93 °C) and water-to-plant material ratio (6.6:1–23.4:1; $v.m^{-1}$). Prediction models and response surfaces for extract yield (EY; $g.100\ g^{-1}$ plant material), aspalathin extraction efficiency (Asp_EE; $g.100g^{-1}$ in plant material) and aspalathin content ($g.100\ g^{-1}$ soluble solids) were generated. Verification of the prediction models showed good predictive ability for EY and Asp_EE. Multi-response optimisation was applied to identify levels of the independent variables which would maximise EY and Asp_EE. Optimal conditions were identified based on these results, along with considerations of cost-efficiency and practicality: extraction time, 29–31 min; extraction temperature, 90–95 °C and water-to-plant material ratio, 9:1–11:1 ($v.m^{-1}$). Validation of the optimal extraction conditions using the 47 commercial GR production batches, (aspalathin content >2.5%) showed that at least 15% EY and 8% aspalathin content in the extract could be achieved. Standardisation of the maximum particle size by sieving out of large particles could potentially improve the overall process efficiency. The CCD for spray-drying included three independent variables: inlet air temperature (150–220 °C), feed concentration (5–35%) and feed flow rate (0.12–0.64 $L.h^{-1}$). Powder yield (g powder recovered per 100 g solids in feed) was the only response for which a statistically significant prediction model was generated. Optimal spray-drying conditions (inlet air temperature of 210–230 °C, feed concentration of 34–36% and feed flow rate of 0.62–0.67 $L.h^{-1}$) were identified and applied in the spray-drying of a pure GRE as well as GRE in a 1:1 mass ratio blend with the carriers, inulin and maltodextrin, respectively. Amorphous powders with low moisture content (<2.2%) and water activity (<0.13) and >89% retention of aspalathin were obtained. The hygroscopic character of the powders was confirmed by moisture sorption analysis, and storage conditions of <25 °C and <40% relative humidity are therefore recommended in order to maintain optimal quality. Inulin improved the flowability and wettability of the powder as compared with maltodextrin. An inulin-GRE formulation was identified as a good candidate for further development as a high-value antidiabetic nutraceutical.

UITTREKSEL

Ongefermenteerde *Aspalathus linearis*, andersins bekend as groen rooibos (GR), bevat hoë vlakke van aspalatien, 'n kragtige *C*-glukosiel dihidrochalkoon antioksidant met anti-diabetiese bioaktiwiteit, uniek aan rooibos. Inherente variasie in die fenoliese samestelling van rooibos sal waarskynlik variasie in die aspalatieninhoud van verskillende produksielotte van GR tot gevolg hê, en dus ook in die kwaliteit van 'n nutraseutiese groen rooibos ekstrak (GRE). Die hoofdoelstelling van hierdie studie was die optimisering van warm water-ekstraksie en sproeidroging in die produksieproses vir 'n rakstabiele GRE. 'n Kwaliteit-deur-ontwerp (KdO) benadering is toegepas, insluitende 'n aanvanklike risiko assessering, een-faktor-op-'n-slag analise, en analises volgens 'n sentrale saamgestelde ontwerp (SSO) om die effek van veranderlikes op die proses uitkomstes te bepaal. Respons-oppervak metodiek (ROM) is toegepas vir die identifisering van toepaslike kontroleruimtes, d.w.s. reikwydtes van die veranderlikes waarbinne optimale uitkomstes, en dus produk kwaliteit, verwag sou kon word. Beduidende variasie in die aspalatieninhoud van verskillende GR produksielotte (n = 47; 2.5–4.5%) is gedemonstreer. Die SSO vir die ekstraksie het drie onafhanklike veranderlikes ingesluit: ekstraksietyd (10–40 min), ekstraksietemperatuur (41–93 °C) en water-tot-plantmateriaal verhouding (6.6:1–23.4:1; $v.m^{-1}$). Voorspellingsmodelle en respons-oppervlaktes vir die ekstrakopbrengs (EO; $g.100\ g^{-1}$ plantmateriaal), aspalatien ekstraksiedoeltreffendheid (Asp_ED; $g.100\ g^{-1}$ in plantmateriaal) en aspalatieninhoud ($g.100\ g^{-1}$ ekstrak), is gegenereer. Verifikasie van die voorspellingsmodelle het goeie voorspellingsvermoë aangedui vir EO en Asp_ED. Multi-respons optimisering is dus toegepas om die optimale waardes van die onafhanklike veranderlikes, waarby maksimum EO en Asp_ED bewerkstellig kan word, te vind. Optimale proses parameters is geselekteer op grond van hierdie resultate, sowel as praktiese oorwegings en koste-doeltreffendheid: ekstraksietyd, 29–31 min; ekstraksietemperatuur, 90–95 °C en water-tot-plantmateriaal verhouding, 9:1–11:1 ($v.m^{-1}$). Validering van die optimale ekstraksiekondisies met die 47 kommersiële GR produksielotte (aspalatieninhoud >2.5%) het aangedui dat ten minste 15% ekstrakopbrengs en 8% aspalatieninhoud in die ekstrak bereikbaar is. Standardisering van die maksimum partikelgroottes deur die uitsifting van groot partikels kan moontlik die algehele ekstraksiedoeltreffendheid verbeter. Die SSO vir sproeidroging het drie onafhanklike veranderlikes ingesluit: inlaat lugtemperatuur (150–220 °C), toevoer konsentrasie (5–35%) en toevoer vloeitempo (0.12–0.64 $L.h^{-1}$). Slegs vir poeier-opbrengs (g poeier herwin per 100 g vastestowwe in toevoer) is 'n statisties beduidende voorspellingsmodel gegenereer. Optimale sproeidrogingskondisies (inlaat lugtemperatuur 210–230 °C), toevoer konsentrasie (34–36%) en toevoer vloeitempo (0.62–0.67 $L.h^{-1}$) is geïdentifiseer en toegepas in die sproeidroging van 'n suiwer GRE sowel as GRE in 'n 1:1 massaverhouding met die draers, maltodekstrien en inulien, onderskeidelik. Die sproeidroging het amorfe poeiers met lae voginhoud (<2.2%) en wateraktiwiteit (<0.13) gelewer, en >89% behoud van aspalatien is bewerkstellig. Die higroskopiese karakter van die poeiers is bevestig deur vogsorpsie-analise. Opbergingstoestande van <25 °C en <40% relatiewe humiditeit word aanbeveel ten einde optimale kwaliteit te handhaaf. Inulien het die vloeikarakter en benatting van die poeier verbeter in vergelyking met maltodekstrien. 'n Inulien-GRE formulasie is geïdentifiseer as 'n goeie kandidaat vir verdere ontwikkeling as 'n hoëwaarde anti-diabetiese nutraseutiese aanvuller.

ACKNOWLEDGEMENTS

Prof. Elizabeth Joubert & Prof. Dalene de Beer of ARC Infruitec-Nietvoorbij (Stellenbosch) — thank you for your expert supervision and significant contributions to this project. The quality of your collective body of work speaks for itself.

Ms Nina Muller — thank you for assisting with administration and for playing a significant supportive role in my application for these postgraduate studies back in 2014.

Nico Walters, Dr Christie Malherbe, Carin de Wet, Chantelle Human, Louise Robertson, George Dico, Neliswa Matrose, Claire Pauck and Lara Alexander — colleagues at ARC Infruitec-Nietvoorbij — thank you for your assistance and advice in and around the laboratory and office.

Chantelle Human — thank you for kindly carrying out the SEM imaging at the electron microbeam unit at the Central Analytical Facility of Stellenbosch University.

Prof. Marique Aucamp of Pharmacen, North West University (Potchefstroom, South Africa) — for carrying out isothermal microcalorimetry, differential thermal and thermogravimetric analyses, moisture sorption studies, contact angle measurements and X-ray powder diffraction. Thank you for assisting in the interpretation of the data.

Prof. Martin Kidd of the Centre for Statistical Consultation of Stellenbosch University and Marieta van der Rijst of the Biometry division at ARC Infruitec-Nietvoorbij — thank you for carrying out statistical analysis and assisting with the interpretation of data.

Ms Colette Cronje & Rooibos Ltd. (Clanwilliam, South Africa) — thank you for providing us with the green rooibos plant material.

Ms Nkuli Khanyeza of Tongaat Hulett Starch (Germiston, South Africa) — for kindly assisting with the sourcing of maltodextrin.

Prof. Gunnar Sigge — thank you for always putting in a good word for me.

My parents, John and Monica — thank you for guiding me through the long journey it took to get to this point. It would not have been possible without your unwavering support.

The author acknowledges the following institutions for project funding and financial support:

- Agricultural Research Council Professional Development Programme
- National Research Foundation (Competitive Programme for Rated Researcher - Grant No. 93438 (project leader: Prof. E. Joubert)
- South African Association of Food Science and Technology (SAAFoST) – Brian Koeppen Memorial Bursary for Masters student in Food Science (2016)

The deepest solace lies in understanding
this ancient, unseen stream
A shudder before the beautiful.

Richard Dawkins

TABLE OF CONTENTS

DECLARATION i

ABSTRACT ii

UITTREKSEL iii

ACKNOWLEDGEMENTS iv

TABLE OF CONTENTS I

1. General Introduction 5

References 11

2. Literature Review 20

2.1. Rooibos (*Aspalathus linearis*) 21

2.1.1. General overview 21

2.1.2. Chemical composition 26

2.1.3. Rooibos quality aspects 43

2.1.4. Medicinal and health-promoting properties 48

2.1.5. Rooibos extracts for food and nutraceutical applications 51

2.2. Quality-by-design (QbD) methodology 52

2.2.1. General overview of QbD 52

2.2.2. Principles of response surface methodology (RSM) 55

2.2.3. Optimisation by design of experiment (DOE) approach 56

2.2.4. Modelling and interpretation of data 56

2.3. Botanical extracts 63

2.3.1. Traditional solvent-based extraction techniques 63

2.3.2. Green extraction concept 66

2.3.3. Factors affecting extraction efficiency 67

2.3.4. Novel or supplementary extraction techniques 71

2.3.5. Extraction kinetics 72
2.3.6. Extraction of *Aspalathus linearis* plant material 73
2.4. Spray-drying of botanical extracts 76
2.4.1. General overview of spray-drying 76
2.4.2. Basic steps in a spray drying process 78
2.4.3. Carrier materials 81
2.4.4. Physicochemical characteristics of spray-dried powders 84
2.4.5. Effect of spray-drying process parameters on product characteristics and yield 90
2.4.6. Spray-drying of rooibos extracts 97
2.5. Conclusion 98
2.6. References 99
3. Optimisation of green rooibos hot water extraction using quality-by-design methodology 121
3.1. Abstract 122
3.2. Introduction 123
3.3. Materials and methods 124
3.3.1. Chemicals and reagents 124
3.3.2. Green rooibos plant material 125
3.3.3. Risk assessment for extraction unit operation 126
3.3.4. One-factor-at-a-time (OFAT) extractions 126
3.3.5. Optimisation of extraction unit operation 127
3.3.6. HPLC analysis of plant material and extracts 128
3.3.7. Gravimetric determination of soluble solids content of extract 129
3.3.8. Total polyphenol content and total antioxidant capacity 129
3.3.9. Statistical analysis 130
3.4. Results and discussion 131
3.4.1. Characterisation of phenolic content of different batches of green rooibos plant material 132
3.4.2. Risk assessment for extraction unit operation 133

3.4.3. One-factor-at-a-time (OFAT) extraction 134
3.4.4. Application of response surface methodology (RSM) 144
3.4.5. Validation of optimum hot water extraction process 165
3.5. Conclusion 178
3.6. References 179
4. Optimisation of spray-drying of green rooibos extract using quality-by-design methodology 185
4.1. Abstract 186
4.2. Introduction 187
4.3. Materials and methods 188
4.3.1. Chemicals and reagents 188
4.3.2. Preparation of freeze-dried extract for spray-drying feed formulations 188
4.3.3. Carriers 189
4.3.4. Spray-drying 189
4.3.5. Physicochemical analyses of spray-dried extracts 194
4.3.6. Statistical analysis 198
4.4. Results and discussion 199
4.4.1. Risk assessment for spray-drying unit operation 199
4.4.2. Preliminary experiments 201
4.4.3. Optimisation of spray-drying by response surface methodology 202
4.4.4. Powder yield and mean outlet air temperature 212
4.4.5. Physicochemical properties of optimised spray-dried extracts 214
4.5. Conclusion 234
4.6. References 235
5. General Discussion and Conclusions 241
References 250
6. Addendum A: Supplementary data pertaining to Chapter 3 254
6.1. Validation of practical optimum hot water extraction parameters 255
6.2. One-factor-at-a-time (OFAT) extractions 257

6.2.1. Effect of extraction time on extraction efficiency 257

6.2.2. Effect of extraction temperature on extraction efficiency 258

6.2.3. Effect of water-to-plant material ratio on extraction efficiency..... 259

6.2.4. Effect of particle size fractions on extraction efficiency..... 260

6.2.5. Effect of various heat treatments on flavonoid contents of green rooibos extract..... 261

6.3. UV-spectrophotometric screening of green rooibos extract..... 263

7. Addendum B: Supplementary data pertaining to Chapter 4.....264

This thesis is presented in the format prescribed by the Department of Food Science at Stellenbosch University. The structure is in the form of one or more research chapters (papers prepared for publication) and is prefaced by an introduction chapter with the study objectives, followed by a literature review chapter and culminating with a chapter for elaborating a general discussion and conclusion. The language, style and referencing format used are in accordance with the requirements of the *International Journal of Food Science and Technology*. This thesis represents a compilation of manuscripts where each chapter is an individual entity and some repetition between chapters has, therefore, been unavoidable.

1. General Introduction

The metabolic syndrome and its related pathognomonic disease states, type 2 diabetes mellitus (T2D) and central obesity, are gaining ground as significant global epidemics, with a great burden being placed on the healthcare infrastructure of developed and developing countries alike (Mathers & Loncar, 2006; Chaturvedi, 2007; Herman, 2011; Guarigata *et al.*, 2014). This is being spurred on by the rampant consumption of foods rich in saturated fats (Riccardi *et al.*, 2004) and refined carbohydrates (Gross *et al.*, 2004), combined with a more sedentary lifestyle, which results in an energy intake far exceeding that required by the body. According to data made available by the International Diabetes Federation (IDF), it is estimated that ≈600 million individuals worldwide will be diagnosed diabetics by 2035, and that the most marked increase will be seen in developing nations (Guariguata *et al.*, 2014). The number of diabetics in South Africa in 2015 were estimated at 2.28 million (about 7% of the population), and this figure is predicted to have doubled by 2040 (IDF, 2016). Dietary intervention therapy is often prescribed as part of the general treatment approach of pre-diabetic and insulin resistant individuals, in combination with other lifestyle changes (Alberti & Zimmett, 1998; Tuomilehto *et al.*, 2001). A 50–60% reduction in progression to T2D has been reported for pre-diabetic subjects who adhered to even minor lifestyle changes geared towards a healthier diet and increased physical activity (Simpson *et al.*, 2003). The worldwide number of obese and overweight individuals has already exceeded the 2.1 billion mark in 2013, which accounts for roughly 30% of the global population, but the more alarming statistic was the rise in childhood obesity by 47% between 1980 and 2013 (Ng *et al.*, 2014). Therefore, it is imperative to take a preventive approach and treat pre-diabetic and/or obese patients, especially at a young age, before the transition into full-blown T2D and metabolic syndrome.

One example of a preventive approach taken by governments is the "sugar tax" on sugar-sweetened beverages, recently also introduced in South Africa. Proponents of this tax advocate that it will reduce consumption of sugar-sweetened beverages, and lead to improved health (Brownell *et al.*, 2009). It is also suggested that taxing of unhealthy foods and beverages may stimulate reformulation of food products by industry such as removal of sugar (Mytton *et al.*, 2012). Finkelstein *et al.* (2010) estimated that sugar tax would result in a decrease in store-bought energy of 101.7.3 kJ per day per person, which would translate into an average weight loss of 0.72 kg during the first year and a cumulative weight loss of 1.3 kg in the long run.

The World Health Organization (WHO) estimates that more than 75% of the population in some developing African and Asian countries makes regular use of traditional medicine (WHO, 2003), which typically involves the utilisation of various kinds of plant materials. There has been a growing global interest in alternatives to single chemical compounds as favoured by the pharmaceutical industry. In many instances, the value of herbal and medicinal plant extracts lies not in a single compound but in their complex phytochemical nature. These complex mixtures of (often unspecified) compounds are able to modulate multiple targets and exhibit pharmacological effects

through synergistic interaction (Schmidt *et al.*, 2008; Efferth & Koch, 2011). Therefore, the development of rationally selected and carefully standardised traditional herbal formulations and botanical drug products, which are supported by robust scientific evidence, have become the subject of a growing number of research studies (Patwardhan & Mashelkar, 2009; Shinde *et al.*, 2009; Qusaj *et al.*, 2012).

Lathiyare & Jain (2015) reviewed the antidiabetic bioactivity of 31 plant species used in various traditional medicine practices, many of which are consumed in the form of aqueous infusions, commonly referred to as herbal teas or tisanes (McKay & Blumberg, 2007). Rooibos (*Aspalathus linearis*), a leguminous shrub endemic to the Western Cape region of South Africa (Dahlgren, 1968; 1988), is one of the better known herbal teas, being especially well-loved and habitually consumed in its native country but also being exported in significant amounts to the global marketplace (Anon., 2014). While it is enjoyed mainly as a refreshing beverage known for its unique flavour profile and slightly sweet taste, rooibos tea has also had a long-standing reputation as a health-promoting beverage, with alleged anxiolytic, anti-allergy, anti-inflammatory and anti-spasmodic effects (McKay & Blumberg, 2007; Joubert & De Beer, 2011; Street & Prinsloo, 2013).

Starting in the late 1990s, an increasing amount of research has been conducted on the link between the health-promoting properties of rooibos and its chemical composition. The discovery that "green" or unfermented rooibos contains significantly higher levels of antioxidant phenolic compounds compared with the traditional fermented variant (Von Gadow *et al.*, 1997; Snijman *et al.*, 2009), resulted in heightened awareness of the potential health benefits to be derived from its consumption. Aspalathin is a *C*-glucosyl dihydrochalcone which is unique to *Aspalathus linearis* (Koeppen & Roux, 1965), and undergoes significant degradation during the traditional fermentation step employed in the production of rooibos tea (Joubert, 1996). A notable disadvantage of consuming green rooibos (GR) herbal tea instead of the traditional fermented variant is that it lacks the slightly sweet taste and herbal-floral aroma typically associated with rooibos tea (Joubert & De Beer, 2014). An alternative to drinking copious volumes of herbal tea with potentially undesirable sensory attributes (Viljoen *et al.*, 2016), whilst still deriving the desirable health benefits, is to consume an enriched, highly concentrated extract of GR as a dietary supplement.

More recent research studies have demonstrated that rooibos extracts and individual rooibos compounds, but particularly aspalathin, display bioactivity with potential antidiabetic and anti-metabolic disease applications. This includes enhancement of glucose uptake *in vitro* and *in vivo* (Kawano *et al.*, 2009; Son *et al.*, 2013), inhibition of adipogenesis (Sanderson *et al.*, 2014), protection of cardiomyocytes in the diabetic heart (Johnson *et al.*, 2016), amelioration of insulin resistance (Mazibuko *et al.*, 2013; Mazibuko *et al.*, 2015) and modulation of oxidative stress (Uličná *et al.*, 2006; Kondo *et al.*, 2013; Hong *et al.*, 2014) and hyperglycaemia-induced inflammation (Ku *et al.*, 2015).

Muller *et al*. (2012) demonstrated that an aspalathin-enriched green rooibos extract (GRE) reduce blood glucose concentrations in streptozotocin-induced diabetic rats. Kamakura *et al.* (2015) showed that GRE significantly enhanced *in vitro* glucose uptake in cultured L6 myotubes under insulin-absent condition through activation of the 5′-adenosine monophosphate-activated protein kinase (AMPK) pathway. This mirrored the results of previous studies which demonstrated that purified aspalathin significantly increased glucose uptake in the same cell model through AMPK activation (Kawano *et al.*, 2009; Son *et al.*, 2013). The AMPK pathway has been previously linked with improving insulin insensitivity, independent of the insulin signalling pathway, through the direct stimulation of glucose uptake by myocytes (Fisher *et al*., 2002; Iglesias *et al*., 2002). At the same aspalathin concentration, GRE was found to be more effective at promoting glucose uptake in L6 myocytes than purified aspalathin (Kamakura *et al.*, 2015). This could be attributed to the presence of other rooibos compounds which have been shown to have hypoglycaemic effects, e.g. rutin (Cai & Lin, 2009; Muller *et al.*, 2012), iso-orientin (Sezik *et al.*, 2005) and phenylpyruvic acid-2-*O*-glucoside (Muller *et al.*, 2013). Additionally, GRE was more effective than aspalathin at protecting pancreatic RIN-5F cells against hyperglycaemia-induced oxidative stress (Kamakura *et al.*, 2015), which plays a significant role in the development of systemic complications of diabetes, e.g. diabetic cardiomyopathy and endarteritis (Fiorentino *et al.*, 2013). Considering these findings, the development of a GRE, containing high levels of aspalathin, for use as a nutraceutical treatment adjunct to pharmaceutical agents and lifestyle management could be a sensible and beneficial pursuit.

A notable challenge associated with the use of plant or other biological material for the preparation of extracts is the variation in chemical composition and overall quality, with the raw materials sometimes containing suboptimal concentrations of the target compound or active pharmaceutical ingredient (API) intended for commercialisation (Taylor *et al*., 2001; Takeuchi *et al*., 2009). Genetic variation is not the sole cause of the substantial variation that may be encountered in raw plant materials — there are also external factors which drive variation, e.g. the development stage of shoots, regional climate, exposure to UV-radiation, salinity stress and differences in post-harvest processing methods (Aherne & O'Brien, 2002; Yao *et al.*, 2005; Cheynier *et al.*, 2013; Di Ferdinando *et al.*, 2013; Tiwari & Cummins, 2013). These are common causes of inconsistent batch-to-batch quality of plant extracts, and a strategy which aims to control the impact of these natural variations would be a first step towards attaining a more reliable level of quality. Some of the bioactive compounds intended for extraction may be prone to undesirable chemical changes during the production process, which can make it even more challenging to establish and maintain an acceptable range of quality attributes (Fischer *et al.*, 2015).

Quality-by-design (QbD) methodology could be applied to address some of these challenges. It refers to a systematic approach which aims to ensure that the desired quality attributes of a product are effectively designed into the manufacturing process, eliminating the traditional reliance

on post-production quality testing to detect deviations (Juran, 1992). QbD has been approved and recommended for use in the biopharmaceutical industry by the United States Food and Drug Administration, and has frequently been applied in recent years (ICH, 2009; Rathore & Winkle, 2009; Khan & Smillie, 2012; Das *et al.*, 2014). A number of statistical tools may be utilised in a QbD approach to analyse experimental processes, including response surface methodology (RSM), which refers to the mathematical modelling of experimental data to obtain visual representations (response surfaces) and data which describe the process in terms of its particular input and output parameters (Bezerra *et al.*, 2008; Granato & De Araújo Calado, 2014). The concept of design of experiments (DOE) is another important element of QbD, and it refers to the systematic and deliberate planning of experiments in such a way as to obtain robust data from which reliable conclusions may be drawn (Dejaegher & Vander Heyden, 2011).

The optimisation of an extraction process by QbD typically aims to increase the efficiency and performance of a system whilst simultaneously minimising the various costs involved (Huang *et al.*, 2009; Zhang *et al.*, 2013). Risk assessment usually precedes the optimisation by experimental design in order to identify those factors which are most likely to have a significant effect on the process output. This preliminary step may be approached in different ways, e.g. the construction of Ishikawa (fishbone) diagrams (Saraph *et al.*, 1989), failure-mode and effect analysis (Gong *et al.*, 2014) or by referring to previous experience or literature (Roy, 2012). The major factors which affect the recovery of bioactive phenolic compounds from plant materials are the solvent type, solvent-to-solid ratio, extraction time, extraction temperature, particle size and pH (Shi *et al.*, 2005; Azmir *et al.*, 2013). Since each type of plant matrix is characterised by unique mass kinetics, an optimised extraction processes should be developed for each type of herbal raw material (Wijngaard *et al.*, 2012).

The bulk of rooibos extract produced each year in South Africa is prepared with fermented plant material, and is used mainly as an ingredient of functional foods and beverages, but the type of rooibos extract can be tailored to suit many different applications (Joubert & De Beer, 2011). In the present study, GR plant material was used as the raw material for production of a potential nutraceutical with a high aspalathin content study since aspalathin undergoes significant oxidative degradation during the production of traditional fermented rooibos (Joubert, 1996). The aspalathin content which has been reported for GR plant material in literature ranges from 2.56% (Joubert & De Beer, 2011) to as high as 13.48% (Joubert *et al.*, 2013). Joubert *et al.* (2012) reported substantial variation in the aspalathin content of fermented rooibos infusions (n = 144), with values ranging from not detected to 15.66 $mg.L^{-1}$ of infusion. The aspalathin content of a fermented rooibos food ingredient extract (n = 74), produced using a simulated industrial extraction process, ranged from 0.16–1.52% (dry basis) (Joubert & De Beer, 2012). These data hint towards the kind of variation which could be expected in the present study.

Plant extracts intended for use as a functional food ingredient or nutraceutical must ultimately be converted into a stable product available in the form of free-flowing powders with sufficiently low moisture content and water activity to facilitate easier handling of the extract and promote storage stability for improved shelf-life (Shah & Rohit, 2005; Azmir *et al.*, 2013). This can be achieved by a variety of methods, e.g. freeze-drying, fluidised bed drying and spouted bed drying (Couto *et al.*, 2011). Spray-drying is, however, one of the most widely used due to its relatively low cost and operational flexibility (Costa *et al.*, 2015).

Spray-drying conditions may expose labile extract constituents to high operating temperatures resulting in their thermal degradation or in unwanted physicochemical attributes of the spray-dried extract (SDE) (Patel *et al.*, 2015). Carrier materials or excipients are often added to extracts before spray-drying to protect heat-labile constituents against high drying temperatures and enhance the physicochemical attributes of the SDE (Sollohub & Cal, 2010; Woo & Bhandari, 2013). Maltodextrin, a derivative of maize starch, is frequently used as excipient in the spray-drying of plant extracts due to its low cost, widespread availability, versatility and food-safe status (Costa *et al.*, 2015). Maltodextrin, however, is metabolised as glucose by the human gastrointestinal system, and its glycaemic index (GI) of 100 might prohibit its use in a nutraceutical preparation with proposed antidiabetic applications (Englyst *et al.*, 1996). Gross *et al.* (2004) demonstrated that there was a strong link between the increased consumption of refined carbohydrate with concomitant reduction in dietary fiber consumption, and the growing trend in the prevalence of T2D. Inulin, a naturally occurring polysaccharide derived mainly from chicory root, is considered a prebiotic and natural dietary fibre which stimulates the growth of beneficial intestinal flora (Kolida *et al.*, 2002), and it has been used as a carrier material in spray-drying of various plant extracts (Saénz *et al.*, 2009; Bakowska-Barczak & Kolodziejczyk, 2011; Hashemiravan *et al.*, 2013). The consumption of non-digestable dietary fiber such as inulin has also been linked to a lower risk for cardiovascular and metabolic diseases, lower body mass index and improved gastrointestinal health (Flamm *et al.*, 2001; Slavin, 2013). The lower energy content of inulin (6.3 $kJ.g^{-1}$ vs. 16.4 $kJ.g^{-1}$ for glucose) and negligible effect on raising of plasma glucose levels makes it a suitable alternative to maltodextrin in the present study, where the promotion of normoglycaemia is a fundamental aspect of the final product (Roberfroid, 1999; Mensink *et al.*, 2015).

While a number of published studies have involved the extraction of rooibos solids or specific subclasses of phenolic compounds, e.g. flavonoids, for analytical purposes (Joubert, 1984, 1988, 1990a, 1990b; Joubert & Hansmann, 1990; Von Gadow *et al.*, 1997; Jaganyi & Wheeler, 2003; Pengilly *et al.*, 2008; Joubert & De Beer, 2012; Coetzee *et al.*, 2014), the extraction process itself has not yet been optimised or described using RSM, DOE or QbD approaches. Similarly, no research has yet been published on the optimisation of spray-drying of rooibos extracts. Since aqueous rooibos infusions have been consumed as a common household beverage for decades, it can be

assumed that hot water extracts would not contain any potentially hazardous constituents which would otherwise be absent in a conventional cup of rooibos tea. The use of water would also streamline the production process by enabling spray-drying of the extract in an "open" configuration, i.e. using atmospheric air, without having to remove organic solvents from the feed preparation (Filkova & Mujumdar, 1995).

In summary, the aim of the present study was to optimise the hot water extraction and spray-drying processes for the production of a shelf-stable GRE with potential nutraceutical applications. This includes the characterisation of a large sample set of commercial GR production batches in terms of its major phenolic content in order to determine the extent of raw material variation to be expected in such a production process. QbD principles were applied to the extraction and spray-drying unit operations, which involved a preliminary risk assessment step, followed by the application of central composite design and RSM to identify suitable control spaces, i.e. ranges of process input factors in which optimal process outputs, i.e. product quality, can be expected (Huang *et al.*, 2009). Maltodextrin, commonly used by industry, and inulin were investigated as carriers of GRE. The physicochemical attributes of the resultant GR SDEs were determined in order to characterise their baseline quality characteristics, assess their shelf-stability and evaluate the overall efficiency of the spray-drying process.

References

Aherne, S.A. & O'Brien, N.M. (2002). Dietary flavonoids: chemistry, food content and metabolism. *Nutrition*, **18**, 75–81.

Alberti, K.G.M.M. & Zimmet, P.F. (1998). Definition, diagnosis and classification of diabetes mellitus and its complications. Part 1: diagnosis and classification of diabetes mellitus. Provisional report of a WHO consultation. *Diabetic Medicine*, **15**, 539–553.

Anonymous (2014). A profile of the South African rooibos tea market value chain. Department of Agriculture, Forestry and Fisheries. Pretoria, South Africa: Government Printing Works.

Azmir, J., Zaidul, I.S.M., Rahman, M.M., Sharif, K.M., Mohamed, A., Sahena, F., Jahurul, M.H.A., Ghafoor, K., Norulaini, N.A.N. & Omar, A.K.M. (2013). Techniques for extraction of bioactive compounds from plant materials: a review. *Journal of Food Engineering*, **117**, 426–436.

Bakowska-Barczak, A.M & Kolodziejczyk, P.P. (2011). Black currant polyphenols: their storage stability and microencapsulation. *Industrial Crops and Products*, **34**, 1301–1309.

Bezerra, M.A., Santelli, R.E., Oliveira, E.P., Villar, L.S. & Escaleira, L.A. (2008). Response surface methodology (RSM) as a tool for optimisation in analytical chemistry. *Talanta*, **76**, 965–977.

Brownell, K.D., Farley, T., Willett, W.C., Popkin, B.M., Chaloupka, F.J., Thompson, J.W. & Ludwig, D.S. (2009). The public health and economic benefits of taxing sugar-sweetened beverages. *New England Journal of Medicine*, **361**, 1599–1605.

Cai, E.P. & Lin, J.K. (2009). Epigallocatechin gallate (EGCG) and rutin suppress the glucotoxicity through activating IRS2 and AMPK signaling in rat pancreatic β cells. *Journal of Agricultural and Food Chemistry*, **57**, 9817–9827.

Chaturvedi, N. (2007). The burden of diabetes and its complications: trends and implications for intervention. *Diabetes Research and Clinical Practice*, **76**, S3–S12.

Cheynier, V., Comte, G., Davies, K.M., Lattanzio, V. & Martens, S. (2013). Plant phenolics: recent advances on their biosynthesis, genetics, and ecophysiology. *Plant Physiology and Biochemistry*, **72**, 1–20.

Coetzee, G., Joubert, E., Van Zyl, W.H. & Viljoen-Bloom, M. (2014). Improved extraction of phytochemicals from rooibos with enzyme treatment. *Food and Bioproducts Processing*, **92**, 393–401.

Costa, S.S., Machado, B.A.S., Martin, A.R., Bagnara, F, Ragadalli, S.A. & Alves, A.R.C. (2015). Drying by spray drying in the food industry: micro-encapsulation, process parameters and main carriers used. *African Journal of Food Science*, **9**, 462–470.

Couto, R.O., Araújo, R.R., Tacon, L.A., Conceição, E.C., Bara, M.T.F., Paula, J.R. & Freitas, A.P. (2011). Development of a phytopharmaceutical intermediate product via spray drying. *Drying Technology*, **29**, 709–718.

Dahlgren, R. (1968). Revision of the genus *Aspalathus.* II. The species with the ericoid and pinoid leaflets. 7. Subgenus Nortiera. With remarks on rooibos tea cultivation. *Botaniska Notiser*, **121**, 165–208.

Dahlgren, R. (1988). Crotalarieae (*Aspalathus*). *Flora of Southern Africa*, **16**, 84–90.

Das, A.K., Mandal, S.C., Mandal, V., Beg, S. & Singh, B. (2014). QbD as an emerging paradigm in extraction technology for developing optimized bioactives. *Pharma Times*, **46**, 50–56.

Dejaegher, B. & Vander Heyden, Y. (2011). Experimental designs and their recent advances in set-up, data interpretation, and analytical applications. *Journal of Pharmaceutical and Biomedical Analysis*, **56**, 141–158.

Di Ferdinando, M., Brunetti, C., Fini, A. & Tattini, M. (2013). Flavonoids as antioxidants in plants under abiotic stresses. In: *Abiotic Stress Responses in Plants: Metabolism, Productivity and Sustainability* (edited by P. Ahmad & M.N.V. Prasads). Pp. 159–179. New York: Springer Science & Business Media.

Efferth, T. & Koch, E. (2011). Complex interactions between phytochemicals. The multi-target therapeutic concept of phytotherapy. *Current Drug Targets*, **12**, 122–132.

Englyst, H.N., Veenstra, J. & Hudson, G.J. (1996). Measurement of rapidly available glucose (RAG) in plant foods: a potential *in vitro* predictor of the glycaemic response. *British Journal of Nutrition*, **75**, 327–337.

Filkova, I. & Mujumdar, A.S. (1995). Industrial spray drying systems. In: *Handbook of Industrial Drying*, 2nd ed., Vol. 1. (edited by S. Mujumdar). Pp. 263–308. Florida: CRC Press.

Finkelstein, E.A., Zhen, C., Nonnemaker, J. & Todd, J.E. (2010). Impact of targeted beverage taxes on higher-and lower-income households. *Archives of Internal Medicine*, **170**, 2028–2034.

Fiorentino, V.T., Prioletta, A., Zuo, P. & Folli, F. (2013). Hyperglycemia-induced oxidative stress and its role in diabetes mellitus related cardiovascular diseases. *Current Pharmaceutical Design*, **19**, 5695–5703.

Fischer, R., Vasilev, N., Twyman, R.M. & Schillberg, S. (2015). High-value products from plants: the challenges of process optimization. *Current Opinion in Biotechnology*, **32**, 156–162.

Fisher, J.S., Gao, J., Han, D.H., Holloszy, J.O. & Nolte, L.A. (2002). Activation of AMP kinase enhances sensitivity of muscle glucose transport to insulin. *American Journal of Physiology-Endocrinology and Metabolism*, **282**, E18–E23.

Flamm, G., Glinsmann, W., Kritchevsky, D., Prosky, L. & Roberfroid, M. (2001). Inulin and oligofructose as dietary fiber: a review of the evidence. *Critical Reviews in Food Science and Nutrition*, **41**, 353–362.

Granato, D. & De Araújo Calado, V.M. (2014). The use and importance of design of experiments (DOE) in process modelling in food science and technology. In: *Mathematical and Statistical Methods in Food Science and Technology*, 1st ed. (edited by D. Granato & G. Ares). Pp. 3–18. New York: John Wiley & Sons.

Gross, L.S., Li, L., Ford, E.S. & Liu, S. (2004). Increased consumption of refined carbohydrates and the epidemic of type 2 diabetes in the United States: an ecologic assessment. *The American Journal of Clinical Nutrition*, **79**, 774–779.

Gong, X., Zhang, Y., Pan, Y. & Qu, H. (2014). Optimization of the ethanol recycling reflux extraction process for saponins using a design space approach. *PLoS one*, **9**, doi: 10.1371/journal.pone.0114300.

Guarigata, L., Whiting, D.R., Hambleton, I., Beagley, J., Linnenkamp, U. & Shaw, J.E. (2014). Global estimates of diabetes prevalence for 2013 and projections for 2035. *Diabetes Research and Clinical Practice*, **103**, 137–149.

Hashemiravan, M., Mazloom, A.S. & Farhaydar, N. (2013). Nano particles of blueberry in inulin and β-cyclodextrin microcapsules. *International Journal of Nanoscience and Nanotechnology*, **9**, 185–192.

Herman, W.H. (2011). The economics of diabetes prevention. *Medical Clinics of North America*, **95**, 373–384.

Hong, I.S., Lee, H.Y. & Kim, H.P. (2014). Anti-oxidative effects of rooibos tea (*Aspalathus linearis*) on immobilization-induced oxidative stress in rat brain. *PLoS one*, **9**(1), doi: 10.1371./journal.pone.0087061.

Huang, J., Kaul, G., Cai, C., Chatlapalli, R., Hernandez-Abad, P., Ghosh, K. & Nagi, A. (2009). Quality by design case study: an integrated multivariate approach to drug product and process development. *International Journal of Pharmaceutics*, **382**, 23–32.

ICH (2009). ICH Harmonised Tripartite Guideline: Pharmaceutical Development Q8(R2). [Internet document]. URL http://www.ich.org/fileadmin/Public_Web_Site/ICH_Products/Guidelines/Quality/Q8_R1/Step4/Q8_R2_Guideline.pdf. 18/08/2016.

IDF (2016). International Diabetes Federation — South Africa. [Internet document]. URL http://www.idf.org/membership/afr/south-africa. 07/12/2016.

Iglesias, M.A., Ye, J.M., Frangioudakis, G., Saha, A.K., Tomas, E., Ruderman, N.B., Cooney, G.J. & Kraegen, E.W. (2002). AICAR administration causes an apparent enhancement of muscle and liver insulin action in insulin-resistant high-fat-fed rats. *Diabetes*, **51**, 2886–2894.

Jaganyi, D. & Wheeler, P.J. (2003). Rooibos tea: equilibrium and extraction kinetics of aspalathin. *Food Chemi*stry, **83**, 121–126.

Johnson, R., Dludla, P., Joubert, E., February, F., Mazibuko, S., Ghoor, S., Muller, C.J.F. & Louw, J. (2016). Aspalathin, a dihydrochalcone *C*-glucoside, protects H9c2 cardiomyocytes against high glucose induced shifts in substrate preference and apoptosis. *Molecular Nutrition & Food Research*, **60**, 922–934.

Joubert, E. (1984). Studies in verband met verkitsing van rooibos tee (*Aspalathus linearis*). MSc Food Science Thesis, Stellenbosch University, South Africa.

Joubert, E. (1988). Effect of batch extraction conditions on yield of soluble solids from rooibos tea. *International Journal of Food Science and Technology*, **23**, 43–47.

Joubert, E. (1990a). Effect of batch extraction conditions on yield of polyphenols from rooibos tea (*Aspalathus linearis*). *International Journal of Food Science and Technology*, **25**, 339–343.

Joubert, E. (1990b). Effect of time on fixed-bed extraction of polyphenols from rooibos tea (*Aspalathus linearis*). *LWT – Food Science and Technology,* **23**, 181–183.

Joubert, E. (1996). HPLC quantification of the dihydrochalcones, aspalathin and nothofagin in rooibos tea (*Aspalathus linearis*) as affected by processing. *Food Chemistry*, **55**, 403–411.

Joubert, E., Beelders, T., De Beer, D., Malherbe, C.J., De Villiers, A.J. & Sigge, G.O. (2012). Variation in phenolic content and antioxidant activity of fermented rooibos herbal tea infusions: role of production season and quality grade. *Journal of Agricultural and Food Chemistry*, **60**, 9171–9179.

Joubert, E. & De Beer, D. (2011). Rooibos (*Aspalathus linearis*) beyond the farm gate: from herbal tea to potential phytopharmaceutical. *South African Journal of Botany*, **77**, 869–886.

Joubert, E. & De Beer, D. (2012). Phenolic content and antioxidant activity of rooibos food ingredient extracts. *Journal of Food Composition and Analysis*, **27**, 45–51.

Joubert, E. & De Beer, D. (2014). Antioxidants of rooibos beverages: role of plant composition and processing. In: *Processing and Impact on Antioxidants in Beverages* (edited by V.R. Preedy). Pp. 131–144. Massachusetts: Elsevier Academic Press.

Joubert, E., De Beer, D., Malherbe, C.J., Muller, N., Bonnet, S.L., Van der Westhuizen, J.H. & Ferreira, D. (2013). Occurrence and sensory perception of *Z*-2-(ß-D-glucopyranosyloxy)-3-phenylpropenoic acid in rooibos (*Aspalathus linearis)*. *Food Chemistry*, **136**, 1078–1085.

Joubert, E. & Hansmann, C.F. (1990). Effect of time on fixed-bed extraction of soluble solids from rooibos tea (*Aspalathus linearis*). *LWT – Food Science and Technology*, **23**, 178–180.

Juran, J.M. (1992). *Juran on Quality by Design: The New Steps for Planning Quality into Goods and Services*. New York: Simon & Schuster.

Kamakura, R., Son, M.J., De Beer, D., Joubert, E., Miura, Y. & Yagasaki, K. (2015). Antidiabetic effect of green rooibos (*Aspalathus linearis)* extract in cultured cells and type 2 diabetic model KK-Ay mice. *Cytotechnology*, **67**, 699–710.

Kawano, A., Nakamura, H., Hata, S., Minakawa, M., Miura, Y. & Yagasaki, K. (2009). Hypoglycemic effect of aspalathin, a rooibos tea component from *Aspalathus linearis*, in type 2 diabetic model db/db mice. *Phytomedicine*, **16**, 437–443.

Khan, I.A. & Smillie, T. (2012). Implementing a "Quality by Design" approach to assure the safety and integrity of botanical dietary supplements. *Journal of Natural Products*, **75**, 1665–1675.

Koeppen, B.H. & Roux, D.G. (1965). Aspalathin: a novel *C*-glycosylflavonoid from *Aspalathus linearis*. *Tetrahedron Letters*, **39**, 3497–3503.

Kolida, S., Tuohy, K. & Gibson, G.R. (2002). Prebiotic effects of inulin and oligofructose. *British Journal of Nutrition*, **87**, S193–S197.

Kondo, M., Hirano, Y., Nishio, M., Furaya, Y., Nakamura, H. & Watanabe, T. (2013). Xanthine oxidase inhibitory activity and hypouricemic effect of aspalathin from unfermented rooibos. *Journal of Food Science*, **78**, 1935–1939.

Ku, S.K., Kwak, S., Kim, Y. & Bae, J.S. (2015). Aspalathin and nothofagin from rooibos (*Aspalathus linearis*) inhibits high glucose-induced inflammation *in vitro* and *in vivo*. *Inflammation*, **38**, 445–455.

Lathiyare, K.B. & Jain, V. (2015). An exhaustive review on herbals used in diabetes mellitus. *International Journal of Pharmaceutical Sciences Letters*, **5**, 546–554.

Mathers, C.D. & Loncar, D. (2006). Projections of global mortality and burden of disease from 2002 to 2030. *PLoS Medicine*, **3**, e442.

Mazibuko, S.E., Muller, C.J.F., Joubert, E., De Beer, D., Johnson, R., Opoku, A.R. & Louw, J. (2013). Amelioration of palmitate-induced insulin resistance in C2C12 muscle cells by rooibos (*Aspalathus linearis*). *Phytomedicine*, **20**, 813–819.

Mazibuko, S.E. Joubert, E. Johnson, R., Louw, J., Opoku, A.R. & Muller, C.J.F. (2015). Aspalathin improves glucose and lipid metabolism in 3T3-L1 adipocytes exposed to palmitate. *Molecular Nutrition & Food Research*, **59**, 2199–2208.

McKay, D.L. & Blumberg, J.B. (2007). A review of the bioactivity of South African herbal teas: rooibos (*Aspalathus linearis*) and honeybush (*Cyclopia intermedia*). *Phytotherapy Research*, **21**, 1–16.

Mensink, M.A., Frijlink, H.W., Van der Voort Maarschalk, K. & Hinrichs, W.L.J. (2015). Inulin, a flexible oligosaccharide II: Review of its pharmaceutical applications. *Carbohydrate Polymers*, **134**, 418–428.

Muller, C.J.F., Joubert, E., De Beer, D., Sanderson, M., Malherbe, C.J., Fey, S.J. & Louw, J. (2012). Acute assessment of aspalathin-enriched green rooibos (*Aspalathus linearis)* extract with hypoglycaemic potential. *Phytomedicine,* **20**, 32–39.

Muller, C.J.F., Joubert, E., Pheiffer, C., Ghoor, S., Sanderson, M., Chellan, N., Fey, S.J. & Louw, J. (2013). *Z*-2-(β-d-glucopyranosyloxy)-3-phenylpropenoic acid, an α-hydroxy acid from rooibos (*Aspalathus linearis*) with hypoglycemic activity. *Molecular Nutrition & Food Research*, **57**, 2216–2222.

Mytton, O.T., Clarke, D. & Rayner, M. (2012). Taxing unhealthy food and drinks to improve health. *British Medical Journal*, **344**, doi: 10.1136/bmj.e2931.

Ng, M., Fleming, T., Robinson, M., Thomson, B., Graetz, N., *et al*. (2014). Global, regional, and national prevalence of overweight and obesity in children and adults during 1980–2013: a systematic analysis for the global burden of disease study 2013. *The Lancet*, **384**, 766–781.

Patel, B.B., Patel, J.K., Chakraborty, S. & Shukla, D. (2015). Revealing facts behind spray dried solid dispersion technology used for solubility enhancement. *Saudi Pharmaceutical Journal*, **23**, 352–365.

Patwardhan, B. & Mashelkar, R.A. (2009). Traditional medicine-inspired approaches to drug discovery: can Ayurveda show the way forward?. *Drug Discovery Today*, **14**, 804–811.

Pengilly, M., Joubert, E., Van Zyl, W.H., Botha, A. & Bloom, M. (2008). Enhancement of rooibos (*Aspalathus linearis*) aqueous extract and antioxidant yield with fungal enzymes. *Journal of Agricultural and Food Chemistry*, **56**, 4047–4053.

Qusaj, Y., Leng, A., Alshihabi, F., Krasniqi, B. & Vandamme, T. (2012). Development strategies for herbal products reducing the influence of natural variance in dry mass on tableting properties and tablet characteristics. *Pharmaceutics*, **4**, 501–516.

Rathore, A.S. & Winkle, H. (2009). Quality by design for biopharmaceuticals. *Nature Biotechnology*, **27**, 26–34.

Riccardi, G., Giacco, R. & Rivellese, A.A. (2004). Dietary fat, insulin sensitivity and the metabolic syndrome. *Clinical Nutrition*, **23**, 447–456.

Roberfroid, M.B. (1999). Caloric value of inulin and oligofructose. *The Journal of Nutrition*, **129**, 1436S–1437S.

Roy, S. (2012). Quality by design: a holistic concept of building quality in pharmaceuticals. *International Journal of Pharmaceutical and Biomedical Research*, **3**, 100–108.

Saénz, C., Tapia, S., Chávez, J. & Robert, P. (2009). Microencapsulation by spray drying of bioactive compounds from cactus pear (*Opuntia ficus-indica*). *Food Chemistry*, **114**, 616–622.

Sanderson, M., Mazibuko, S.E., Joubert, E., De Beer, D., Johnson, R., Pheiffer, C., Louw, J. & Muller, C.J. (2014). Effects of fermented rooibos (*Aspalathus linearis*) on adipocyte differentiation. *Phytomedicine*, **21**, 109–117.

Saraph, J.V., Benson, P.G. & Schroeder, R.G. (1989). An instrument for measuring the critical factors of quality management. *Decision Sciences*, **20**, 810–829.

Schmidt, B., Ribnicky, D.M., Poulev, A., Logendra, S., Cefalu, W.T. & Raskin, I. (2008). A natural history of botanical therapeutics. *Metabolism*, **57**, S3–S9.

Sezik, E., Aslan, M., Yesilada, E. & Ito, S. (2005). Hypoglycaemic activity of *Gentiana olivieri* and isolation of the active constituent through bioassay-directed fractionation techniques. *Life Sciences*, **76**, 1223–1238.

Shah, M.V. & Rohit, M.C. (2013). Novel techniques for isolation and extraction of phyto-constituents from herbal plants. *American Journal of Phytomedicine and Clinical Therapeutics*, **1**, 338–350.

Shinde, V.M., Dhalwal, K., Potdar, M. & Mahadik, K.R. (2009). Application of quality control principles to herbal drugs. *International Journal of Phytomedicine*, **1**, 4–8.

Shi, J., Nawaz, H., Pohorly, J., Mittal, G., Kakuda, Y. & Jiang, Y. (2005). Extraction of polyphenolics from plant material for functional foods — engineering and technology. *Food Reviews International*, **21**, 139–166.

Simpson, R.W., Shaw, J.E. & Zimmet, P.Z. (2003). The prevention of type 2 diabetes -lifestyle change or pharmacotherapy? A challenge for the 21st century. *Diabetes Research and Clinical Practice*, **59**, 165–180.

Slavin, J. (2013). Fiber and prebiotics: mechanism and health benefits. *Nutrients*, **5**, 1417–1435.

Snijman, P.W., Joubert, E., Ferreira, D., Li, X.C., Ding, Y., Green, I.R. & Gelderblom, W.C.A. (2009). Antioxidant activity of the dihydrochalcones aspalathin and nothofagin and their corresponding flavones in relation to other rooibos (*Aspalathus linearis*) flavonoids, epigallocatechin gallate, and trolox. *Journal of Agricultural and Food Chemistry*, **57**, 6678–6684.

Sollohub, K. & Cal, K. (2010). Spray drying technique. II. Current applications in pharmaceutical technology. *Journal of Pharmaceutical Sciences*, **99**, 587–597.

Son, M.J., Minikawa, M., Miura, Y. & Yagasaki, K. (2013). Aspalathin improves hyperglycaemia and glucose intolerance in obese diabetic *ob/ob* mice. *European Journal of Nutrition*, **52**, 1607–1619.

Street, R.A. & Prinsloo, G. (2013). Commercially important medicinal plants of South Africa: a review. *Journal of Chemistry*, **2013**, doi: 10.1155/2013/205048.

Takeuchi, T.M., Pereira, C.G., Braga, M.E.M., Maróstica, M.R., Leal, P.F. & Meireles, M.A.A. (2009). Low-pressure solvent extraction (solid-liquid extraction, microwave assisted, and ultrasound assisted) from condimentary plants. In: *Extracting Bioactive Compounds for Food Products: Theory and Applications* (edited by Meireles, M.A.A.). Pp 138–211. New York: Taylor & Francis Group, LLC.

Taylor, J.L.S., Rabe, T., McGaw, L.J., Jäger, A.K. & Van Staden, J. (2001). Towards the scientific validation of traditional medicinal plants. *Plant Growth Regulation*, **34**, 23–37.

Tiwari, U. & Cummins, E. (2013). Factors influencing levels of phytochemicals in selected fruit and vegetables during pre-and post-harvest food processing operations. *Food Research International*, **50**, 497–506.

Tuomilehto, J., Lindström, J., Eriksson, J.G., Valle, T.T., Hämäläinen, H., Ilanne-Parikka, P., Keinänen-Kiukaanniemi, S., Laakso, M., Louheranta, A., Rastas, M. & Salminen, V. (2001). Prevention of type 2 diabetes mellitus by changes in lifestyle among subjects with impaired glucose tolerance. *New England Journal of Medicine*, **344**, 1343–1350.

Uličná, O., Vančová, O., Božek, P., Čársky, J., Šebekova, K., Boor, P., Nakano, M. & Greksák, M. (2006). Rooibos tea (*Aspalathus linearis*) partially prevents oxidative stress in streptozotocin-induced diabetic rats. *Physiological Research*, **55**, 157–164.

Viljoen, M., Muller, M., De Beer, D. & Joubert, E. (2016). Identification of broad-based sensory attributes driving consumer preference of ready-to-drink rooibos iced tea with increased aspalathin content. *South African Journal of Botany*, doi: 10.1016/j.sajb.2016.07.019

Von Gadow, A., Joubert, E. & Hansmann, C.F. (1997). Comparison of the antioxidant activity of rooibos tea (*Aspalathus linearis*) with green, oolong and black tea. *Food Chemistry*, **60**, 73–77.

WHO (2003). Traditional medicine. World Health Organization Fact Sheet No. 134. [Internet document]. URL http://www.who.int/mediacentre/factsheets/2003/fs134/en/. 18/08/2016.

Wijngaard, H., Hossain, M.B., Rai, D.K. & Brunton, N. (2012). Techniques to extract bioactive compounds from food by-products of plant origin. *Food Research International*, **46**, 505–513.

Woo, M.W. & Bhandari, B. (2013). Spray drying for food powder production. In: *Handbook of Food Powders: Processes and Properties* (edited by B. Bhandari). Pp. 29–56. Cambridge: Woodhead Publishing.

Yao, L., Caffin, N., D'Arcy, B., Jiang, Y., Shi, J., Singanusong, R., Liu, X., Datta, N., Kakuda, Y. & Xu, Y. (2005). Seasonal variations of phenolic compounds in Australia-grown tea (*Camellia sinensis*). *Journal of Agricultural and Food Chemistry*, **53**, 6477–6483.

Zhang, L., Yan, B., Gong, X., Yu, L.X. & Qu, H. (2013). Application of quality by design to the process development of botanical drug products: a case study. *AAPS PharmSciTech*, **14**, 277–286.

2. Literature Review

2.1. Rooibos (*Aspalathus linearis*)

2.1.1. General overview

2.1.1.1. Taxonomy and geographical distribution

Fabaceae (or Leguminosae), referred to colloquially as the bean/legume/pea family, is the third largest land-plant family in terms of absolute number of species, with over 19 000 documented in more than 630 genera, including a number of species of agricultural and economic importance, e.g. *Pisum sativum* (pea), *Cicer arietinum* (chickpea) and *Arachis hypogeae* (peanut) (Anon., 2013). One of these, *Aspalathus* (subfamily Faboideae; tribe Crotalariae), contributes over 270 species to that total. These are nearly all endemic to the south-western fynbos biome of South Africa, with over 50 occurring exclusively in the Cape Peninsula region (Joubert & De Beer, 2011). *Aspalathus linearis* (Burm.f.) Dahlg., commonly known as *rooibos* (literally "red bush"), is the most well-known of these and can be found growing naturally in the south-eastern and western regions of the Western Cape Province and, to a lesser extent, in the south-western area of the Northern Cape Province (Figs. 2.1a & 2.1b) (Dahlgren, 1968; 1988).

Despite a wide variety of distinct biotypes having been observed in the wild (Van Heerden *et al.*, 2003; Malgas *et al.*, 2010; Hawkins *et al.*, 2011; Kotina *et al.*, 2012), the red/Rocklands type is currently the only type of *Aspalathus linearis* being used to manufacture herbal tea on a commercial level. The unacceptable and inconsistent quality of other rooibos types (e.g. red-brown, grey and black), which were also initially used for tea production, led to discontinuation of their use in 1966 (Anon., 1967). The red/Rocklands type has been subcategorised further as either the selected and improved Nortier type or the wild-growing Cederberg type, discernable by its coarser and broader leaves (Morton, 1983). Due to the unique attributes of rooibos which are closely related to its geographical location, it has recently been granted a geographical indication (GI) certification. This formally recognises that rooibos occurs specifically in the Fynbos biome of the Cape Floristic Region, one of 25 locations previously identified as "global diversity hotspots". GI certification should ensure that rooibos is not cultivated outside of South Africa and that its moniker is not unjustly exploited for commercial purposes (Biénabe *et al.*, 2009; Anon., 2014b).

2.1.1.2. Applications throughout history

The indigenous Khoi practice of consuming a rooibos beverage was reportedly first described by Carl Thunberg, a Swedish naturalist, during his African expedition of 1772 (Morton, 1983). Benjamin Ginsberg was the first to realise the commercial potential of rooibos at the beginning of the 20th century when he observed inhabitants of the Clanwilliam district of the Western Cape harvesting

and processing the rooibos plant for preparation of a hot water infusion. Modern-day industrial rooibos processing mirrors the traditional basic steps used to process rooibos, i.e. cutting, bruising, "sweating" (later called "fermentation") and sun-drying (Joubert & De Beer, 2011).

Following shortages of Ceylon tea during World War II, rooibos was increasingly being used as an alternative. Loose-leaf tea, consisting of blended leaves and stems, was infused with hot water to brew a strong, red-coloured and full-flavoured beverage, typically with milk and sugar added according to taste. The modern consumer generally prefers the teabag rather than loose-leaf tea owing to its convenience and ease of disposal. The average rooibos teabag contains approximately 2 g of refined leaves, which requires 2–5 min of infusion with freshly boiled water (250 mL per teabag) to release the characteristic flavour and develop the distinctive red colour (Joubert & De Beer, 2011). In recent years, a variety of new rooibos-derived consumer products have been introduced to the marketplace, including exotically flavoured rooibos teas and ready-to-drink iced teas, slimming products and cosmetics, *Red Espresso* (a rooibos-derived tea espresso available in various flavours), instant rooibos cappuccino and rooibos-flavoured yogurts and breakfast cereals (Biénabe *et al.*, 2009; Wynberg *et al.*, 2009; Joubert & De Beer, 2011; Joubert & De Beer, 2014). Most recently, rooibos has been incorporated as an ingredient in *Albany's Ultima* "Rooibos and Rye" whole-wheat bread variant, which is promoted for its high antioxidant content and is marketed as a health-promoting product (Anon., 2015a). Rooibos plant material has also been used in the production of the *Audacia* range of sulphite-free wines (Anon., 2015b) and an innovative niche craft beer known as *Stellenbrau Governor's Red* (Anon., 2015c).

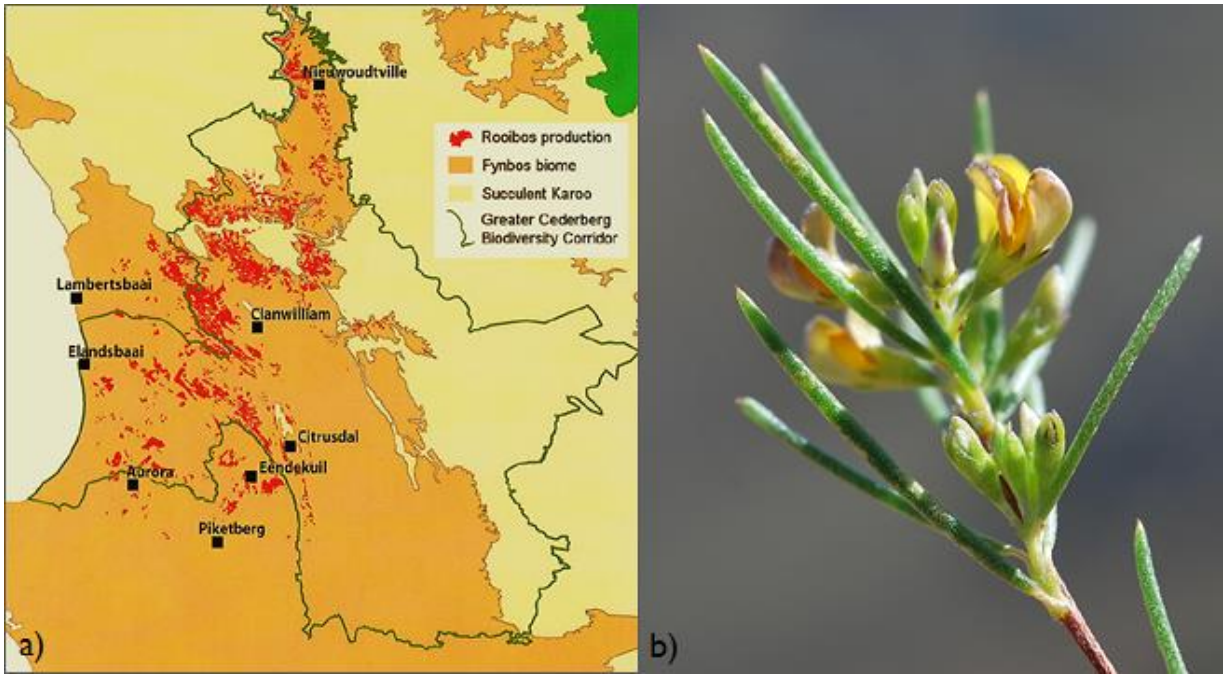

Figure 2.1 (a) Geographical distribution pattern of rooibos (map supplied by South African Rooibos Council) (Joubert & De Beer, 2011); (b) Typical needle-like leaves of wild-growing *Aspalathus linearis* (Image credit: Charles Stirton, 2011; http://www.ispotnature.org/node480116).

2.1.1.3. Rooibos Industry

The growing global demand for rooibos tea eventually resulted in the establishment of a lucrative export market, but total annual exports were still less than 800 tonnes by the early 1990s. This sluggish increase from an initial 544 tonnes, reported in 1955, to 750 tonnes in 1993 was eclipsed considerably since then, with the industry reaching its hitherto unseen peak of 7 176 tonnes exported in 2007 (Joubert & De Beer, 2011). *Unfermented* or *green* rooibos (GR) has been available on the market since the early 2000s due to growing interest in a product with higher antioxidant and/or aspalathin content (see section 2.1.2). The unfermented product lacks the typical herbal-floral, woody and honey-like flavour notes and sweet taste of fermented rooibos, and instead possesses a grassy, hay-like aroma (Joubert & De Beer, 2014; Viljoen *et al.*, 2016).

Fig. 2.2 shows the amounts of conventional (fermented) and GR exported to each of the top five rooibos export countries for the period 2004–2014. Germany was consistently the top export destination by a considerable margin, with Netherlands, the United Kingdom, the United States of America and Japan constituting the rest of the top five. Smaller emerging markets like Spain and Sri Lanka have all recently shown promising growth as well. Conventional rooibos consistently outsells green Oriental and GR tea both individually and combined, having been established as a product on the market for much longer and being lower in price and more readily available. Organic and GR have maintained a stable market share of 12% of exports between 2004 and 2013 (Anon., 2014a). GR has seen a three-fold increase in export tonnage since 2003, most likely due to the discovery of its higher polyphenolic content compared with conventional rooibos, suggesting a more potent antioxidant effect (Von Gadow *et al.*, 1997).

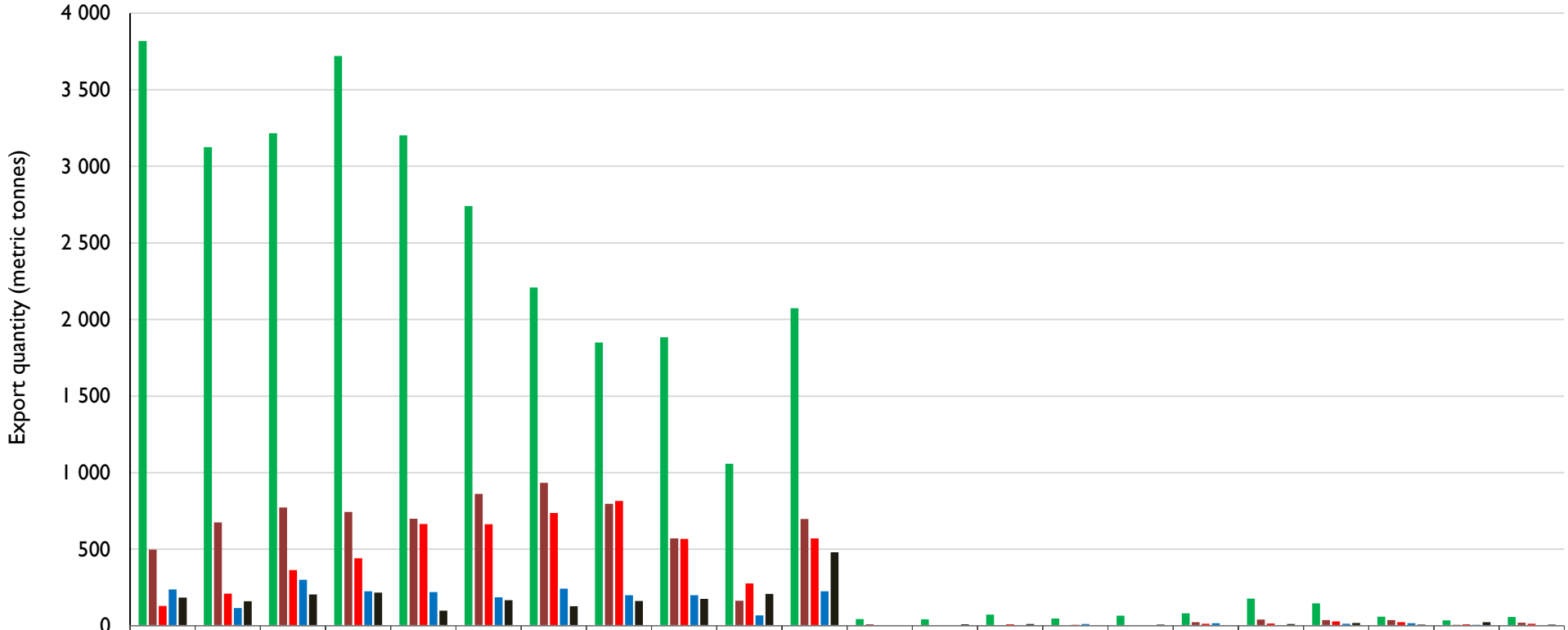

	Conventional Rooibos (metric tonnes)											Green Rooibos (metric tonnes)										
	2004	2005	2006	2007	2008	2009	2010	2011	2012	2013	2014	2004	2005	2006	2007	2008	2009	2010	2011	2012	2013	2014
Germany	3 817.0	3 126.0	3 216.0	3 720.0	3 203.0	2 740.0	2 209.0	1 850.0	1 884.0	1 058.0	2 074.1	43.6	42.7	72.4	48.2	66.7	81.4	178.2	147.1	59.3	36.3	57.9
Netherlands	496.4	674.5	773.2	743.0	699.1	861.4	932.6	796.3	570.1	164.2	696.7	9.7	3.1	5.4	0.0	5.5	23.7	40.3	37.5	37.1	6.5	19.4
UK	129.5	209.7	363.5	440.1	665.3	662.8	736.3	815.7	566.7	276.0	570.8	1.5	3.3	10.1	6.0	2.4	14.0	14.2	29.5	22.8	10.6	13.5
USA	237.4	116.7	299.7	225.6	219.6	186.5	241.8	199.8	198.9	67.3	224.9	0.0	2.1	0.3	11.5	0.0	16.0	5.0	12.8	16.0	5.9	2.6
Japan	183.6	160.5	205.5	216.0	98.0	166.8	127.8	162.2	176.1	207.4	480.6	5.5	9.3	11.0	0.0	9.0	4.8	11.1	18.9	8.5	22.8	8.0

Figure 2.2 Exported quantities of South African conventional (fermented) and green (unfermented) rooibos by top five export destinations from 2004–2014 (adapted from Anon., 2014a).

2.1.1.4. Agroprocessing and distribution of rooibos plant material

There are an estimated 350 to 550 farmers producing rooibos in South Africa, predominantly in the Cederberg area, where the cultivated Nortier type rooibos has been successfully propagated using seedlings (Anon., 2014a). Planting usually takes place in the winter months at about 8 000–10 000 plants to a hectare of land, and after approximately eight months the plants are trimmed to a height of 30 cm in order to stimulate further branching. Eighteen months of growth are required before the first harvest can be undertaken, and it typically takes double that amount of time to attain a fully feasible production programme (Joubert & Schulz, 2006). The average dry yield per hectare cultivated is approximately 300 kg (Anon., 2014a). When harvested in the summer and early Autumn (January to April), the entire rooibos bush is topped to a height of about 45 cm. Many producers make use of a central processing yard for primary processing of rooibos. Such processing yards are situated in Clanwilliam, Graafwater and Nieuwoudtville. The central processing yards sell the processed plant material to secondary processors for further value-addition and the production and development of consumer products. Secondary processing of rooibos is currently dominated by eight large processors who are collectively responsible for about 90% of the market share (Biénabe *et al.*, 2009; Anon., 2014a).

In 1986 a steam-pasteurisation process was introduced by the Rooibos Tea Board to address the issue of microbial contamination of plant material, which had caused significant losses to the industry in the preceding years (Snyman, 2000). Because plant material from various origins are often blended to standardise quality, the potential for introducing contamination increases, and the subsequent fermentation process creates conditions favourable to bacterial growth. Microbial contamination is therefore essentially unavoidable, and the practice of steam pasteurisation for 2 min at 99.5 °C prior to packing has been recommended to reduce the microbial load to acceptable levels (Du Plessis & Roos, 1986). Steam pasteurisation for 60 s at 96 °C is currently the method employed by South Africa's largest rooibos processor. An additional drying step is also carried out to reduce the moisture content to 10% or less (Koch *et al.*, 2012) in accordance with the official South African regulations relating to quality standards for rooibos (Anon., 2010a). The low final moisture content of processed rooibos tea makes it a well-preserved product which is generally considered microbiologically safe under prescribed storage conditions (Joubert & De Beer, 2011).

Oxidation of the processed plant material should be kept to a minimum in the production of GR, and this can be achieved by a number of methods: steaming or drying of fresh, whole shoots to inactive enzymes before shredding; rapid drying of shredded plant material under vacuum or initial low temperature drying followed by high-temperature drying of the shredded plant material (Joubert & De Beer, 2014). The most commonly used drying method for GR, however, is by spreading out the freshly shredded plant material in thin layers under direct sunlight. It is of critical importance

that this is carried out effectively, as too much residual moisture could significantly affect the tea quality in the long term (Joubert *et al.*, 2008a; Joubert & De Beer, 2011). This method requires no additional equipment or trained operators, but may still result in slow browning of the plant material and loss of phenolic content since it is not always easy to control and subject to the specific environmental conditions (Joubert & De Beer, 2014).

2.1.2. Chemical composition

The desirable attributes of rooibos and other commercially significant plant species are often linked to the presence of a particular chemical compound or chemical constitution. Chemical compounds in plant material may be broadly classified as primary or secondary metabolites. Primary metabolites are those compounds which are involved in the basic anabolic and catabolic processes required for cell maintenance and growth, whereas secondary metabolites are those involved in "non-essential" processes which confer specific advantages in terms of survival and environmental stress protection (Lattanzio *et al.*, 2008; Petrussa *et al.*, 2013). Phenolics are the most widely distributed class of secondary plant metabolite, and refers to an aromatic ring bearing one hydroxyl group (*phenol*), or more than one hydroxyl group (*polyphenol*) (Di Ferdinando *et al.*, 2013). In general, the term "plant phenolics" refers to secondary metabolites (monomeric or polymeric) which arise biogenetically from either the shikimate (phenylpropanoid) pathway or the malonate pathway, and which play a significant role in a wide range of physiological processes (Quideau, 2006).

Phenolics are arguably the most important class of chemical compounds in rooibos in terms of its overall contribution to the characteristics of the plant material and its derived products. The major phenolic compounds of interest to this study, as well as the factors which affect their content and distribution in rooibos, will be discussed in the following section. A brief overview of non-phenolic rooibos compounds is presented at the end of the section, but a more extensive review has been published by Joubert *et al.* (2008a).

2.1.2.1. Phenolic composition

The majority of the phenolic compounds present in rooibos belong to the *flavonoid* subclass, a specific type of low-molecular-weight polyphenolic compound formed by the reaction of acetic acid with derivatives of phenylalanine (via the shikimate pathway) (Tzin & Galili, 2010). The specific chemical properties of flavonoids depend on their structural class, degree of polymerisation, substitutions, conjugations and hydroxylation (Aherne & O'Brien, 2002). The structure of the basic flavan nucleus (Fig. 2.3) allows for a large number of substitutions to be made in the A, B and C

rings, which results in a large number of potential flavonoid subclasses with unique chemical properties (Aherne & O'Brien, 2002).

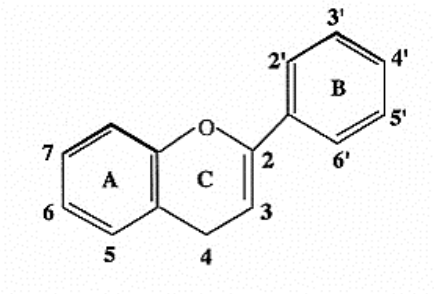

Figure 2.3 Basic flavan nucleus with rings and carbon number numberings indicated (Aherne & O'Brien, 2002).

Flavonoids may be categorised into classes, including anthocyanidins, dihydrochalcones, catechins, flavones, flavanols, isoflavones and flavanones, based on the level of oxidation on the C-ring. Two of these classes, flavones and flavonols, have been identified in almost all plant species (Di Ferdinando *et al*., 2013). Flavonoid molecules which do not have sugar moieties attached are known as flavonoid *aglycones*, whereas those with sugar moieties are known as flavonoid *glycosides*. With the exception of catechins, flavonoids are not present in plants in the aglycone form. D-glucose is the most common sugar moiety, but arabinose, galactose, and xylose moieties do occur. Glycosylation results in an increase in the polarity of the flavonoid molecule, which promotes its storage in plant vacuoles (Aherne & O'Brien, 2002). It has been suggested that glycosylation of the flavonoids, besides enhancing their solubility in the aqueous cellular environment, serves to protect the most reactive groups from auto-oxidation (Di Ferdinando *et al*., 2013). Sugar moieties can be linked to the flavan nucleus by an *O* or *C*-glycosidic bond (Fig. 2.4), the latter type being more resistant to hydrolysis than the *O*-glycosidic bond type, which is readily broken down enzymatically or chemically (Brazier-Hicks & Edwards, 2013). Water solubility also generally increases with the number of hydroxyl groups present (Lattanzio *et al*., 2008). The various flavonoids which have been identified in rooibos have been discussed more extensively elsewhere (Joubert *et al*., 2008a; Iswaldi *et al*., 2011; Beelders *et al*., 2012; Joubert & De Beer, 2014), but a number of compounds of interest to the present study are shown in Table 2.1.

Aspalathis linearis is unique in that it is the only plant species which has so far been found to contain the bioflavonoid aspalathin, a *C*-glucosyl dihydrochalcone (Koeppen & Roux, 1965a). Dihydrochalcones are the major type of flavonoid in apple trees (*Malus* sp.) and are found in large amounts (up to 5% dry weight) in immature fruits and leaves, where they have been shown to play a role in maintaining the overall redox homeostasis (De Bernonville *et al*., 2010). They were initially thought to be unique to *Malus* sp., but dihydrochalcones have since also been identified in *Symplocos*, *Fragaria* and *Balanophora* (De Bernonville *et al*., 2010). Another rooibos dihydrochalcone, nothofagin,

also present in substantial quantities in the unfermented plant material, has been found thus far in only two other natural sources, *Nothofagus fusca* and *Schoepfia sinensis*, and only the absence of a hydroxyl group on the ß-ring distinguishes it from aspalathin in terms of chemical structure (Hillis & Inoue, 1967; Joubert *et al.*, 2008a).

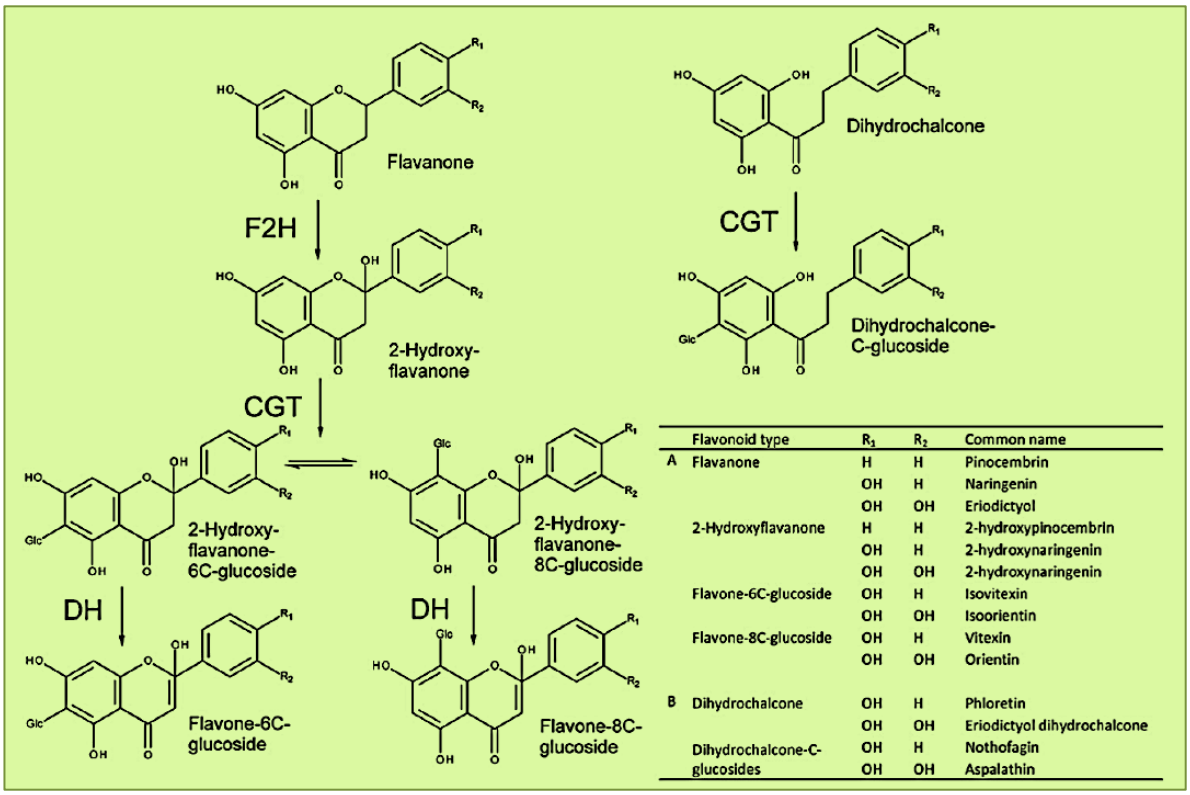

	Flavonoid type	R_1	R_2	Common name
A	Flavanone	H	H	Pinocembrin
		OH	H	Naringenin
		OH	OH	Eriodictyol
	2-Hydroxyflavanone	H	H	2-hydroxypinocembrin
		OH	H	2-hydroxynaringenin
		OH	OH	2-hydroxynaringenin
	Flavone-6C-glucoside	OH	H	Isovitexin
		OH	OH	Isoorientin
	Flavone-8C-glucoside	OH	H	Vitexin
		OH	OH	Orientin
B	Dihydrochalcone	OH	H	Phloretin
		OH	OH	Eriodictyol dihydrochalcone
	Dihydrochalcone-C-glucosides	OH	H	Nothofagin
		OH	OH	Aspalathin

Figure 2.4 Biosynthesis of flavone-*C*-glycosides and dihydrochalcone-*C*-glycosides in plants. F2H, flavanone-2-hydroxylase; CGT, *C*-glucosyltransferase; DH, dehydratase (Brazier-Hicks & Edwards, 2013).

Aspalathin is converted to orientin and iso-orientin (also known as homo-orientin) during fermentation of the plant material, and rooibos plant material therefore contains diastereomeric mixtures of the 6-C and 8-C flavanones, (*R*)- and (*S*)-eriodictyol-6-*C*-ß-D-glucopyranoside and (*R*)- and (*S*)-eriodictyol-8-*C*-ß-D-glucopyranoside, intermediates which are formed during this conversion process (Koeppen & Roux, 1965a; Marais *et al.*, 2000; Krafczyk & Glomb, 2008). Joubert *et al.* (2004) showed that fermentation significantly decreased the aspalathin content of ethyl acetate-soluble fractions of aqueous rooibos extracts (from 547 to 36.4 $mg.g^{-1}$) and that aspalathin was the major contributor to the total polyphenol content of the unfermented extract.

Rooibos also contains monomeric flavonoids from the *flavonol* and *flavone* subclasses. The flavones include the *C*-glucosyl flavones (vitexin, isovitexin, orientin and iso-orientin) as well as the flavone aglycone, luteolin, its *O*-glucoside, luteolin-7-*O*-glucoside, and its 3-*O*-methyl analogue, chrysoeriol. Quercetin is a flavonol aglycone isolated from rooibos along with its *O*-glycosides, rutin,

isoquercitrin, quercetin-3-*O*-robinobioside and hyperoside (Joubert & De Beer, 2011). The dimeric procyanidin B3 and the trimeric bis-fisetinidol-(4ß, 6:4ß,8)-catechin are further examples of flavonols that have been identified in rooibos (Ferreira *et al.*, 1995; Krafczyk & Glomb, 2008).

Phenolic acids present in rooibos include the hydroxybenzoic acids (*p*-hydroxybenzoic acid, salicylic acid, gallic acid, vanillic acid and gentisic acid) as well as the hydroxycinnamic acid derivatives, *p*-coumaric acid, ferulic acid and caffeic acid. The latter three compounds occur alongside their 3,4,5-trihydroxy analogues, which confirms that the hydroxycinnamic acids play a key role in the biosynthesis of phenylpropanoid metabolites (derivatives of phenylalanine) (Rabe *et al.*, 1994). Tannins are astringent polyphenolic compounds which also play a protective role in a variety of plant species, and rooibos tannins are of the procyanidin type (Joubert *et al.*, 2004). The tannin content of fermented rooibos leaves, reported as 3.2% (Reynecke *et al.*, 1949) and 4.4% (Blommaert & Steenkamp, 1979), is relatively low compared with fermented Oriental tea, and rooibos is generally considered a low-tannin herbal tea (Morton, 1983). No data has been published to date on the tannin content of unfermented rooibos tea. Aspalathin is a potent antioxidant which compares favourably with epigallocatechin gallate (EGCG), the major antioxidant flavonoid in green Oriental tea (*Camellia sinensis*) (Joubert & De Beer, 2014). Schulz *et al.* (2003) found that the total aspalathin content in unfermented rooibos plant material correlated well ($R^2 = 0.812$) with the total antioxidant activity. Joubert *et al.* (2004) investigated the radical scavenging capacity of rooibos flavonoids and tannin as well as crude phenolic fractions and aqueous extracts of fermented and unfermented rooibos. Aspalathin had higher superoxide anion and α,α-diphenyl-β-picrylhydrazyl radical scavenging capacity than Trolox, the water-soluble analogue of α-tocopherol. The greatest anti-radical capacities and the highest aspalathin and total polyphenol contents were observed in the ethyl acetate-soluble fractions of the aqueous unfermented rooibos extract and in the crude aspalathin fraction.

Table 2.1 Secondary metabolites identified in *Aspalathus linearis* plant material (adapted from Joubert & De Beer, 2014).

General Structure	Compound type Name and substituents
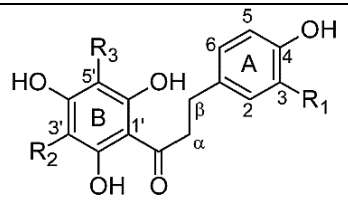	**Dihydrochalcones** Aspalathin [a,b,c,d,f,g,k]: R_1 = OH, R_2 = ß-D-glucopyranosyl Nothofagin [e,f,g,k]: R_1 = H, R_2 = ß-D-glucopyranosyl
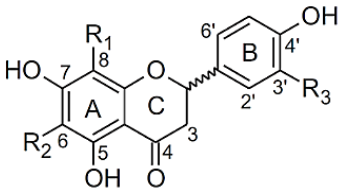	**Flavanones** Hemiphlorin [g]: R_1 = ß-D-glucopyranosyl, R_2 = R_3 = H *(R)/(S)*-eriodictyol-8-*C*-glucoside [f,g,k]: R_1 = ß-D-glucopyranosyl, R_2 = H, R_3 = OH *(R)/(S)*-eriodictyol-6-*C*-glucoside [f,g,k]: R_1 = H, R_2 = ß-D-glucopyranosyl, R_3 = OH
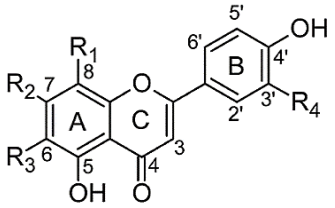	**Flavones** Orientin [a,c,f,g,h,i,k]: R_1 = β-D-glucopyranosyl, R_2 = R_4 = OH, R_3 = H Iso-orientin [c,f,h,i,k]: R_1 = H, R_2 = R_4 = OH, R_3 = D-glucopyranosyl Vitexin [a,c,f,g,k]: R_1 = β-D-glucopyranosyl, R_2 = OH, R_3 = R_4 = H Isovitexin [c,f,g,k]: R_1 = R_4 = H, R_2 = OH, R_3 = β-D-glucopyranosyl Luteolin [c,f,g,k]: R_1 = R_3 = H, R_2 = R_4 = OH Luteolin-7-*O*-glucoside [d]: R_1 = R_3 = H, R_2 = β-D-glucopyranosyloxy, R_4 = OH Chrysoeriol [c,f,k]: R_1 = R_3 = H, R_2 = OH, R_4 = OCH_3

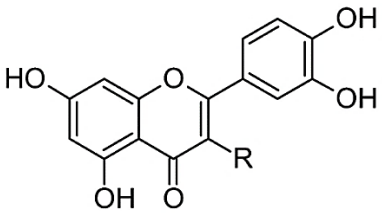

Flavonols

Quercetin [c,f,g,k] : R = H

Isoquercitrin [c,f,g,i,k] : R = β-D-glucopyranosyloxy

Hyperoside [f,g,k] : R = β-D-pyranosyloxy

Rutin [f,i,k] : R = α-L-rhamnopyranosyl-(1→6)-β-D-glucopyranosyloxy

Quercetin-3-β-D-robinoside [g] : R = α-L-rhamnopyranosyl-(1→6)-β-D-galactopyranosyloxy

---

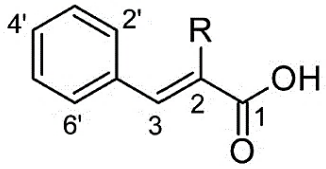

Phenylpropanoid

Phenylpyruvic acid-2-*O*-glucoside (PPAG) [l] : R = 2-β-D-glucopyranosyloxy

---

[a] Koeppen & Roux, 1965a (identification by NMR); [b] Koeppen & Roux, 1966 (identification by NMR); [c] Rabe *et al*., 1994 (identification by NMR); [d] Ferreira *et al*., 1995 (identification by NMR); [e] Joubert, 1996 (identification by co-elution with pure standard); [f] Bramati *et al*., 2002 (identification by LC-MS); [g] Shimamura *et al*., 2006 (identification by NMR); [h] Koeppen & Roux, 1965b (identification by NMR); [i] Koeppen *et al*., 1962 (identification by NMR); [j] Marais *et al*., 1996 (identification by NMR); [k] Krafczyk & Glomb, 2008 (identification by NMR); [l] Joubert *et al*., 2013 (identification by NMR).

2.1.2.2. Factors affecting the phenolic content of rooibos and rooibos extracts

The plant kingdom features a wide variety of phenolic compounds, with some plant tissues containing several grams per kilogram, their biosynthesis stimulated by extreme or harsh environmental conditions (Lattanzio *et al.*, 2008). The accumulation of phenolics in plant tissue is thought to be an evolved defence mechanism which deters predation by animals and insects, as well as to repair damage caused by oxidative stress (Petrussa *et al.*, 1996). Flavonoid glycosides in particular are thought to play a major role in the protection of plants against ultraviolet (UV) light-induced oxidative damage and are often most highly concentrated in the epidermal and sub-epidermal cell layers of leaves and stems, flowers and other peripheral parts of the plant (e.g. skin or peel), and tend to decrease in concentration towards the core of the plant matrix (Aherne & O'Brien, 2002; Winkel-Shirley, 2002; Lattanzio *et al.*, 2008). The formation of oxidised forms of the basic flavonoid structure is accelerated by direct exposure to sunlight (especially UV-B radiation), which explains their higher concentration in external and/or aerial plant tissues and their diminished content in greenhouse-cultivated plants. With the exception of onions, flavonoids are mostly found in plant parts above soil level (Aherne & O'Brien, 2002).

Fundamentally, all plant material varies greatly in its phenolic composition as a result of genetic variation, but a number of other factors have been shown to affect this significantly, i.e. climate, seasonal effects, diurnal cycles, development stage of shoots and post-harvest processing methods (Aherne & O'Brien, 2002; Yao *et al.*, 2005; Joubert *et al.*, 2008a). Di Ferdinando *et al.* (2013) reviewed the various abiotic stressors which have been reported to affect the accumulation of flavonoids in plants, including UV radiation, nitrogen depletion, heavy metals, solar intensity, cold, drought, ozone and salinity stress. None of the factors that could affect the phenolic composition of rooibos has been investigated to date as it would require large amounts of plant material that are unavailable at this stage due to the demands of the industry. A number of studies using large sample sets have confirmed, however, that significant variation occurs in the phenolic composition of cultivated rooibos (Joubert & Schulz, 2006; Manley *et al.*, 2006; Joubert & De Beer, 2011; Joubert *et al.*, 2012; Joubert *et al.*, 2013).

Seasonal variation in flavonoid levels has also been demonstrated in leafy vegetables like leek and lettuce, with levels typically peaking in summer months (Aherne & O'Brien, 2002). Yao *et al.* (2005) observed a similar trend for Australian-grown *Camellia sinensis*, with fresh shoots harvested in warmer months containing significantly higher levels of antioxidant flavonoids than those harvested during cooler months ($P < 0.05$). Changes in abiotic and biotic stress have been shown to result in variation in the dihydrochalcone content of other plant species over time (Petrussa *et al.*, 1996; Treutter, 2001). It has been suggested that dihydrochalcones help to reduce oxidative damage in

apple (*Malus domestica*) leaves, which were also found to contain significantly lower levels of dihydrochalcone when matured (De Bernonville *et al*., 2010).

Joubert *et al*. (2012), investigating the phenolic content and antioxidant activity of hot water infusions of batches of fermented rooibos (n = 114) from different production seasons (2009, 2010 and 2011), reported significant variation in the individual content values of phenolic compounds ($P < 0.05$). Aspalathin values ranged from not detected to 15.66 $mg.L^{-1}$ of infusion. The effect of production season did not significantly affect ($P > 0.05$) the total polyphenol content or the aspalathin and orientin content of the infusions, but the nothofagin and iso-orientin content were significantly higher ($P < 0.05$) in the production seasons of 2009 and 2011, respectively. Joubert *et al.* (2016) analysed a large sample set (n = 209) of fermented, unpasteurised rooibos collected from two major production areas (Northern and Western Cape Provinces, South Africa) over the production period of 2011 to 2013. Hot water infusions were prepared to quantify the content of the major flavonoids and PPAG in each production batch. Analysis of variance (ANOVA) indicated a significant production area x production year interaction ($P < 0.05$) for the flavonol subclass of phenolic compounds, whereas the dihydrochalcone content was significantly affected by the production area, with samples from the Western Cape having higher aspalathin ($P < 0.0001$) and nothofagin ($P = 0.0207$) content than those originating from the Northern Cape. Neither the production year nor production area significantly affected the flavone content. Iso-orientin and orientin, the major rooibos flavones, were the most predominant phenolic compounds in the fermented rooibos infusions, indicating that significant oxidative degradation of aspalathin had taken place.

Processing methods may affect the phenolic composition of rooibos significantly, especially the typically uncontrolled fermentation process which renders the dihydrochalcones, aspalathin and nothofagin, susceptible to enzymatic oxidative degradation (Joubert, 1996). Oxidative degradation of orientin, iso-orientin and nothofagin is slow compared with that of aspalathin, suggesting that the C-ring configuration and the hydroquinone moiety of the B-ring plays a key role in the oxidation process (Krafczyk *et al.*, 2009). Fig. 2.5 illustrates the initial oxidation reactions involving aspalathin. An aspalathin dimer may also form during fermentation due to oxidative coupling of the A- and B-rings. Aspalathin and nothofagin are also both converted to higher molecular weight compounds during oxidation which contribute to browning of the plant material (Krafczyk *et al.*, 2009). Heinrich *et al.* (2012) showed the presence of dibenzofuran derivatives in oxidised aspalathin solution. Joubert (1996) demonstrated rapid browning and decrease in dihydrochalcone content as soon as the leaves were cut into small pieces (comminuted). Less than 80% of the initial aspalathin content of the leaf remains 15 min after oxidation is initiated by cutting, and ca. 33% remains after 210 min of oxidation. A major portion of the aspalathin may therefore be degraded before fermentation has even been commenced. Fermentation of the plant material (Fig. 2.6) results in a further sharp

decrease in the aspalathin content, with less than 7% of the initial amount remaining in the fermented product (Joubert, 1996).

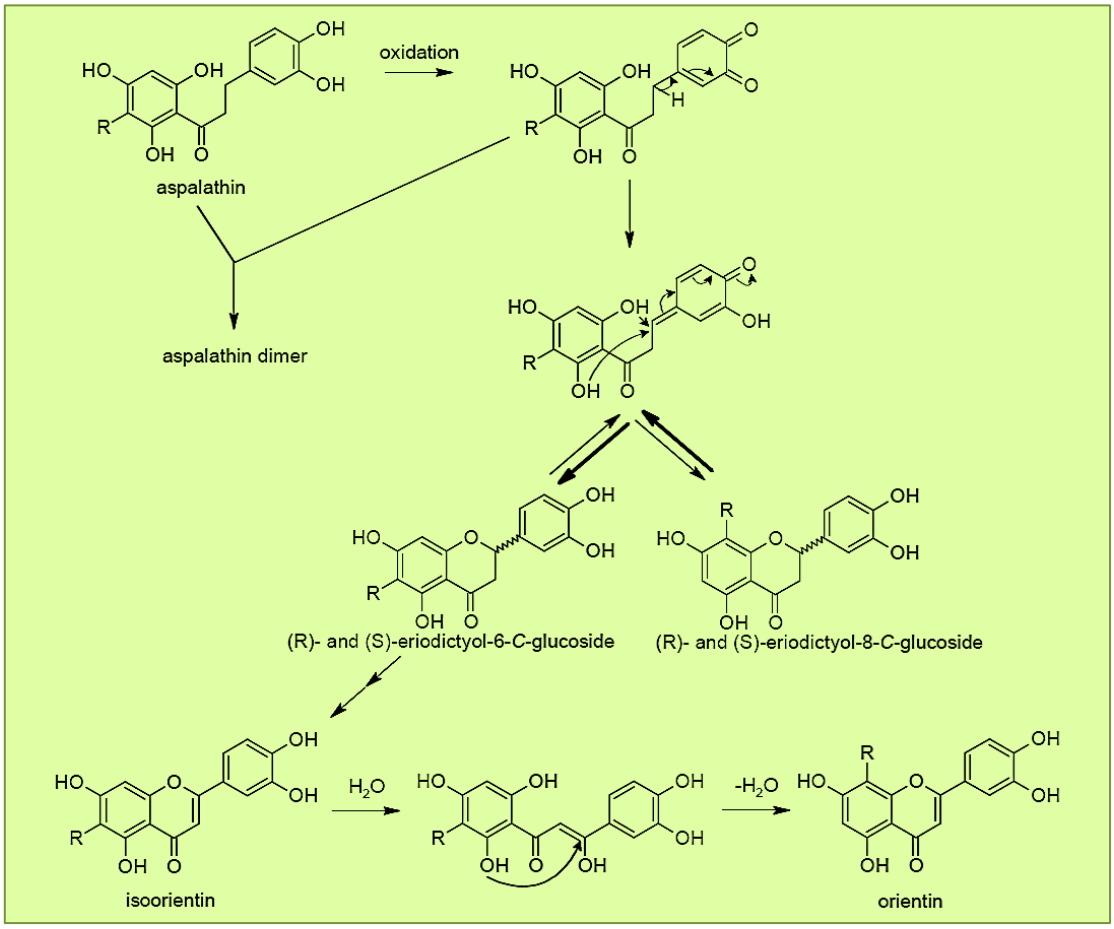

Figure 2.5 Mechanism of aspalathin oxidation (Joubert & De Beer, 2011).

Figure 2.6 Fermentation of rooibos plant material in moist, aerated heaps, resulting in colour change from green to reddish brown (inset) (Image credit: Carmien Tea Pty Ltd., 2016; http://rooibos-route.co.za).

Similar trends were observed for nothofagin, with ca. 8% of the initial content remaining after fermentation. The total polyphenol content did not decrease to the same degree as the total dihydrochalcone content, while the ratio of dihydrochalcones to total polyphenols in the plant material decreased significantly during fermentation, indicating that dihydrochalcones were converted to other phenolic compounds in the process (Joubert, 1996). Joubert & De Villiers (1997) investigated the effects of fermentation temperature (30–42 °C), drying temperature (40–70 °C) and drying method (sun-drying vs. controlled drying) on the subjective tea quality and objective colour measurement of fermented rooibos. The drying method had no significant effect on the subjective tea quality, but sun-dried rooibos had a significantly darker colour ($P = 0.003$) than that dried under controlled conditions. The subjective tea quality improved with increasing fermentation temperature and decreased with increasing drying temperature ($P < 0.05$). The drying method (deep-bed drying vs. thin-layer drying) for fermented rooibos did not significantly affect its overall quality (based on aroma, taste and colour).

The effects of fermentation, steam pasteurisation, sieving and sun-drying on the total polyphenol content and soluble solids content of aqueous extracts of unfermented and fermented rooibos were investigated by Standley *et al.* (2001). It was found that steam pasteurisation caused a significant increase in the percentage total polyphenols and water-soluble solids, but this was attributed to the removal of stems, which have low water-soluble phenolic content, prior to steam pasteurisation. The samples used were also randomly collected at different points during processing, and the plant material used could have originated from different plantations (different age) in addition to inherent genetic variation.

Schulz *et al.* (2003) reported that substantial losses of aspalathin and nothofagin were observed after the fermentation process. The ratio of the total antioxidant activity to the total polyphenol content was also lower for fermented samples, indicating that oxidative changes during fermentation resulted in a significant loss of antioxidant capacity. The effects of various processing unit operations on the soluble solids and total polyphenol content of fermented and unfermented samples of rooibos ($n = 6$), originating from the same plant material, were investigated by Joubert *et al.* (2008c). Results demonstrated that fermentation of the plant material caused a significant reduction in the total polyphenolic content and the yield of dried aqueous extract. Koch *et al.* (2013) found that steam-pasteurisation (1 min at 96 °C) of fermented rooibos caused significant decreases in the soluble solids, aspalathin and total polyphenol contents of the corresponding hot water infusions ($P < 0.05$). The decreases in the total polyphenol and total soluble solids contents were strongly positively correlated, suggesting that the decrease in soluble solids could be strongly attributed to the decrease in the soluble polyphenol content.

The use of rooibos extract in commercial, ready-to-drink rooibos iced tea products prompted a study investigating the effects of various heat treatments on the orientin, iso-orientin and aspalathin content of rooibos iced tea formulations, prepared either with fermented rooibos extract, aspalathin-enriched green rooibos extract (GRE) or a nanomicellar solution of aspalathin-enriched GRE (Joubert *et al.*, 2009; Joubert *et al.*, 2010). Rooibos extract with no added ascorbic or citric acid had reduced aspalathin, orientin and iso-orientin content after normal temperature sterilisation (5 min at 121 °C) and high-temperature sterilisation (4 min at 135 °C). The reduction in aspalathin content was substantially greater than the reduction in orientin and iso-orientin content, possibly explained by the fact that aspalathin is partially converted to orientin and iso-orientin by oxidative degradation (Krafczyk *et al.*, 2009). Pasteurisation (30 min at 93 °C) caused a decrease in the aspalathin content, but conversely led to an increase in the orientin and iso-orientin content. This could be attributed to the aforementioned oxidative degradation of aspalathin. When the intended final product is green or unfermented rooibos, the bruising, wetting and fermentation steps are omitted to minimise oxidative changes to retain the green leaf colour and prevent a significant decrease in the total phenolic content. By drying the plant material to a critical moisture level before shredding is carried out, or by steam-treating the shoots to inactivate pro-oxidative enzymes, this can be achieved fairly successfully. Quick drying under vacuum conditions is another strategy to achieve this, although often prohibitively expensive. The same degree of oxidative degradation of aspalathin occurs under controlled-drying conditions in the absence of sunlight as under simple sun-drying conditions (Joubert, 1996).

2.1.2.3. Characterisation of phenolic profile by reversed-phase high-performance liquid chromatography (RP-HPLC)

Various high-performance liquid chromatography methods have been developed and used to quantify rooibos phenolic compounds, requiring run times ranging from 16 to 125 min per sample (Table 2.2). Recently, a method was developed specifically for GR (De Beer, D., 2016, ARC Infruitec-Nietvoorbij, Stellenbosch, personal communication, 9 June) which provides reproducible results within a comparatively short analysis time (16 min) by reducing the number of analytes to just four (De Beer *et al.*, 2015). The method thus provides an efficient means of quantifying these compounds, especially when large numbers of experimental runs are to be conducted and a less comprehensive phenolic profile is required. The major flavonoid contents of a variety of rooibos sample types, as determined by RP-HPLC, are summarised in Table 2.3.

Table 2.2 Summarised details of studies using high-performance liquid chromatography methods to quantify rooibos polyphenolic compounds.

Reference	Aim of study	Sample types	Mobile Phase	Stationary Phase	Analytes	Column Temperature	Analysis Time	Detection Method
Joubert, 1996	Quantification of the dihydrochalcones, aspalathin and nothofagin, as a function of processing parameters	Ethyl acetate soluble fractions of rooibos plant material at various stages of processing	Gradient elution with methanol and 2% (v.v^{-1}) aqueous formic acid Flow Rate: 0.4–1.2 mL.min^{-1}	Merck LiChrospher 100 RP-18 (250 x 4.0 mm, 5 µm)	Protocatechuic acid; *p*-hydroxybenzoic acid; vanillic + caffeic acid; *p*-coumaric acid; aspalathin; orientin + ferulic acid; iso-orientin; vitexin; nothofagin; rutin + isoquercitrin.	38 °C	125 min	Variable wavelength detection
Bramati *et al.*, 2002; 2003	Quantitative characterisation of flavonoid compounds in fermented and unfermented rooibos tea (*Aspalathus linearis*)	Aqueous and methanolic extracts of commercial fermented and unfermented rooibos	Gradient elution with acetonitrile and 0.1% (v.v^{-1}) aqueous acetic acid Flow Rate: 0.8 mL.min^{-1}	Waters Symmetry Shield C18 (250 x 4.6 mm, 5 µm)	Iso-orientin; orientin; aspalathin; vitexin; rutin; isovitexin; isoquercitrin + hyperoside; luteolin; quercetin; chrysoeriol	Ambient temperature	30 min	Diode array detection & mass spectrometry
Schulz *et al.*, 2003	Development of a method for the reliable identification of the	Aqueous extract of unfermented rooibos	Gradient elution with acetonitrile and 1% (v.v^{-1}) aqueous	Agilent Zorbax SB-C18 (150 x 3.0 mm, 3.5 µm)	Iso-orientin; orientin; aspalathin; rutin;	35 °C	40 min	Diode array detection & mass spectrometry

Reference	Aim of study	Sample types	Mobile Phase	Stationary Phase	Analytes	Column Temperature	Analysis Time	Detection Method
	most relevant flavonoids occurring in rooibos		formic acid Flow Rate: 0.5–0.7 mL.min^{-1}		isoquercitrin; nothofagin			
Stalmach *et al.*, 2009	Quantification of flavonoids in 500 mL of unfermented and fermented rooibos teas; and aspalathin and eriodictyol metabolites in urine	Commercial ready-to-drink rooibos tea (fermented and unfermented) Urine and plasma samples of 10 human test subjects	Gradient elution with acetonitrile and 0.1% (v.v^{-1}) aqueous formic acid Flow Rate: 1.0 mL.min^{-1}	Phenomenex Synergi (C12) RP-MAX 80A (250 x 4.6 mm, 4 µm)	Aspalathin; nothofagin; eriodictyol-C-glucosides (4); orientin; iso-orientin; vitexin; isovitexin; hyperoside; isoquercitrin; rutin; rutin isomer; luteolin; quercetin in rooibos teas. Aspalathin and eriodictyol metabolites in urine	40 °C	75 min	Diode array detection & mass spectrometry
Joubert *et al.*, 2009 Joubert *et al.*, 2010 De Beer *et al.*, 2012	Quantification of the dihydrochalcone aspalathin and its corresponding flavones orientin and iso-orientin in fermented rooibos iced tea.	2009: Samples obtained at 6 different stages of production of commercial powdered aqueous rooibos extract; Commercial ready-to-drink rooibos iced teas and fruit	Gradient elution with acetonitrile and 2% (v.v^{-1}) aqueous acetic acid Flow Rate: 0.8 mL.min^{-1}	Agilent Zorbax Eclipse XDB-C18 (150 x 4.6 mm, 5 µm)	Aspalathin; orientin; iso-orientin	38 °C	23 min	Diode array detection

Reference	Aim of study	Sample types	Mobile Phase	Stationary Phase	Analytes	Column Temperature	Analysis Time	Detection Method
		juice blends 2010: Different formulations of ready-to-drink beverages containing unfermented rooibos extract 2012: Different formulations of ready-to-drink beverages containing unfermented and fermented rooibos extracts subjected to various storage conditions						
Breiter *et al*., 2011	Quantification of the major flavonoids in aqueous extract of dried green rooibos tea leaves; also unchanged flavonoids in plasma after ingestion of rooibos tea or active fraction isolated from rooibos tea	Aqueous extract of unfermented rooibos Urine and plasma of 10 human test subjects	Gradient elution with acetonitrile and 2% ($v.v^{-1}$) aqueous acetic acid Flow Rate: 0.5 $mL.min^{-1}$	Phenomenex Luna Phenyl-Hexyl (250 x 4.6 mm, 5 µm)	Aspalathin; nothofagin; iso-orientin; orientin; rutin; hyperoside; isoquercitrin; vitexin; isovitexin; luteolin-*O*-galactoside in aqueous extract of green rooibos.	Ambient temperature	±80 min	Diode array detection

Reference	Aim of study	Sample types	Mobile Phase	Stationary Phase	Analytes	Column Temperature	Analysis Time	Detection Method
					Aspalathin; iso-orientin; and orientin in plasma.			
Beelders *et al.*, 2012	Development of a routine quantification method for major rooibos phenolic compounds	Aqueous infusions of fermented and unfermented rooibos	Gradient elution with acetonitrile and 2% (v.v^{-1}) aqueous acetic acid Flow Rate: 1.0 mL.min^{-1}	Agilent Zorbax SB-C18 (50,100 x 4.6 mm, 1.8 µm) Phenomenex Gemini C18 (150 x 4.6 mm, 5.0 µm)	Aspalathin; nothofagin; iso-orientin; orientin; vitexin; isovitexin; luteolin; luteolin-7-*O*-glucoside; chrysoeriol; quercetin; isoquercitrin; hyperoside; rutin; phenylpyruvic acid-2-*O*-glucoside; ferulic acid	25 °C	37 min	Diode array detection & mass spectrometry
De Beer *et al.*, 2015	Quantification of major dihydrochalcones and flavones during development of a high-performance countercurrent chromatography isolation protocol	Polyphenol-enriched fractions of aqueous green rooibos extract	Gradient elution with acetonitrile and 0.1% (v.v^{-1}) aqueous formic acid Flow Rate: 1.0 mL.min^{-1}	Poroshell SB-C18 (50 x 4.6 mm, 2.7 µm)	Aspalathin; iso-orientin; orientin; nothofagin	30 °C	16 min	Diode array detection

Table 2.3 Phenolic composition of various rooibos sample types as quantified by high-performance liquid chromatography.

Reference	Sample Type	Aspalathin	Iso-orientin	Orientin	Nothofagin	PPAG
Beelders *et al*., 2012	Unfermented rooibos aqueous infusion, P_1 (n = 5)[1]	8.4 ± 1.4	0.72 ± 0.12	0.48 ± 0.080	0.69 ± 1.2	0.25 ± 0.051
	Unfermented rooibos aqueous infusion, P_2 (n = 5)[1]	12.4 ± 1.0	1.3 ± 0.6	0.81 ± 0.080	1.7 ± 0.16	0.44 ± 0.056
	Fermented rooibos aqueous infusion (n = 10)[1]	0.64 ± 0.17	1.3 ± 0.084	0.92 ± 0.053	0.10 ± 0.026	0.53 ± 0.10
Bramati *et al*., 2002	Fermented rooibos (n = 1)[1]	0.12 ± 0.001	0.08 ± 0.0007	0.10 ± 0.001	-	-
Bramati *et al*., 2003	Unfermented rooibos (n = 1)[1]	4.99 ± 0.08	0.36 ± 0.018	0.23 ± 0.005	-	-
Joubert & Schulz, 2006	Unfermented whole dried shoots (n = 97)[2]	6.60 (3.80–9.70)	-	-	0.70 (0.20–1.20)	-
	Fermented product (n = 97)[2]	0.30 (0.02–1.20)	-	-	0.10 (nd–0.40)	-
	Fermented aqueous extract (n = 9)[3]	0.35	0.05	0.16	0.11	-
Joubert & De Beer, 2011	Unfermented whole dried shoots (n = 3)[2]	2.56	0.45	0.26	0.25	-
	Fermented product (n = 3)[2]	0.42	0.33	0.20	0.04	-
Joubert & De Beer, 2012	Fermented rooibos food ingredient extract (n = 74)[3]	0.58 (0.16–1.52)	0.83 (0.47–1.03)	0.79 (0.44–0.90)	0.069 (0.03–0.18)	-

Reference	Sample Type	Aspalathin	Iso-orientin	Orientin	Nothofagin	PPAG
Joubert & De Beer, 2012	Fermented rooibos infusions (n = 20)[1]	0.53 (0.264–0.979)	1.12 (1.11–1.36)	0.94 (0.86–1.04)	0.06 (0.03–0.09)	-
Joubert *et al.*, 2012	Fermented rooibos infusions (n = 114)[4]	5.80 (nd–15.66)	15.03 (7.40–20.47)	10.84 (10.33–14.31)	0.95 (nd–2.76)	6.91 (2.72–14.81)
Joubert *et al.*, 2013	Unfermented dried leaves (n = 54)[2]	9.68 (5.97–13.48)	1.52 (0.85–2.24)	0.83 (0.48–1.19)	0.97 (0.49–1.75)	0.14 (nd–0.75)
	Fermented product (n = 10)[2]	0.10 (0.04–0.14)	0.34 (0.30–0.37)	0.22 (0.19–0.24)	0.01 (0.01–0.02)	0.07 (0.03–0.11)
	Industrial hot water extracts of fermented rooibos (n = 18)[1]	0.59 (nd–2.79)	1.07 (0.34–1.41)	1.01 (0.69–1.16)	0.03 (nd–0.18)	0.57 (0.09–0.81)
	Fermented rooibos infusions (n = 10)[4]	5.86 (2.69–8.38)	14.17 (12.15–16.09)	11.10 (9.54–12.61)	0.65 (0.40–0.98)	7.80 (3.77–11.27)
Schulz *et al.*, 2003	Unfermented whole dried shoots (n = 20)[2]	4.89 ± 0.93	-	-	-	-
	Fermented product (n = 20)[2]	0.11 ± 0.05	-	-	-	-

[1] Values reported as g.100 g^{-1} soluble solids; [2] Values reported as g.100 g^{-1} plant material; [3] Values reported as g.100 g^{-1} dried extract; [4] Values reported as mg.L^{-1} infusion; nd = not detected; P_1 and P_2 indicate different producers; PPAG = phenylpyruvic acid-2-*O*-glucoside.

2.1.2.4. Non-phenolic compounds

While the purported medicinal properties of rooibos are mainly associated with its phenolic content, a number of non-phenolic compounds in rooibos have been identified and investigated as discussed in a comprehensive review by Joubert *et al.* (2008a). Volatile constituents contribute to the characteristic aroma and flavour of rooibos, and examples of these which have been identified so far include breakdown products of ß-carotene, i.e. damascenone and ß-ionone (Habu *et al.,* 1985; Kawakami *et al.*, 1993), which are present in relatively high concentrations and have prompted further investigation by Sefton *et al.* (2011). No caffeine has been documented in rooibos, but the related alkaloid sparteine has been reported in rooibos by Van Wyk & Verdoorn (1989).

Phenylpyruvic acid (PPA) is an intermediate in the shikimate pathway, which is used by microorganisms and plants to produce aromatic amino acids (Tzin & Galili, 2010). The enolic glucoside derivative of PPA, enolic *O*-ß-D-glucopyranoside of PPA (or PPAG), has been isolated from unfermented rooibos (Joubert *et al.*, 2013). Recent studies have demonstrated that this compound may help to increase glucose uptake, ameliorate insulin resistance and offer protective effects against hyperglycaemic-induced cardiovascular and pancreatic damage properties (Muller *et al.*, 2013; Mathijs *et al.*, 2014, Dludla *et al.*, 2015).

2.1.3. Rooibos quality aspects

Ninfali *et al.* (2009) proposed the use of two parameters in combination to standardise the quality of herbal extracts. This could involve the quantification of a marker compound (defined as the active ingredient which imparts the intended pharmacological activity) and the total antioxidant capacity as determined with the oxygen radical absorbance capacity (ORAC) or α,α-diphenyl-β-picrylhydrazyl (DPPH) methods. Rutin was investigated as a potential marker compound for rooibos, but it was found to not be representative of the antioxidant activity of the extract. Aspalathin is unique to rooibos and its use as a marker compound would therefore have the additional benefit of authenticating true rooibos products, but this might be complicated by the fact that some wild types of *Aspalathus linearis* have been found to contain little or no aspalathin (Joubert & Schulz, 2006; Van Heerden *et al.*, 2003). HPLC analysis of commercial ready-to-drink rooibos iced teas, claiming to contain hot water extracts of fermented rooibos, demonstrated that some of the products contained neither aspalathin nor its oxidation products, iso-orientin and orientin (Joubert *et al.*, 2009). This suggests that less than the stated amount of rooibos extracts, or extracts of poor quality, had been added to these products. A food product claiming to contain the equivalent of "six cups of rooibos tea" in a single portion has been introduced to the South African market in the past,

but no indication was given of which criteria were used to ensure the purported "six cups" content in the final product (Joubert & De Beer, 2012).

Aspalathin is pH and heat-labile (Joubert *et al.*, 2009; De Beer *et al.*, 2012; De Beer *et al.*, 2015) and its concentration varies significantly between genotypes (Joubert & De Beer, 2011), but orientin and iso-orientin are more resistant to heat processing (Joubert *et al.*, 2009) and varying pH conditions (De Beer *et al.*, 2012) than aspalathin and represent oxidation products of aspalathin (Krafczyk & Glomb, 2008), making these two compounds perhaps a more feasible option in terms of standardisation.

The use of total antioxidant capacity (TAC) and total polyphenol content (TPC) as quality indicators has also been extensively studied, with Joubert *et al.* (2008a) finding a strong correlation between the TPC and TAC of unfermented rooibos, and also between the aspalathin content and the TAC of unfermented rooibos (Joubert *et al.*, 2008a). There are no minimum values specified for TAC and TPC of rooibos despite the association these attributes have with its reported health-promoting reputation, but some manufacturers of rooibos extracts have opted to use TPC and TAC as quality parameters (Joubert & De Beer, 2011).

The Agricultural Product Standards Act (APSA) of South Africa and its various amendments provide regulations pertaining to the packaging and labelling, moisture content and the level of microbial, foreign matter, pest and chemical residue contamination of rooibos (Anon., 2010a). Moisture content of not more than 10% is currently the legal requirement. Rooibos intended for export is monitored by the Perishable Products Export Control Board (PPECB) (Joubert & De Beer, 2011). The required sensory quality attributes of rooibos as stipulated in the APSA is that it should have "the clean, characteristic taste and aroma and clear, distinctive colour of rooibos" (Anon., 2010a). However, no reference standards are provided, making the quality grading a highly subjective process which cannot be validated scientifically.

Rooibos manufacturers often have their own set of sensory evaluation protocols and standards for the purpose of quality grading. One example, as described by Koch *et al.* (2012), employed expert graders who evaluated the colour and clarity of rooibos infusions and the appearance of dry leaves, in addition to the flavour, in order to grade batches according to quality. Sensory quality evaluation relies on subjective criteria, and there is heightened interest in the development of objective quality parameters and quality assurance protocols. Recently, a flavour and mouthfeel wheel was developed intended to facilitate sensory evaluation. It includes negative and positive sensory properties and descriptors, and a preliminary sensory lexicon to assist the evaluator in the assessment. The sensory wheel also serves to improve communication between processors and marketers regarding sensory attributes as it provides a "common language" (Koch *et al.*, 2012).

Typically, dried rooibos plant material is mechanically sieved/refined to remove coarse material (>10 mesh) and dust (<40 mesh) and the percentage of this fraction is taken into account when the price per kg, paid to the producer, is determined. The refined product is then used to determine the quality grade (Koch *et al.*, 2012). Quality considerations may differ depending on the intended use. Some plant material unsuitable for use in teabags could, for instance, be used in loose-leaf tea blends. Kotina *et al.* (2012) published detailed anatomical descriptions of commercial fermented rooibos plant material in order to evaluate the pharmacognostic value of the various anatomical characteristics. The rooibos tea consisted of differing proportions of leaf, stem, wood and bark fragments, ranging in length from about 2 to 5 mm. Although fermented leaf and stem fragments were similar in their appearance, the stem fragments were firmer in texture. The ratio between the various fragments types varied significantly between samples, but the authors suggested that good quality unrefined tea should comprise of roughly equal proportions of leaves and stems, which together should make up at least 60% of the total bulk of the plant material. No more than 40% of the total should be comprised of wood and bark fragments, which are generally present in a 3:1 mass ratio (Kotina *et al.*, 2012).

Reddish-brown oxidation products are localised mainly in the epidermal cells of rooibos leaves and stem fragments. Wood and bark fragments contain mostly colourless phloem and xylem, i.e. little or no oxidation products. Sieving of the unrefined plant material to remove the coarse, woody fragments therefore increases the amount of desirable phenolic compounds to deliver a higher quality product for the herbal tea market. The woody fragments were once discarded, but have more recently been a valuable raw material for the production of extracts (Kotina *et al.*, 2012). Fermented rooibos remains the primary raw material used for the production of commercial spray-dried hot water extracts (Joubert & De Beer, 2012), which are mainly used in functional food and beverage applications. Since the appearance of the plant material is of less importance in extract production, fermented rooibos used for this purpose is often used "as-is", i.e. unrefined and containing waste material which would otherwise be removed for the herbal tea market (Joubert & De Beer, 2012).

Joubert *et al.* (2012) demonstrated that there was significant variation present in the individual contents of certain individual phenolic compounds, soluble solids content and total antioxidant activity of fermented rooibos infusions within quality grades (A, highest; B; C; D, lowest). The plant material was obtained from the same supplier as the one used in a contemporaneous study by Joubert & De Beer (2012), and grading of the plant material was performed using the same protocols and quality parameters (leaf colour, infusion flavour and colour and yield of refined fraction). Infusions were prepared according to a method recommended by the South African Rooibos Council when collecting data on the composition of a typical "one-cup serving" (Joubert *et al.*, 2012). This briefly entailed the following: 2.5 g of the refined, pasteurised plant material was

infused in 200 mL of freshly boiled, distilled water for 5 min with no further agitation, passed through a tea-strainer and finally through Whatman No. 4 filter paper. Higher quality grade samples were associated with higher levels of phenolic compounds, with the aspalathin content of the "Grade A" infusions being twice as high as that of the "Grade D" infusions (Table 2.4). The highest and lowest total polyphenol content values were measured in the "Grade A" and Grade D" infusions, respectively. Large variation in the aspalathin content was also observed between the different quality grades. This suggested that the presence of these phenolic compounds could contribute to the positive attributes of the rooibos infusions and similar quality grading could be carried out on the basis of their content in the plant material. It was concluded that consumers could potentially benefit most from consuming grade A rooibos tea.

The bulk of fermented rooibos produced annually for the herbal tea market is of grade B or C, with the low-quality grade D destined mainly for extract production (Joubert *et al.*, 2012). This implies that the majority of rooibos extract is currently not produced for optimal health-promoting qualities as such, but rather to add the distinctive rooibos flavour and/or colour to established consumer products. Low-quality production batches of fermented rooibos (e.g. Grade D) would not be the ideal raw material for the production of an extract high in aspalathin, but might be acceptable for the production of extracts for such general applications.

Table 2.4 Mean values[1] for total antioxidant activity (TAA) and individual phenolic compound, total polyphenol and soluble solids contents of aqueous infusions of fermented rooibos infusions of different quality grades (adapted from Joubert *et al.*, 2012).

Parameter	**Grade A** (n = 30)[2]	**Grade B** (n = 30)	**Grade C** (n = 29)	**Grade D** (n = 25)
Total polyphenols [3]	332 ± 47 a[4]	298 ± 35 b	282 ± 36 bc	266 ± 52 c
Soluble solids	1258 ± 157 a	1170 ± 137 b	1116 ± 133 b	1146 ± 138 b
TAA_{ORAC} [5]	10908 ± 1808 a	10113 ± 1378 ab	9913 ± 1558 b	9014 ± 1583 c
TAA_{DPPH} [5]	2465 ± 377 a	2234 ± 314 b	2137 ± 337 b	1939 ± 394 c
Aspalathin	7.70 ± 3.33 a	5.84 ± 2.83 b	5.83 ± 3.30 b	3.35 ± 2.24 c
Iso-orientin	15.92 ± 2.35 a	15.55 ± 1.93 a	14.95 ± 2.73 a	13.44 ± 2.37 b
Orientin	11.37 ± 1.38 a	11.15 ± 1.29 a	10.72 ± 1.60 ab	9.95 ± 1.80 b
Nothofagin	1.04 ± 0.38 a	1.02 ± 0.52 a	1.04 ± 0.57 a	0.64 ± 0.48 b
PPAG [6]	7.29 ± 2.09 a	7.39 ± 1.98 a	6.86 ± 2.27 a	5.94 ± 1.40 b

[1] $mg.L^{-1}$ ± standard deviation; [2] number of samples; [3] Gallic acid equivalents; [4] Means in the same row but with different letters are significantly different ($P < 0.05$); [5] TAA determined using DPPH radical scavenging and ORAC assays and expressed as µmol Trolox equivalents; [6] Phenylpyruvic acid-2-*O*-glucoside

Joubert & De Beer (2012) investigated the flavonoid content, TPC and TAA of fermented rooibos extracts produced using plant material from two classes of quality grade (Grade B or C, as per supplier). Grading was carried out by the supplier according to standard protocols using leaf

colour, infusion colour, infusion flavour and the yield of refined fractions as parameters. The parameters tested in this study are not routinely used as quality parameters in rooibos grading, but the results suggested that a combination of TPC, TAC_{ORAC} and the content of a single marker compound could be used as an alternative means of classifying quality grades for rooibos.

It would be necessary to conduct screening analyses of plant material intended for aspalathin-enriched extract production. Manley *et al.* (2006) reported that a minimum level of 4% aspalathin in dried, GR plant material has been specified by a major extract manufacturer in order to produce extracts containing at least 15% aspalathin. Quantification of the flavonoid content in plant material is usually conducted by HPLC analysis due to its high selectivity and accuracy, but typically requires additional sample preparation. In an industrial setting, however, such comprehensive and time-consuming analyses are usually not required, and rapid screening methods for raw plant materials at an early stage of production are therefore of great interest. This would allow for the identification of batches of plant material which meet the minimum quality criteria in terms of the target compound content.

Colourimetry and UV-visible spectroscopy can be used for screening of plant material, but they require an initial solvent extraction step and trained personnel. Near-infrared spectroscopy (NIRS) has been used to develop prediction models for the total antioxidant activity and the total soluble solids, polyphenol, aspalathin, nothofagin and dihydrochalcone contents of dried, unfermented rooibos plant material, as well as for the aspalathin content in aqueous extracts of the same plant material (Manley *et al.*, 2006). The NIRS prediction models could reliably predict the aspalathin and dihydrochalcone contents of GR plant material with coefficients of determination (R^2) of 0.87 and 0.88, respectively. These models were deemed as suitably accurate and robust for use in the industry to rapidly quantify the content of aspalathin and dihydrochalcones at an early stage of production. The prediction models developed for TPC, TAA and flavonoid content in the aqueous extracts showed poor accuracy and were therefore not acceptable for use in industry. This was attributed to the relatively low concentrations of the target compounds in the aqueous extracts (Manley *et al.*, 2006).

Schulz *et al.* (2003) developed a NIRS method to rapidly discriminate between unfermented and fermented rooibos and additionally to predict the aspalathin content of unfermented samples. A large number of samples (n = 119) was used to develop a NIRS calibration model, reference-analysed by HPLC, for the aspalathin content in GR. By applying the newly developed NIRS method, it would be possible to rapidly assess the degree of fermentation and classify individual batches of plant material for quality assurance and screening purposes. Baranska *et al.* (2006) used Fourier Transmission-Raman (FT-Raman) spectroscopy for in-situ identification and quantification of dihydrochalcones in dried GR plant material. Partial least squares regression models for the rapid quantification of aspalathin (R^2 = 0.83), nothofagin (R^2 = 0.78) and dihydrochalcones (R^2 = 0.84) were

developed based on spectral data and HPLC reference values from a large sample set (n = 100) of production batches from different areas and production seasons. The aspalathin and nothofagin contents of the dried plant material ranged between 0.59–10.59 g.100 g^{-1} and 0.067–1.23 g.100 g^{-1}, respectively. The greater the number of data points used and the wider the range of flavonoid content of the samples, the more reliable the calibration model will be (Baranska *et al*., 2006). FT-Raman spectroscopy has also been utilised to identify and quantify various secondary plant metabolites, and notable advantages of this technique are that it is non-destructive and requires minimal training (Gierlinger & Schwanninger, 2007).

Joubert *et al*. (2008b) investigated the potential of UV spectrophotometry and an aluminium chloride ($AlCl_3$) colourimetric methods as alternative to HPLC to quantify the dihydrochalcone content of unfermented rooibos. These methods can be used for quantification of classes of compounds especially if they are present in large amounts relative to others, as is the case with dihydrochalcones in unfermented rooibos. UV-Vis spectrophotometers are also less expensive than NIRS and HPLC equipment, and could be adapted for use with a microplate reader for more efficient use. The dihydrochalcone content of the aqueous GREs, determined with UV spectroscopy, correlated strongly with the sum of the aspalathin and nothofagin contents as quantified by HPLC (r = 0.97). A linear model generated using the correlation data was used to predict the dihydrochalcone content of extracts based on spectrophotometric measurements with reasonable accuracy (R^2 = 0.92). It was also demonstrated that the total polyphenol content (TPC) of aqueous rooibos extracts could be determined accurately (r = 0.99) by UV spectrophotometry with pure aspalathin as a reference standard. UV spectrophotometry requires no additional reaction time or special chemical reagents, making it a potentially advantageous alternative to the Folin-Ciocalteau method for determining TPC. The total antioxidant activity of the unfermented rooibos extract correlated strongly with both its total polyphenol content (r = 0.99) and its aspalathin content (r = 0.96). This was ascribed to aspalathin comprising a major part of the TPC and its potent antioxidant properties.

2.1.4. Medicinal and health-promoting properties

Watt & Breyer-Brandwijk (1932) first documented rooibos as a medicinal plant in a treatise on South African medicinal and poisonous plants, but no clearer details of its alleged uses were provided at the time. Rooibos tea was initially consumed for its anecdotal medicinal attributes only to gradually become firmly entrenched in the public consciousness as a non-medicinal beverage consumed mainly for refreshment (Joubert *et al*., 2008a). It was the discovery by Annetjie Theron in 1968 that a rooibos infusion calmed her colicky infant — and her subsequent media advocacy of the aforementioned and other alleged health benefits — that led to rooibos growing steadily as a

commercial entity and within the public consciousness as a health-promoting beverage. In addition to its established use as herbal tea, rooibos extracts were later developed to produce a range of cosmetic products under the trademark *Annique* (Morton, 1983).

Rooibos continues to be promoted as an indigenous medicinal plant, and anecdotal reports have suggested that rooibos acts as an effective anxiolytic, digestive aid, allergy treatment, appetite stimulant and even as a sleep remedy due to a mild sedative effect (Joubert & De Beer, 2011; Street & Prinsloo, 2013). More recently, the health-promoting aspects of rooibos have been attributed to its phenolic content, and these confirmed benefits include antidiabetic, antioxidant, phyto-oestrogenic, hepatoprotective, anticarcinogenic and anti-inflammatory properties. These and other attributes (including alleged anti-ageing, antimicrobial, immunoprotective and antihemolytic properties) have been thoroughly reviewed (Joubert & Ferreira, 1996; Joubert *et al*., 2008a; Joubert & De Beer, 2011; Muller *et al*., 2016). Research by Marnewick *et al*. (2011) demonstrated that consumption of six cups of traditional rooibos per day could significantly improve the lipid profile as well as redox status, both relevant to heart disease, in adults at risk for developing cardiovascular disease. Extracts delivering the equivalent of six cups of rooibos has subsequently became a "gold standard" in industry as it relates to the quantity perceived as eliciting a measurable beneficial health effect (Joubert & De Beer, 2012).

Flavonoids function as antioxidants in the human body and confer their protective benefits by increasing the levels of endogenous antioxidant defence systems, e.g. catalase, superoxide dismutase and glutathione peroxidase, allowing for the increased elimination of reactive oxygen species (ROS) which induce oxidative stress (Jiang *et al*., 2010; Zhang *et al*., 2014b). The antioxidant activity of rooibos flavonoids was investigated by Snijman *et al*. (2009), with Trolox and epigallocatechin gallate (EGCG) as reference standards, using the $ABTS^{\cdot+}$ radical cation, metal chelating and Fe(II)-induced microsomal lipid peroxidation assays. Aspalathin and EGCG, the major antioxidant flavonoid in green Oriental tea, showed similar results and were the most potent radical scavengers (IC_{50} = 3.33 and 3.46 µM, respectively).

Diabetes mellitus — specifically the lifestyle-related type 2 diabetes mellitus (T2D) — has been identified as contributing significantly to the burden of disease and mortality in developing countries, with the prevalence likely to increase in the approaching decades (Mathers & Loncar, 2006). This can partially be attributed to the increased consumption of highly processed foods, rich in saturated fats and refined carbohydrates, coupled with a less active, sedentary lifestyle. According to information published by the International Diabetes Federation (Guariguata *et al*., 2014), it has been estimated that 592 million people globally will suffer from diabetes by 2035, and that the most marked increase will be seen in developing nations. The same study predicted a prevalence of 9.9% for diabetes amongst the South African population by 2035. This would represent a proportional increase in diabetic sufferers of more than twice the projected population increase for the same

period (Guariguata *et al.*, 2014). With treatment of T2D inextricably linked to the individual's dietary habits (Tuomilehto *et al.*, 2001), the use of specialised nutraceuticals as a treatment adjunct to oral therapy and lifestyle management could be a worthwhile avenue of research.

Phloridzin and its aglycone form, phloretin, are the predominant dihydrochalcones present in apples (*Malus* sp.) and have been hypothesised to play a role in UV-protection and pathogen resistance (Gosch *et al.*, 2010). Phloridzin has been shown to exhibit hypoglycaemic effects in animal models (Ehrenkranz *et al.*, 2005). De Bernonville *et al.* (2010) reported that sieboldin, a dihydrochalcone obtained from *Malus domestica* leaves, demonstrated the ability to prevent oxidative-dependent formation of advanced glycosylation end-products (AGEs), which have been linked to many complications associated with diabetes. This points towards its and other dihydrochalcone-*C*-glycosides' potential use in an antidiabetic dietary supplement or nutraceutical.

The potential of rooibos extracts and individual rooibos flavonoids as a treatment adjunct for metabolic disease has been investigated by a number of studies in recent years. They have demonstrated that aspalathin enhances glucose uptake *in vitro* and *in vivo* (Kawano *et al.*, 2009; Muller *et al.*, 2012; Son *et al.*, 2013, Schloms *et al.*, 2014), inhibits adipogenesis (Sanderson *et al.*, 2014), ameliorates insulin resistance (Mazibuko *et al.*, 2013; Mazibuko *et al.*, 2015), modulates oxidative stress (Uličná *et al.*, 2006; Kondo *et al.*, 2013; Hong *et al.*, 2014) and high glucose-induced inflammation (Ku *et al.*, 2015). It has also been reported that aqueous extracts of fermented rooibos showed a protective effective on cultured cardiomyocytes, derived from diabetic Adult Wistar rats, against experimentally-induced oxidative stress and ischaemia (Dludla *et al.*, 2014), and significantly reduced serum cholesterol, triglycerides and free fatty acid concentrations in hyperlipidaemic mice (Beltrán-Debón *et al.*, 2011).

Exposure to chronic hyperglycaemia results in the production of ROS which may play a role in the pathogenesis of diabetic cardiomyopathy (Flores-Mateo *et al.*, 2009; Khullar *et al.*, 2010; Ansley & Wang, 2013). The impaired equilibrium between the generation and elimination of ROS in the diabetic individual often results in structural remodelling of the myocardium and subsequent left ventricular dysfunction, one of the hallmarks of diabetic heart disease (Ansley & Wang, 2013). Aspalathin was shown to increase glucose oxidation and modulate fatty acid utilisation, resulting in a favourable substrate shift, in H9c2 cardiomyocytes exposed to high glucose-induced oxidative stress (Johnson *et al.*, 2016). Aspalathin was also shown to be as effective as metformin, a well-known oral antidiabetic agent, in inhibiting glucose-induced fatty acid oxidation and the resultant oxidative stress. As an additional point of interest, a synergistic effect between aspalathin and metformin was also noted (Johnson *et al.*, 2016).

2.1.5. Rooibos extracts for food and nutraceutical applications

Research studies undertaken during the 1980s and early 1990s showed that rooibos could be further processed for value-addition by preparing liquid extracts and powders (Joubert, 1984; 1988a; 1990a). However, it was only at the turn of the century that the commercial value of these forms of rooibos was realised. The majority of rooibos extract produced annually is prepared from fermented rooibos and is used mainly as an ingredient of functional foods and beverages, but the type of rooibos extract (in terms of raw materials used) can be tailored to suit many different applications (Joubert & De Beer, 2011). Adding rooibos extract to food products provides not only the distinctive rooibos flavour characteristics, but the polyphenol content of rooibos may potentially confer health benefits.

Joubert & De Beer (2012) investigated the phenolic composition and total antioxidant activity of simulated industrial aqueous rooibos extracts, adjusted to correspond with the equivalent of six cups of rooibos standard infusion in terms of soluble solids content. They reported that the simulated industrial extracts would deliver the same total polyphenol, aspalathin and nothofagin contents ($P < 0.05$), but lower flavone content than six cups of freshly steeped rooibos infusion ($P < 0.05$). They noted that food products containing the equivalent of six cups of rooibos infusion would require at least 1.3 g of aqueous rooibos extract based on these results, and this might adversely affect the flavour and colour of the product.

Extract of fermented rooibos has been shown to be effective in stabilising açai fruit anthocyanins, indicating potential new applications (Pacheco-Palencia & Talcott, 2010). Huang *et al.* (2008) reported that the rate of transport of aspalathin across intestinal epithelial (CaCo2) cells is concentration-dependent and significantly enhanced when aspalathin is present in the form of a rooibos extract rather than in pure form. The presence of other phytoconstituents in the extract could explain this increased transfer rate, highlighting the potential benefit of consuming rooibos extract in a concentrated, encapsulated form for the maximal absorption of its bioactive compounds from the gastrointestinal tract.

The polymerisation of phenolic compounds during rooibos fermentation reduces their solubility, and it has been confirmed that the total polyphenol content of unfermented rooibos plant material is significantly higher (Joubert, 1984). The use of unfermented rooibos could thus allow for the production of an extract with higher phenolic content and an associated higher antioxidant activity. According to regulations under the South African Foodstuffs, Cosmetics and Disinfectants Act (No. 54 of 1972), information or declarations implying that a foodstuff or one of its constituents has health-giving properties are strictly prohibited either on labelling or advertising material (Anon, 2010b). No studies on specific products containing rooibos extract have been conducted to date.

2.2. Quality-by-design (QbD) methodology

2.2.1. General overview of QbD

The concept of quality-by-design (QbD) refers to an approach in which the desired quality attributes of a product is effectively designed into the manufacturing process rather than relying on extensive post-production quality testing, and was first proposed by Joseph M. Juran in a widely cited treatise on quality management (Juran, 1992). This approach has been approved for and increasingly been applied in the biopharmaceutical industry in recent years (ICH, 2009; Rathore & Winkle, 2009). In QbD, the critical material attributes (CMAs) and critical process parameters (CPPs) which impact on the critical quality attributes (CQAs) of the final product are identified, and the ultimate goal is to describe a "design space", i.e. the range of CQAs which would be acceptable for that particular unit operation (Huang *et al.*, 2009; Lebrun *et al.*, 2012; Das *et al.*, 2014; Gong *et al.*, 2014a; Gong *et al.*, 2014b; Yan *et al.*, 2014).

Despite the widespread use of herbal drug preparations, there have been relatively few reports of QbD being applied in their manufacturing process. This could be attributed to two chief differences between herbal and chemical drugs. In the first instance, the quality variation seen in herbal raw materials are decidedly greater than that seen in chemical drugs (Rathore & Winkle, 2009; Khan & Smillie, 2012). Plant material harvested at different times or grown in different regions may vary significantly in terms of their chemical composition, and in some cases may even have suboptimal concentrations of the desired compounds. This is a common cause of erratic batch-to-batch quality, and a strategy which aims to control the impact of these natural variations would be a first step towards attaining a more reliable level of quality (Shinde *et al.*, 2009). Secondly, herbal drugs typically contain one or more active pharmaceutical ingredients (APIs), which are often prone to undergo undesirable chemical changes during the production process. This can make it difficult to establish an acceptable range of CQAs (Roy, 2012).

Yan *et al.* (2014) proposed a feedforward control strategy for the manufacturing of herbal drugs. It entailed establishing the relationship between CMAs/CPPs and CQAs, and then generating an optimisation model for the adjustment of process parameters. The most desirable processing parameters can then be determined from this model, with the intent to reduce the variation in CQAs. Fig. 2.7 depicts a schematic diagram of a hypothetical manufacturing process wherein process 1 produces intermediate 1, which in turn is used as an input material for process 2, which then produces intermediate 2 and so forth, until the final product is ultimately obtained. Intermediate 1 will have a set of attributes which will serve as the critical quality attributes (CQAs) for process 1, while simultaneously being the critical material attributes (CMAs) of process 2. The CMA and CQA ranges frequently overlap completely. Thus, if process 2 uses specific process parameters based on the CMAs of intermediate 1, and it produces an acceptable intermediate 2,

then these CMAs of intermediate 1 (which are the CQAs of process 1 are acceptable (Yan *et al.*, 2014).

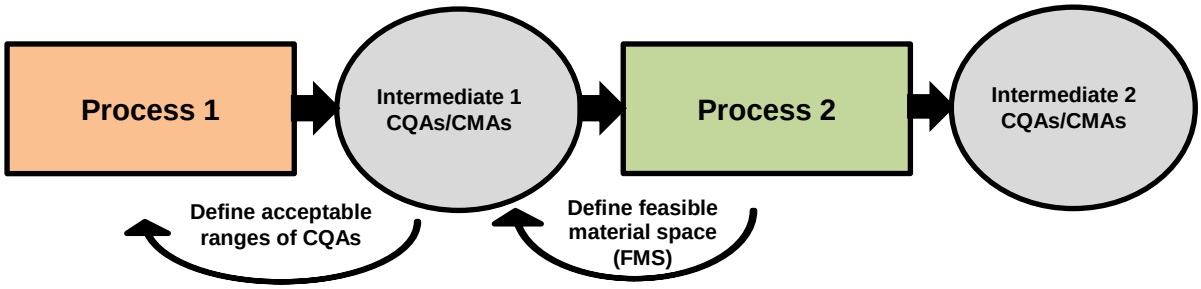

Figure 2.7 Schematic diagram of method described to define acceptable critical quality attributes (adapted from Yan *et al.,* 2014).

These ranges of CMAs can then be defined as the feasible material space (FMS). The feasible material space of process 2 can thus be used to define the CQAs of process 1. Furthermore, the feasible material space of the final process must be based on the desired quality profile of the target product, and only then can the range of CQAs for the penultimate process be established. When applying QbD to the production process of herbal drugs, every step should ideally be designed in this manner (Gong *et al.*, 2014a; Gong *et al.*, 2014b; Yan *et al.*, 2014).

The feedforward control strategy for QbD implementation as described by Yan *et al.* (2014) is shown in Fig. 2.8. The first step entails modelling the effects of the input CMAs and CPPs on the CQAs simultaneously. The optimisation model for determining the best process parameters is then established, followed by defining of the FMS. A more basic approach to defining these material specifications is based on only the quality of those input materials which have historically been associated with products of acceptable quality – but this approach fails to take into account the effect of adjusting process parameters. This makes the acceptable ranges of input material attributes obtained very small, and this could lead to misclassification of acceptable material as unacceptable simply due to the restricted range (Nagar *et al.*, 2010; Roy, 2012).

QbD provides a number of tools for the assessment of the possible inputs to a process in order to establish which of them would have the most significant effect on the output. The Ishikawa (fishbone) diagram is a useful means of identifying and grouping the potential factors expected to cause a variation with the system (Nagar *et al.*, 2010). Fig. 2.9 depicts an Ishikawa diagram as presented in a study by Gong *et al.* (2014b) in which the extraction of saponins from *Panax notoginseng* was optimised using a design space approach. The major categories of process inputs were identified, viz. solvent, material, environmental, equipment and extraction-related factors. These categories were populated by specific factors known to affect extraction performance, based on prior experience and a review of existing data. To narrow down the significant inputs for further investigation, a failure mode and effect analysis (FMEA) was conducted, in which each parameter is

assigned a severity score (S) on a scale of 1 to 4 based on its impact on the process. Each parameter was also assigned a numerical score based on occurrence probability of failure (O) and on the likelihood of the operator to detect process failure (D). These scores were all based on existing literature and prior experience. The mathematical product of the three individual scores was reported as the risk priority number (RPN) for each individual parameter, and those with the highest RPN were identified as the critical process parameters to be investigated in subsequent experiment.

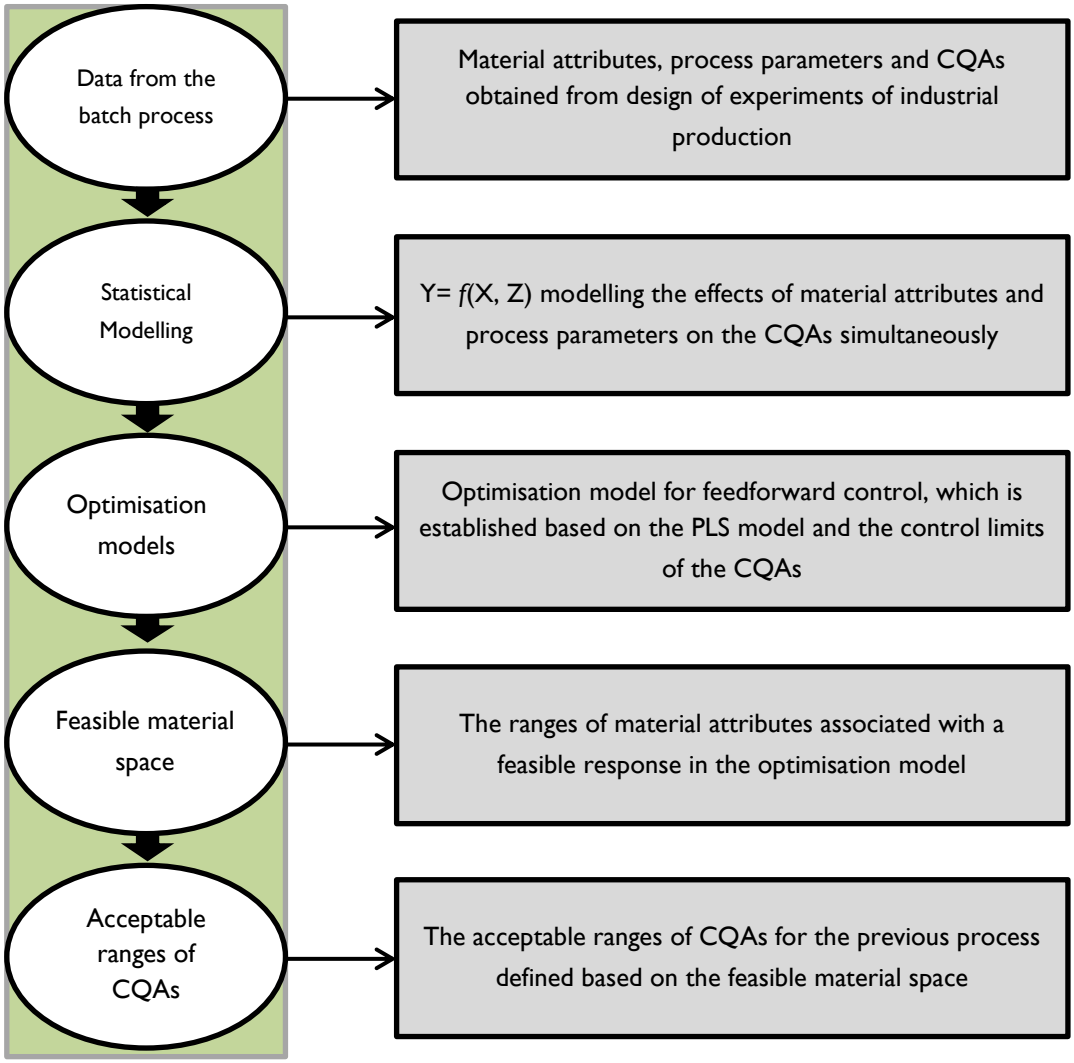

Figure 2.8 Implementation steps of the feedforward control strategy and the method for defining the acceptable ranges of critical quality attributes (adapted from Yan *et al.*, 2014).

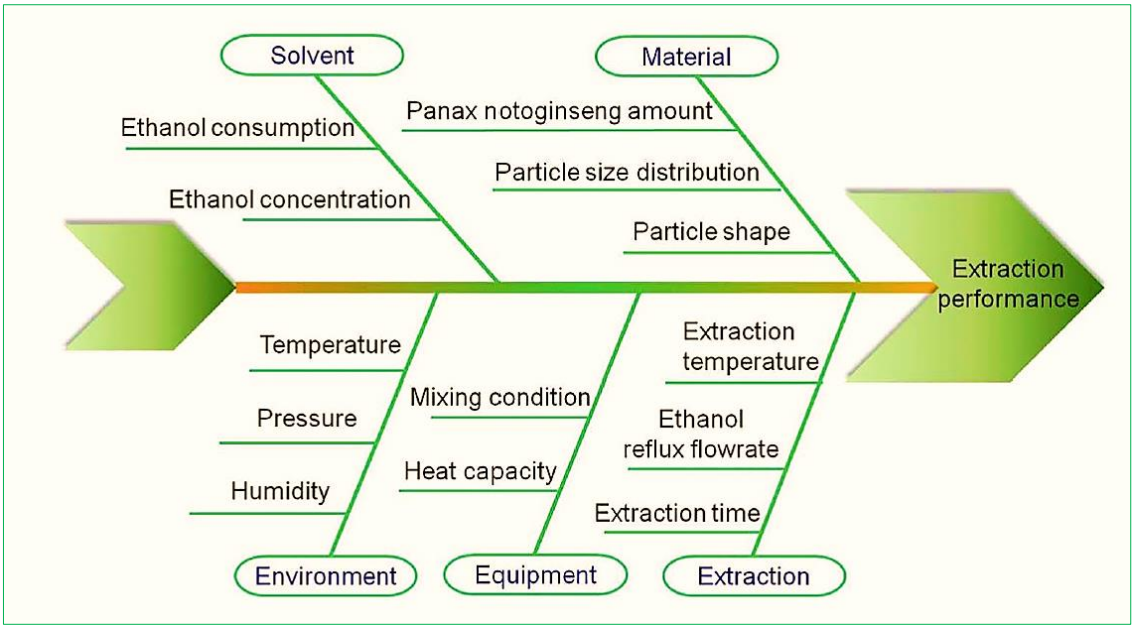

Figure 2.9 Ishikawa diagram showing inputs of extraction process with potential to cause variation (Gong *et al*., 2014b).

2.2.2. Principles of response surface methodology (RSM)

QbD represents a systematic approach to quality assurance in which a variety of statistical tools may be utilised to describe experimental processes and their inputs/outputs. One such statistical tool is response surface methodology (RSM), which refers to the use of mathematical modelling to obtain *response surfaces* based on experimental data from which reliable conclusions about the experimental process can be drawn (Bezerra *et al*., 2008). The *response* refers to the measured quantity or attribute which is being optimised (e.g. the yield of soluble solids from an extraction process), and this response is the result of the interaction of independent experimental factors. The *response surface* (usually a plot in two or three dimensions) refers to the relationship of a response to values of one or multiple factors, while *model* refers to a polynomial equation which describes the relationship between factors and a response. Responses can thus be predicted based on known input factors (Steinberg & Bursztyn, 2010). The most important factors expected to affect the response should be identified in an initial screening phase followed by an optimisation phase. Screening designs which can be used include full factorial, fractional factorial, Plackett-Burman and Taguchi designs (Dejaegher & Vander Heyden, 2011; Das *et al*., 2014; Gong *et al*., 2014a).

The most notable advantage of RSM is that it uses a small number of experiments to generate a large amount of data whilst minimising reagent-, energy- and raw material usage. It also investigates the interaction effects between factors on the process outcomes (Bezerra *et al*., 2008). One of the main disadvantages of RSM is that the second-order polynomial model cannot always be

used to fit all the data obtained from various systems. Making adjustments to the ranges of individual parameters or transforming the data to a different form (e.g. logarithmic scale) could be a potential solution to this problem (Das *et al.*, 2014).

2.2.3. Optimisation by design of experiment (DOE) approach

It is necessary to first identify those factors which will have a significant effect on the responses before an optimisation study can be embarked upon. This is accomplished by conducting preliminary trials which usually highlight two or three parameters to be optimised. More than three factors require large numbers of experiments and could complicate the interpretation of the response surface (Huang *et al.*, 2009; Hibbert, 2012).

The concept of *design of experiments* (DOE) is another element of QbD, and it entails the systematic planning of experiments so that any obtained data can be used to draw reliable conclusions (Granato & De Araújo Calado, 2014). By intentionally altering the process input factors, the effect on process output variables can be observed, and when multiple input variables are changed simultaneously, polynomial functions are generated to describe the relationship of the input factors to the response. The *level* of the factor indicates the value ascribed to that factor and the number of factor levels is typically used to name the design type, e.g. two or three-level design (Leardi, 2009). The setting of different factor levels, e.g. different operating temperatures or particles sizes for extraction, should be considered with care as it could complicate the optimisation process if extremes of experimental ranges, or levels which are too close in value, are used (Das *et al.*, 2014). Examples of experimental designs used in a DOE approach include central composite, Box-Behnken and Doehlert designs (Ferreira *et al.*, 2007; Bezerra *et al.*, 2008; Hibbert, 2012; Maran *et al.*, 2015). Optimisation of a process aims to increase the yield and performance of a system whilst minimising the various costs involved (Huang *et al.*, 2009). An approach in which optimisation of only one process variable is undertaken is known as a "one-factor-at-a-time" (OFAT) technique, but this is not always a feasible approach when more than one variable requires optimisation, as the amount of experimental work required could become excessive and impractical. Furthermore, OFAT does not account for the possible interaction between factors (Lundstedt *et al.*, 1998; Bezerra *et al.*, 2008).

2.2.4. Modelling and interpretation of data

Once an experimental design has been completed, a model equation is established and regression coefficients are predicted (Bezerra *et al.*, 2008). In RSM, a second-order polynomial model is typically used to fit the data:

$$\hat{Y} = \beta_0 + \Sigma_{j=1}^{k}\beta_j X_J + \Sigma_{j=1}^{k}\beta_{jj}X_j^2 + \Sigma\Sigma_{i<j}\beta_{ij}X_iX_j + \varepsilon$$

where β_0, β_j, β_{jj}, and β_{ij} represent regression coefficients for intercept, linear, quadratic and interaction terms, respectively. The response value (dependent variable) is represented by $\hat{Y}$, and X_i and X_j represent the level of the independent variables (factors). The term k represents the number of factors under investigation, while ε represents the residual error associated with the experiment. Analysis of variance (ANOVA) is then performed to determine how well the proposed model will fit the data, and to estimate how the process parameters and their interactions affect the measured responses. The experimental procedure is repeated to validate the generated model and to compare results with predicted values (Baş & Boyaci, 2007; Bezerra *et al.*, 2008; Dejaegher & Vander Heyden, 2011).

Response surface plots graphically depict the responses observed due to the combined effect of multiple variables. If three or more variables are present, the plot visualisation is only possible if one or more variables are kept at a constant value. Steep slopes (i.e. rounded peaks) on the response surface are indicative of a significant effect of factors on the response, whereas a flat surface represents no significant effect. The critical/stationary point of a response refers to the optimum value in a range of tested parameters, and it can be determined with the aid of the second-order polynomial equation. It is not always possible to identify a single optimum value in RSM, in which case an optimum region of values may be indicated on the response surface instead (Bezerra *et al.*, 2008; Granato & De Araújo Calado, 2014).

Figs. 2.10a and 2.10b depict response surfaces where the maximum response is located within the experimental design space. Fig. 2.10b differs in that a plateau is present in relation to variable X_2, which indicates that adjustment of its levels does not affect the level of the response (y). The response surface in Fig. 2.10c depicts a situation in which the maximum response does not lie entirely within the experimental region. The experimental design would have to be displaced to attain a maximal response, i.e. extended ranges of the independent variable would have to be incorporated in the experimental design. Fig. 2.10d shows a minimum point located within the experimental domain, and Fig. 2.10e depicts a *saddle point*, which represents an inflexion point between a relative maximum and a relative minimum. Saddle point coordinates do not serve as valid optimal values when the intent is to obtain a minimum or maximum response in a system (Bezerra *et al.*, 2008).

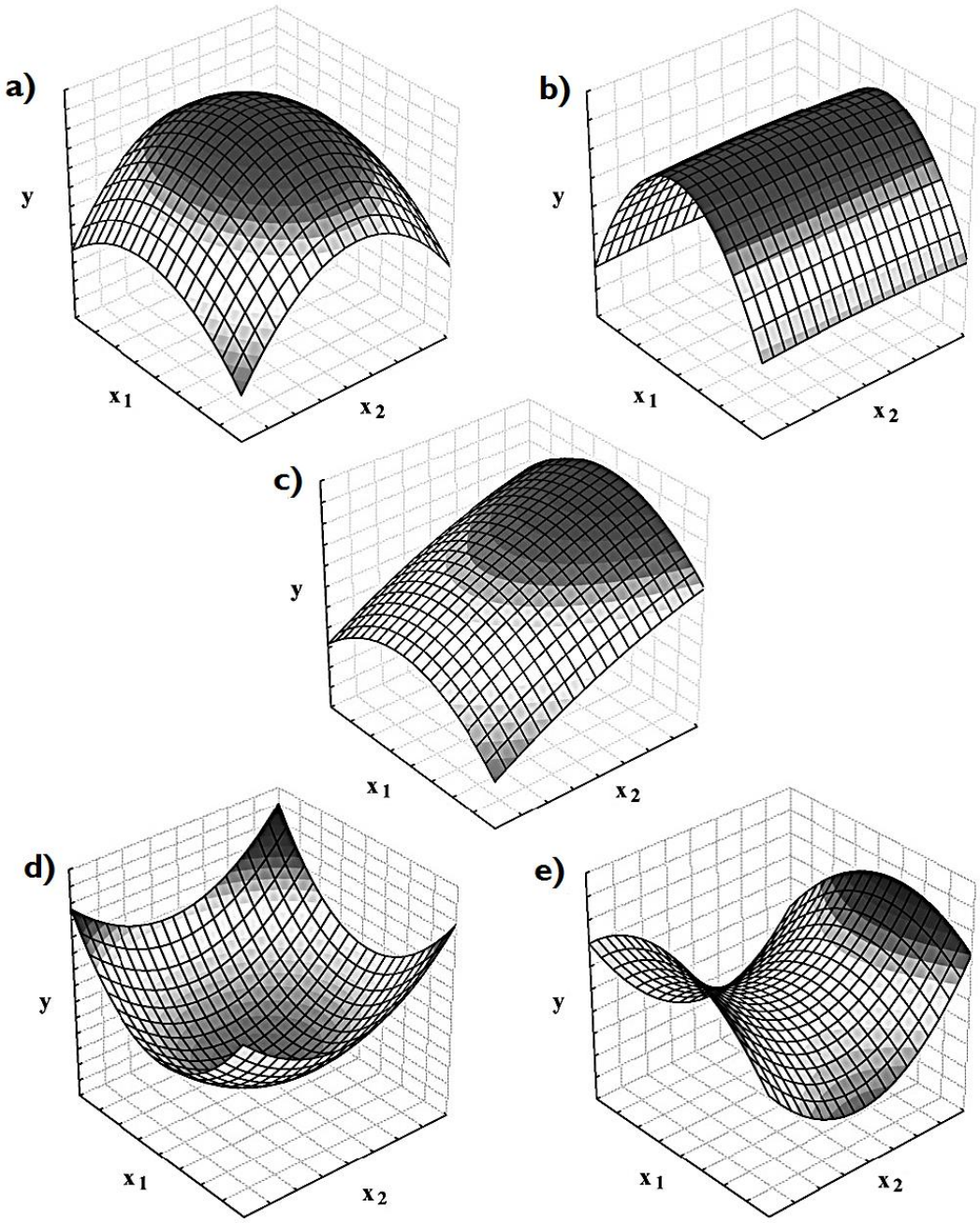

Figure 2.10 Examples of hypothetical response surface plots obtained in the optimisation of two variables, x_1 and x_2, depicting (a) maximum, (b) plateau, (c) maximum outside the experimental region, (d) minimum, and (e) saddle surfaces (Bezerra *et al.*, 2008).

Zou *et al.* (2013) successfully applied RSM to optimise the extraction of astaxanthin from *Haematocoocus pluvialis*. Amongst others, the combined effect of the solvent composition (axis A: Ratio of ethanol to ethyl acetate) and extraction temperature (axis B) on the astaxanthin yield (vertical/y-axis) was visualised on a three-dimensional response surface plot which showed that a maximum response was attained within the experimental domain (Fig. 2.11).

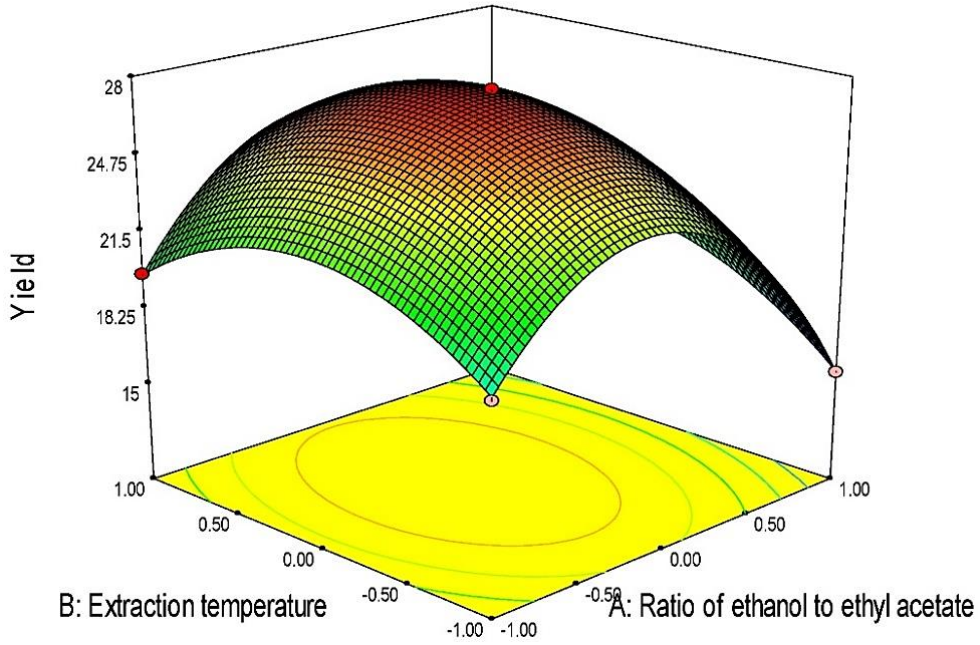

Figure 2.11 Response surface plot showing the effect of two process variables on the yield of astaxanthin from ultrasound-assisted extraction of *Haematococcus pluvialis* (Zou *et al.*, 2013).

Response surfaces may also be depicted as two-dimensional *contour plots*, on which plotlines in close proximity (i.e. darker areas) indicate that slight changes to the input factors are associated with significant changes in the response value. Elliptical contour plots represent significant interactions, while circular plots represent non-significant interactions (Steinberg & Bursztyn, 2010). Wen *et al.* (2015) optimised microwave-assisted extraction of anthocyanin from blackberry, using two-dimensional contour plots to illustrate the effect of four process variables on the extraction efficiency. Fig. 2.12 shows the effect of microwave power (X_1) and microwave time (X_4) on the anthocyanin yield at a fixed solvent concentration and liquid-solid ratio. The elliptical shape of the contour plot indicates a significant quadratic effect, and the maximal response was located within the experimental design space where the microwave power was ca. 430 W and the microwave time was ca. 2.8 min.

Response surfaces are typically also presented as three-dimensional (3D) surface plots combined with their corresponding two-dimensional (2D) contour plots (Fig. 2.13). Li *et al.* (2012) optimised the extraction of mycelial polysaccharide from *Fusarium oxysporum* and used combined plots to show the effect of process variables X_1 (extraction time) and X_2 (extraction time) on the extraction yield. The elliptical shape of the contour plot indicates that there was a significant interaction between these two variables, and the optimal ranges were identified as 1.40–2.39 h (extraction time) and 89.92–99.35 °C (extraction temperature).

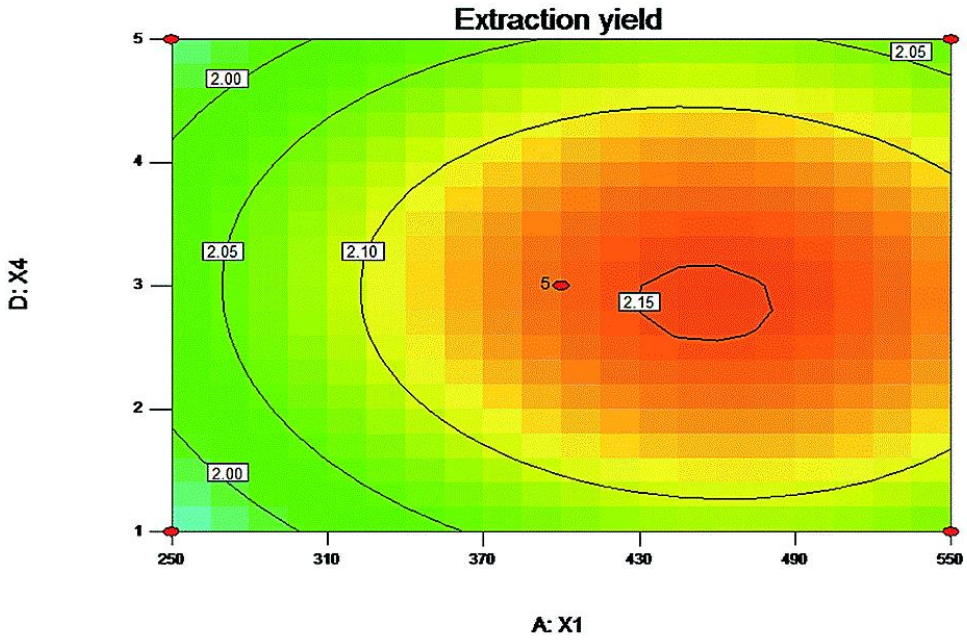

Figure 2.12 Elliptical contour plot showing combined effect of microwave power (X_1) and microwave time (X_4) on extraction yield (Wen *et al.*, 2015).

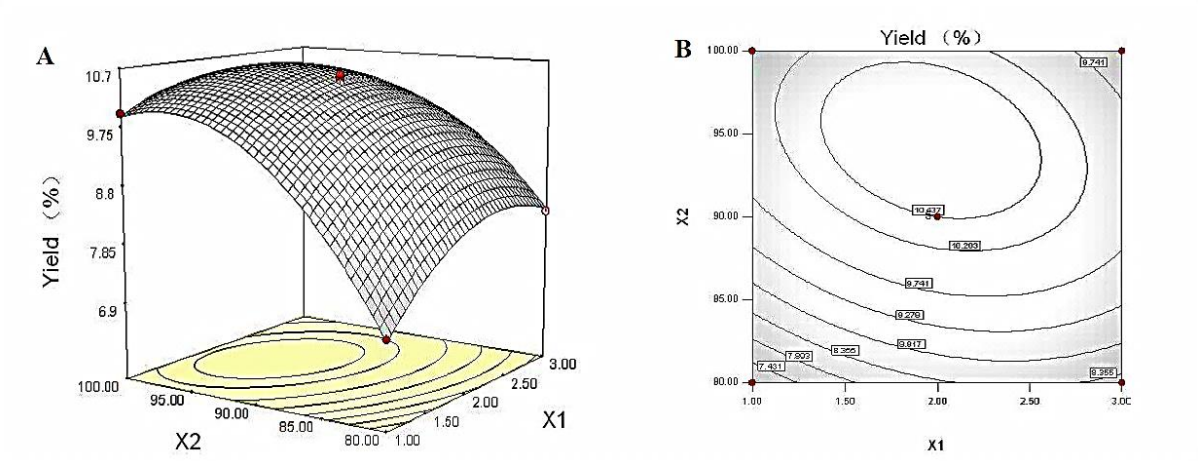

Figure 2.13 Combined response surface plot (a) and corresponding contour plot (b) showing effects of two variables (X_1 = extraction time; X_2 = extraction temperature) on extraction yield (Li *et al.*, 2012).

Fig. 2.11, discussed previously, is also an example of a combined plot, comprising a 3D fitted surface with an underlying contour plot. In this instance, the levels of the two independent variables were presented in coded form, with -1, 0 and +1 representing the minimum, centre point and maximum values of the variables, respectively.

The significance of linear, quadratic and interaction effects can also be graphically demonstrated using standardised Pareto charts. Horizontal bars represent various factors and their interactions, and those bars which intersect the vertical line represent significant effects at a 5% level of significance (P = 0.05). The length of a horizontal bar is proportional to the magnitude of its estimated effect, while a negative value bar length indicates a negative effect on the measured

response (Das *et al.*, 2014). Khan *et al.* (2010) investigated the effects of sonication power (P), extraction temperature (T) and ethanol: water ratio (E) on the efficiency of an ultrasound-assisted extraction process for orange (*Citrus sinensis)*, and presented their ANOVA data in a standardised Pareto chart (Fig. 2.14).

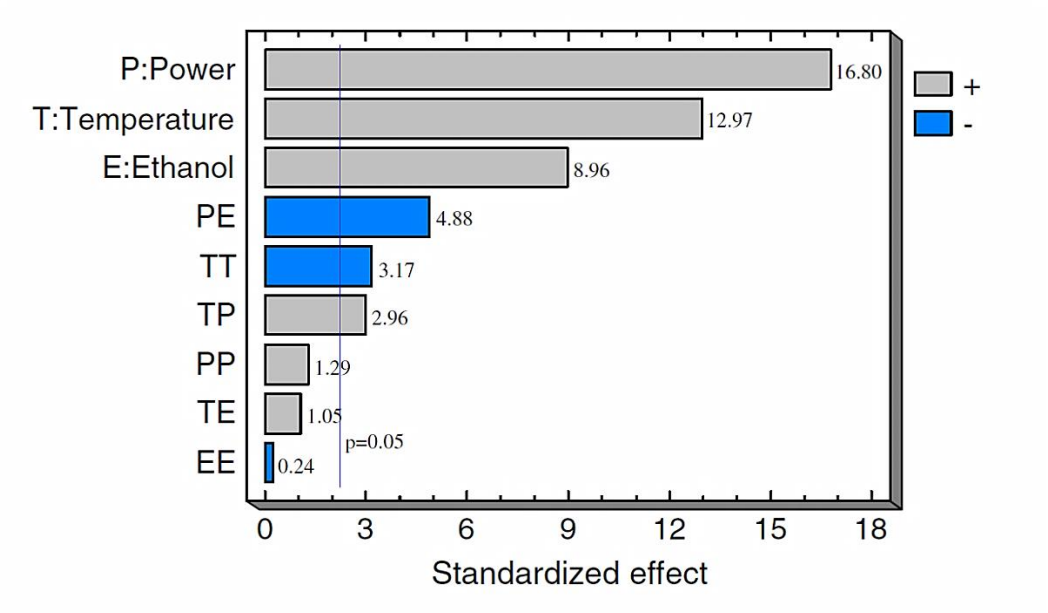

Figure 2.14 Standardised Pareto chart for total phenolic content at 30 min extraction (Khan *et al.*, 2010).

The magnitude and significance ($P < 0.05$) of the linear, quadratic and interaction effects of the three tested factors on the total phenolic content (TPC) of the extract, at a fixed extraction time of 30 min, was graphically depicted on the Pareto chart. Six out of the nine horizontal bars representing these terms crossed the vertical blue line which denotes the 5% significance level. The linear effects of P, T and E had the most significant positive effect on the response, as reflected in the relative size of their bars and the standardised effect values (8.96–16.80). The interaction of sonication power and ethanol: water ratio (PE) and the quadratic term of extraction temperature (TT) both had significant negative effects on the TPC, and the interaction of extraction temperature and sonication power (TP) had a significant positive effect on the response, but these effects were considerably smaller than those of the three linear terms. The three terms represented by the remaining three bars on the Pareto chart did not have significant effects on the response.

If several responses have to be optimised simultaneously, then multi-criteria methodology, like desirability profiling, can be used. This method determines the levels of factors that result in maximum overall desirability for the process in terms of output (Bezerra *et al.*, 2008). Since factors can have opposite effects on the measured responses, an optimal compromise has to be made. The desirability function for each response is determined by assigning a dimensionless score to the predicted values, ranging from 0 (very undesirable) to 1 (very desirable). This allows for the calculation of an overall desirability function by applying the geometric mean, after which an

algorithm is applied to the desirability function to obtain the set of variable values which maximises it (Ferreira *et al*., 2007; Bezerra *et al*., 2008).

Bosman (2014) applied multi-response desirability profiling in the simultaneous maximisation of extract and mangiferin yield in an ethanolic extraction process for honeybush (*Cyclopia genistoides*). Compound prediction profiles were generated which show the effect of the two independent variables under investigation (extraction temperature and ethanol concentration) on the desirability of predicted extract and mangiferin yield (Fig. 2.15). Blue horizontal lines on the prediction profiles indicate 95% confidence intervals which aid in the assessment of prediction reliability. Vertical red lines intersecting the *x*-axes and apices of the desirability curves (green) indicate the levels of the independent variables which would result in the most desirable (i.e. maximum) extract and mangiferin yields. In this case, the optimal levels were an extraction temperature of 70 °C and an ethanol concentration of 40%.

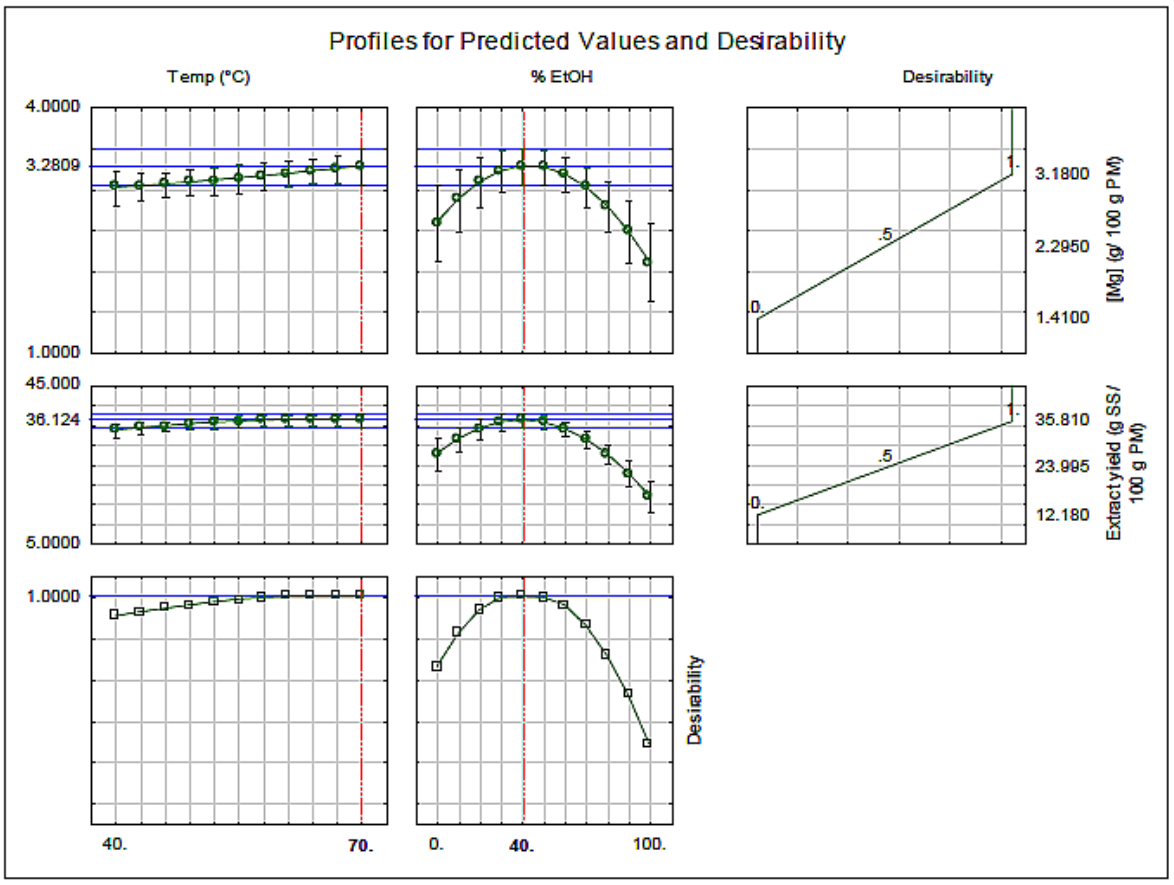

Figure 2.15 Multi-response desirability profiles for maximum extract and mangiferin yield in ethanolic extraction process for *Cyclopia genistoides* (Bosman, 2014).

2.3. Botanical extracts

Plant materials have long been a valuable source of bioactive chemical compounds, obtained by an extraction process and commercialised as functional food ingredients or nutraceuticals. Grape seed (Hernández-Jiménez *et al.*, 2012), ginseng (Corbit *et al.*, 2005) and St. John's Wort (Cossuta *et al.*, 2012) are just a few established examples, but the investigation of new, sustainable raw materials and more efficient extraction methods is of paramount importance. The choice of extraction technique will have a significant impact on the yield, purity and extraction rate, but the chosen method should be appropriate for the end use of the product whilst also taking into account economical, logistic, practical and environmental considerations. The use of organic solvent based techniques is usually associated with greater yields (Shi *et al.*, 2005; Pasrija & Anandharamakrishnan, 2015), but may make the extracted product unsuitable for human consumption, necessitating further purification steps. Methods requiring elevated temperatures for prolonged periods may cause degradation of target compounds, but the application of auxiliary methods like sonication may present solutions to these problems. Compounds other than the target compound may sometimes enhance the antioxidant potential of extracts. Examples of such compounds, referred to as *synergists*, are the polyvalent organic acids, amino acids, chelating agents and phospholipids (lecithin) (Takeuchi *et al.*, 2009).

The commonly used extraction techniques for plant bioactive compounds, and the factors which affect their efficiency, are discussed in the following section along with some recent innovations in the use of *green* extraction techniques, i.e. those which aim to consume less energy and chemical solvents (Pasrija & Anandharamakrishnan, 2015).

2.3.1. Traditional solvent-based extraction techniques

The process of solvent-based extraction involves the use of a liquid to selectively dissolve and remove the soluble fraction (solute) from a permeable, insoluble solid matrix, with probably one of the best known examples of solid-liquid extraction applied in the food industry being the production of fixed oils (vegetable oils) from oleaginous plants (Takeuchi *et al.*, 2009). Traditional methods of solvent-based extraction like maceration with alcohol, Soxhlet extraction and distillation rely on the extracting capacity of various solvents and the application of heat and/or mixing. Some solvent extraction methods have specific terminology: *decoction* refers to extraction with the solvent at its boiling point, *lixiviation* is used when the target compounds are alkalis, and *elution* is used when the soluble solids are at the surface of the plant matrix (Takeuchi *et al.*, 2009).

The use of these traditional extraction techniques is sometimes associated with some disadvantages like the use of harsh chemicals, overheating of the plant material sample and inactivation of important compounds, high energy, time and solvent consumption, and poor

extraction selectivity. Furthermore, the choice of chemical solvent and process parameters can affect the efficiency of the extraction technique to a great degree (Azmir *et al.*, 2013). Due to the differences in the polarities of the various chemical solvents available, it is expected that the solubility and extraction efficiency of individual compounds would vary with the use of different solvents or combinations of solvents (Liu *et al.*, 2016). Ethanol, methanol and water are polar protic solvents with dielectric constants of 24, 33 and 80, respectively, whereas ethyl acetate and acetone are non-polar and polar aprotic solvents of dielectric constants 6 and 21, respectively (Wang *et al.*, 2011). The relative extraction efficiencies of these solvents for the recovery of phenolics from pomegranate peel are shown in Fig. 2.16. The higher the dielectric constant of the solvent, i.e. the more polar the solvent, the higher were the yields of total phenolics, proanthocyanidins and flavonoids.

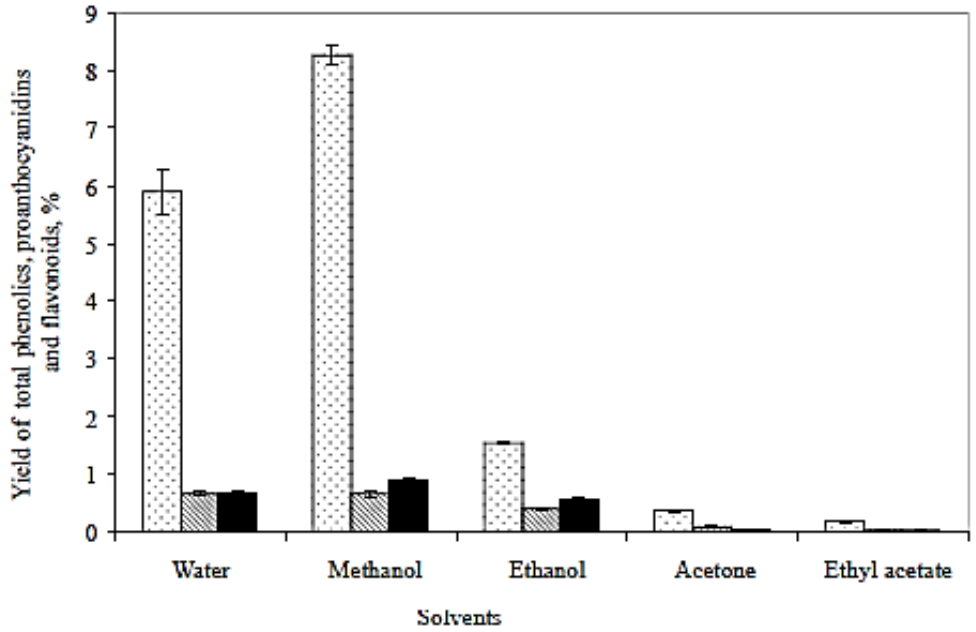

Figure 2.16 The effect of various solvents on the yield of phenolic compounds from ground pomegranate (*Punica granatum* L.) peels extracted at 40 °C, solvent-to-solid ratio of 15:1 ($v.m^{-1}$) and 40 mesh particle size; ⚀ total phenolics ▨ proanthocyanidins ■ flavonoids. (Wang *et al*, 2011).

The rate of extraction of plant constituents is, to a large extent, affected by the mass transfer rate and the equilibrium state, but the Soxhlet method improves the mass transfer rate and displaces the transfer equilibrium by continuously exposing the solid matrix to an influx of fresh solvent (Wang & Weller, 2006).

Hot water extraction (HWE) refers to the sole use of H_2O as solvent, and is thus less effective at extracting non-polar compounds. For non-polar target compounds, co-solvents like ethanol or a chemical modifier are often added to increase the extraction capacity (Azmir *et al.*, 2013). The polar nature of water enables its use as a solvent for natural water-soluble products like organic acids, sugars, proteins as well as inorganic materials (Chemat *et al.*, 2012).

Another specialised type of solvent-based extraction technique, in which carbon dioxide (CO_2) is commonly used, is supercritical fluid extraction (SFE), in which organic solvents are used at temperatures and pressures above their critical points, and pressurised gas is used to collect the extract. Carbon dioxide (CO_2) is a commonly used solvent for the extraction of non-polar molecules due to its food-grade status, widespread availability, relatively low cost and low critical pressure (7.4 MPa) and critical temperature (31.1 °C) (Azmir *et al.*, 2013; Maran *et al.*, 2015). One of the notable disadvantages of CO_2 as a solvent is its low polarity, which limits its usefulness mainly to the extraction of lipids, fats and non-polar substances. The addition of chemical modifiers, e.g. dichloromethane or diethylamine, to enhance the polarity of CO_2 has been successfully applied as a solution to this problem (Lang & Wai, 2001; Azmir *et al.*, 2013).

The phenolic compounds present in plant material may range from simple to highly polymerised. The different types and amounts of phenolic acids, tannins, anthocyanins and phenylpropanoids also differ between plant types, and these may interact with proteins and carbohydrates to form insoluble complexes. The complete recovery of phenolics from plant material is therefore not always possible unless the appropriate solvent and process parameters are used in conjunction with pre-treatment of the sample to promote recovery of the target compounds (Takeuchi *et al.*, 2009). In an industrial setting, the feasibility of an extraction process will rely on the optimal combination of process parameters that would maximise the process efficiency and reduce costs. Water, ethanol, isopropanol and their use in combination have been certified with GRAS (Generally Recognised as Safe) status by the United States Food and Drug Administration, and these solvents are therefore appropriate for the manufacture of nutraceuticals (Wang & Weller, 2006).

Extraction at high temperatures may cause degradation of heat-labile chemical compounds, therefore the concurrent use of elevated operating pressures is beneficial in that it allows the use of lower temperatures to achieve the same extraction efficiency (Wijngaard *et al.*, 2012). Under SFE operating conditions, the solvation capacity is improved due to the solvent remaining in one phase but having the properties of both gas and liquid. SFE is a useful alternative when extracting heat sensitive compounds, but disadvantages may include relatively high cost and long operating times (Shah & Rohit, 2013).

Enzyme-assisted extraction (EAE) involves treating the source material with enzyme preparations (e.g. pectinase or cellulase), which facilitates the release of the target bioactive compounds from the polysaccharide-lignin matrices which they are bound to. It may be prohibitively expensive, however, for processing larger volumes of plant material (Puri *et al.*, 2012). The use of enzymes to enhance the extraction of polyphenols from unripe apples (*Malus pumila*) was also investigated by Zheng *et al.* (2009). Experimental results indicated that the total polyphenol content (mg gallic acid equivalents.100 g^{-1}) and extraction yield were three and two times higher than in controls, respectively.

Chandini *et al.* (2011) investigated the effect of *Aspergillus*-derived pectinase and tannase pre-treatments on the quality of aqueous black tea (*Camellia sinensis*) extracts and found that pectinase improved the yield of total soluble solids by up to 11.5% without a concomitant improvement in the yield of total polyphenols, whereas tannase pre-treatment resulted in an improvement in both the total soluble solids and polyphenol yields (11.1% and 14.3%, respectively). The use of both the enzyme preparations, either simultaneously or in succession, was not as effective as the use of the tannase preparation alone in terms of improving the overall extract quality. In another study (Chen *et al.*, 2011), the EAE of flavonoids from *Ginkgo biloba* was investigated using *Penicillium decumbens* cellulase, *Trichoderma reesei* cellulase and *Aspergillus niger* pectinase with maltose as the glycosyl donor. *P. decumbens* cellulase performed significantly better in enhancing the extraction efficiency than the other two enzymes due to its high transglycosylation capacity, which converts flavonol aglycones to more polar and therefore more soluble flavonoid glucosides. These results indicate that the use of carbohydrate-hydrolysing enzyme facilitates the release of polyphenols complexed in cell walls, and therefore may bring about a higher polyphenol yield. Examples of EAE of rooibos documented in literature are covered under section 2.3.6.

2.3.2. Green extraction concept

Extraction processes often require large amounts of chemical solvents and consume both time and energy, whilst not always guaranteeing a good yield (Chemat *et al.,* 2012). In the interest of striving towards more efficient and environmentally friendly practices, the concepts of "green" engineering and -chemistry have recently been introduced. Green chemistry can be sub-classified further into those technologies which recycle industrial waste and co-products into food additives and biofuels, and those technologies which aim to improve the sustainability of existing techniques by adapting them to use eco-friendlier solvents and processing parameters (Chemat *et al.*, 2012). In the green extraction approach, the plant source should be renewable and in constant supply, and solvents like water or biodegradable compounds should replace traditional chemical solvents.

Natural ionic liquids and deep eutectic solvents (NADES), composed of natural compounds, have recently been discovered and may offer many advantages, like high solvation power for polar and non-polar compounds, biodegradability, favourable toxicity profiles and sustainability (Du *et al.*, 2009; Paiva *et al.*, 2014). Successful applications include the extraction of polyphenols from safflower (*Carthamus tinctorius* L.) (Dai *et al.*, 2013), green coffee beans (Paiva *et al.*, 2014) and shrimp byproducts (Zhang *et al.*, 2014a).

By recycling solvents as much as possible and recovering and re-using any energy produced, energy consumption can be significantly reduced. Modification of existing processes to be more efficient, or the use of brand new techniques could potentially lead to further energy savings. By

performing regular maintenance of equipment, equipment efficiency could be improved and reduce the energy consumption even more. The energy consumption of a system can be determined by exergy analysis, which helps to identify where the greatest energy losses occur (Van Gool, 1992).

2.3.3. Factors affecting extraction efficiency

The major factors which affect the recovery of phenolic compounds from plant materials are the solvent type, solvent-to-solid ratio, extraction time, extraction temperature, particle size and pH. The effect of each of these factors on the mass transfer kinetics is unique to each type of plant matrix, and optimised extraction processes should therefore be developed for each type of botanical raw material (Wijngaard *et al.*, 2012). The choice of solvent should be guided by considerations of its selectivity and capability in terms of extracting the target compound, cost, reactivity, interfacial tension, stability, toxicity and viscosity (Takeuchi *et al.*, 2009).

Plant materials are complex by nature, and the extraction of compounds they contain is influenced by process parameters like temperature, solvent type, mechanical action (e.g. shaking or ultrasonication) and the solubility of the target compounds. The distribution of the target compounds may differ from one type of plant material to the next. The target antioxidant compounds in rosemary, oregano and sage are located on the leaf surfaces, but they may be located in the seeds and roots of other plant materials (Takeuchi *et al.*, 2009). The appropriate choice of solvent should therefore be accompanied by pre-treatment of the raw material in order to facilitate the optimal extraction of these compounds from the plant matrix and maximise the process yield.

The polarity of the solvent used will affect the efficiency of the extract process. Water is an effective solvent for polar target compounds, but for non-polar compounds the use of a less polar solvent (e.g. ethanol) will be required to achieve the same effect (Wang & Weller, 2006). The pH of the reaction solution may affect the rate of cell wall hydrolysis and polyphenol extraction, as shown by Zheng *et al.* (2009), who used acetate and sodium hydroxide to control pH in a study on the effect of pH on the total polyphenol content (TPC) of a ethanolic extract of unripe apple (*Malus pumila*). The TPC was highest when a pH of 3.7 was maintained, and significantly decreased when the pH was increased above 4.0. In a study conducted on methanolic extraction of finger millet (*Eleusine coracana*) polyphenols, it was found that a highly acidic to near-neutral pH (6.5) was associated with higher total polyphenol content than a higher, more alkaline pH (Chethan & Malleshi, 2007). High solvent: solid ratios will increase the concentration gradient, speeding up the extraction process, but will produce a more dilute extract which will necessitate further treatment to remove the large volumes of solvent remaining (Shah & Rohit, 2013).

The preparation of the solid material is often cited as the first important factor to consider in an industrial extraction unit operation (Takeuchi *et al.*, 2009; Wijngaard *et al.*, 2012; Azmir *et al.*,

2013). In most cases, the target compounds are stored in intracellular spaces, capillaries or cell structures as opposed to the outermost surface. Comminuting or grinding of the raw material increases the contact area between the solvent and the plant matrix and decreases the diffusion distance of target compounds from the interior to the solid matrix surface. FT-Raman mapping can be used to identify a target compound as well as to describe its distribution within the plant matrix. Fig. 2.17 shows FT-Raman maps of aspalathin in transverse and longitudinal sections of dried rooibos leaf. Heterogeneous distribution of aspalathin can be observed, with the highest concentration situated in the innermost parts of the leaf. Smaller particle size will reduce the limitations of mass transfer and increase the extraction rate due to a shorter diffusion distance for solutes within the plant matrix. However, excessively fine plant material could complicate filtering of the extract or cause blockage of extraction equipment. The effect of particle size on rooibos extraction as documented in literature is covered under section 2.3.6.

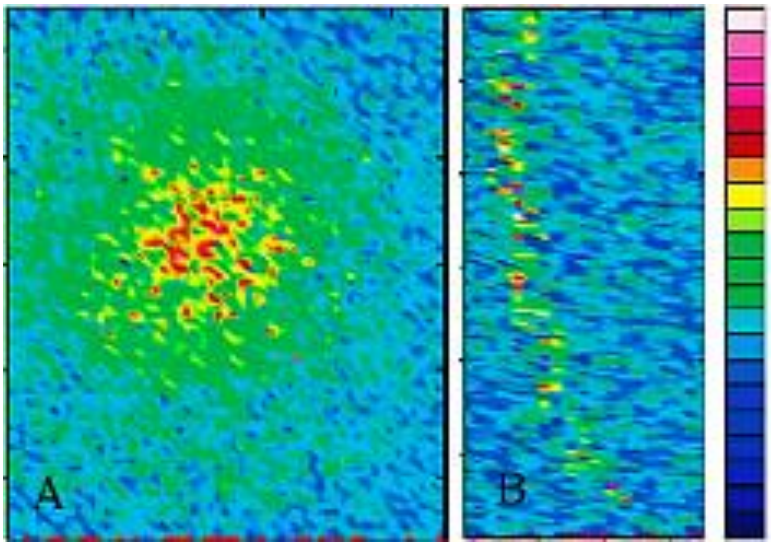

Figure 2.17 FT-Raman maps obtained from transverse (A) and longitudinal (B) sections of *Aspalathus linearis* leaves, coloured according to the individual band intensity for aspalathin at 784 cm^{-1} (Baranska *et al.*, 2006).

Particle size can significantly enhance mass transfer, but very small particles tend to agglomerate and may thus negatively affect the mass transfer kinetics by forming preferential flow channels, preventing effective penetration of the solvent in the solid matrix (Pinelo *et al.*, 2005). Bucić-Kojić *et al.* (2007) reported that smaller particle sizes (0.125–0.16 mm) were associated with the highest recovery of gallic acid from grape seeds using a 50% aqueous ethanol extraction process at 80 °C and 40:1 solvent-to-solid ratio ($mL.g^{-1}$). There was an exponential decrease in gallic acid recovery with increased particle size, and the enhancing influence of extraction temperature became more pronounced as the particle size increased. Laroze *et al.* (2010) investigated the use of solid waste from industrial berry juice production as a raw material for the extraction of polyphenols and confirmed that extraction rates and total polyphenol yields consistently increased with decreasing

particle size. Naidu *et al.* (2007), studying the effect of ground maize particle sizes (separated by mesh screen sizes of 0.5, 1, 2, 3, 4 and 5 mm) on the ethanol and soluble solids yields from thin stillage, noted an 22% increase in ethanol yield as the mesh screen size decreased from 5 to 0.5 mm (Fig. 2.18). Soluble solids recovery was also highest with 0.5 mm particle size, but no significant differences were seen between the soluble solids recovery achieved with larger particle sizes.

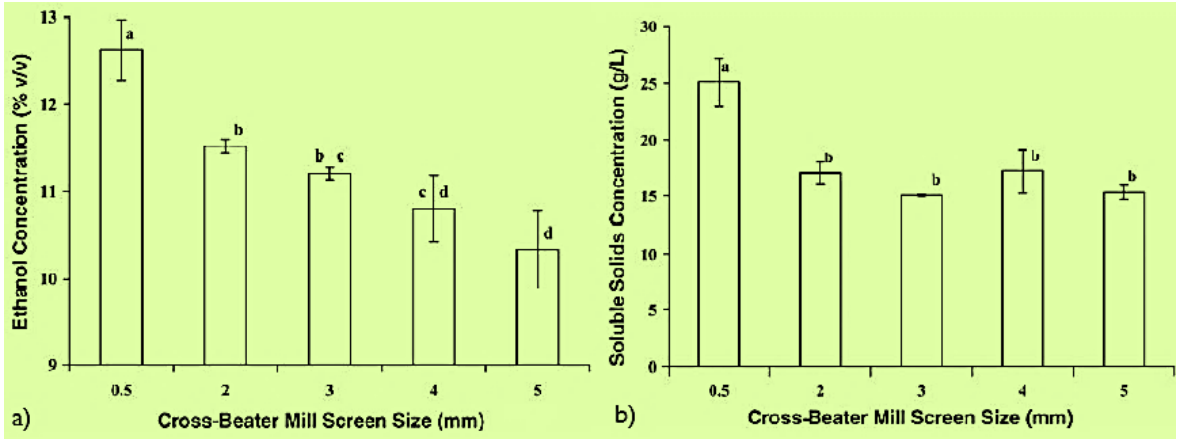

Figure 2.18 The effect of particle size on the ethanol and soluble solids yield from ground maize stillage (values with the same letters within each bar chart are not significantly different; $P < 0.05$) (Naidu *et al.*, 2007).

The effect of different particle sizes on the extraction yield of phenolics from ground pomegranate (*Punica granatum* L.) peel, using distilled water at 60 °C and a 15:1 solvent-to-solid ratio ($mL.g^{-1}$), was investigated by Wang *et al.* (2011). Mesh screen sizes of 10, 20, 30 and 40 were used to obtain 5 different particle size fractions (>10, 10>x>20, 20>x>30, 30>x>40 and <40 mesh), which were extracted for 2, 20 and 60 min. Fig. 2.19 shows that decreasing particle size significantly increased the yield, but this effect was greatest at the shortest extraction time (2 min). This suggests that the use of smaller particle size could allow for the use of shorter extraction times to achieve the same yields and therefore reduce energy and time consumption.

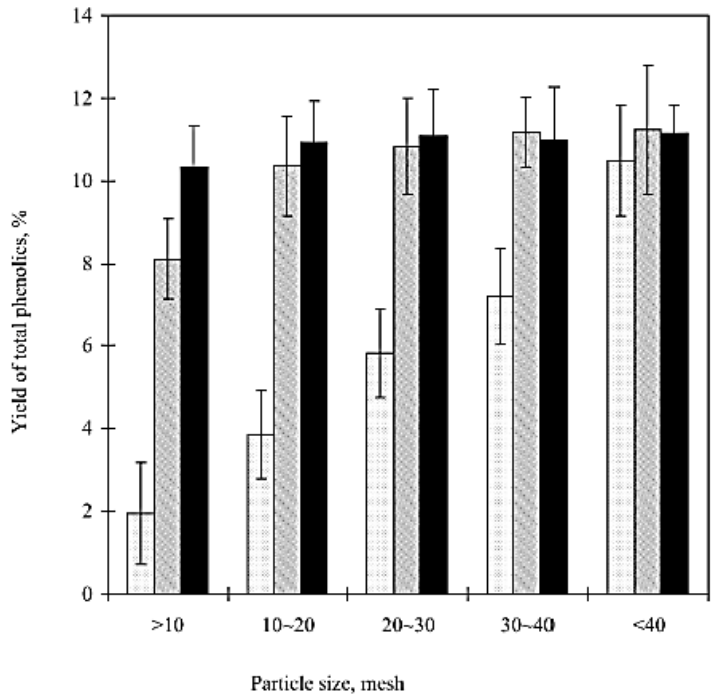

Figure 2.19 The effect of particle sizes on the yield of phenolics from ground pomegranate peel extracted with distilled water at 60 °C (15:1 mL.g^{-1} solvent-to-solids ratio). Extraction times: □ 2 min, ▒ 20 min, ■ 60 min (Wang *et al.*, 2011).

According to the principles of mass transfer, the driving force of the extraction process is the concentration gradient of the solute between the solid and the bulk of the solvent. This concentration gradient is higher when a higher solvent-to-solid ratio is used, independent of the type of solvent used (Takeuchi *et al.*, 2009). This would imply that a greater yield of soluble solids would be obtained with a higher solvent-to-solid ratio, but since this would increase the solvent consumption and have a direct impact on the cost efficiency of the process, it should be carefully considered when the optimal process parameters are selected.

The enhanced extraction of polyphenols with increasing temperature is a result of increased solubility, particularly of polymeric fractions, at higher temperatures as well as increased mass transfer of solutes (Azmir *et al.*, 2013). However, prolonged exposure of phenolic compounds to sufficiently high temperatures would negate this enhancing effect on the extraction kinetics by promoting their oxidative degradation (Shi *et al.*, 2005; Yang *et al.*, 2010). Vuong *et al.* (2011) optimised the hot water extraction of catechins from green tea (*Camellia sinensis*), investigating the combined effects of extraction temperature, time, pH, tea-to-water ratio and tea particle size. The yield of all catechins under investigation sharply increased with an increase in extraction temperature. The optimal combination of treatment levels which maximised catechin yield, whilst minimising thermal degradation of catechin, was established to be a temperature of 80 °C, pH <6.0, tea-to-water ratio of 50:1 (mL.g^{-1}), 30 min of extraction time and a particle size of 1 mm.

Jokić *et al.* (2010) investigated the extraction of polyphenols from milled soybeans (*Glycine max*), using 50% aqueous ethanol and a fixed solvent-to-solid ratio (40:1; $mL.g^{-1}$), and found that higher yields of polyphenols were obtained with increasing extraction time and temperature (Fig. 2.20). The sharpest increase in polyphenol yields was observed in the first 40 min, after which it had less of an effect. Multifactorial optimisation of the extraction process was not performed in this study, and the economically unfeasible notion of employing a 120 min extraction time (despite achieving only a marginal increase in yield compared with 40 min) was not highlighted. The addition of mechanical processes like stirring, shaking, pressure application and sonication of the plant material will also have an effect on the extraction rate by disrupting cell membranes and allowing for faster dissolution of compounds and more effective blending of reactants for chemical processes to take place within the system (Shi *et al.*, 2005; Wang & Weller, 2006).

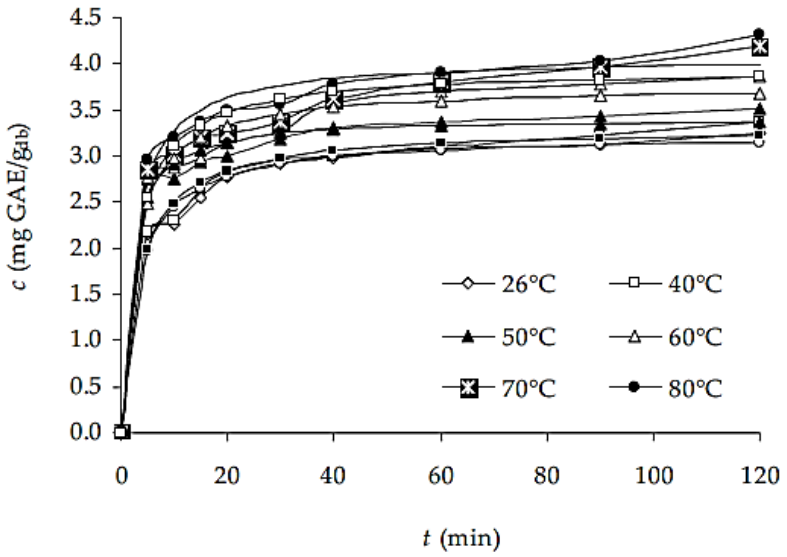

Figure 2.20 The effect of extraction time at various extraction temperatures on the yield of phenolics ($mg.g^{-1}$ dry extract) from milled soybeans (Jokić *et al.* 2010). GAE, gallic acid equivalents.

2.3.4. Novel or supplementary extraction techniques

There are a number of supplementary techniques which have been described to improve the efficiency of traditional solvent-based extraction methods. Microwave-assisted extraction (MAE) is an adapted technique which allows more effective extraction to be achieved at higher rates and shorter durations. Microwaves (typically 300 MHz to 300 GHz) are used to heat the sample by a dual mechanism of dipole rotation and ionic conduction, applied individually or in combination (Pasrija & Anandharamakrishnan, 2015). MAE uses electromagnetic radiation to rupture and create cavitations in the cellular structure and break weak hydrogen bonds in polar molecules, thus releasing active compounds (Tatke & Jaiswal, 2011). Non-polar or volatile molecules are less

efficiently extracted by MAE, however (Shah & Rohit, 2013). MAE has been applied to improve the extraction of a number of botanical bioactive compounds, including astragalosides from *Radix astragala* (Yan *et al.*, 2010), proanthocyanidins from peanut skins (Ballard *et al.*, 2010), and gallic acid from the fruit hull of *Camellia oleifera* (Zhang *et al.*, 2011).

Ultrasound-assisted extraction (UAE) make use of sound waves (20 kHz to 100 MHz) to cavitate plant material in a liquid medium, allowing more efficient and faster penetration of solvent into the material and facilitates recovery of target compounds (Shah & Rohit, 2013). The application of ultrasound enhances the mass transfer kinetics and is based on the phenomenon of acoustic cavitation, which involves the formation, growth and bursting of miniscule bubbles within the solvent (Chemat *et al.*, 2011). Virot *et al.* (2010) applied RSM to optimise the UAE of polyphenols from apple pomace (*Malus domestica*), and found that yield of polyphenols was increased by nearly 20% when ultrasound treatment was added to a previously optimised extraction procedure using 50% aqueous ethanol. Pulsed-electric field extraction (PEF) makes use of electrodes to create a transmembrane potential across plant material, resulting in repulsion between charged molecules within the cells. This leads to the formation of pores in weak areas of the membrane, allowing target molecules to be extracted with greater ease (Azmir *et al.*, 2013). PEF is an ideal choice for heat-sensitive compounds, as it can induce extensive membrane damage without generating much heat (Wijngaard *et al.*, 2012).

2.3.5. Extraction kinetics

The discovery of a plethora of health benefits associated with polyphenols during the past few decades has shifted attention towards harnessing the full potential of raw materials and optimum recovery of bioactive phytochemicals for potential cosmetic, pharmaceutical and food applications. A major aim of most extraction processes is to recover the largest possible amount of target compounds from the plant material in as little time as possible in order to maximise the efficiency and economy. An understanding of the reaction kinetics involved is important when attempting to optimise such a process. Once a solvent is added to plant material, an equilibrium concentration gradient is established between the solutes still inside the plant material and those solutes dissolved in the solvent (Gertenbach, 2002). The relationship between these factors can be described by the equation:

$$K = \frac{C_e}{C_{dm}}$$

with, K representing the equilibrium constant, C_e the concentration of a specified compound in the solvent and C_{dm} the concentration of a specified compound in the dry plant material. K is subject to the temperature and type of solvent used, as well as the initial content of the specified compound in

the plant material (Gertenbach, 2002). Large *K* values are desirable as they indicate that large amounts of the given compound will dissolve into the solvent.

The extraction of compounds from plant material to a bulk solution involves four stages. In the first stage the solvent penetrates and diffuses into the solid particles. This is followed by dissolution of the target compounds into the solvent. The third stage involves diffusion of the dissolved solutes through the plant matrix to the particle surface. The solute-rich solvent which accumulates at the particle surface then diffuses back into the bulk solvent (Gertenbach, 2002).

Price & Spitzer (1993; 1994) have described first-order diffusion mechanisms based on Fick's Law for the extraction of flavanols and caffeine from green and black Oriental tea. The rate-limiting step in polyphenol extraction from tea leaves is the diffusion of the various constituents from within the leaf to the particle exterior (internal diffusion), and this process can be described by using Fick's Second Law (Fick, 1855). The relationship can be expressed as follows:

$$\frac{\delta C}{\delta t} = D\frac{\delta^2 C}{\delta x^2}$$

where *C* is the solute concentration, *t* is time, *D* is the coefficient of diffusivity and *x* is the particle diameter. The concentration gradient between the amount of target compounds within the plant particle and the amount at its surface therefore drives the extraction process. Franco *et al.* (2007) used first-order mathematical models derived from Fick's Second Law to describe the kinetics of an ethanolic extraction process for rosehip seeds (*Rosa rubiginosa*). Resveratrol extraction from grape cane (*Vitis vinifera*) has also been comprehensively studied using a similar approach (Karacabey & Mazza, 2008).

2.3.6. Extraction of *Aspalathus linearis* plant material

The use of solvent-based extraction is currently the standard method for the commercial production of rooibos extracts and for analysis of plant material samples. Aspalathin is a highly water-soluble, hydrophilic molecule (Huang *et al.*, 2008), and hot water extraction is a safe and energy-efficient method for rooibos extraction particularly if it is for the production of food-grade extracts. Since aqueous rooibos infusions have been consumed as a household beverage for generations, it is generally accepted that hot water extracts would not contain any potentially hazardous constituents which would otherwise be absent in a conventional cup of rooibos tea. The sole use of water also facilitates more efficient production by spray-drying, since the system can then be operated in an "open configuration" without the need for removing organic solvents (Büchi, 2009). The soluble solids and polyphenol content of botanical extracts are affected by the average particle size and stem content of the ingoing plant material, and lower concentrations of soluble

solids and polyphenols were obtained when higher fractions of coarse fermented plant material (including stems) were used (Joubert, 1984).

Aside from the nature of the raw material used, the extraction conditions and type of solvents used also affect the level of aspalathin recovery from the plant material and enrichment in the final product. There is a limited amount of published literature on the optimisation of rooibos extraction processes. Those available mostly studied the effect of one factor at a time (temperature, time and solid: leaf ratio) on total polyphenol and soluble solids yield from fermented rooibos. Higher extraction temperatures, and higher water-to-leaf ratios as well as longer extraction times are associated with higher soluble solids and polyphenol content in the final product (Joubert, 1988b, 1990b, 1990c; Joubert & Hansmann, 1990).

Joubert investigated the effects of temperature (23–90 °C), water-to-tea mass ratio (5:1 and 10:1) and water flow rate (0.1 and 0.2 $m^3.h^{-1}$) on the yield of soluble solids (1988b) and polyphenols (1990b) from fermented rooibos extracted by single-stage batch extraction. The soluble solids and polyphenol yields increased linearly with an increase in extraction temperature and mass ratio, whereas the both were decreased at a higher water flow rate. There was also significant interaction between the extraction temperature and water: tea mass ratio ($P < 0.01$) and flow rate ($P < 0.01$), with the effect of temperature less pronounced at lower mass ratios and higher flow rates. The extraction temperature had a more pronounced positive effect on the extraction of flavonoids than non-flavonoid phenols, and it was demonstrated that the increase in the total polyphenol content was largely attributable to an increase in the flavonoid content.

Joubert (1990c) investigated the hot water extraction of total polyphenols, flavonoid and non-flavonoid phenols from fermented rooibos using a fixed-bed system at 90 °C and flow rates of 0.09 and 0.18 $m^3.hr^{-1}$. An increase in the flow rate at a fixed extraction time was associated with a decrease in the yield of total polyphenols. The yield of flavonoids and total polyphenols increased with increasing extraction time up to 8 min, whereas non-flavonoid phenols were much less significantly affected by the extraction time. The total polyphenol content of the extract was comprised mainly of flavonoids (59–68%, depending on extraction time). The extraction process conditions used by a major rooibos extract manufacturer are based on the results of these studies (Van Breda, R., 2015, Afriplex, Paarl, personal communication, 24 September).

Von Gadow *et al.* (1997) demonstrated that longer extraction time resulted in increased phenolic content in fermented rooibos extracts, and that its antioxidant activity was stable during additional heat exposure. Jaganyi & Wheeler (2003) determined that approximately 50% of the aspalathin in fermented rooibos is extracted within 5 min in water at 80 °C, with a steady state reached after ca. 60 min. No additional studies on the extraction kinetics of rooibos flavonoids have been conducted.

Joubert & De Beer (2012) described the composition of 74 batches of unrefined (i.e. comminuted but not sieved) fermented rooibos plant material in terms of three particle size fractions: >10 (coarse), 10>x>40 (refined tea) and <40 mesh (dust). The coarse tea fraction represented on average 12.97% of the unrefined tea (range: 4.45–23.82%). There was a weak (r = 0.300) but significant (P = 0.009) negative correlation between the size of the coarse fraction and the yield of soluble solids from the unrefined tea (Fig. 2.21). It was previously shown that rooibos waste material provided a low yield of soluble solids (8.9%) compared with the refined fraction (20.4%) (Joubert, 1984), which would explain the lower yields observed when larger coarse fractions (i.e. waste material) were present in the plant material.

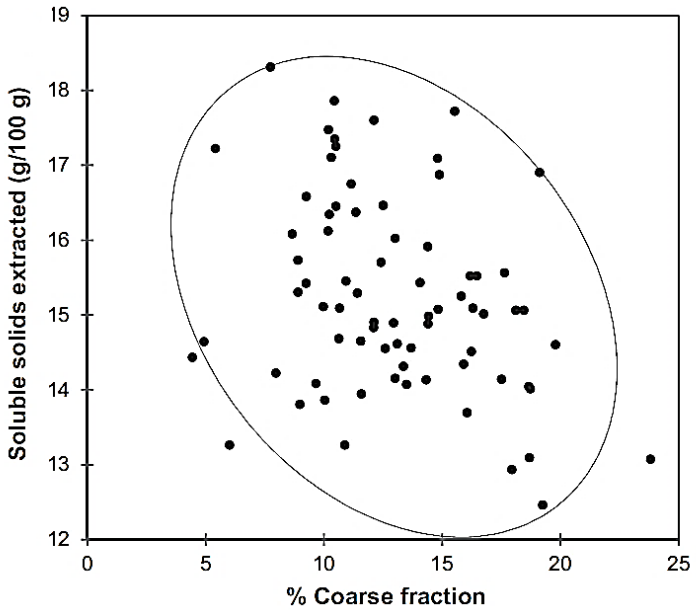

Figure 2.21 Correlation between soluble solids extract from unrefined, fermented rooibos tea and percentage coarse fraction in the unrefined tea (Joubert & De Beer, 2012).

Pengilly *et al.* (2008) investigated the effect of using different enzyme preparations of *Rhizopus oryzae* in hot water extraction of soluble solids and phenolic compounds from fermented rooibos. The type of culture medium used to produce the enzyme cocktail had a significant effect on the extraction efficiency. When the enzyme cocktail was cultured in yeast peptone-wheat straw medium, the yield of soluble solids was improved by 47%, and >95% of both the total polyphenol content and the antioxidant activity ($ABTS^{\cdot+}$ scavenging assay) were retained in the extract. The enzyme cocktail prepared with potato dextrose culture medium did not improve the yield of soluble solids, but it did increase the total polyphenol content and antioxidant capacity of the extract. When the fermented plant material was treated with an enzyme cocktail of *R. oryzae*, (cultured using yeast peptone-wheat straw medium) for 2 h at 40 °C, and subsequently extracted according to a simulated industrial process, the soluble solids and total polyphenol yields were improved by 30 and

31%, respectively. Coetzee *et al.* (2014) reported that subjecting fermented and GR plant material to pre-treatment with food-grade cellulase, pectinase or ferulic acid esterase resulted in higher contents of soluble solids in hot water infusions. However, the total polyphenol content and antioxidant content were reduced when enzyme pre-treatment was carried out due to the concomitant extraction of non-polyphenolic soluble matter.

No studies have been done on GR extraction optimisation. In order to manufacture an extract with a consistent set of quality attributes, the process must be investigated and well understood. The interaction effects of process parameters could contribute significantly to the process efficiency, and multivariate statistical methodology like RSM could be utilised to investigate these effects after a risk assessment process guided by QbD principles.

2.4. Spray-drying of botanical extracts

2.4.1. General overview of spray-drying

Spray-drying refers to a unit operation in which a liquid product containing suspended or dissolved solids is atomised in a heated drying gas current to produce powdered solids. Air is most commonly used as drying gas, but some applications may involve the use of an inert gas like nitrogen (Ré, 1998). Spray-drying is an established technique in the food and pharmaceutical industries, and it can provide the dual benefit of drying a product by removing moisture and simultaneously creating a more physicochemically stable microencapsulated product. Microencapsulation refers to the process in which small particles are enveloped in a coating material or embedded in a homogenous or heterogeneous matrix (Patel *et al.*, 2015). Such microcapsules may be produced by other established techniques like spray-chilling, freeze-drying, liposomal entrapment and centrifugal extrusion, but spray drying remains the most commonly applied technique owing to its relatively low implementation and maintenance costs, ease of scale-up, continuous processing capacity and less potential thermal damage to the product (Gharsallaoui *et al.*, 2007; Lebrun *et al.*, 2012; Murugesan & Orsat, 2012; Costa *et al.*, 2015).

The development of microencapsulation techniques has enabled the production of previously unfeasible products due to the protective effect of the encapsulating agent (also referred to as wall, coating or carrier material) on the material contained inside, or the "core". The latter may be composed of one or more ingredients, which may be in solution, emulsion, or a suspension of solids or smaller microcapsules. The coating material may likewise be composed of more than one type of material (Gharsallaoui *et al.*, 2007; Costa *et al.*, 2015).

Microencapsulation is typically applied in the food and pharmaceutical industry for one or a combination of the following indications: to protect and reduce the transfer rate of the core material

to the environment, allow controlled release of the core material, facilitate ease of handling and to dilute the core material to a desired concentration (Gharsallaoui *et al.*, 2007; Woo & Bhandari, 2013). Another major function of microencapsulation by spray-drying is the removal of moisture and reduction of water activity, which confers microbiological and biochemical stability, reduces storage and transport costs, and may provide a product with specific desired quality attributes (e.g. flowability, solubility and hygroscopicity) (Ré, 1998; Fitzpatrick, 2013).

Depending on the material attributes and operating parameters selected, spray-drying may produce a very fine, homogenous powder (⌀ = 10–50 µm) or larger particles of irregular morphology (⌀ = 2–3 mm) (Murugesan & Orsat, 2012). The typical size ranges of particles produced by various spray-drying configurations are shown in Table 2.5. Various particles morphologies may also be achieved with spray-drying, and these different particle sizes and shapes can be tailored towards a variety of applications (Patel *et al.*, 2015).

Table 2.5 Typical size ranges of particles obtained by various spray-drying processes (Woo & Bhandari, 2013).

Spray-drying process/system	Average particle size (µm)
Bench spray dryer	5–20
Pilot-scale dryer	20–40
Commercial spray dryers (two-stage)	200–400
Agglomerated powders	200–2000

The physicochemical properties which determine the quality of the dried product obtained may also vary greatly depending on the conditions under which the drying steps took place. The large number of parameters which may affect responses in the spray-drying process makes mathematical modelling of experimental data an often challenging task (Gharsallaoui *et al.*, 2007).

Spray-drying has been widely utilised for the production of a variety of consumer goods ranging from pharmaceuticals to microencapsulated salt and instant soup powders (Ré, 1998). Various types of botanical extracts with health-promoting antioxidants and phenolic compounds or desirable aromatic constituents have been microencapsulated by spray-drying, amongst others extract of sumac (*Rhus coriaria* L.) (Caliskan & Dirim, 2013), *Eugenia dysenterica* (Couto *et al.*, 2011), rosemary (*Rosmarinus officinalis* L.) (De Barros Fernandes *et al.*, 2013), blueberry (*Vaccinium* ssp.) (Jiménez-Aguilar *et al.*, 2011; Hashemiravan *et al.*, 2013), ginger (*Zingiber officinale*) (Jangam & Thorat, 2010), pineapple (*Ananas comosus*) (Jittanit *et al.*, 2010; Wong *et al.*, 2015), bitter melon (*Momordica charantia*) (Kaur *et al.*, 2015; Tan *et al.*, 2015), acerola (*Malpighia emarginata* D.C.) (Moreira *et al.*, 2009), flaxseed (*Linum usitatissimum*) (Oomah & Mazza, 2011), Oriental tea (*Camellia sinensis*) (Pandey & Manimehalai, 2014; Belščak-Cvitanović *et al.*, 2015; Pasrija *et al.*, 2015), cactus pear (*Opuntia ficus-indica*) (Saénz *et al.*, 2009), mountain tea (*Sideritis stricta*) (Şahin-Nadeem *et al.*, 2011), sage (*Salvia fruticosa*) (Şahin-Nadeem *et al.*, 2013), jaboticaba peel (*Myrciaria jaboticaba*) (Silva *et al.*, 2013),

Brazilian orchid (*Bauhinia forficata*) (Souza & Oliveira, 2006), betel leaf (*Piper betle*) (Tee *et al.*, 2012) and chicory root (*Cichorium intybus*) (Toneli *et al.*, 2010). RSM is frequently applied in these studies to evaluate the effect of multiple process parameters on the process output, since the large number of process parameters typically involved necessitates the use of multivariate statistical analysis (Lebrun *et al.*, 2012).

2.4.2. Basic steps in a spray drying process

The various stages in a standard spray-drying process have been extensively described in a number of previous studies (Gharsallaoui *et al.*, 2007; Lebrun *et al.*, 2012; Woo & Bhandari, 2013; Costa *et al.*, 2015), but will be briefly summarised in the following section. Figs. 2.22 depicts the basic functional principles and components of a typical spray-drying system for illustrative purposes.

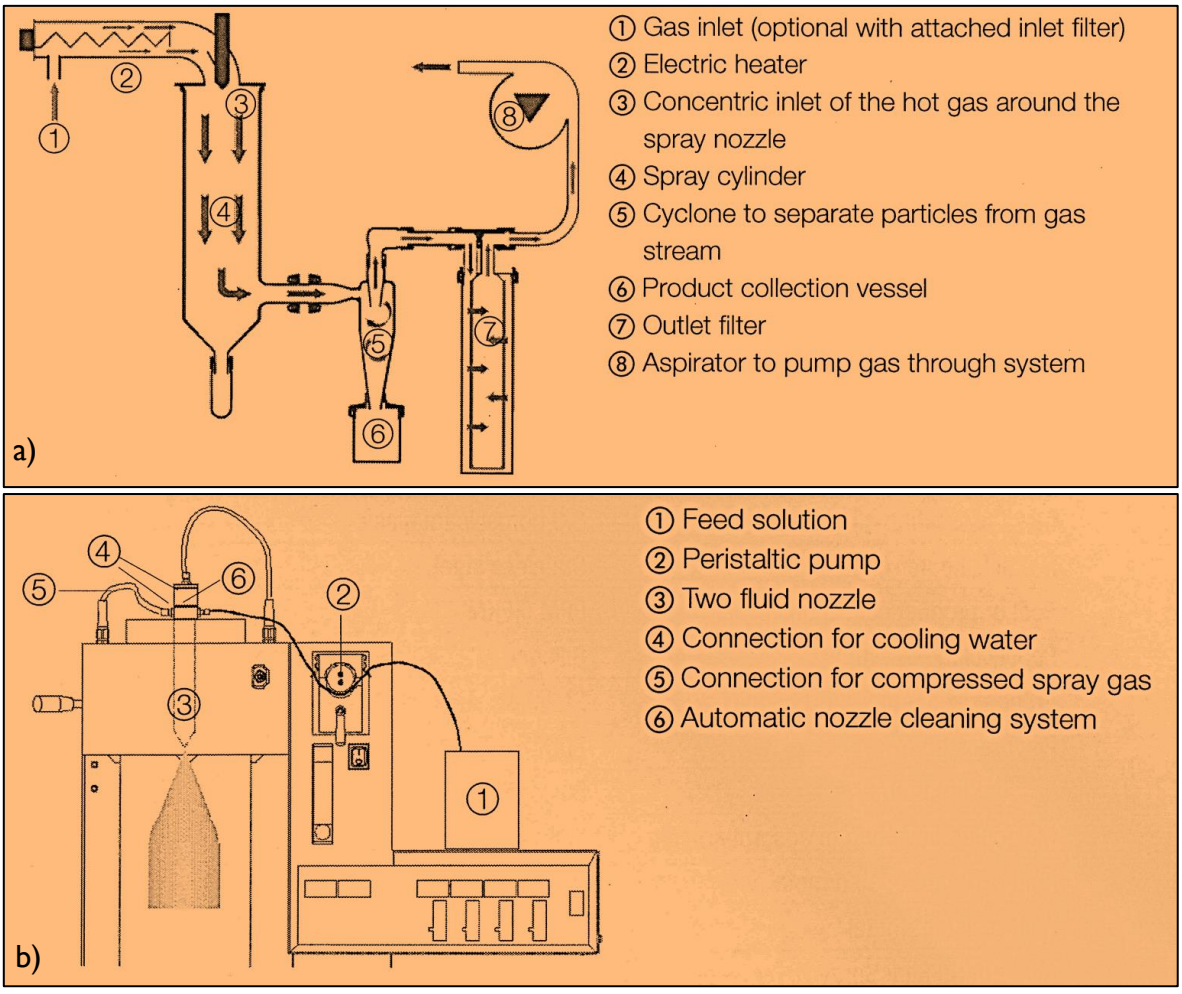

Figure 2.22 Functional principles and components of (a) typical spray-drying system and (b) spray-drying sample feed and dispersion system (Büchi, 2009).

2.4.2.1. Atomisation

The first step involves the conversion of the feed material to small aerosolised droplets by the application of centrifugal energy or pressure. In the model system depicted in Fig. 2.22, atomisation is achieved by the application of compressed air to the feed solution, which is then forced through the narrow orifice of the spray nozzle and dispersed inside the spray cylinder in aerosolised form. This increases the available surface area for heat transfer and mass transfer between the drying air and the solvent (Patel *et al.*, 2015). The greater the amount of energy applied in the atomisation process, the finer the resultant particles. An increase in the feed rate or viscosity of the feed material at the same atomisation energy will result in larger particles (Woo & Bhandari, 2013; Costa *et al.*, 2015).

2.4.2.2. Air-droplet contact

Air-droplet contact initiates the drying stage and occurs during atomisation. *Concurrent* spray-drying refers to a set-up in which the liquid feed is sprayed in the same direction as the hot air current, which is typically at a temperature in the range 150 to 220 °C, causing instantaneous evaporation of moisture and exposure of the dried particles to moderate temperatures within the range 50–80 °C (Gharsallaoui *et al.*, 2007). This is the desired configuration when heat-sensitive compounds are present within the core. *Countercurrent* spray-drying, which involves the spraying of the liquid feed against the flow of hot air, exposes the dried product to higher temperatures and thus limits its use, although it has been noted that countercurrent configurations consume less energy (Woo & Bhandari, 2013; Patel *et al.*, 2015). Fig. 2.23 illustrates the basic drying process of an individual atomised droplet in a typical spray drying set-up. The heating of an atomised droplet is driven by the temperature gradient between the droplet surface and the drying air. The temperature gradient within the droplet itself is usually negligible due to the small particle sizes and the high rates of heat transfer, and the droplet itself is usually considered uniform in temperature (Chen, 2005; Patel & Chen, 2008). The heating of a droplet can be roughly described by the following equation:

$$\frac{\Delta T}{\Delta t} = hA\left(T_{air} - T_{droplet}\right) - \frac{\Delta m}{\Delta t}\Delta H_{evap}$$

where $\Delta T/\Delta t$ is the rate of temperature change ($K.s^{-1}$), h is the convective heat transfer coefficient ($W.m^{-2}.K^{-1}$), A is the droplet surface area (m^2), (T_{air} - $T_{droplet}$) is the temperature difference (K), $\Delta m/\Delta t$ is the drying rate ($kg.s^{-1}$) and ΔH_{evap} is the latent heat of evaporation ($kJ.kg^{-1}$) (Woo & Bhandari, 2013).

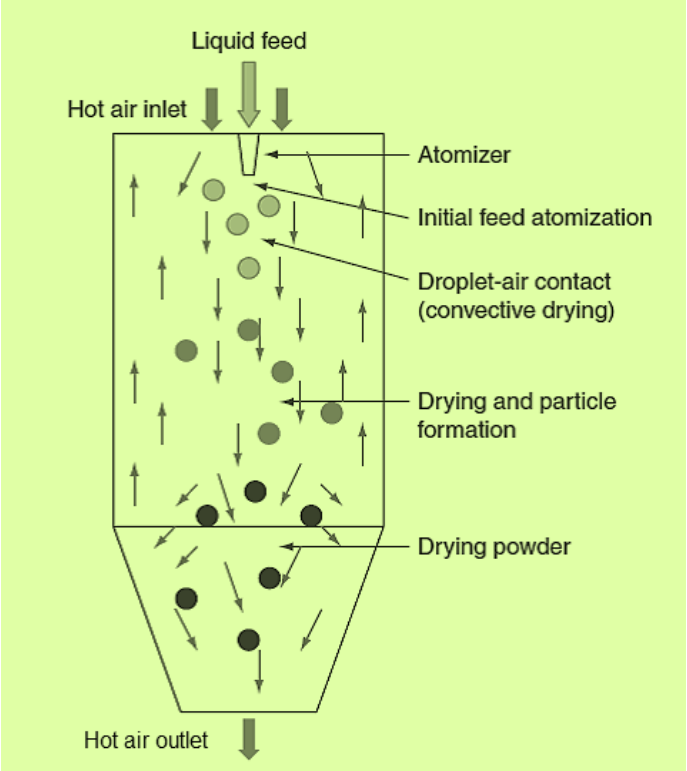

Figure 2.23 Simplified diagram of basic spray drying process (Woo & Bhandari, 2013).

The drying rate is also driven by the difference between the droplet surface vapour concentration and the drying air vapour concentration (Patel *et al.*, 2009). The humidity of the drying air will therefore significantly affect the rate of moisture loss of the droplet. Mathematically, it can be expressed as follows:

$$\frac{dm}{dt} = h_m A(\rho_{droplet,surface} - \rho_{air})$$

where $\Delta m/\Delta t$ is the rate of moisture loss ($kg.s^{-1}$), h_m is the convective mass transfer coefficient ($m.s^{-1}$) and ($\rho_{droplet,surface}$ - ρ_{air}) is the vapour concentration difference ($kg.m^{-3}$) (Woo & Bhandari, 2013).

2.4.2.3. Evaporation of moisture

As soon as the aerosolised droplets are exposed to the heated drying air, temperature and partial vapour pressure balances are established between the gas and liquid phases. Heat transfer is then carried out from the drying air towards the product due to a temperature gradient, and water is transferred from the droplet to the surrounding air along a pressure gradient (Ré, 1998). Fig. 2.24 describes the basic mass and heat transfer principles which affect the formation of solid particles in spray-drying.

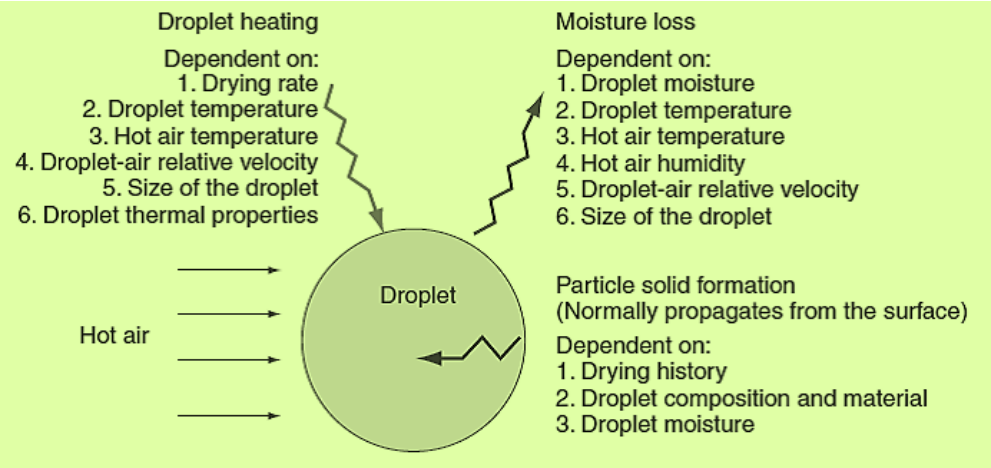

Figure 2.24 Convective heat and mass transfer and particle formation in spray-drying (Woo & Bhandari, 2013).

The fundamental theory of drying states that three distinct phases or steps are present (Gharsallaoui *et al.*, 2007): (1) the transfer of heat increases the droplet temperature to a constant level, at which point (2) the evaporation of moisture occurs at constant temperature and partial water vapour pressure. It is generally assumed that the rate of water diffusion from the droplet center to the surface is constant and equal to the rate of evaporation from the surface (Cal & Sollohub, 2010). Once the droplet moisture content (MC) falls below a material-specific critical limit, a dry crust forms at the surface which then limits the rate of diffusion of water to the environment. The drying stage ends (3) when the temperature of the dried particle is equal to that of the air. The duration of these steps may differ based on the operating parameters and the nature of the product. For instance, when the air inlet temperature is high, the formation of the dry crust occurs rapidly due to the high rate of evaporation. In addition, the large surface to volume ratio of the aerosolised particles increases the rate of heat transfer (Patel *et al.*, 2009; Costa *et al.*, 2015).

The dry product is usually separated from the air by means of a cyclone system with an aspirator pump, which improves the product yield by diverting the fine particles into a collection vessel and reduces losses to the environment and clogging of outlet filters (Woo & Bhandari, 2013).

2.4.3. Carrier materials

Carrier materials for spray drying should be selected on the basis of their physicochemical properties like crystallinity, solubility, sensory characteristics, emulsifying properties and molecular weight as it pertains to the application in question (Sollohub & Cal, 2010). The economic feasibility of their use should also be considered, since many remain prohibitively expensive. It has been established that the highest losses of volatile compounds during spray drying occur before the

formation of the dry crust in the early stages of drying (Patel *et al.*, 2009). The addition of *carrier* materials to the feed can modify the drying attributes of the microcapsule by enhancing dry crust formation and increasing the hydrophilicity of the coating (Woo & Bhandari, 2013; Costa *et al.*, 2015). A wide variety of natural and synthetic polymers can be used as carrier materials. Good solubility in water is an important requirement for most spray drying applications since aqueous solutions are typically used as feed material (Ré, 1998). Low viscosity and good emulsifying and film-forming properties are also desirable (Costa *et al.*, 2015). Natural gums like carrageenan, gum arabic and alginates have been successfully used as carrier materials, along with proteins of varied origin and other complex carbohydrates like waxes and maltodextrin. The selection of carrier material often involves a trial-and-error approach in which different options are evaluated based on their microencapsulation efficiency in terms of process yield, core material retention, storage stability and particle size and morphology, amongst others (Gharsallaoui *et al.*, 2007).

Carbohydrates like maltodextrin, inulin and lactose have been widely used as encapsulating agents due to their generally low viscosity at high concentrations and good solubility in water, but they often lack the good interfacial properties associated with gums and proteins (Sollohub & Cal, 2010). Maltodextrin is a polymer of D-glucose obtained from acid or enzymatic hydrolysis of corn starch, and is available in different dextrose equivalents (DE), which correspond with the degree of hydrolysis of the starch. The DE is therefore also inversely related to the average molecular weight (Costa *et al.*, 2015). Maltodextrin is commonly used in spray drying due to its neutral smell and taste, high solubility in cold water, low cost, low hygroscopicity, and low viscosity at high concentrations (Ré, 1998). It has also been shown to exhibit an antioxidant effect and good volatile retention. It lacks good emulsifying properties, but this can be addressed by the addition of a second carrier which does provide that function, like gum arabic (Costa *et al.*, 2015). Gum arabic, a polysaccharide containing mainly D-glucoronic acid, D-galactose, L-rhamnose and L-arabinose, is one of the most commonly used carriers due to its excellent solubility, low viscosity, high oxidative stability and good emulsifying properties, which is attributed to a small protein fraction (2%) found among its constituents. This makes it an excellent choice for the encapsulation of lipids (De Barros Fernandes *et al.*, 2012). High costs and limited supplies often prohibit the more widespread use of gum arabic, however, and alternatives have been proposed, e.g. mesquite gum (Jimenez-Aguilar *et al.*, 2011).

Inulin, produced on a commercial level mainly from extracts of chicory (*Cichorium intybus*) roots, Dahlia (*Dahlia pinuata*) and Jerusalem artichoke (*Helianthus tuberosus*), is a polysaccharide and non-digestible dietary fibre composed of β(2→1) linked D-fructosyl residues (n = 2–60) which has been applied as carrier agent in a number of spray drying operations, besides its other uses in the food and pharmaceutical industries as fat replacer, protein stabiliser, texture modifier and diagnostic aid (Mensink *et al.*, 2015a; Mensink *et al.*, 2015b). Inulin is only partially hydrolysed in the

gastrointestinal tract and does not result in the production of monosaccharides, and therefore does not result in elevated blood glucose concentrations (Kolida *et al.,* 2002; Mensink *et al*., 2015b). This would be an important consideration in the selection of a carrier material for an antidiabetic nutraceutical, since the beneficial hypoglycaemic effects of the bioactive compounds would be diminished if a carrier with a high glycaemic index were part of the formulation. Inulin has the additional advantage of acting as a prebiotic by stimulating the growth of beneficial gastrointestinal bifidobacteria (Kolida *et al*., 2002). The increased consumption of dietary fiber has been linked to a lower risk for cardiovascular diseases, lower body mass index and improved gastrointestinal health (Slavin, 2013). The latter is particularly associated with *prebiotic* dietary fibers, i.e. those which stimulate the growth and/or activity of specific gut microflora to the benefit of the host. Inulin has been shown to stimulate the growth of the beneficial genus *Bifidobacterium* in a number of studies (Costabile *et al*., 2010; Ramnani *et al*., 2010). A number of large-scale cohort studies have demonstrated a strong inverse relationship between the regular consumption of dietary fiber and the development of T2D (Meyer *et al*., 2000; Hopping *et al*., 2010; Nazare *et al*., 2011; Slavin, 2013). Gargari *et al.* (2013) studied the effects of high-performance inulin supplementation on glycaemic control indices and antioxidant status in women (n = 49) with T2D. The control group (n = 25), who received 10 g per day of maltodextrin for 2 months, had significantly higher ($P < 0.05$) fasting plasma glucose (8.74%), glycosylated haemoglobin (10.43%) and malondialdehyde (37.21%) levels than the treatment group (n = 24), who received 10 g of inulin per day for the same period. The inulin group also had significantly higher ($P < 0.05$) superoxide dismutase activity (4.36%) and total antioxidant capacity (18.82%) than the control group. Yang *et al.* (2012) reported that the combined intake of catechin-rich green tea and inulin may have an anti-obesity effect in obese and overweight adults. Experimental subjects who received a green tea infusion with added inulin for 6 weeks had significantly reduced body weight and fat mass compared with the control group, who received only the green tea infusion.

Proteins exhibit many functional characteristics which allow their successful application as spray-drying carriers. Two of the most long-established carrier proteins are gelatin, derived from animal collagen, and milk or whey proteins. The latter has been used extensively in the dairy industry for the production of microencapsulated milk fat (e.g. instant coffee creamers) by spray drying and is often associated with very favourable product yields (Young *et al*., 1993; Gunasekaran *et al*., 2007). In addition, the use of pea protein concentrates as carrier for spray-dried ascorbic acid and alpha-tocopherol has been investigated with promising results (Pierucci *et al*., 2006, Pierucci *et al*., 2007). The use of proteins should take into account the processing conditions, as heat treatment could lead to denaturation of the protein structure and subsequent loss of its desired functional properties. Other limitations associated with the use of some proteins include the potential of allergenicity, precipitation in products with pH near the iso-electric point of the carrier, and the

matter of religious or cultural prohibitions against the consumption of some animal-derived products (Sollohub & Cal, 2010).

2.4.4. Physicochemical characteristics of spray-dried powders

Spray-dried powders can vary greatly in their physicochemical attributes depending on how efficiently the drying, dispersion and collection of particles were carried out. These attributes can be quantified by a number of established analytical techniques for the purposes of quality assessment and evaluation of the spray-drying process. Measurable attributes of powders can be classified as particle properties or bulk properties. Particle properties include particle density, composition, internal structure, shape and size distribution, whereas bulk properties refer to the bulk density, flowability and dustiness (Fitzpatrick, 2013). The MC of powders may also significantly affect both its particle and bulk properties, and is therefore usually included in powder quality assessment. Particle properties have a direct influence on processing behaviour, product quality and bulk properties, and particle properties themselves may be directly affected by a number of process variables (Patel *et al.*, 2015).

2.4.4.1. Yield

One of the most important properties to consider in evaluating the efficiency and economic feasibility of the spray drying process is the process yield, i.e. the mass of spray-dried solids collected at the system outlet relative to the total mass of solids that was present in the ingoing feed solution. Spray-drying generally provides favourable yields if the process is carried out optimally, but what is considered acceptable varies amongst investigators, with minimum acceptability criteria ranging from at least 60% to at least 80% mass yield (Murugesan & Orsat, 2012; Woo & Bhandari, 2013; Costa *et al.*, 2015), but even yields as low as >45% have been cited as acceptable (Sollohub & Cal, 2010). Maury *et al.* (2005) and Amaro *et al.* (2011) reported that powder yields were greater at a higher drying air inlet temperature due to the improved drying rate and reduced deposition of particles on the drying chamber walls. Studies by Prinn *et al.* (2002) and Maltesen *et al.* (2008) have demonstrated that an increased feed solution concentration was associated with higher yields due to low MC and less stickiness in the final product. The yield is greatly dependent on the amount of spray-dried particles which stick to the interior of the drying chamber, and the degree of stickiness is related to the glass transition characteristics of the specific materials (see section 2.4.4.3.) (Keshani *et al.*, 2015; Patel *et al.*, 2015).

2.4.4.2. Moisture content and water activity

Moisture content (MC) refers to the total amount of water present in a material, regardless of its availability to partake in chemical reactions, and can be expressed on a volumetric or gravimetric basis. Spray-dried powders, if properly produced, should have a low MC since the primary function of the unit operation is to remove moisture. MC of below 5% has been specified as a requirement for powders to ensure effective packaging, handling and storage stability (Sinija *et al.*, 2007; Şahin-Nadeem *et al.*, 2013). Food-grade powders are usually analysed for MC by thermogravimetric analysis at temperatures between 102 and 110 °C until a constant sample mass is reached, but alternative chemical methods are available, e.g. Karl-Fischer titration, for accurately determining MC below 1% (Fitzpatrick, 2013).

Water activity (a_w) is a concept commonly applied in food safety and quality assessment and refers to the amount of water available (at equilibrium) for hydration of the material, taking part in chemical reactions and to support microorganism and enzyme activity (Rockland & Nishi, 1980; Sablani *et al.*, 2007). The a_w of a product is largely a function of its MC and the conditions of the surrounding air. A value of zero indicates the total absence of water, while the maximum value of 1 corresponds to pure water. Below a value of 0.5, the occurrence of microbial growth and biochemical degradation is greatly reduced, thereby ensuring safety and shelf-stability (Woo & Bhandari, 2013). The relationship between a_w and MC is complex, but an increase in MC generally corresponds with an increase in a_w in a non-linear fashion. The equilibrium relationship between moisture in the powder at a given temperature and moisture in the atmosphere can be described by moisture sorption isotherms, which are determined experimentally for each individual type of material (Al-Muhtaseb *et al.*, 2002; Fitzpatrick, 2013).

2.4.4.3. Glass transition and solid state characteristics

Spray-dried powders may be described as solid dispersions, i.e. the dispersion of one or more active ingredients in an inert matrix (carrier) where the active ingredients may exist in an amorphous, solubilised or crystalline state (Patel *et al.*, 2015). Spray-drying may result in two basic types of solid dispersions: amorphous and crystalline. The amorphous-type system features the carrier in an amorphous state rather than crystalline, and can be further classified as solid glassy suspensions, solid glassy solutions and solid crystalline suspension (Baird & Taylor, 2012). Spray-dried botanical extracts typically exist in the amorphous state as it exits the drying chamber, but may subsequently transform to a crystalline state during storage, especially in the presence of residual moisture (Chiou & Langrish, 2007). Crystallisation is undesirable as it may cause disruption of the particles and subsequent losses of encapsulated compounds, as well as agglomeration and caking of powders with

resultant poor flowability (Palzer, 2005; Chadha & Bhandari, 2014). The degree of crystallinity of a powder may also affect a number of its physicochemical characteristics, e.g. stickiness, solubility, porosity and flowability (Patel *et al.*, 2015). A key role of the added excipient in a spray-dried dispersion is to reduce the molecular mobility and avoid phase separation and re-crystallisation during storage (Sareen *et al.*, 2012).

Powdered extracts may undergo a number of such physicochemical changes during various processing stages and storage, and an understanding of these phase transitions are helpful in identifying optimal processing and storage conditions. The temperatures at which phase transitions take place can be characterised by thermal analysis techniques, which is a frequently used index of stability for products with pharmaceutical applications (Šimon *et al.*, 2004). Most notably, thermal analysis is used to determine the glass transition temperature (T_G), which refers to the temperature (or temperature range) at which an amorphous system transforms from a glassy to a rubbery, viscoelastic state (Le Meste *et al.*, 2002; Roos, 2010). Molecular mobility is significantly reduced in the glassy state and at low MC due to high viscosity of the matrix (Sablani *et al.*, 2007). The plasticising effect of moisture has been investigated by Konno & Taylor (2006), who observed that the T_G of a solid dispersion was increased towards that of the pure excipient in the absence of moisture, and much lower in the presence of moisture. This indicates that the presence of moisture increases the molecular mobility and tendency towards re-crystallisation. Differential scanning calorimetry (DSC) is a commonly used thermal analysis technique which measures the change in the heat capacity of a material as it is subjected to a heating cycle (usually in the range of 30–300 °C), and can be used to characterise the glass transition and crystallisation temperature ranges, heat of fusion, polymorphism and purity of a powder (Shreshtha *et al.*, 2007; Chadha & Bhandari, 2014). X-ray powder diffraction (XRPD) is used to distinguish between products in amorphous or crystalline state by plotting the intensity of X-ray diffraction against the diffraction angle. Materials in a crystalline state have a characteristic reflection pattern with more clearly defined peaks compared with amorphous substances, which have a typical "halo" appearance on the XRPD graph due to less clearly defined peaks (Cortes-Rojas & Oliveira, 2012; Chadha & Bhandari, 2014).

Solid glassy solutions contain the bioactive compound and carrier in a single, dispersed homogenous phase, and are characterised by DSC thermograms showing a single glass transition temperature peak. Solid glassy solutions are the best types of solid dispersions for optimal solubility and storage stability of powders (Dhirendra *et al.*, 2009; Patel *et al.*, 2015). Solid glassy suspensions, also known as two-phase blends, contain the bioactive compound in a partially miscible state with the excipient and tend to undergo phase separation more easily during storage. Solid crystalline suspensions contain the excipient in an amorphous state while the bioactive compound is in a crystalline state. This is reflected in DSC by the presence of two separate peaks for the excipient and the bioactive compound, which is an indication of no miscibility between the two (Dhirendra *et*

al., 2009; Baird & Taylor, 2012). Molecular diffusion is very slow in the glassy state, which results in improved shelf stability of products stored below the glass transition temperature, since the rate of chemical reactions and microbial growth is greatly reduced (Sablani *et al.*, 2007). The long-term stability of spray-dried food powders is often enhanced by the addition of pharmaceutically suitable excipients, surfactants and stabilisers to reduce the molecular mobility and prevent re-crystallisation. The presence of useful moieties like hydrogen donors/acceptors is an additional benefit of some excipients, due to their inhibitory effect on re-crystallisation from a glassy solution. General physical instability or nucleation is increased below the T_G due to higher molecular mobility, therefore the use of excipients with higher glass transition temperature are usually preferred (Vasconcelos *et al.*, 2007; Van den Mooter, 2012).

2.4.4.4. Colour

Practically all food and consumer products are associated with a specific physical appearance which serves as an indicator of quality, and colour is perhaps one of the most important. Spray-dried botanical extracts may be prone to colour changes as a result of ongoing oxidative degradation or moisture uptake (Cortes-Rojas *et al.*, 2012). Objective colour measurements can be obtained by a number of methods, but one of the most common methods is by using the CIE colour space, defined by the Commission International de l'Eclairage in 1976 and commonly referred to as CIE*L*a*b**. It provides a standardised three-dimensional representation for the perception of colour stimuli (Liew, *et al.*, 2008; Pathare *et al.*, 2013) (Fig. 2.25). The vertical axis represents the lightness (*L**) coordinate with a value ranging from 0 (black) to 100 (white). The chroma coordinates, *a** and *b**, represent the red/green and yellow/blue colour stimuli, respectively.

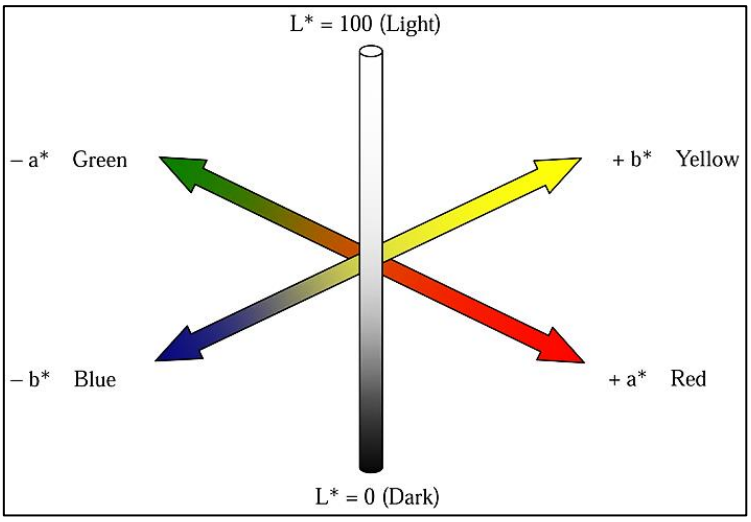

Figure 2.15 Graphic representation of CIE*L*a*b** colour space (Liew *et al.*, 2008).

2.4.4.5. Density and flow characteristics

The flow characteristics of powders intended for nutraceutical/pharmaceutical processing have an important effect on its handling properties in a number of other unit operations. Poor flowability of powders have, in extreme cases, resulted in the failure of some preparations to reach pilot-scale production (Prescott & Barnum, 2000). Since powder flow is complex, multidimensional and influenced by a host of factors, no single test can ever be used to quantify flowability. Powder flowability has been defined as "the ability of a powder to flow in a desired manner in a specific piece of equipment" (Prescott & Barnum, 2000). The interaction between various flow properties, e.g. density/compressibilty, cohesive strength and internal friction, may dictate what kind of manufacturing processes and rates are possible. Unit operations which are particularly affected by flow properties include powder transfer, storage, separation of small quantities from the bulk, blending, compaction and fluidisation process (Schwedes & Schulze, 1990; Prescott & Barnum, 2000).

The bulk density (ρ_B) of a powder is calculated by dividing its total mass by its bulk volume, which will differ depending on how compact the particles are arranged within the bulk. This is typically measured by pouring a specified mass of powder into a graduated cylinder and recording the resultant volume. This is sometimes called the *poured* bulk density as opposed to the *tapped* bulk density (or simply tapped density, ρ_T), which is calculated after subjecting the same mass of powdered sample in the cylinder to a standardised tapping treatment. This agitates the cylinder and allows the powder to settle into a more compact structure of lower volume, which is then used to calculate the tapped bulk density (Tenou *et al.*, 1999).

Flowability of powders are related to their capacity to overcome resistance to flow and move over each other, which involves the overcoming of surface interactions like *internal friction* and *cohesion*. The former is the Coulomb frictional resistance of one particle moving across another under normal atmospheric pressure. In the absence of pressure, forces of cohesion between particles may still cause resistance to flow, but these forces are also often strengthened by increased atmospheric pressure. In dry powders, Van der Waals forces are the major contributor to cohesion, but electrostatic and magnetic forces may also contribute (Fitzpatrick, 2013). Liquid also contributes to the strength of cohesive forces since liquid bridges will form between particles above a certain MC, and this will produce capillary forces through surface tension. Van der Waals forces will be significantly reduced by the increased MC, but the capillary forces tend to be much stronger and will result in a net increase in cohesion (Tenou *et al.*, 1999).

Several techniques are available to measure powder flowability, varying from advanced to simple techniques (Tenou *et al.*, 1999; Prescott & Barnum, 2000; Sarraguca *et al.*, 2010). The Hausner ratio, defined as the ratio of the tapped to the poured bulk density of a powder, serves as an index of its flow characteristics (Table 2.6). Higher Hausner ratio values (>1.35) denote a greater value difference between the tapped and poured bulk densities, thus indicating that greater intra-

particle cohesive forces were present before tapping of the cylinder was carried out. Greater cohesion between particles result in poorer flowability, and increasing ranges of Hausner ratio values are labelled accordingly. A value equal to 1.0 indicates that tapped and poured bulk densities were equal, with tapping having caused no additional compaction of the bulk. This would be associated with excellent free-flowing properties due to the low or non-existent cohesive forces between particles.

Powder flow properties can also be assessed by measuring the angle of repose (Fig. 2.26), which refers to the angle relative to the horizontal plane formed by a standardised heap of powder, with a sharper angle indicative of less cohesive, highly flowable powder (Fitzpatrick, 2013). A number of methods are available to measure the angle of repose, and values may differ depending on whether a wedge-shaped, conical or rotating drum-type heap is used (Schulze, 2006). The Carr compressibility index (CCI) is another indirect measure of the resistance to flow (Table 2.6), with a lower Carr index value indicating better flowability (Carr, 1965). It can be calculated using the formula:

$$\mathrm{CCI} = 100\left(1 - \frac{\rho_B}{\rho_T}\right)$$

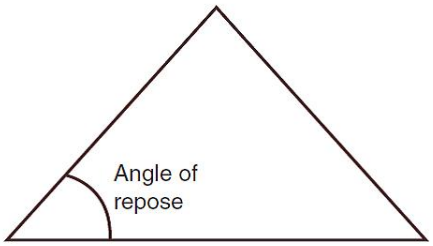

Figure 2.26 Angle of repose as index of powder flowability (Fitzpatrick, 2013).

Table 2.6 Powder flow characteristics based on Carr index and Hausner ratio (Carr, 1965; Fitzpatrick, 2013).

Flow character	Carr compressibility index (%)	Hausner ratio
Very, very poor	>38	>1.60
Very poor	32–37	1.46–1.59
Poor	26–31	1.35–1.45
Passable	21–25	1.26–1.34
Fair	16–20	1.19–1.25
Good	11–15	1.12–1.18
Excellent	0–10	1.00–1.11

2.4.4.4. Wettability

The solubility and dispersibility of botanical extract powders in an aqueous environment are important attributes to consider in the development such products for nutraceutical applications. The wettability of a powder will have a substantial effect on its overall solubility, since wetting is a precursor to dissolution (Mitsui & Takada, 1969; Anderson, 1986). One of the commonly employed methods for the characterisation of wettability properties of powders is measurement of the contact angle, which briefly entails the following: a sample of powder is pressed flat, whereafter a droplet of deionised water is deposited on the surface, and the interaction between the water and the powder sample is recorded by high-definition video imaging equipment. The first frame of video that depicts a well-defined and vibration-free droplet is then used to measure the contact angle through the liquid phase (Aucamp, M., 2016, Department of Pharmaceutical Sciences, North West University, personal communication, 8 March)

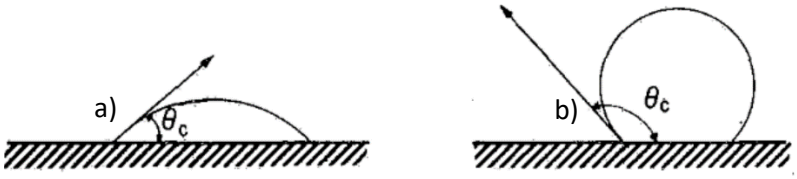

Figure 2.27 Contact angle (θ_c) measurements of a) <90° and b) >90°, indicating good and poor wettability properties, respectively (adapted from Anderson, 1986).

The magnitude of the contact angle (Fig. 2.27) is inversely related to the degree of wettability, i.e. the smaller the contact angle the more wettable the powder, and, in general, contact angles below 90 °C indicate good wettability properties (Anderson, 1986). Powders with poor wettability properties will have minimal contact with surface of the water droplet and appear to "repel" the droplet, resulting in an obtuse contact angle value (Hogekamp & Schubert, 2009; Yuan & Lee, 2013).

2.4.5. Effect of spray-drying process parameters on product characteristics and yield

The efficient spray-drying of any material will depend greatly on the choice of processing parameters and the nature of the ingoing feed. The process parameters which are generally considered to have the most significant effect on product quality are the inlet air temperature, outlet air temperature, feed concentration, feed temperature, feed flow rate and drying air flow rate (Gharsallaoui *et al.*, 2007; Woo *et al.*, 2007; Patel *et al.*, 2009; Lebrun *et al.*, 2012; Woo & Bhandari, 20013; Costa *et al.*, 2015; Patel *et al.*, 2015). Table 2.7 and Fig. 2.28 summarise the effects of various processing parameters on the process output.

The inlet air temperature is directly related to the drying rate and the MC of the final product (Patel *et al.*, 2015). An extremely high inlet air temperature can cause rapid evaporation of moisture and subsequent formation of defects and cracks in the coating, with resultant degradation of core material. A low inlet temperature leads to a lower evaporation rate and the subsequent development of dense microcapsule crusts, and a final product with high MC and increased tendency to agglomerate. Bakowska-Barczak & Kolodziejczyk (2011) investigated the microencapsulation of black currant (*Ribes nigrum* L.) polyphenols by spray drying using maltodextrins DE11, DE18 and DE21 and inulin as wall material. Maltodextrin DE11 provided higher yields and better polyphenol encapsulation than DE 18 and 21. Although inulin was less effective than maltodextrin in the encapsulation of polyphenols, the yield obtained with inulin did not significantly differ from maltodextrin DE11, which provided the highest overall yield. Drying air inlet temperatures of 150–205 °C were evaluated and it was shown that higher temperatures were associated with lower MC. The MC of all powders ranged from 1.8 to 3.9%.

Table 2.7 Summarised effects of various spray-drying process parameters on process outputs (adapted from Patel *et al.*, 2015).

Parameter	Effect on spray drying process
Use of organic solvent	1. Produces smaller particles due to lower surface tension
Increased drying air inlet temperature	1. Increases outlet temperature proportionally 2. Increases yield 3. Less sticky product
Increased drying air flow rate	1. Decreased outlet temperature 2. Smaller powder particles sizes due to decreased size of atomised droplets at nozzle outlet
Increased spray drying solution feed rate	1. Decreased outlet temperature 2. Increased moisture content in final product 3. Increased droplet size at nozzle outlet resulting in larger powder particles
Increased drying air humidity	1. Increased moisture content in final product 2. Decreased yield due to adherence of moist particles to drying chamber
Increased feed solution solids concentration and viscosity	1. Higher outlet temperature due to proportionally less solvent content and therefore less heat consumption for drying 2. May increase particle size due to higher solids content in atomised droplet 3. Decreased moisture content in final product
Increased aspirator rate	1. Decreased outlet temperature 2. Decreased moisture content in final product 3. More effective separation of particles in cyclone with resultant higher yield

Dependent variable (responses)	Independent variable (parameter)						
	Aspirator flow rate ↑	**Humidity of drying air** ↑	**Inlet air temperature** ↑	**Inlet air flow rate** ↑	**Feed flow rate** ↑	**Feed concentration** ↑	**Organic solvent instead of water** ↑
Outlet temperature	↑↑	↑	↑↑↑	↓	↓↓	↑↑	↑↑↑
Particle size	X	X	X	↓↓↓	↑	↑↑↑	↓
Humidity in final product	↓↓	↑↑	↓↓	X	↑↑	↓	↓↓↓
Yield	↑↑	X	↑	X	↑	↑	↑↑

Legend			
↑↑↑	High influence		Increasing parameter
↑↑	Moderate influence		Increasing dependent variable
↑	Minor influence		Decreasing dependent variable
X No influence			

Figure 2.28 Influence of various parameters on responses in typical spray-drying process (adapted from Büchi, 2009).

Belščak-Cvitanović *et al.* (2015) investigated the use of different natural biopolymers (alginate, pectin, carrageenan, modified corn starch, acacia gum, guar gum, xanthan, locust bean gum, whey proteins, pea flour, oligofructose and inulin) as encapsulants for a green tea extract spray-dried with a Büchi B-290 Mini spray-dryer. The inlet air temperature, air flow rate, rate of liquid feed, atomisation pressure and pump speed were 130 °C, 536 $L.h^{-1}$, 8 $mL.min^{-1}$, 6 psi and 30%, respectively. All powders had sufficiently low MC to ensure good storage stability (<2.35%).

The outlet air temperature is usually measured between the drying cylinder outlet and the cyclone and is considered one of the most important parameters to consider when developing and optimising the process, since it is the highest temperature to which the product is exposed in the drying space and will therefore have a significant impact on the characteristics of the dried product collected at the outlet (Büchi, 2009; Costa *et al.*, 2015). The outlet air temperature is not under direct control of the operator, as it depends on the drying characteristics of the given material, the inlet air temperature, aspiration rate and the flow rate of product through the drying space (Patel *et al.*, 2015). An increase in the feed flow rate leads to a decrease in the outlet air temperature due to the increased amount of water entering the system and subsequent increase in evaporative cooling. However, an excessive increase in the feed flow rate could lead to deposition of droplets on the walls of the drying cylinder due to inadequate drying of the increased water content in the system.

This would lead to an undesirable decrease in the process yield and the feed flow rate must therefore be adjusted accordingly (Keshani *et al.*, 2015).

The feed concentration and characteristics will also affect the powder characteristics. The presence of low molecular weight substances with a low T_G in the feed will lead to high molecular mobility (even at relatively low temperatures), a highly hygroscopic, sticky powder and lower yields (Gharsallaoui *et al.*, 2007). Spray-drying of products with a high sugar or fat content is often associated with this type of problem, but the addition of carriers with higher molecular weight typically improves the yield significantly by increasing the glass transition temperature (Le Meste *et al.*, 2002). The feed temperature affects the viscosity and flow properties of the ingoing material and thus also its capacity to be spray-dried homogeneously. Higher feed temperature leads to decreased viscosity and smaller droplet size (Cal & Sollohub, 2010). The feed flow rate regulates the amount of feed which is delivered to the atomiser per time unit, and should be adjusted so that each sprayed droplet attains the desired level of drying before it reaches the surface of the drying chamber (Patel *et al.*, 2015).

2.4.5.1. Optimisation of spray drying by response surface methodology (RSM)

A multivariate statistical method can be applied to determine various processing parameters and material attributes which may have individual and interactive effects on the product characteristics. With RSM the number of experiments required can be limited (Steinberg & Bursztyn, 2010). The frequent use of spray drying in the production of microencapsulated plant extracts, and the associated problem of varying quality of natural raw materials, prompted the application of quality-by-design methodology by researchers in an attempt to describe a feasible design space for these processes. Details of selected studies and process parameters investigated, using laboratory-scale spray-dryer equipment, are summarised in Table 2.8.

Baldinger *et al.* (2012) applied QbD methodology to optimise the physicochemical properties and yield of an inhalable spray-dried powder obtained from an aqueous solution of 10% trehalose: mannitol (9:1). The factors most likely to have a significant effect on the final product quality were identified by means of a risk assessment screening step based on data in the existing knowledge space. An Ishikawa (fishbone) diagram was constructed to group these factors in a systematic fashion, with those ultimately selected for further investigation indicated with bold italic script (Fig. 2.29). The effect of the inlet air temperature (110–220 °C), atomisation air flow rate (7.3–29.1 $L.min^{-1}$) and feed flow rate (2.5–7.5 $mL.min^{-1}$) were investigated. Spray drying was carried out with a concurrent flow Büchi Mini spray-dryer B-290 (Büchi Labortechnik AG, Flawil, Switzerland) equipped with a 0.7 mm two-fluid nozzle set at 100% aspiration rate. It was found that the particle diameter increased with increased inlet air temperature in a positive non-linear fashion, and that increasing the

feed flow rate and atomisation air flow rate both showed minor negative effects on the particle size. The yield, expressed as the ratio between the obtained amount of powder and the expected amount of powder, ranged between 7.7 and 91% (Fig. 2.30). The inlet air temperature had a marked negative effect on the yield, and this was explained by the fact that the higher the inlet air temperature, the higher the outlet temperature at the end of the drying zone. The increased outlet temperature increased agglomeration of the trehalose-mannitol blend in the spray-dryer due to the rubbery state of trehalose at this temperature, which is above its glass transition temperature of 107 °C (Baldinger *et al.*, 2012).

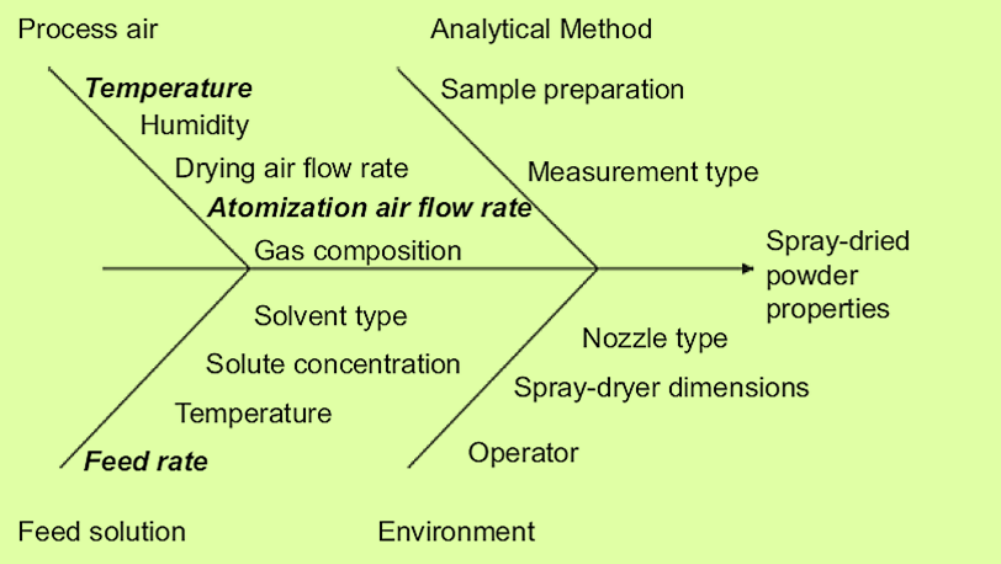

Figure 2.29 Risk assessment using Ishikawa (fishbone) diagram showing factors which may affect the quality of spray-dried powder (Baldinger *et al.*, 2012).

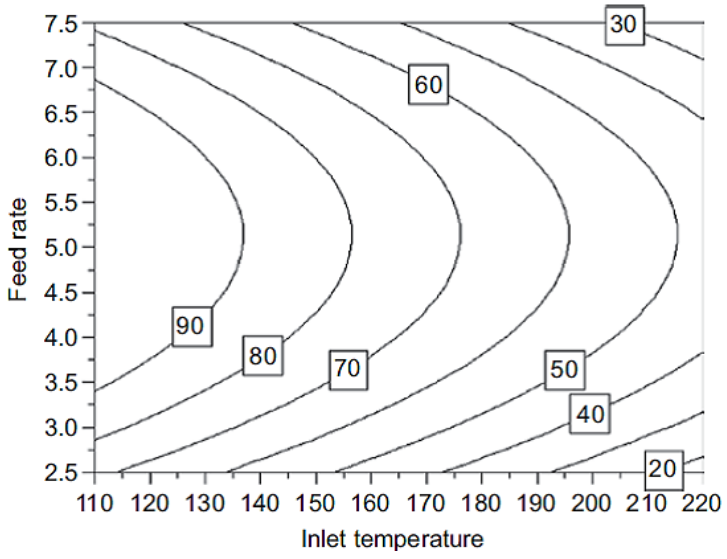

Figure 2.30 Two-dimensional contour response surface indicating ranges of inlet temperature (°C) and feed rates (mL.min^{-1}) within which optimal product yields can be achieved for the production by spray-drying of an inhalable mannitol-trehalose powder (Baldinger *et al.*, 2012).

Chaubal & Popescu (2008) also used the Büchi Mini B-290 spray-dryer to investigate the effect of air inlet temperatures between 80 and 120 °C on the microencapsulation efficiency of itraconazole preparations using mannitol, lactose, dextrose and sucrose as carriers. High inlet temperatures were associated with excessive sticking of particles to the drying chamber, whereas lower inlet temperatures produced microcapsules with higher residual MC. The carriers with lower glass transition temperatures, e.g. sucrose (T_G = 62 °C) and dextrose (T_G = 32 °C), were associated with sticky powders, but those with higher glass transition temperatures, e.g. mannitol (T_G = 87 °C) and lactose (T_G = 101 °C) produced free-flowing powders. The choice of carrier was also shown to affect the quality of the final product, with the lactose-containing formulation exhibiting higher residual MC (4–6%) than the mannitol-containing formulations (<2% MC). Mannitol was ultimately selected as the ideal carrier based on it satisfying the widest array of criteria for high product quality. The authors concluded that particle sizes and morphologies were affected mainly by spray-drying process parameters and less so by the type of carrier material used.

Cortes-Rojas & Oliviera (2012) obtained the highest product yield (86.9%) with a formulation containing microcrystalline cellulose and colloidal silicon dioxide in a 3:1 mass ratio. The cellulose served to reduce the stickiness of the powder, similar to results reported by Cano-Chauca *et al.* (2005). The blend of colloidal silicon dioxide and maltodextrin exhibited a lower yield (65.5%) due to the stickiness of the product. The T_G of the carrier had a significant impact on the recovery of product, because the heating of amorphous materials above their glass transition temperatures causes a transition to a rubbery state prone to excessive stickiness (Le Meste *et al.*, 2002). The T_G of maltodextrins are inversely related to their dextrose equivalents (DE), which is an indication of the reducing sugar content compared with glucose (DE = 100), and increasing molecular weight is also associated with an increase in the T_G (Costa *et al.*, 2015).

De Barros Fernandes *et al.* (2013) investigated the effect of varying inlet air temperature (135–195 °C), wall material concentration (10–30%) and feed flow rate (0.5–1.0 $L.h^{-1}$) on the microencapsulation efficiency of rosemary oil with gum arabic as carrier and using a two-fluid atomiser with air flow at 40 $L.min^{-1}$. By increasing the inlet air temperature higher yields were obtained, while an increase in the feed solids concentration reduced the yield. The highest solid concentration possible should be aimed for in optimisation, as this reduces the relative amount of water to be removed from the feed, but this decision should take into account the potential disadvantages of high feed concentrations, i.e. clogging of the atomiser nozzle and reduced yields (Gharsallaoui *et al.*, 2007). The inlet air temperature had the most significant effect on the hygroscopicity of the powders, with lower temperatures resulting in lower hygroscopicity values. Powders produced at lower inlet temperatures typically have a higher residual MC, and therefore exhibit a lower water concentration gradient between the atmosphere and the product. The higher the feed flow rate, the lower were the hygroscopicity values, which resulted from the higher residual

MC in the samples caused by a relatively short residence time within the drying cylinder. Optimised conditions for spray-drying (wall material concentration of 19.3%, feed flow rate of 0.92 $L.h^{-1}$, and an inlet air temperature of 171 °C) were identified using RSM and desirability profiling.

Jangam & Thorat (2010) optimised the spray drying of ginger (*Zingiber officinale*) extract and found that the inlet air temperature was the most significant factor affecting yield and retention of polyphenols, with a higher inlet temperature leading to lower levels of 6-gingerol, which was attributed to heat degradation of the compound in question. Increasing the atomisation pressure also had a negative effect on retention of polyphenols, since the higher pressure probably produced smaller aerosolised droplets with an increased surface area to volume ratio which facilitated increased losses of the 6-gingerol.

Table 2.8 Details of selected spray-drying optimisation studies.

Reference	Product Spray-dryer model	Carriers	Experimental design	Process parameters	Responses investigated
Moreira *et al.*, 2009	Acerola (*Malpighia emarginata*) pomace extract Büchi B-290	MD (DE ns) CTG	• CCD • 3 factors • 17 treatments • 3 reps of CP	<u>Varied:</u> • IT: 170–200 °C • C:E ratio (2:1–5:1) • MD:CTG mass ratio (0–1.0) <u>Constant:</u> • Feed FR: 0.49 $kg.h^{-1}$ • Pump rate: 1.23 $kg.h^{-1}$ • Aspirator FR: 5.51×10^4 $kg.h^{-1}$	• Flowability (AOR) • Hygroscopicity • MC • WS
Tan *et al.*, 2015	Aqueous bitter melon (*Momordica charantia* L.) extract Büchi B-290	MD (DE 18) GA	• CCD • 2 factors • 11 treatments • 3 reps of CP	<u>Varied:</u> • Carrier solution concentration: 23–37% • Extract: carrier solution ratio ($g.g^{-1}$) (0.3–1.71) <u>Constant:</u> • IT: 150 ± 2 °C • OT: 85 ± 2 °C • Feed FR: 14–16 $mL.min^{-1}$ • Drying air flow rate 35 $m^3.h^{-1}$ • Aspirator capacity 70% • Compressed air flow rate 473 $L.h^{-1}$ • MD:GA mass ratio 1:1	• MC • TPC • Saponins content • Flavonoid content • TAA • Yield
Tee *et al.*, 2012	Sirih (*Piper betle* L.) leaf extract Büchi B-290	MD (DE 9-12)	• BBD • 3 factors • 17 treatments • 5 reps of CP	<u>Varied:</u> • IT: 120–160 °C • Feed FR: 5–15 $mL.min^{-1}$ • Aspirator rate 80–100% <u>Constant:</u> • MD concentration 5% $m.v^{-1}$	• Hydroxychavicol content • PSD • MC • Yield • Hygroscopicity

				• C:E mass ratio (1:1)	
Tonon *et al.*, 2008	Açai (*Euterpia olaraceae* Mart.) pulp LabPlant SD-05	MD (DE 9-12)	• CCD • 3 factors • 17 treatments • 3 reps of CP	<u>Varied:</u> • IT: 138–202 °C • Feed FR (5-25 $g.min^{-1}$) • MD concentration (10–30%) <u>Constant:</u> • Drying air FR: 73 $m^3.h^{-1}$ • Compressor air pressure 0.006 MPa	• Anthocyanin content • Hygroscopicity • MC • Powder morphology • PSD • Yield
Toneli *et al.*, 2010	Chicory (*Cichorium* intybus) root inulin Büchi B-191	None	• 2^3 factorial design • 3 factors • 10 treatments • 2 reps of CP	<u>Varied:</u> • IT: 130–210 °C • Pump Speed (5.0-35.5%) • Feed temperature: 25-60 °C <u>Constant:</u> • Drying air FR: 600 $L.h^{-1}$ • Aspirator capacity 70%	• OT • Powder morphology • Yield

AOR, angle of repose; BBD, Box-Behnken Design; CCD, central composite design; C: E, carrier: extract; CTG, cashew tree gum; CP, centre point; DE, dextrose equivalent; FR, flow rate; GA, gum arabic; IT, inlet temperature; MC, moisture content; MD, maltodextrin; ns, not stated; OT, outlet temperature; PSD, particle size distribution; TAA, total antioxidant activity; TPC, total polyphenol content; WS, water solubility.

2.4.6. Spray-drying of rooibos extracts

No published studies as of the time of writing have focussed exclusively on the optimisation of the spray-drying of rooibos extracts. The first published article on this topic (Joubert, 1988a) investigated the effect of agglomeration on the properties of spray-dried rooibos tea, using a fixed-bed extractor with water at 60 °C and a flow rate of 0.1 $m^3.hr^{-1}$ for 24 min to obtain an extract, after which it was concentrated to the desired level (22%; $m.m^{-1}$) using a climbing film evaporator. No investigations were carried out on the effects of the extraction conditions on process responses (e.g. yield or polyphenol retention), since this study was concerned mainly with the powder agglomeration unit operation. The aqueous rooibos extract was combined with maltodextrin (DE 10) in a 1:1 mass ratio to a final concentration of 36% soluble solids. Drying was carried out using an Anhydro pilot plant-scale spray-dryer, with the inlet and outlet air temperatures maintained at 200±10 and 90±10 °C, respectively. The feed solution (at ambient temperature) was fed into the system at a rate of ca. 120 $kg.hr^{-1}$. A fine, light-brown powder with a bulk density of 0.654 $g.mL^{-1}$ and MC of 3.3% was obtained. Agglomeration of the spray-dried powder was then carried out using a laboratory-scale spray granulator. There was a significant difference in the particle size distribution of the powder before and after agglomeration. Before agglomeration, only 3.5% of the particles were larger than 180 µm, compared with 45.1% after agglomeration. The agglomerated powder had

higher MC (5.6%), a darker colour, decreased bulk density (0.497 $g.mL^{-1}$) and improved bulk flow and wettability properties.

Another study (Joubert, 1990a) investigated and compared the chemical and sensory attributes of spray- and freeze-dried rooibos extracts. Soluble solids which precipitated upon cooling of a freshly prepared rooibos concentrate were isolated, and their effects on the sensory qualities and chemical composition of the tea were investigated. The method of drying and the removal of the precipitate did not significantly affect the sensory attributes of the dried tea extract, but the total polyphenol, flavonoid, flavonol, tannin and proanthocyanidin content of the dried extract were all significantly reduced by the removal of the precipitate. The spray-dried and freeze-dried extracts differed significantly in their physical appearance and reconstitutability. The spray-dried powder was lighter in colour than the freeze-dried flakes, which can be attributed to the light scattering of trapped air between and within the hollow particles (Pintauro, 1970).

A study by Joubert *et al.* (2009) investigated whether spray-drying reduced the aspalathin, orientin and iso-orientin content rooibos extract concentrate. Samples for analysis were taken on-line during commercial production. Spray-drying was found to have no significant effect ($P < 0.05$) on the content of these three compounds. These results have not yet been confirmed under controlled conditions in a laboratory. No other articles have been published in which the rooibos extract spray-drying process itself was investigated or optimised.

2.5. Conclusion

Unfermented or green rooibos (GR) has in recent years gained a small foothold in the local and export market for herbal teas. The oxidative changes which are induced in the production of conventional fermented rooibos are deliberately minimised in the production of GR, resulting in the presence of significantly higher levels of aspalathin, a phenolic compound unique to rooibos. The higher aspalathin content of GR was shown to result in significantly higher antioxidant activity, and subsequent research studies have revealed a number of potential health-promoting effects associated with aspalathin. The potential antidiabetic effect of aspalathin, either in pure form or in an aspalathin-enriched green rooibos extract (GRE), has garnered a notable amount of attention. Aspalathin is a highly water-soluble flavonoid which could be safely extracted using water alone. Spray-drying of such an extract in the presence of a suitable carrier material would be a relatively simple and cost-effective method of converting it to a low-moisture, encapsulated powder, which would serve to protect the desirable phenolic content against further oxidative degradation and allow for its incorporation into tablet or capsule form. GREs containing high levels of aspalathin could be commercialised as an antidiabetic functional food ingredient or nutraceutical. The natural variation in the raw plant material intended for extraction, as well as the large number of variables involved in both the extraction and spray-drying unit operations, could lead to inconsistent batch-to-

batch quality, however. Quality-by-design (QbD) methodology could be applied to the extraction and spray-drying processes to gain a deeper understanding of the interplay between the various process parameters and material attributes and their effects on the process outputs. QbD, as advocated by the United States Food and Drug Administration, has been applied to optimised the extraction and spray-drying processes of a wide variety of food and pharmaceutical products, and the application of its principles to GRE production would be a first step towards establishing a feasible design space in which a consistent level of quality could be maintained.

2.6. References

Aherne, S.A. & O'Brien, N.M. (2002). Dietary flavonoids: chemistry, food content and metabolism. *Nutrition*, **18**, 75–81.

Al-Muhtaseb, A.H., McMinn, W.A.M. & Magee, T.R.A. (2002). Moisture sorption isotherm characteristics of food products: a review. *Food and Bioproducts Processing*, **80**, 118–128.

Amaro, M.I., Tajber, L., Corrigan, O.I. & Healy, A.M. (2011). Optimisation of spray drying process conditions for sugar nanoporous microparticles (NPMPs) intended for inhalation. *International Journal of Pharmaceutics*, **421**, 99–109.

Anderson, W.G. (1986). Wettability literature survey – part 2: wettability measurement. *Journal of Petroleum Technology*, **38**, 1246–1261.

Anonymous (1967). Rooibos Tea Control Board 12th Annual Report. Clanwilliam, South Africa.

Anonymous (2010a). Agricultural Product Standards Act. Act No. 119 of 1990. G.N.R. 568/2010. Pretoria, South Africa: Government Printing Works.

Anonymous (2010b). Foodstuffs, Cosmetics and Disinfectants Act. Act No. 54 of 1972. G.N.R. 146/2010. Pretoria, South Africa: Government Printing Works.

Anonymous (2013). The Plant List Version 1.1. [Internet document]. URL http://www.theplantlist.org. 04/02/2016.

Anonymous (2014a). A profile of the South African rooibos tea market value chain. Department of Agriculture, Forestry and Fisheries. Pretoria, South Africa: Government Printing Works.

Anonymous (2014b). Rooibos name protected in EU trade pact. South African Press Association. [Internet document]. URL http://www.fin24.com/Companies/Agribusiness/Rooibos-name-protected-in-EU-trade-pact-20140722. 04/02/2016.

Anonymous (2015a). Albany Ultima health range. [Internet document]. URL http://www.albany.co.za/ultima.php. 09/11/2015.

Anonymous (2015b). Rooibos wooded wines. [Internet document]. URL http://www.audacia.co.za/wines.html. 09/11/2015.

Anonymous (2015c). Stellenbrau — our story. [Internet document]. URL http://stellenbrau.co.za/pages/our-story.php. 09/11/2015.

Ansley, D.M. & Wang, B. (2013). Oxidative stress and myocardial injury in the diabetic heart. *Journal of Pathology*, **229**, 232-241.

Azmir, J., Zaidul, I.S.M., Rahman, M.M., Sharif, K.M., Mohamed, A., Sahena, F., Jahurul, M.H.A., Ghafoor, K., Norulaini, N.A.N. & Omar, A.K.M. (2013). Techniques for extraction of bioactive compounds from plant materials: a review. *Journal of Food Engineering*, **117**, 426–436.

Baird, J.A. & Taylor, L.S. (2012). Evaluation of amorphous solid dispersion properties using thermal analysis techniques. *Advanced Drug Delivery Reviews*, **64**, 396–421.

Bakowska-Barczak, A.M & Kolodziejczyk, P.P. (2011). Black currant polyphenols: their storage stability and microencapsulation. *Industrial Crops and Products*, **34**, 1301–1309.

Baldinger, A., Clerdent, L., Rantanen, J., Yang, M. & Groghanz, H. (2012). Quality by design approach in the optimization of the spray drying process. *Pharmaceutical Development and Technology*, **17**, 389–397.

Ballard, T.S., Mallikarjunan, P., Zhou, K. & O'Keefe, S. (2010). Microwave-assisted extraction of phenolic antioxidant compounds from peanut skins. *Food Chemistry*, **120**, 1185–1192.

Baş, D. & Boyaci, I.H. (2007). Modelling and optimisation I: usability of response surface methodology. *Journal of Food Engineering*, **78**, 836–845.

Baranska, M., Schulz, H., Joubert, E. & Manley, M. (2006). In situ flavonoid analysis by FT-Raman spectroscopy: identification, distribution, and quantification of aspalathin in green rooibos (*Aspalathus linearis*). *Analytical Chemistry*, **78**, 7716–7721.

Beelders, T., Sigge, G.O., Joubert, E., De Beer, D. & De Villiers, A. (2012). Kinetic optimisation of the reversed phase liquid chromatographic separation of rooibos tea (*Aspalathus linearis*) phenolics on conventional high-performance liquid chromatographic instrumentation. *Journal of Chromatography A*, **1219**, 128–139.

Belščak-Cvitanović, A., Lević, S. Kalušević, A., Špoljarić, I., Đorđević, V., Komes, D., Mršić, G. & Nedović, V. (2015). Efficiency assessment of natural biopolymers as encapsulants of green tea (*Camellia sinensis* L.) bioactive compounds by spray drying. *Food and Bioprocess Technology*, **8**, 2444–2460.

Beltrán-Debón, R., Rull, A., Rodríguez-Sanabria, F., Iswaldi, I., Herranz-López, M., Aragonès, G., Camps, J., Alonso-Villaverde, C., Menéndez, J.A., Micol, V. & Segura-Carretero, A. (2011). Continuous administration of polyphenols from aqueous rooibos (*Aspalathus linearis*) extract ameliorates dietary-induced metabolic disturbances in hyperlipidemic mice. *Phytomedicine*, **18**, 414–424.

Bezerra, M.A., Santelli, R.E., Oliveira, E.P., Villar, L.S. & Escaleira, L.A. (2008). Response surface methodology (RSM) as a tool for optimisation in analytical chemistry. *Talanta*, **76**, 965–977.

Biénabe, E., Bramley, C. & Kirsten, J. (2009). An economic analysis of the evolution in intellectual property strategies in the South African agricultural sector: the rooibos industry. In: *The Economics of Intellectual Property in South Africa* (edited by E. Burrone & P. Rai). Pp. 56–83. Geneva: World Intellectual Property Organisation.

Blommaert, K.L.J. & Steenkamp, J. (1978). Tannin and possible caffeine content of rooibos tea, *Aspalathus* (Subgen. Nortiera) *linearis* (Burm.Fil) R. Dahlgr. [Afrikaans]. *Agroplantae*, **10**, 49.

Bosman, S.C. (2014). Development of a xanthone-enriched honeybush tea extract. MSc Food Science Thesis, Stellenbosch University, South Africa.

Bramati, L., Minoggio, M., Gardana, C., Simonetti, P., Mauri, P. & Pietta, P. (2002). Quantitative characterization of flavonoid compounds in rooibos tea (*Aspalathus linearis*) by LC-UV/DAD. *Journal of Agricultural and Food Chem*istry, **50**, 5513–5519.

Bramati, L., Aquilano, F. & Pietta, P. (2003). Unfermented rooibos tea: quantitative characterization of flavonoids by HPLC-UV and determination of the total antioxidant activity. *Journal of Agricultural and Food Chemistry*, **51**, 7472–7474.

Brazier-Hicks, M. & Edwards, R. (2013). Metabolic engineering of the flavone-*C*-glucoside pathway using polyprotein technology. *Metabolic Engineering*, **16**, 11–20.

Breiter, T., Laue, C., Kressel, G., Gröll, S., Engelhardt, U.H. & Hahn, A. (2011). Bioavailability and antioxidant potential of rooibos flavonoids in humans following the consumption of different rooibos formulations. *Food Chemistry*, **128**, 338–347.

Büchi (2009). *B-290 Operation Manual Version H.* Flawil, Switzerland: Büchi Labortechnik AG.

Bucić-Kojić, A., Planinić, M., Tomas, S., Bilić, M. & Velić, D. (2007). Study of solid-liquid extraction kinetics of total polyphenols from grape seeds. *Journal of Food Engineering*, **81**, 236–242.

Cal, K. & Sollohub, K. (2010). Spray drying technique. I: Hardware and process parameters. *Journal of Pharmaceutical Sciences*, **99**, 575–586.

Caliskan, G. & Dirim, S.N. (2013). The effects of the different drying conditions and the amounts of maltodextrin addition during spray drying of sumac extract. *Food and Bioproducts Processing*, **91**, 539–548.

Cano-Chauca, M., Stringheta, P.C., Ramos, A.M. & Cal-Vidal, J. (2005). Effect of the carriers on the microstructure of mango powder obtained by spray drying and its functional characterization. *Innovative Food Science and Emerging Technologies*, **6**, 420–428.

Carr, R.L. (1965). Classifying flow properties of solids. *Chemical Engineering*, **72**, 69–72.

Chadha, R. & Bhandari, S. (2014). Drug-excipient compatibility screening — role of thermoanalytical and spectroscopic techniques. *Journal of Pharmaceutical and Biomedical Analysis*, **87**, 82–97.

Chandini, S.K., Rao, L.J., Gowthaman, M.K., Haware, D.J. & Subramanian, R. (2011). Enzymatic treatment to improve the quality of black tea extracts. *Food Chemistry*, **127**, 1039–1045.

Chaubal, M.V. & Popescu, C. (2008). Conversion of nanosuspensions into dry powders by spray drying: a case study. *Pharmaceutical Research*, **25**, 2302–2307.

Chemat, F., Huma, Z.-E. & Khan, M.K. (2011). Applications of ultrasound in food technology: processing, preservation and extraction. *Ultrasonics Sonochemistry*, **18**, 813–835.

Chemat, F., Vian, M.A. & Cravotto, G. (2012). Green extraction of natural products: concept and principles. *International Journal of Molecular Sciences,* **13**, 8615–8627.

Chen, X.D. (2005). Air drying of food and biological materials — modified Biot and Lewis number analysis. *Drying Technology*, **23**, 2239–2248.

Chen, S., Xing, X.H., Huang, J.J. & Xu, M.S. (2011). Enzyme-assisted extraction of flavonoids from *Ginkgo biloba* leaves: improvement effect of flavonol transglycosylation catalyzed by *Penicillium decumbens* cellulase. *Enzyme and Microbial Technology*, **48**, 100–105.

Chethan, S. & Malleshi, N.G. (2007). Finger millet polyphenols: optimization of extraction and the effect of pH on their stability. *Food Chemistry*, **105**, 862–870.

Chiou, D. & Langrish, T. (2007). Development and characterisation of novel nutraceuticals with spray drying technology. *Journal of Food Engineering*, **82**, 84–91.

Coetzee, G., Joubert, E., Van Zyl, W.H. & Viljoen-Bloom, M. (2014). Improved extraction of phytochemicals from rooibos with enzyme treatment. *Food and Bioproducts Processing*, **92**, 393–401.

Corbit, R.M., Ferreira, J.F.S., Ebbs, S.D. & Murphy, L.L. (2005). Simplified extraction of ginsenosides from American ginseng (*Panax quinquefolius* L.) for high-performance liquid chromatography-ultraviolet analysis. *Journal of Agricultural and Food Chemistry*, **53**, 9867–9873.

Cortes-Rojas, D.F. & Oliveira, W.P. (2012). Physicochemical properties of phytopharmaceutical preparations as affected by drying methods and carriers. *Drying Technology*, **30**, 921–934.

Cossuta, D., Vatai, T., Báthori, M., Hohmann, J., Keve, T. & Simándi, B. (2012). Extraction of hyperforin and hypericin from St. John's Wort (*Hypericum perforatum*) with different solvents. *Journal of Food Process Engineering*, **35**, 222–235.

Costa, S.S., Machado, B.A.S., Martin, A.R., Bagnara, F, Ragadalli, S.A. & Alves, A.R.C. (2015). Drying by spray drying in the food industry: micro-encapsulation, process parameters and main carriers used. *African Journal of Food Science*, **9**, 462–470.

Costabile, A., Kolida, S., Klinder, A., Gietl, E., Bauerlein, M., Frohburg, C., Landschutze, V. & Gibson, G.R. (2010). A double-blind, placebo-controlled, cross-over study to establish the bifidogenic effect of a very-long chain inulin extracted from globe artichoke (*Cynara scolymus*) in healthy subjects. *British Journal of Nutrition*, **104**, 1007–1017.

Couto, R.O., Araújo, R.R., Tacon, L.A., Conceição, E.C., Bara, M.T.F., Paula, J.R. & Freitas, A.P. (2011). Development of a phytopharmaceutical intermediate product via spray drying. *Drying Technology*, **29**, 709–718.

Dahlgren, R. (1968). Revision of the genus *Aspalathus*. II. The species with the ericoid and pinoid leaflets. 7. Subgenus Nortiera. With remarks on rooibos tea cultivation. *Botaniska Notiser*, **121**, 165–208.

Dahlgren, R. (1988). Crotalarieae (*Aspalathus*). *Flora of Southern Africa*, **16**, 84–90.

Dai, Y., Witkamp, G.J., Verpoorte, R. & Choi, Y.H. (2013). Natural deep eutectic solvents as a new extraction media for phenolic metabolites in *Carthamus tincorius*. *Analytical Chemistry*, **85**, 6272–6278.

Das, A.K., Mandal, S.C., Mandal, V., Beg, S. & Singh, B. (2014). QbD as an emerging paradigm in extraction technology for developing optimized bioactives. *Pharma Times*, **46**, 50–56.

De Barros Fernandes, R.V., Borges, S.V., Botrel, D.A, Silva, E.K., Da Costa, J.M.G. & Queioz, F. (2013). Microencapsulation of rosemary essential oil: characterization of particles. *Drying Technology*, **31**, 1245–1254.

De Beer, D., Joubert, E., Viljoen, M. & Manley, M. (2012). Enhancing aspalathin stability in rooibos (*Aspalathus linearis*) ready-to-drink iced teas during storage: the role of nano-emulsification and beverage ingredients, citric and ascorbic acids. *Journal of the Science of Food and Agriculture*, **94**, 272–284.

De Beer, D., Malherbe, C.J., Beelders, T., Willenburg, E.L., Brand, D.J. & Joubert, E. (2015). Isolation of aspalathin and nothofagin from rooibos (A*spalathus linearis*) using high-performance countercurrent chromatography: sample loading and compound stability considerations. *Journal of Chromatography A*, **1381**, 29–36.

De Bernonville, T.D., Guyot, S., Paulin, J.P, Gaucher, M., Loufrani, L., Henrion, D., Derbré, S., Guilet, D., Richomme, P., Dat, J.F. & Brisset, M.N. (2010). Dihydrochalcones: implication in resistance to oxidative stress and bioactivities against advanced glycation end-products and vasoconstriction. *Phytochemistry*, **71**, 443–452.

Dejaegher, B. & Vander Heyden, Y. (2011). Experimental designs and their recent advances in set-up, data interpretation, and analytical applications. *Journal of Pharmaceutical and Biomedical Analysis*, **56**, 141–158.

Dhirendra, K., Lewis, S., Udupa, N. & Atin, K. (2009). Solid dispersions: a review. *Pakistan Journal of Pharmaceutical Sciences*, **22**, 234–246.

Di Ferdinando, M., Brunetti, C., Fini, A. & Tattini, M. (2013). Flavonoids as antioxidants in plants under abiotic stresses. In: *Abiotic Stress Responses in Plants: Metabolism, Productivity and Sustainability* (edited by P. Ahmad & M.N.V. Prasads). Pp. 159–179. New York: Springer Science & Business Media.

Dludla, P.V., Muller, CJ.F., Louw, J., Joubert, E., Salie, R., Opoku, A.R. & Johnson, R. (2014). The cardioprotective effect of an aqueous extract of fermented rooibos (*Aspalathus linearis*) on cultured cardiomyocytes derived from diabetic rats. *Phytomedicine*, **21**, 595–601.

Dludla, P.V., Joubert, E., Louw, J., Muller, C.C.J., Huisamen, B., Essop, M.F. & Johnson, R. (2015). A phenylpropenoic acid glucoside (PPAG) of *Aspalathus linearis* protects H9c2 cardiomyocytes against hyperglycemia-induced cell apoptosis. *Planta Medica*, **81**, doi:10.1055/s-0035-1565572.

Du., F-Y., Xiao, X-H., Luo, X-J. & Li, G-K. (2009). Application of ionic liquids in the microwave-assisted extraction of polyphenolic compounds from medicinal plants. *Talanta*, **78**, 1177–1184.

Du Plessis, H.J. & Roos, I.M.M. (1986). Recovery of coliforms, *Escherichia coli* type I and *Salmonella* species from rooibos tea (*Aspalathus linearis*) and decontamination by steam. *Phytophylactica,* **18**, 177–181.

Ehrenkranz, J.R.L., Lewis, N.G., Kahn, C.R. & Roth, J. (2005). Phloridzin: a review. *Diabetes/Metabolism Research & Reviews*, **21**, 31–38.

Ferreira, D., Marais, C., Steenkamp, J.A. & Joubert, E. (1995). Rooibos as a likely health food supplement. In: *Recent Developments in Technologies on Functional Foods for Health*. Pp. 73–88. Seoul, South Korea: Korean Society of Food Science and Technology.

Ferreira, S.L.C., Bruns, R.E., Ferreira, H.S., Matos, G.D., David, J.M., Brandão, G.C., Da Silva, E.G.P., Portugal, L.A., Dos Reis, P.S., Souza, A.S. & Dos Santos, W.N.L. (2007). Box-Behnken design: an alternative for the optimization of analytical methods. *Analytica Chimica Acta*, **597**, 179–186.

Fick, A. (1855). Ueber diffusion. *Annalen der Physik*, **170**, 59–86.

Fitzpatrick, J. (2013). Powder properties in food production systems. In: *Handbook of Food Powders: Processes and Properties* (edited by B. Bhandari). Pp. 285–308. Cambridge: Woodhead Publishing.

Flores-Mateo, G., Carrillo-Santisteve, P., Elosua, R., Guallar, E., Marrugat, J., Bleys, J. & Covas, M.I. (2009). Antioxidant enzyme activity and coronary heart disease: meta-analyses of observational studies. *American Journal of Epidemiology*, **170**, 135–147.

Franco, D., Sineiro, J., Pinelo, M. & Nuñez, M.J. (2007). Ethanolic extraction of *Rosa rubiginosa* soluble substances: oil solubility equilibria and kinetic studies. *Journal of Food Engineering*, **79**, 150–157.

Gargari, B.P, Dehghan, P., Aliasgharzadeh, A. & Jafar-abadi, M.A. (2013). Effects of high-performance inulin supplementation on glycemic control and antioxidant status in women with type 2 diabetes. *Diabetes & Metabolism Journal*, **37**, 140–148.

Gertenbach, D.D. (2002). Solid-liquid extraction technologies for manufacturing nutraceuticals. In: *Functional Foods: Biochemical and Processing Aspects*, Volume II. Pp. 332–339. Florida: CRC Press LLC.

Gharsallaoui, A., Roudaut, G., Chambin, O., Voilley, A. & Saurel, R. (2007). Applications of spray drying in microencapsulation of food ingredients: an overview. *Food Research International*, **40**, 1107–1121.

Gierlinger, N. & Schwanninger, M. (2007). The potential of Raman microscopy and Raman imaging in plant research. *Spectroscopy*, **21**, 69–89.

Gong, X., Chen, H., Chen, T & Qu, H. (2014a). Unit operation optimization for the manufacturing of botanical injections using a design space approach: a case study of water precipitation. *PLoS one*, **9**, doi: 10.1371/journal.pone.0104493.

Gong, X., Zhang, Y., Pan, Y. & Qu, H. (2014b). Optimization of the ethanol recycling reflux extraction process for saponins using a design space approach. *PLoS one*, **9**, doi: 10.1371/journal.pone.0114300.

Gosch, C., Halbwirth, H. & Stich, K. (2010). Phloridzin: biosynthesis, distribution and physiological relevance in plants. *Phytochemistry*, **71**, 838–843.

Granato, D. & De Araújo Calado, V.M. (2014). The use and importance of design of experiments (DOE) in process modelling in food science and technology. In: *Mathematical and Statistical Methods in Food Science and Technology* (1st ed.) (edited by D. Granato & G. Ares). Pp. 3–18. New York: John Wiley & Sons.

Guarigata, L., Whiting, D.R., Hambleton, I., Beagley, J., Linnenkamp, U. & Shaw, J.E. (2014). Global estimates of diabetes prevalence for 2013 and projections for 2035. *Diabetes Research and Clinical Practice*, **103**, 137–149.

Gunasekaran, S., Ko, S. & Xiao, L. (2007). Use of whey proteins for encapsulation and controlled delivery applications. *Journal of Food Engineering*, **83**, 31–40.

Habu, T., Flath, R.A., Mon, T.R. & Morton, J.F. (1985). Volatile compounds of rooibos tea (*Aspalathus linearis*). *Journal of Agricultural and Food Chemistry*, **33**, 249–254.

Hashemiravan, M., Mazloom, A.S. & Farhaydar, N. (2013). Nano particles of blueberry in inulin and β-cyclodextrin microcapsules. *International Journal of Nanoscience and Nanotechnology*, **9**, 185–192.

Hawkins, H.J., Malgas, R. & Biénabe, E. (2011). Ecotypes of wild rooibos (*Aspalathus linearis* (Burm. F) Dahlg., Fabaceae) are ecologically distinct. *South African Journal of Botany*, **77**, 360–370.

Heinrich, T., Willenberg, I. & Glomb, M.A. (2012). Chemistry of color formation during rooibos fermentation. *Journal of Agricultural and Food Chemistry*, **60**, 5221–5228.

Hernández-Jiménez, A., Kennedy, J.A., Bautista-Ortín, A.B. & Gómez-Plaza, E. (2012). Effect of ethanol on grape seed proanthocyanidin extraction. *American Journal of Enology and Viticulture*, **63**, 57–61.

Hibbert, D.B. (2012). Experimental design in chromatography: a review. *Journal of Chromatography B*, **910**, 2–13.

Hillis, W.E. & Inoue, T. (1967). The polyphenols of Nothofagus species — II: the heartwood of *Nothofagus fusca*. *Phytochemistry*, **6**, 59–67.

Hogekamp, S. & Schubert, H. (2003). Rehydration of food powders. *Food Science and Technology International,* **9**, 223–235.

Hong, I.S., Lee, H.Y. & Kim, H.P. (2014). Anti-oxidative effects of rooibos tea (*Aspalathus linearis*) on immobilization-induced oxidative stress in rat brain. *PLoS one*, **9**, doi: 10.1371./journal.pone.0087061.

Hopping, B.N., Erber, E., Grandinetti, A., Park, S.Y., Kolonel, L.N. & Maskarinec, G. (2010). Dietary fiber, magnesium, and glycemic load alter risk of type 2 diabetes in a multiethnic cohort in Hawaii. *Journal of Nutrition*, **140**, 68–74.

Huang, M., Du Plessis, J., Du Preez, J., Hamman, J. & Viljoen, A. (2008). Transport of aspalathin, a rooibos tea flavonoid, across the skin and intestinal epithelium. *Phytotherapy Research*, **22**, 699–704.

Huang, J., Kaul, G., Cai, C., Chatlapalli, R., Hernandez-Abad, P., Ghosh, K. & Nagi, A. (2009). Quality by design case study: an integrated multivariate approach to drug product and process development. *International Journal of Pharmaceutics*, **382**, 23–32.

ICH (2009). ICH Harmonised Tripartite Guideline: Pharmaceutical Development Q8(R2). [Internet document]. URL http://www.ich.org/fileadmin/Public_Web_Site/ICH_Products/Guidelines/Quality/Q8_R1/Step4/Q8_R2_Guideline.pdf. 18/08/2016.

Iswaldi, I., Arraez-Roman, D., Rodriguez-Medina, I., Beltran-Debon, R., Joven, J., Segura-Carretero, A. & Fernandez-Gutierrez, A. (2011). Identification of phenolic compounds in aqueous and ethanolic rooibos extracts (*Aspalathus linearis*) by HPLC-ESI-MS (TOF/IT). *Analytical and Bioanalytical Chemistry*, **400**, 3643–3654.

Jaganyi, D. & Wheeler, P.J. (2003). Rooibos tea: equilibrium and extraction kinetics of aspalathin. *Food Chemistry*, **83**, 121–126.

Jangam, S.V & Thorat, B.N. (2010). Optimization of spray drying of ginger extract. *Drying Technology*, **28**, 1426–1434.

Jiang, F., Chang, C. W. & Dusting, G. J. (2010). Cytoprotection by natural and synthetic polyphenols in the heart: novel mechanisms and perspectives. *Current Pharmaceutical Design,* **16**, 4103–4112.

Jiménez-Aguilar, D.M., Ortega-Regules, A.E., Lozada-Ramírez, J.D., Pérez-Pérez, M.C.I., Vernon-Carter, E.J. & Welti-Chanes, J. (2011). Color and chemical stability of spray-dried blueberry extract using mesquite gum as wall material. *Journal of Food Composition and Analysis*, **24**, 889–894.

Jittanit, W., Niti-Att, S. & Techanuntachaikul, O. (2010). Study of spray drying of pineapple juice using maltodextrin as an adjunct. *Chiang Mai Journal of Science*, **37**, 498–506.

Johnson, R., Dludla, P., Joubert, E., February, F., Mazibuko, S., Ghoor, S., Muller, C.J.F. & Louw, J. (2016). Aspalathin, a dihydrochalcone *C*-glucoside, protects H9c2 cardiomyocytes against high glucose induced shifts in substrate preference and apoptosis. *Molecular Nutrition & Food Research*, **60**, 922–934.

Jokić, S., Velić, D., Bilić, M., Bucić-Kojić, A., Planinić, M. & Tomas, S. (2010). Modelling of the process of solid-liquid extraction of total polyphenols from soybeans. *Czech Journal of Food Science*, **28**, 206–212.

Joubert, E. (1984). Studies in verband met verkitsing van rooibos tee (*Aspalathus linearis*). MSc Food Science Thesis, Stellenbosch University, South Africa.

Joubert, E. (1988a). Technical note: effect of agglomeration on the properties of spray-dried rooibos tea. *International Journal of Food Science and Technology*, **23**, 203–207.

Joubert, E. (1988b). Effect of batch extraction conditions on yield of soluble solids from rooibos tea. *International Journal of Food Science and Technology*, **23**, 43–47.

Joubert, E. (1990a). Chemical and sensory analyses of spray- and freeze-dried extracts of rooibos tea (*Aspalathus linearis*). *International Journal of Food Science and Technology*, **25**, 344–349.

Joubert, E. (1990b). Effect of batch extraction conditions on yield of polyphenols from rooibos tea (*Aspalathus linearis*). *International Journal of Food Science and Technology*, **25**, 339–343.

Joubert, E. (1990c). Effect of time on fixed-bed extraction of polyphenols from rooibos tea (*Aspalathus linearis*). *LWT – Food Science and Technology,* **23**, 181–183.

Joubert, E. (1996). HPLC quantification of the dihydrochalcones, aspalathin and nothofagin in rooibos tea (*Aspalathus linearis*) as affected by processing. *Food Chemistry*, **55**, 403–411.

Joubert, E., Beelders, T., De Beer, D., Malherbe, C.J., De Villiers, A.J. & Sigge, G.O. (2012). Variation in phenolic content and antioxidant activity of fermented rooibos herbal tea infusions: role of production season and quality grade. *Journal of Agricultural and Food Chemistry*, **60**, 9171–9179.

Joubert, E. & De Beer, D. (2011). Rooibos (*Aspalathus linearis*) beyond the farm gate: from herbal tea to potential phytopharmaceutical. *South African Journal of Botany*, **77**, 869–886.

Joubert, E. & De Beer, D. (2012). Phenolic content and antioxidant activity of rooibos food ingredient extracts. *Journal of Food Composition and Analysis*, **27**, 45–51.

Joubert, E. & De Beer, D. (2014). Antioxidants of rooibos beverages: role of plant composition and processing. In: *Processing and Impact on Antioxidants in Beverages* (edited by V.R. Preedy). Pp. 131–144. Massachusetts: Elsevier Academic Press.

Joubert, E., De Beer, D., Malherbe, C.J., Muller, N., Bonnet, S.L., Van der Westhuizen, J.H. & Ferreira, D. (2013). Occurrence and sensory perception of *Z*-2-(ß-D-glucopyranosyloxy)-3-phenylpropenoic acid in rooibos (*Aspalathus linearis)*. *Food Chemistry*, **136**, 1078–1085.

Joubert, E. & De Villiers, O.T. (1997). Effect of fermentation and drying conditions on the quality of rooibos tea. *International Journal of Food Science and Technology*, **32**, 127–134.

Joubert, E. & Ferreira, D. (1996). Antioxidants of rooibos tea – a possible explanation for its health promoting properties?. *The South African Journal of Food Science and Nutrition*, **8**, 79–83.

Joubert, E., Gelderblom, W.C.A., Louw, A. & De Beer, D. (2008a). South African herbal teas: *Aspalathus linearis*, *Cyclopia* spp. and *Athrixia phylicoides*. A review. *Journal of Ethnopharmacology*, **119**, 376–412.

Joubert, E. & Hansmann, C.F. (1990). Effect of time on fixed-bed extraction of soluble solids from rooibos tea (*Aspalathus linearis*). *LWT – Food Science and Technology*, **23**, 178–180.

Joubert, E., Jolley, B., Koch, I.S., Muller, M., Van der Rijst, M. & De Beer, D. (2016). Major production areas of rooibos (*Aspalathus linearis*) deliver herbal tea of similar phenolic and phenylpropenoic acid glucoside content. *South African Journal of Botany*, **103**, 162–169.

Joubert, E., Manley, M. & Botha, M. (2008b). Evaluation of spectroscopic methods for screening of green rooibos (*Aspalathus linearis*) and green honeybush (*Cyclopia genistoides*) extracts for high levels of bio-active compounds. *Phytochemical Analysis*, **19**, 169–178.

Joubert, E., Richards, E.S., Van der Merwe, D., De Beer, D., Manley, M. & Gelderblom, W.C.A. (2008c). Effects of species variation and processing on phenolic composition and in vitro antioxidant activity of aqueous extracts of *Cyclopia* spp. (honeybush tea). *Journal of Agricultural and Food Chemistry*, **56**, 954–963.

Joubert, E. & Schulz, H. (2006). Production and quality aspects of rooibos tea and quality products. A review. *Journal of Applied Botany and Food Quality*, **80**, 138–144.

Joubert, E., Winterton, P., Britz, T.J. & Ferreira, D. (2004). Superoxide anion and α,α-diphenyl-β-picrylhydrazyl radical scavenging capacity of rooibos (*Aspalathus linearis*) aqueous extracts, crude phenolic fractions, tannin and flavonoids. *Food Research International*, **37**, 133–138.

Joubert, E., Viljoen, M., De Beer, D., Malherbe, C.J., Brand, D.J. & Manley, M. (2010). Use of green rooibos (*Aspalathus linearis*) extract and water-soluble nanomicelles of green rooibos extract encapsulated with ascorbic acid for enhanced aspalathin content in ready-to-drink iced teas. *Journal of Agricultural and Food Chemistry*, **58**, 10965–10971.

Joubert, E., Viljoen, M., De Beer, D. & Manley, M. (2009). Effect of heat on aspalathin, iso-orientin, and orientin contents and color of fermented rooibos (*Aspalathus linearis*) iced tea. *Journal of Agricultural and Food Chemistry*, **57**, 4204–4211.

Juran, J.M. (1992). *Juran on Quality by Design: The New Steps for Planning Quality into Goods and Services*. New York: Simon & Schuster.

Karacabey, E. & Mazza, G. (2008). Optimization of solid-liquid extraction of resveratrol and other phenolic compounds from milled grape canes (*Vitis vinifera*). *Journal of Agricultural and Food Chemistry*, **56**, 6318–6325.

Kaur, P., Singh, S.K., Garg, V., Gulati, M. & Vaidya, Y. (2015). Optimization of spray drying process for formulation of solid dispersion containing polypeptide-k powder through quality by design approach. *Powder Technology*, **284**, 1–11.

Kawakami, M., Kobayashi, A. & Kator, K. (1993). Volatile constituents of rooibos tea (*Aspalathus* linearis) as affected by extraction process. *Journal of Agricultural and Food Chemistry*, **41**, 633–636.

Kawano, A., Nakamura, H., Hata, S., Minakawa, M., Miura, Y. & Yagasaki, K. (2009). Hypoglycemic effect of aspalathin, a rooibos tea component from *Aspalathus linearis*, in type 2 diabetic model db/db mice. *Phytomedicine*, **16**, 437–443.

Keshani, S., Daud, W.R.W., Nourouzi, M.M., Namvar, F. & Ghasemi, M. (2015). Spray drying: an overview on wall deposition, process and modeling. *Journal of Food Engineering*, **146**, 152–162.

Khan, M.K., Albert-Vian, M., Fabiano-Tixier, A.S., Dangles, O. & Chemat, F. (2010). Ultrasound-assisted extraction of polyphenols (flavanone glycosides) from orange (*Citrus sinensis* L.) peel. *Food Chemistry*, **119**, 851–858.

Khan, I.A. & Smillie, T. (2012). Implementing a "Quality by Design" approach to assure the safety and integrity of botanical dietary supplements. *Journal of Natural Products*, **75**, 1665–1675.

Khullar, M., Al-Shudiefat, A. A., Ludke, A. & Binepal, G. (2010). Oxidative stress: a key contributor to diabetic cardiomyopathy. *Canadian Journal of Physiology and Pharmacology*, **88**, 233–240.

Koch, I.S., Muller, M., Joubert, E., Van der Rijst, M. & Næs, T. (2012). Sensory characterization of rooibos tea and the development of a rooibos sensory wheel and lexicon. *Food Research* International, **46**, 217−228.

Koch, I.S., Muller, N., De Beer, D., Næs, T. & Joubert, E. (2013). Impact of steam pasteurization on the sensory profile and phenolic composition of rooibos (*Aspalathus linearis*) herbal tea infusions. *Food Research International*, **53**, 704–712.

Koeppen, B.H. & Roux, D.G. (1965a). Aspalathin: a novel *C*-glycosylflavonoid from *Aspalathus linearis*. *Tetrahedron Letters*, **39**, 3497–3503.

Koeppen, B.H. & Roux, D.G. (1965b). *C*-glycosylflavonoids. The chemistry of orientin and iso-orientin. *Biochemistry Journal*, **97**, 444–448.

Koeppen, B.H., & Roux, D.G. (1966). *C*-Glycosylflavonoids. The chemistry of aspalathin. *Biochemistry Journal*, **99**, 604–609.

Koeppen, B.H., Smit, C.J.B. & Roux, D.G. (1962). The flavone *C*-glycosides and flavanol *O*-glycosides of *Aspalathus acuminatus* (Rooibos tea). *Biochemistry Journal*, **83**, 507–511.

Kolida, S., Tuohy, K. & Gibson, G.R. (2002). Prebiotic effects of inulin and oligofructose. *British Journal of Nutrition*, **87**, S193–S197.

Kondo, M., Hirano, Y., Nishio, M., Furaya, Y., Nakamura, H. & Watanabe, T. (2013). Xanthine oxidase inhibitory activity and hypouricemic effect of aspalathin from unfermented rooibos. *Journal of Food Science*, **78**, 1935–1939.

Konno, H. & Taylor, L.S. (2006). Influence of different polymers on the crystallization tendency of molecularly dispersed amorphous felodipine. *Journal of Pharmaceutical Sciences*, **95**, 2692–2705.

Kotina, E.L., Stepanova, A.V., Tilney, P.M. & Van Wyk, B.-E. (2012). The pharmacognostic value of leaf and stem anatomy in rooibos tea (*Aspalathus linearis*). *South African Journal of Botany*, **82**, 129–133.

Krafczyk, N. & Glomb, M.A. (2008). Characterization of phenolic compounds in rooibos tea. *Journal of Agricultural and Food Chemistry*, **56**, 3368–3376.

Krafczyk, N., Heinrich, T., Porzel, A. & Glomb, M.A. (2009). Oxidation of the dihydrochalcone aspalathin leads to dimerization. *Journal of Agricultural and Food Chemistry*, **57**, 6838–6843.

Ku, S.K., Kwak, S., Kim, Y. & Bae, J.S. (2015). Aspalathin and nothofagin from rooibos (*Aspalathus linearis*) inhibits high glucose-induced inflammation *in vitro* and *in vivo*. *Inflammation*, **38**, 445–455.

Lang, Q. & Wai, C.M. (2001). Supercritical fluid extraction in herbal and natural product studies — a practical review. *Talanta*, **53**, 771–782.

Laroze, L.E., Díaz-Reinoso, B., Moure, A., Zúñiga, M.E. & Domínguez, H. (2010). Extraction of antioxidants from several berries pressing wastes using conventional and supercritical solvents. *European Food Research and Technology*, **231**, 669–677.

Lattanzio, V., Kroon, P.A., Quideau, S. & Treutter, D. (2008). Plant phenolics — secondary metabolites with diverse functions. In: *Recent Advances in Polyphenol Research, Vol. 1* (edited by F. Daayf & V. Lattanzio). Pp. 1–35. New Jersey: Wiley-Blackwell.

Leardi, R. (2009). Experimental design in chemistry: a tutorial. *Analytica Chimica Acta*, **652**, 161–172.

Lebrun, P., Krier, F., Mantanus, J., Grohganz, H., Yang, M., Rozet, E., Boulanger, B., Evrard, B., Rantanen, J. & Hubert, P. (2012). Design space approach in the optimization of the spray drying process. *European Journal of Pharmaceutics and Biopharmaceutics*, **80**, 226–234.

Le Meste, M., Champion, D., Roudaut, G., Blond, G. & Simatos, D. (2002). Glass transition and food technology: a critical appraisal. *Journal of Food Science*, **67**, 2444–2458.

Li, P., Lu, S., Shan, T., Mou, Y., Li, Y., Sun, W. & Zhou, L. (2012). Extraction optimization of water-extracted mycelial polysaccharide from endophytic fungus *Fusarium oxysporum* Dzf17 by response surface methodology. *International Journal of Molecular Sciences*, **13**, 5441–5453.

Liew, O.W., Chong, P.C.J., Li, B. & Asundi, A.K. (2008). Signature optical cues: emerging technologies for monitoring plant health. *Sensors*, **8**, 3205–3239.

Liu. J.L., Li, L.Y. & He, G.H. (2016). Optimization of microwave-assisted extraction conditions for five major bioactive compounds from Flos Sophorae Immaturus (Cultivars of *Sophora japonica* L.) using response surface methodology. *Molecules*, **21**, 295–322.

Lundstedt, T., Seifert, E., Abramo, L., Thelin, B., Nyström, Å., Petterson, J. & Bergman, R. (1998). Experimental design and optimization. *Chemometrics and Intelligent Laboratory Systems*, **42**, 3–40.

Malgas, R.R., Potts, A.J., Oettlé, N.M., Koelle, B., Todd, S.W., Verboom, G.A. & Hoffman, M.T. (2010). Distribution, quantitative morphological variation and preliminary molecular analysis of different growth forms of wild rooibos (*Aspalathus linearis*) in the northern Cederberg and on the Bokkeveld Plateau. *South African Journal of Botany*, **76**, 72–81.

Maltesen, M.J., Bjerregaard, S., Hovgaard, L., Havelund, S. & Van de Weert, M. (2008). Quality by design — spray drying of insulin intended for inhalation. *European Journal of Pharmaceutics and Biopharmaceutics*, **70**, 828–838.

Manley, M., Joubert, E. & Botha, M. (2006). Quantification of the major phenolic compounds, soluble solid content and total antioxidant activity of green rooibos (*Aspalathus linearis*) by means of near infrared spectroscopy. *Journal of Near Infrared Spectroscopy*, **14**, 213–222.

Marais, C., Steenkamp, J.A. & Ferreira, D. (1996). The occurrence of phenylpyruvic acid in woody plants: biosynthetic significance. *Tetrahedron Letters*, **37**, 5763–5764.

Marais, C., Van Rensburg, W.J., Ferreira, D. & Steenkamp, J.A. (2000). (*S*)- and (*R*)-eriodictyol-6-*C*-β-D glucopyranoside, novel keys to fermentation of rooibos (*Aspalathus linearis*). *Phytochemistry*, **55**, 43–49.

Maran, J.P., Manikandan, S., Priya, B. & Gurumoorthi, P. (2015). Box-Behnken design based multi-response analysis and optimization of supercritical carbon dioxide extraction of bioactive flavonoid compounds from tea (*Camellia sinensis* L.) leaves. *Journal of Food Science and* Technology, **52**, 92–104.

Marnewick, J.L., Rautenbach, F., Venter, I., Neethling, H., Blackhurst, D.M., Wolmarans, P. & Macharia, M. (2011). Effects of rooibos (*Aspalathus linearis*) on oxidative stress and biochemical parameters in adults at risk for cardiovascular disease. *Journal of Ethnopharmacology*, **133**, 46–52.

Mathers, C.D. & Loncar, D. (2006). Projections of global mortality and burden of disease from 2002 to 2030. *PLoS Medicine*, **3**, e442.

Mathijs, I., Da Cunha, D.A., Himpe, E., Ladriere, L., Chellan, N., Roux, C.R., Joubert, E., Muller, C., Cnop, M., Louw, J. & Bouwens, L. (2014). Phenylpropenoic acid glucoside augments pancreatic beta cell mass in high-fat diet-fed mice and protects beta cells from ER stress-induced apoptosis. *Molecular Nutrition & Food Research*, **58**, 1980–1990.

Maury, M., Murphy, K., Kumar, S., Shi, L. & Lee, G. (2005). Effects of process variables on the powder yield of spray-dried trehalose on a laboratory spray-dryer. *European Journal of Pharmaceutics and Biopharmaceutics*, **59**, 565–573.

Mazibuko, S.E., Muller, C.J.F., Joubert, E., De Beer, D., Johnson, R., Opoku, A.R. & Louw, J. (2013). Amelioration of palmitate-induced insulin resistance in C2C12 muscle cells by rooibos (*Aspalathus linearis*). *Phytomedicine*, **20**, 813–819.

Mazibuko, S.E. Joubert, E. Johnson, R., Louw, J., Opoku, A.R. & Muller, C.J.F. (2015). Aspalathin improves glucose and lipid metabolism in 3T3-L1 adipocytes exposed to palmitate. *Molecular Nutrition & Food Research*, **59**, 2199–2208.

Mensink, M.A., Frijlink, H.W., Van der Voort Maarschalk, K. & Hinrichs, W.L.J. (2015a). Inulin, a flexible oligosaccharide I: Review of its physicochemical characteristics. *Carbohydrate Polymers*, **130**, 405–419.

Mensink, M.A., Frijlink, H.W., Van der Voort Maarschalk, K. & Hinrichs, W.L.J. (2015b). Inulin, a flexible oligosaccharide II: Review of its pharmaceutical applications. *Carbohydrate Polymers*, **134**, 418–428.

Meyer, K.A., Kushi, L.H., Jackobs, D.R., Slavin, J., Sellers, A.A. & Folsom, A.R. (2000). Carbohydrates, dietary fiber, and incident type 2 diabetes in older women. *American Journal of Clinical Nutrition*, **71**, 921–930.

Mitsui, T. & Takada, S. (1969). On factors influencing dispersibility and wettability of powder in water. *Journal of the Society of Cosmetic Chemists*, **20**, 335–351.

Moreira, G.E.G., Costa, M.G.M., Souza, A.C.R., Brito, E.S., Medeiros, M.F.D. & Azeredo, H.M.C. (2009). Physical properties of spray dried acerola pomace extract as affected by temperature and drying aids. *Food Science and Technology*, **42**, 641–645.

Morton, J.F. (1983). Rooibos tea, *Aspalathus linearis*, a caffeineless, low-tannin beverage. *Economic Botany*, **37**, 164–173.

Muller, C.J.F., Joubert, E., De Beer, D., Sanderson, M., Malherbe, C.J., Fey, S.J. & Louw, J. (2012). Acute assessment of aspalathin-enriched green rooibos (*Aspalathus linearis)* extract with hypoglycaemic potential. *Phytomedicine,* **20**, 32–39.

Muller, C.J.F., Joubert, E., Pheiffer, C., Ghoor, S., Sanderson, M., Chellan, N., Fey, S.J. & Louw, J. (2013). *Z*-2-(β-d-glucopyranosyloxy)-3-phenylpropenoic acid, an α-hydroxy acid from

rooibos (*Aspalathus linearis*) with hypoglycemic activity. *Molecular Nutrition & Food Research*, **57**, 2216–2222.

Muller, C.J.F., Malherbe, C.J., Chellan, N., Yagasaki, K., Miura, Y. & Joubert, E. (2016). Potential of rooibos, its major *C*-glucosyl flavonoids and *Z*-2-(β-D-glucopyranoloxy)-3-phenylpropenoic acid in prevention of metabolic syndrome. *Critical Reviews in Food Science and Nutrition*, doi: 10.1080/10408398.2016.1157568.

Murugesan, R. & Orsat, V. (2012). Spray drying for the production of nutraceutical ingredients — a review. *Food and Bioprocess Technology*, **5**, 3–14.

Nagar, M., Panwar, K.S., Chopra, V.S., Bala, I. & Trivedi, P. (2010). Quality by design: a systemic approach to pharmaceutical development. *Der Pharmacia Lettre*, **2**, 111–130.

Naidu, K., Singh, V., Johnston, D.B., Rausch, K.R. & Tumbleson, M.E. (2007). Effects of ground corn particle size on ethanol yield and thin stillage soluble solids. *Cereal Chemistry*, **84**, 6–9.

Nazare, J.A., Sauvinet, V., Normand, S., Guerin-Deremaux, L., Gabert, L., Desige, M., Wils, D. & Laville, M. (2011). Impact of a resistant dextrin with a prolonged oxidation pattern on day-long ghrelin profile. *The Journal of the American College of Nutrition*, **30**, 63–72.

Ninfali, P., Gennari, L., Biagotti, E., Cangi, F., Mattoli, L. & Maidecchi, A. (2009). Improvement in botanical standardisation of commercial freeze-dried herbal extracts by using the combination of antioxidant capacity and constituent marker concentrations. *Journal of AOAC International*, **92**, 797–805.

Oomah, B.D. & Mazza, G. (2001). Optimization of a spray drying process for flaxseed gum. *International Journal of Food Science and Technology*, **36**, 135–143.

Pacheco-Palencia, L.A. & Talcott, S.T. (2010). Chemical stability of açai fruit (*Euterpe oleracea* Mart.) anthocyanins as influenced by naturally occurring and externally added polyphenolic cofactors in model systems. *Food Chemistry*, **118**, 17–25.

Paiva, A., Craveiro, R., Aroso, I., Martins, M., Reis, R. & Duarte, A.R.C. (2014). Natural deep eutectic solvents — solvents for the 21st century. *ACS Sustainable Chemistry & Engineering*, **2**, 1063–1071.

Palzer, S. (2005). The effect of glass transition on the desired and undesired agglomeration of amorphous food powders. *Chemical Engineering Science*, **60**, 3959–3968.

Pandey, R.K. & Manimehalai, N. (2014). Production of instant tea powder by spray drying. *International Journal of Agriculture and Food Science Technology*, **5**, 197–202.

Pasrija, D. & Anandharamakrishnan, C. (2015). Techniques for extraction of green tea polyphenols: review. *Food and Bioprocess Technology*, **8**, 935–950.

Pasrija, D., Ezhilarasi, P.N., Indrani, D. & Anandharamkrishnan, C. (2015). Microencapsulation of green tea polyphenols and its effect on incorporated bread quality. *LWT – Food Science and Technology*, **64**, 289–296.

Patel, K. & Chen, X.D. (2008). Surface-center temperature differences within milk droplets during convective drying and drying-based Biot number analysis. *Journal of AiChE*, **54,** 3273–3290.

Patel, R.P., Patel, M.P. & Suthar, A.M. (2009). Spray drying technology: an overview. *Indian Journal of Science and Technology*, **2**, 44–47.

Patel, B.B., Patel, J.K., Chakraborty, S. & Shukla, D. (2015). Revealing facts behind spray dried solid dispersion technology used for solubility enhancement. *Saudi Pharmaceutical Journal*, **23**, 352–365.

Pathare, P.B., Opara, U.L. & Al-Said, F.A.J. (2013). Colour measurement and analysis in fresh and processed foods: a review. *Food and Bioprocess Technology*, **6**, 36–60.

Pengilly, M., Joubert, E., Van Zyl, W.H., Botha, A. & Bloom, M. (2008). Enhancement of rooibos (*Aspalathus linearis*) aqueous extract and antioxidant yield with fungal enzymes. *Journal of Agricultural and Food Chemistry*, **56**, 4047–4053.

Petrussa, E., Braidot, E., Zancani, M., Peresson, C., Bertolini, A., Patui, S. & Vianello, A. (2013). Plant flavonoids — biosynthesis, transport and involvement in stress responses. *International Journal of Molecular Science*, **14**, 14950–14973.

Pierucci, A.P.T.R., Andrade, L.R., Baptista, E.B., Volpato, N.M., & Rocha-Leao, M.H.M. (2006). New microencapsulation system for ascorbic acid using pea protein concentrate as coat protector. *Journal of Microencapsulation*, **23**, 654–662.

Pierucci, A.P.T.R., Andrade, L.R., Farina, M., Pedrosa, C. & Rocha-Leão, M.H.M. (2007). Comparison of a-tocopherol microparticles produced with different wall materials: pea protein a new interesting alternative. *Journal of Microencapsulation*, **24**, 201–213.

Pinelo, M., Rubilar, M., Jerez, M., Sineiro, J. & Nuñez, M.J. (2005). Effect of solvent, temperature, and solvent-to-solid ratio on the total phenolic content and antiradical activity of extracts from different components of grape pomace. *Journal of Agricultural and Food Chemistry*, **53**, 2111–2117.

Pintauro, N.D. (1970). *Soluble Tea Production Processes.* Pp. 143–162. Park Ridge, NJ: Noyes Data Corporation.

Prescott, J.K. & Barnum, R.A. (2000). On powder flowability. *Pharmaceutical Technology*, **23**, 60–84.

Price, W.E. & Spitzer, J.C. (1993). The temperature dependence of the rate of extraction of soluble constituents of black tea. *Food Chemistry*, **46**, 133–136.

Price, W.E. & Spitzer, J.C. (1994). The kinetics of extraction of individual flavanols and caffeine from a Japanese green tea (Sen Cha Uji Tsuyu) as a function of temperature. *Food Chemistry*, **50**, 19–23.

Prinn, K.B., Costantino, H.R. & Tracy, M. (2002). Statistical modeling of protein spray drying at the lab scale. *Aaps Pharmscitech*, **3**, 32–39.

Puri, M., Sharma, D. & Barrow, C.J. (2012). Enzyme-assisted extraction of bioactives from plants. *Trends in Biotechnology*, **30**, 37–44.

Quideau, S. (2006). Why bother with polyphenols?. *Polyphénols Actualités*, **24**, 10–14.

Rabe, C., Steenkamp, J.A., Joubert, E., Burger, J.F.W. & Ferreira, D. (1994). Phenolic metabolites from rooibos tea (*Aspalathus linearis*). *Phytochemistry*, **35**, 1559–1565.

Ramnani, P., Gaudier, E., Bingham, M., Van Bruggen, P., Tuohy, K.M. & Gibson, G.R. (2010). Prebiotic effect of fruit and vegetable shots containing Jerusalem artichoke inulin: a human intervention study. *British Journal of Nutrition*, **104**, 233–240.

Rathore, A.S. & Winkle, H. (2009). Quality by design for biopharmaceuticals. *Nature Biotechnology*, **27**, 26–34.

Ré, M.I. (1998). Microencapsulation by spray drying. *Drying Technology*, **16**, 1195–1236.

Reynecke, J., Coetzee, W.H.K. & Bester, J.J.A. (1949). Rooibos tea. A preliminary report on the composition. *Farming in South Africa*, **24**, 397–412.

Rockland, L.B., & Nishi, S.K. (1980). Influence of water activity on food product quality and stability. *Food Technology*, **34**, 42–51.

Roos, Y.H. (2010). Glass transition temperature and its relevance in food processing. *Annual Review of Food Science and Technology*, **1**, 469–496.

Roy, S. (2012). Quality by design: a holistic concept of building quality in pharmaceuticals. *International Journal of Pharmaceutical and Biomedical Research*, **3**, 100–108.

Sablani, S.S., Kasapis, S. & Rahman, M.S. (2007). Evaluating water activity and glass transition concepts for food stability. *Journal of Food Engineering*, **78**, 266–271.

Saénz, C., Tapia, S., Chávez, J. & Robert, P. (2009). Microencapsulation by spray drying of bioactive compounds from cactus pear (*Opuntia ficus-indica)*. *Food Chemistry*, **114**, 616–622.

Şahin-Nadeem, H., Torun, M. & Özdemir, F. (2011). Spray drying of the mountain tea (*Sideritis stricta*) water extract by using different hydrocolloid carriers. *LWT – Food Science and Technology*, **44**, 1626–1635.

Şahin-Nadeem, H., Dinçer, C., Torun, M., Topuz, A. & Özdemir, F. (2013). Influence of inlet air temperature and carrier material on the production of instant soluble sage (*Salvia fruticosa* Miller) by spray drying. *LWT – Food Science and Technology*, **52**, 31–38.

Sanderson, M., Mazibuko, S.E., Joubert, E., De Beer, D., Johnson, R., Pheiffer, C., Louw, J. & Muller, C.J. (2014). Effects of fermented rooibos (*Aspalathus linearis*) on adipocyte differentiation. *Phytomedicine*, **21**, 109–117.

Sareen, S., Mathew, G. & Joseph, L. (2012). Improvement in solubility of poor water-soluble drugs by solid dispersion. *International Journal of Pharmaceutical Investigation*, **2**, 12–17.

Sarraguca, M.C., Cruz, A. V., Soares, S.O., Amaral, H.R., Costa, P.C. & Lopes, J.A. (2010). Determination of flow properties of pharmaceutical powders by near infrared spectroscopy. *Journal of Pharmaceutical and Biomedical Analysis*, **52**, 484–492.

Schloms, L., Smith, C., Storbeck, K.H., Marnewick, J.L, Swart, P. & Swart, A.C. (2014). Rooibos influences glucocorticoid levels and steroid ratios in vivo and in vitro: a natural approach in the management of stress and metabolic disorders?. *Molecular Nutrition & Food Research*, **58**, 537–549.

Schulz, H., Joubert, E. & Schütze, W. (2003). Quantification of quality parameters for reliable evaluation of green rooibos (*Aspalathus linearis*). *European Food Research and Technology*, **216**, 539–543.

Schulze, D. (2006). The behaviour of powders and bulk solids. Braunschweig/Wolfenbuttel, Germany: University of Applied Sciences. [Internet document]. URL http://www.dietmar-schulze.de/grdle1pr.html. 11/06/2016.

Schwedes, J. & Schulze, D. (1990). Measurement of flow properties of bulk solids. *Powder Technology*, **61**, 59–68.

Sefton, M.A., Skouroumounis, G.K., Elsey, G.M. & Taylor, D.K. (2011). Occurence, sensory impact, formation and fate of damascenone in grapes, wines, and other foods and beverages. *Journal of Agricultural and Food Chemistry*, **59**, 9717–9746.

Shah, M.V. & Rohit, M.C. (2013). Novel techniques for isolation and extraction of phyto-constituents from herbal plants. *American Journal of Phytomedicine and Clinical Therapeutics*, **1**, 338–350.

Shrestha, A.K., Ua-arak, T., Adhikari, B.P., Howes, T. & Bhandari, B.R. (2007). Glass transition behavior of spray dried orange juice powder measured by differential scanning calorimetry (DSC) and thermal mechanical compression test (TMCT). *International Journal of Food Properties*, **10**, 661–67.

Shi, J., Nawaz, H., Pohorly, J., Mittal, G., Kakuda, Y. & Jiang, Y. (2005). Extraction of polyphenolics from plant material for functional foods — engineering and technology. *Food Reviews International*, **21**, 139–166.

Shimamura, N., Miyase, T., Umehara, K., Warashina, T. & Fujii, S. (2006). Phytoestrogens from *Aspalathus linearis*. *Biological and Pharmaceutical Bulletin*, **29**, 1271–1274.

Shinde, V.M., Dhalwal, K., Potdar, M. & Mahadik, K.R. (2009). Application of quality control principles to herbal drugs. *International Journal of Phytomedicine*, **1**, 4–8.

Silva, P.I., Stringheta, P.C., Teófilo, R.F. & De Oliveira, I.R.N. (2013). Parameter optimization for spray drying microencapsulation of jaboticaba (*Myrciaria jaboticaba*) peel extracts using simultaneous analysis of responses. *Journal of Food Engineering*, **117**, 538–544.

Šimon, P., Veverka, M. & Okuliar, J. (2004). New screening method for the determination of stability of pharmaceuticals. *International Journal of Pharmaceutics*, **270**, 21–26.

Sinija, V.R., Mishra, H.N. & Bal, S. (2007). Process technology for production of soluble tea powder. *Journal of Food Engineering*, **82**, 276–283.

Slavin, J. (2013). Fiber and prebiotics: mechanism and health benefits. *Nutrients*, **5**, 1417–1435.

Snijman, P.W., Joubert, E., Ferreira, D., Li, X.C., Ding, Y., Green, I.R. & Gelderblom, W.C.A. (2009). Antioxidant activity of the dihydrochalcones aspalathin and nothofagin and their corresponding flavones in relation to other rooibos (*Aspalathus linearis*) flavonoids, epigallocatechin gallate, and trolox. *Journal of Agricultural and Food Chemistry*, **57**, 6678–6684.

Snyman, S. (2000). *Wesgro Background Report. The Rooibos Industry in the Western Cape*. Cape Town: Wesgro.

Sollohub, K. & Cal, K. (2010). Spray drying technique. II. Current applications in pharmaceutical technology. *Journal of Pharmaceutical Sciences*, **99**, 587–597.

Son, M.J., Minikawa, M., Miura, Y. & Yagasaki, K. (2013). Aspalathin improves hyperglycaemia and glucose intolerance in obese diabetic *ob/ob* mice. *European Journal of Nutrition*, **52**, 1607–1619.

Souza, C.R.F. & Oliveira, P. (2006). Powder properties and system behaviour during spray drying of *Bauhinia forficata* link extract. *Drying Technology*, **24**, 735–749.

Stalmach, A., Mullen, W., Pecorari, M., Serafini, M. & Crozier, A. (2009). Bioavailability of *C*-linked dihydrochalcone and flavanone glucosides in humans following ingestion of unfermented and fermented rooibos teas. *Journal of Agricultural and Food Chemistry*, **57**, 7104–7111.

Standley, L., Winterton, P., Marnewick, J.L., Gelderblom, W.C.A., Joubert, E. & Britz, T.J. (2001). Influence of processing stages on antimutagenic and antioxidant potentials of rooibos tea. *Journal of Agricultural and Food Chemistry*, **49**, 114–117.

Steinberg, D.M. & Bursztyn, D. (2010). Response surface methodology in biotechnology. *Quality Engineering*, **22**, 78–87.

Street, R.A. & Prinsloo, G. (2013). Commercially important medicinal plants of South Africa: a review. *Journal of Chemistry*, **2013**, doi: 10.1155/2013/205048.

Takeuchi, T.M., Pereira, C.G., Braga, M.E.M., Maróstica, M.R., Leal, P.F. & Meireles, M.A.A. (2009). Low-pressure solvent extraction (solid-liquid extraction, microwave assisted, and ultrasound assisted) from condimentary plants. In: *Extracting Bioactive Compounds for Food Products: Theory and Applications* (edited by Meireles, M.A.A.). Pp 138–211. New York: Taylor & Francis Group, LLC.

Tan, S.P., Kha, T.C., Parks, S., Stathopoulos, C. & Roach, P.D. (2015). Optimising the encapsulation of an aqueous bitter melon extract by spray drying. *Foods*, **3**, 400–419.

Tatke, P. & Jaiswal, Y. (2011). An overview of microwave assisted extraction and its applications in herbal drug research. *Research Journal of Medicinal Plant*, **5**, 21–31.

Tee, L.H., Luqman Chuah, A., Pin, K.Y., Abdull Rashih, A. & Yusof, Y.A. (2012). Optimization of spray drying process parameters of *Piper betle* L. (Sirih) leaves extract coated with maltodextrin. *Journal of Chemical and Pharmaceutical Research*, **4**, 1833–1841.

Tenou, E., Fitzpatrick, J.J. & Synnot, E.C. (1999). Characterisation of food powder flowability. *Journal of Food Engineering*, **39**, 31–37.

Tuomilehto, J., Lindström, J., Eriksson, J.G., Valle, T.T., Hämäläinen, H., Ilanne-Parikka, P., Keinänen-Kiukaanniemi, S., Laakso, M., Louheranta, A., Rastas, M. & Salminen, V. (2001). Prevention of type 2 diabetes mellitus by changes in lifestyle among subjects with impaired glucose tolerance. *New England Journal of Medicine*, **344**, 1343–1350.

Toneli, J., Park, K., Negreiros, A. & Murr, F. (2010). Spray drying process optimization of chicory root inulin. *Drying Technology*, **28**, 369–379.

Tonon, R.V., Brabet, C. & Hubinger, M.D. (2008). Influence of process conditions on the physicochemical properties of açai (*Euterpe oleracea* Mart.) powder produced by spray drying. *Journal of Food Engineering*, **88**, 411–418.

Treutter, D. (2001). Biosynthesis of phenolic compounds and its regulation in apple. *Plant Growth Regulation*, **34**, 71–89.

Tzin, V. & Galili, G. (2010). New insights into the shikimate and aromatic amino acids biosynthesis pathways in plants. *Molecular Plant*, **3**, 956–972.

Uličná, O., Vančová, O., Božek, P., Čársky, J., Šebekova, K., Boor, P., Nakano, M. & Greksák, M. (2006). Rooibos tea (*Aspalathus linearis*) partially prevents oxidative stress in streptozotocin-induced diabetic rats. *Physiological Research*, **55**, 157–164.

Van Gool, W. (1992). Exergy analysis of industrial processes. *Energy*, **17**, 791–803.

Van den Mooter, G. (2012). The use of amorphous solid dispersions: a formulation strategy to overcome poor solubility and dissolution rate. *Drug Discovery Today: Technologies*, **9**, 79–85.

Van Heerden, F.R., Van Wyk, B.-E., Viljoen, A.M. & Steenkamp, P.A. (2003). Phenolic variation in wild populations of *Aspalathus linearis* (rooibos tea). *Biochemical Systematics and Ecology*, **31**, 885–895.

Van Wyk, B.-E. & Verdoorn, G.H. (1989). Alkaloids of the genera *Aspalathus*, *Rafnia* and *Wiborgia* (Fabaceae-Crotalariaea). *South African Journal of Botany*, **55**, 520–522.

Vasconcelos, T., Sarmento, B. & Costa, P. (2007). Solid dispersions as strategy to improve oral bioavailability of poor water soluble drugs. *Drug Discovery Today*, **12**, 1068–1075.

Viljoen, M., Muller, M., De Beer, D. & Joubert, E. (2016). Identification of broad-based sensory attributes driving consumer preference of ready-to-drink rooibos iced tea with increased aspalathin content. *South African Journal of Botany*, doi: 10.1016/j.sajb.2016.07.019.

Virot, M., Tomao, V., Le Bourvellec, C., Renard, C.M. & Chemat, F. (2010). Towards the industrial production of antioxidants from food processing by-products with ultrasound-assisted extraction. *Ultrasonics Sonochemistry*, **17**, 1066–1074.

Von Gadow, A., Joubert, E. & Hansmann, C.F. (1997). Comparison of the antioxidant activity of rooibos tea (*Aspalathus linearis*) with green, oolong and black tea. *Food Chemistry*, **60**, 73–77.

Vuong, Q.V., Golding, J.B., Stathopoulos, C.E., Nguyen, M.H. & Roach, P.D. (2011). Optimizing conditions for the extraction of catechins from green tea using hot water. *Journal of Separation Science*, **34**, 3099–3106.

Wang, Z., Pan, Z., Ma, H. & Atungulu, G.G. (2011). Extract of phenolics from pomegranate peels. *The Open Food Science Journal*, **5**,17–25.

Wang, L. & Weller, C.L. (2006). Recent advances in extraction of nutraceuticals from plants. *Trends in Food Science and Technology*, **17**, 300–312.

Watt, J.M. & Breyer-Brandwijk, M.G. (1932). The medicinal and poisonous plants of southern Africa. Pp. 70–71. Edinburgh: E & S Livingstone.

Wen, Y., Chen, H., Zhou, X., Deng, Q., Zhao, Y., Zhao, C. & Gong, X. (2015). Optimization of the microwave-assisted extraction and antioxidant activities of anthocyanins from blackberry using a response surface methodology. *RSC Advances*, **5**, 19686–19695.

Wijngaard, H., Hossain, M.B., Rai, D.K. & Brunton, N. (2012). Techniques to extract bioactive compounds from food by-products of plant origin. *Food Research International*, **46**, 505–513.

Winkel-Shirley, B. (2002). Biosynthesis of flavonoids and effects of stress. *Current Opinion in Plant Biology*, **5**, 218–223.

Wong, C.W., Pui, L.P. & Ng, J.M.L. (2015). Production of spray-dried pineapple (*Ananas comosus*) powder from enzyme liquefied puree. *International Food Research Journal*, **22**, 1631–1636.

Woo, M.W. & Bhandari, B. (2013). Spray drying for food powder production. In: *Handbook of Food Powders: Processes and Properties* (edited by B. Bhandari). Pp. 29–56. Cambridge: Woodhead Publishing.

Wynberg, R., Silveston, J. & Lombard, C. (2009). Value adding in the Southern African natural products sector: how much do patents matter?. In: *The Economics of Intellectual Property in South Africa* (edited by E. Burrone & P. Rai). Pp. 18–55. Geneva: World Intellectual Property Organisation.

Yan, M., Liu, W., Fu, Y., Zu, Y., Chen, C & Luo, M. (2010). Optimisation of the microwave-assisted extraction process for four main astragalosides in *Radix astragali*. *Food Chemistry*, **119**, 1663–1670.

Yan, B., Li, Y., Guo, Z. & Qu, H. (2014). Quality by design for herbal drugs: a feedforward control strategy and an approach to define the acceptable ranges of critical quality attributes. *Phytochemical Analysis*, **29**, 59–65.

Yang, L., Cao, Y.L., Jiang, J.G., Lin, Q.S., Chen, J. & Zhu, L. (2010). Response surface optimization of ultrasound-assisted flavonoids extraction from the flower of *Citrus aurantium* L. var. amara Engl. *Journal of Separation Science*, **33**, 1349–1355.

Yang, H.U., Yang, S.C., Chao, J.C.J. & Chen, J.R. (2012). Beneficial effects of catechin-rich green tea and inulin on the body composition of overweight adults. *British Journal of Nutrition*, **107**, 749–754.

Yao, L., Caffin, N., D'Arcy, B., Jiang, Y., Shi, J., Singanusong, R., Liu, X., Datta, N., Kakuda, Y. & Xu, Y. (2005). Seasonal variations of phenolic compounds in Australia-grown tea (*Camellia sinensis*). *Journal of Agricultural and Food Chemistry*, **53**, 6477–6483.

Young, S.L., Sarda, X., & Rosenberg, M. (1993). Microencapsulation properties of whey proteins. 1. Microencapsulation of anhydrous milk fat. *Journal of Dairy Science*, **76**, 2868–2877.

Yuan, Y. & Lee, T.R. (2013). Contact angle and wetting properties. In: *Surface Science Techniques* (edited by G. Bracco and B. Holst). Pp. 3–34. Berlin: Springer-Verlag. GmbH.

Zhang, L., Wang, Y., Wu, D., Xu, M. & Chen, J. (2011). Microwave-assisted extraction of polyphenols from *Camellia oleifera* fruit hull. *Molecules*, **16**, 4428–4437.

Zhang, L., Yan, B., Gong, X., Yu, L.X. & Qu, H. (2013). Application of quality by design to the process development of botanical drug products: a case study. *AAPS PharmSciTech*, **14**, 277–286.

Zhang, H., Tang, B. & Row, K. (2014a). A green deep eutectic solvent-based ultrasound-assisted method to extract astaxanthin from shrimp byproducts. *Analytical Letters*, **47**, 742–749.

Zhang, P.Y., Xu, X. & Li, X.C. (2014b). Cardiovascular diseases: oxidative damage and antioxidant protection. *European Review for Medical and Pharmacological Sciences*, **18**, 3091–3096.

Zheng, H., Hwang, I. & Chung, S.K. (2009). Enhancing polyphenol extraction from unripe apples by carbohydrate-hydrolyzing enzymes. *Journal of Zhejiang University Science B*, **10**, 912–919.

Zou, T., Jia, Q., Li, H.W., Wang, C. & Wu, H. (2013). Response surface methodology for ultrasound-assisted extraction of astaxanthin from *Haematococcus pluvialis*. *Marine Drugs*, **11**, 1644–1655.

3. Optimisation of green rooibos hot water extraction using quality-by-design methodology

Elements of this chapter have been published as part of:

De Beer, D., Miller, N. & Joubert, E. (2016). Production of dihydrochalcone-rich green rooibos (*Aspalathus linearis*) extract taking into account seasonal and batch-to-batch variation in phenolic composition of plant material. *South African Journal of Botany*, [in press], doi:10.1016/j.sajb.2016.02.198.

3.1. Abstract

Unfermented *Aspalathus linearis* plant material, otherwise known as green rooibos (GR), has been shown to contain high levels of health-promoting flavonoids, particularly aspalathin, a *C*-glucosyl dihydrochalcone which is unique to *A. linearis*. Aspalathin is a potent antioxidant and has demonstrated antidiabetic effects in a variety of cell-based studies. Green rooibos extract (GRE) could be commercialised as an antidiabetic nutraceutical, but the batch-to-batch quality of such botanical extracts are often compromised by the inherent natural variability in the raw material. Rooibos is cultivated using seedlings and is subject to external and genetic factors which is likely to lead to significant variability in the aspalathin content of different production batches of GR. Quality-by-design (QbD) methodology was applied to optimise the hot water extraction process of GR for maximum aspalathin and soluble solids yields. Risk assessment was conducted to identify critical process parameters or critical material attributes likely to have a major effect on the extraction efficiency. The extraction temperature, extraction time, water-to-plant material ratio and rooibos particle size were selected for further investigation using preliminary one-factor-at-a-time (OFAT) experiments, in which the individual effects of each parameter was tested at fixed levels of the remaining parameters and using a single production batch of commercial GR plant material. Ranges of the chosen parameters were identified in which optimal values for maximum process efficiency would most likely be located. The extraction process was then optimised using multifactorial response surface methodology. Hot water extractions were carried out according to a central composite design with three independent variables: extraction time (10–40 min), extraction temperature (41–93 °C) and water-to-plant material ratio (6.59–23.41:1, $v.m^{-1}$). Prediction models and combined response surfaces for extract yield (EY; $g.100\ g^{-1}$ plant material), aspalathin extraction efficiency (Asp_EE; $g.100g^{-1}$ in plant material) and aspalathin content $g.100\ g^{-1}$ soluble solids) were generated. Verification of the prediction models showed good predictive ability of the prediction models for EY and Asp_EE. Therefore, multiple desirability profiling was applied to identify the optimal values of the independent variables which would maximise the EY and Asp_EE. Optimal conditions were identified based on these results, along with considerations of cost-efficiency: extraction time: 29–31 min, extraction temperature: 90–95 °C and water-to-plant material ratio: 9–11:1 ($v.m^{-1}$). Validation of the optimal extraction parameters was carried out by extracting ten different production batches of commercial GR. The soluble solids and aspalathin yields predicted by the regression models were not obtained in all of the validation experiments, which was attributed to the differences in the composition and average particle sizes of the production batches. This reflects the natural variability which accompanies the use of herbal raw materials. The validation batches were then subjected to particle size reduction treatments by sieving out larger size fractions of plant material. Removal of large particles (>12 mesh) resulted in highly improved

aspalathin extraction and soluble solids yields in certain batches which contained higher amounts of stems and coarse material. In general, higher yields and extraction efficiency were associated with smaller particle sizes and minimal stem/wood content. In order to achieve optimal yields and extraction of aspalathin in a hot water extraction process of GR, it is therefore recommended that the leaves be cut as short as possible and the inclusion of undesirable coarse material and stems be avoided. This would require the application of risk assessment and quality assurance steps at the primary processing and distribution stages.

3.2. Introduction

Plant materials have been utilised for many years as a renewable source of bioactive chemical compounds for the production of phytopharmaceuticals. Recent years has seen renewed interest in plant extracts specifically for commercialisation as functional food ingredients or nutraceuticals. Well-established examples include *Ginkgo biloba* (Chen *et al.*, 2011), *Panax notoginseng* (Ng, 2006; Uzayisenga *et al.*, 2014), Oriental tea (Astill *et al.*, 2001; Yao *et al.*, 2005; Zimmerman & Gleichenhagen, 2011), St. John's Wort (*Hypericum perforatum*) (Cossuta *et al.*, 2012; Karakashov *et al.*, 2015) and grape seed (Hernández-Jiménez *et al.*, 2012). Sustainability has become a critical point of differentiation in the nutraceuticals market (Moloughney, 2016), emphasising the importance of optimising extraction processes to limit resource usage and waste generation.

A notable challenge involved in the use of plant material for preparation of extracts is the variation in chemical composition and overall quality, with some raw materials containing suboptimal concentrations of the desired compounds to be extracted for commercialisation (Takeuchi *et al.*, 2009). Apart from inherent genetic variation present in plant material, there are also external factors which promote variation, e.g. climate, salinity stress, UV-radiation, seasonal effects, diurnal cycles, development stage of shoots and post-harvest processing methods (Aherne & O'Brien, 2002; Yao *et al.*, 2005; Di Ferdinando *et al.*, 2013). These are common causes of variable batch-to-batch quality of plant extracts, and a strategy which aims to control the impact of these natural variations would be a first step towards attaining a more reliable level of quality. Some of the bioactive compounds intended for extraction may be prone to undesirable chemical changes during the production process, which can make it even more challenging to establish and maintain an acceptable range of quality attributes (Fischer *et al.*, 2015).

The concept of quality-by-design (QbD) refers to an approach in which the desired quality attributes of a product is effectively designed into the manufacturing process rather than relying on extensive post-production quality testing. This approach has been approved for use in the biopharmaceutical industry by the United States Food and Drug Administration and is increasingly being applied in this area in recent years (ICH, 2009; Rathore & Winkle, 2009; Das *et al.*, 2014).

Numerous statistical tools may be utilised in a QbD approach to describe experimental processes and their input/output factors. One such statistical tool is response surface methodology (RSM), which refers to the use of mathematical modelling of experimental data to obtain response surfaces and associated data from which reliable conclusions about the experimental process can be drawn (Bezerra *et al*., 2008; Granato & De Araújo Calado, 2014). The concept of *design of experiments* (DOE) is another element of QbD, and it entails the systematic planning of experiments so that any obtained data can be used to draw reliable conclusions (Dejaegher & Vander Heyden, 2011). By intentionally altering the process input factors, the effect on process output variables can be observed. Optimisation of a process by QbD typically aims to increase the yield and performance of a system whilst minimising the various costs involved (Huang *et al*., 2009; Leardi, 2009).

Rooibos (*Aspalathus linearis*), a fynbos species endemic to the Western Cape region of South Africa, has been successfully commercialised as herbal tea both locally and internationally. Known for many years as a healthy beverage (Joubert & De Beer, 2011), demonstration of antidiabetic properties for rooibos extracts and aspalathin, a novel rooibos *C*-glucosyl dihydrochalcone (Kawano *et al*., 2009; Muller *et al*., 2012; Mazibuko *et al*., 2013; Son *et al*., 2013; Kamakura *et al*., 2015; Mazibuko *et al*., 2015) motivated the present investigation into the production of rooibos extract containing high levels of this compound. The major factors which affect the recovery of phenolic compounds from plant materials are the solvent type, solvent-to-solid ratio, extraction time, extraction temperature, particle size and pH (Shi *et al*., 2005). The effect of each of these factors on the mass transfer kinetics is unique to each type of plant matrix, and optimised extraction processes should therefore be developed for each type of botanical raw material (Wijngaard *et al*., 2012). For the present study, "unfermented" green rooibos (GR) plant material was chosen as raw material since aspalathin undergoes significant oxidative degradation during the production of traditional "fermented" rooibos (Joubert, 1996). Furthermore, water at natural pH was selected as extraction solvent given the common consumption of rooibos as a hot water infusion for many generations.

In summary, the aim of the present study was to optimise the hot water extraction process of GR plant material by applying QbD methodology. Risk assessment and preliminary investigations were conducted in order to identify potential critical process parameters (CPPs) and critical material attributes (CMAs). These parameters and their effects on the critical quality attributes (CQAs) of the green rooibos extract (GRE) were then investigated using multivariate RSM.

3.3. Materials and methods

3.3.1. Chemicals and reagents

Authentic reference standards with purity >95% were obtained from the South African Medical Research Council (PROMEC Division, Bellville, South Africa; aspalathin and nothofagin) and

Extrasynthese (Genay, France; iso-orientin and orientin). Formic acid (≥99.8%) was purchased from Merck Millipore (Darmstadt, Germany), and Chromasolv Plus gradient grade "far ultraviolet (UV)" acetonitrile (≥99.9%) and ascorbic acid were purchased from Sigma-Aldrich (St. Louis, MO, USA). Deionised water prepared using an Elix Advantage 5 water purification system (Merck Millipore) was purified further to obtain high performance liquid chromatography (HPLC) grade water using a Milli-Q Reference water purification system (Merck Millipore). Deionised water was used in all extraction experiments and for the preparation of aqueous solutions.

3.3.2. Green rooibos plant material

A large sample set (n = 47) drawn from individual production batches (Batches A1 to A47; ≈1.5 kg per batch) of unfermented rooibos plant material from a single plantation was obtained from Rooibos Ltd. (Clanwilliam, South Africa) with the aim to determine the variation in the content of the major flavonoids in GR, as well as to determine the variation in their content in the optimised extract, prepared from each batch. Their production took place over a 48-day period (27 January to 16 March 2015). An aliquot of each sample (≈10 g) was finely ground with a Retsch MM301 ball mill (Retsch GmbH, Haan, Germany) and stored at <5 °C until required for quantification of the phenolic content of the plant material (i.e. water-acetonitrile extraction and HPLC analysis). The unmilled plant material was stored at <5 °C until it was used "as-is" for hot water extraction (optimum conditions).

For optimisation of extraction conditions, a large sample of unfermented rooibos plant material (≈18 kg) from an individual production batch (Batch B; production date 20 August 2014) was obtained from Rooibos Ltd (Clanwilliam, South Africa). An aliquot of this plant material (≈700 g) was milled to a fine powder, using a Retsch SM 100 cutting mill (1 mm sieve; Retsch GmbH, Haan, Germany) followed by 2 min in a Retsch MM301 ball mill. Another aliquot (1 kg; in triplicate) of this plant material was sieved for 90 seconds using a SMC Mini-Sifter (J.M. Quality Control Services, Wynberg, South Africa) fitted with three mesh sieves and a pan to collect the fractions >12, 16<x<12, 20<x<16 and <20 mesh. The fractions were weighed to the nearest 3 decimals using a Sartorius L420P balance (Sartorius AG, Göttingen, Germany) to determine the relative contribution of each size fraction of plant material to the overall mass of the plant material received. Aliquots (≈10 g) of each of the four recovered size fractions from Batch B were milled to a fine powder for 2 min in a Retsch MM301 ball mill and stored at <5 °C until required for determination of their flavonoid content and subsequent HPLC analysis. The remaining unmilled plant material from Batch B was stored at <5 °C until it was used "as-is" for extract optimisation experiments. Preliminary investigations showed that it was impractical to use finely milled plant material due to rapid clogging of the filtration equipment and impractical delays in operations.

3.3.3. Risk assessment for extraction unit operation

Prior to conducting one-factor-at-a-time (OFAT) investigations on the effect of process input factors on the extraction efficiency, risk assessment was carried out to identify the various factors which should be taken into consideration. An Ishikawa diagram (Saraph *et al*., 1989) was constructed to group together the process parameters and material attributes which would most likely have a significant effect on the extraction efficiency. The latter refers to the capacity of the process to extract the maximum possible amount of bioactive compound whilst simultaneously providing acceptable yields of extracted rooibos solids and minimal practical limitations. Previous practical experience with extraction of fermented rooibos (Joubert, 1984; 1988a; 1988b; 1990a; 1990b; 1990c; Joubert & Hansmann, 1990), as well as a similar risk assessment step carried out by Gong *et al.* (2014), was considered in the selection of input factors for further investigation.

3.3.4. One-factor-at-a-time (OFAT) extractions

Prior to the development of response surface models, the individual effects of the extraction time, extraction temperature, water-to-plant material ratios and particle sizes were investigated in a series of OFAT experiments. The factor under investigation in a particular experiment was tested at different levels while all other factors were kept at a constant level. This was done in order to determine the ranges of the independent variables in which an optimum response is likely to be achievable. These ranges formed the basis for selecting an appropriate experimental design for subsequent RSM experiments.

The general extraction procedure entailed weighing the GR plant material (25 g; Batch B – unrefined and unmilled) into 1 L Schott bottles. Hot water extraction was commenced by adding the required amount of deionised water (preheated to the experimental temperature in question) to the plant material, and placing the Schott bottle in a preheated water-bath. Extraction time was recorded from the moment that the water was added to the plant material. The contents of each sealed Schott bottle were agitated for 5 s at 5 min intervals for the duration of the extraction period. Once the extraction time had elapsed, the contents were immediately filtered through Whatman No. 4 filter paper (ø = 150 mm; Whatman International Ltd., Maidstone, England) using a vacuum-assisted Büchner filtration apparatus. The filtrate was used to determine the soluble solids content of the hot water extract and aliquots of the remaining extract were stored at -18 °C for subsequent analysis.

The effect of various extraction times (10, 20, 30, 40, 50 and 60 min) on the extraction efficiency of the plant material was determined by extraction at a fixed temperature (93 °C) and

water-to-plant material ratio (10:1; v.m^{-1}). The effect of temperature (30, 45, 60, 75 and 90 °C) on the extraction efficiency was determined at a fixed extraction time (20 min) and water-to-plant material ratio (10:1). The extractions were performed in triplicate over three days in a completely randomised order. The effect of different water-to-plant material ratios (5:1, 10:1, 15:1 and 20:1; v.m^{-1}) on the extraction efficiency was determined at a fixed extraction temperature (60 °C) and extraction time (20 min). The ratios were achieved by adding the appropriate volume of re-heated water (125, 250, 325 or 500 mL) to 25 g plant material. The effect of different size fractions on the extraction efficiency was determined using four size fractions as described in section 3.3.2. The other extraction conditions were fixed at 60 °C, 20 min and 15:1 water-to-plant material ratio. For this experiment, 15 g of plant material were extracted with 225 mL water. All extractions were performed in triplicate in completely randomised order for each factor.

3.3.5. Optimisation of extraction unit operation

A central composite design (CCD) consisting of 16 experimental runs was used to optimise the extraction process. The independent variables under investigation were extraction temperature (°C), extraction time (min) and water-to-plant material ratio (v.m^{-1}). The ranges of treatment levels of the independent variables (Table 3.1) were chosen based on the results of the preliminary OFAT extractions. The effect of different particle size fractions on the extraction efficiency was not investigated in the central composite design since the size fractions are discrete, fixed values which are not amenable to optimisation. Furthermore, the particle size distribution, as well as the stem and leaf content of the various plant material size fractions, may differ significantly from batch to batch. As with the preliminary single factor extractions, a single batch of plant material (Batch B) was used for all the RSM experimental runs. The 16 experimental runs of the CCD were performed in triplicate in a completely randomised order over 10 days. The same general extraction procedure was followed as with the preliminary OFAT hot water extractions.

Table 3.1 Independent variables and their levels as applied in central composite design for green rooibos hot water extraction optimisation.

Factor	Symbol	Levels				
		-α (-1.68)	**-1**	**0**	**+1**	**+α (1.68)**
Extraction time (min)	X_1	10	16	25	34	40
Extraction temperature (°C)	X_2	41	51	67	82	93
Water-to-plant material ratio (v.m^{-1})	X_3	6.59	10	15	20	23.41

The experimental data obtained from the central composite design were used to generate regression coefficients and fitted to a second order polynomial equation:

$$y = \beta_0 + \Sigma_{j=1}^{k}\beta_j X_J + \Sigma_{j=1}^{k}\beta_{jj}X_j^2 + \Sigma\Sigma_{i<j}\beta_{ij}X_iX_j + \varepsilon$$

where β_0, β_j, β_{jj}, and β_{ij} represent regression coefficients for intercept, linear, quadratic and interaction terms, respectively. The response value (dependent variable) is represented by y, and X_i and X_j represent the level of the independent variables (factors). The term k represents the number of factors under investigation, while ε represents the residual error associated with the experiment. Verification of the prediction models for the dependent variables was carried out by conducting an additional replication of the CCD. Validation of the optimal extraction conditions was carried out by performing extractions (in triplicate) on ten randomly selected batches of commercial green plant material (30 g per sample) from the large sample set.

All the commercial plant material batches (n = 47) were also extracted at the optimal conditions (in duplicate) and the filtrates freeze-dried to allow (1) comparison with literature data of similarly prepared extracts of fermented rooibos plant material (Joubert & De Beer, 2012) and (2) determination of the relationship between the flavonoid content of the extract and the plant material. The freeze-dried extracts (FDE) were stored at <5 °C until HPLC, total polyphenol content (TPC) and total antioxidant capacity (TAC) analysis.

3.3.6. HPLC analysis of plant material and extracts

Sample preparation for the determination of the flavonoid content of the plant material entailed a procedure, using 33% ($v.v^{-1}$) acetonitrile as solvent, adapted from Joubert *et al.* (2014). Briefly, 80 mg of milled plant material were weighed into 5 mL glass reaction vials, 3 mL solvent added to each vial and the sealed vials heated in a Stuart SBH220D/3 block heater (Bibby Scientific Ltd., Staffordshire, UK) set at 100 °C for 20 min. Following sonication for 5 min in a Branson B-12 Ultrasonic Cleaner (50/60 Hz, 80 W; Branson Ultrasonics, Danbury, CT, USA), the samples were cooled to room temperature (ca. 22°C) and 0.5 mL of a 10% ascorbic acid solution ($m.v^{-1}$) added to prevent oxidation of the phenolic compounds during subsequent HPLC analysis. The water-acetonitrile extracts were further diluted prior to HPLC analysis by adding 300 µL to 1000 µL deionised water Similarly, the hot water extracts, defrosted before analysis or reconstituted in deionised water, were protected against oxidation by adding 100 µL of the extract to 1000 µL 1% aqueous ascorbic acid.

Reverse-phase high performance liquid chromatography with diode array detection (RP-HPLC-DAD) was performed to quantify the four major rooibos flavonoids of all extracts using a rapid screening method (16 min) as described by De Beer *et al.* (2015). An Agilent 1200 HPLC system consisting of a quaternary pump, autosampler, on-line degasser, column oven and diode-array

detector controlled by Chemstation 3D LC software (Agilent Technologies Inc., Santa Clara, CA, USA) was used. Separation was achieved on a Poroshell SB-C18 column (50x4.6 mm, 2.7 µm particle size) (Agilent Technologies Inc.), protected by an Acquity UPLC in-line filter (Waters; 0.2 µm) and an Acquity UPLC VanGuard pre-column (Waters; Stationary phase: BEH C18 1.7 µm) maintained at 30 °C. Gradient elution was performed using 0.1% aqueous formic acid (A) and acetonitrile (B) at 1 mL.min^{-1} as follows: 0–10 min, 12.4–16.6% B; 10–10.5 min, 16.6–80% B; 10.5–11.5 min, 80% B; 11.5–12 min, 80–12.4% B; 12–16 min, 12.4% B. UV-Vis spectra were recorded for all samples from 220 to 450 nm with quantification of the dihydrochalcones at 288 nm and the flavones at 350 nm, respectively. Stock solutions of authentic reference standards (ca. 1 mg.mL^{-1}) in dimethyl sulfoxide were used to prepare a standard calibration mixture. It was injected at different injection volumes to obtain 7-point calibration curves for aspalathin, iso-orientin, orientin and nothofagin. The results were expressed as a percentage of the plant material (dry basis) or soluble solids content of the extracts (g.100 g^{-1} = %; m.m^{-1}). UV-Vis spectra and retention times of the peaks corresponding to those of aspalathin, iso-orientin, orientin and nothofagin were compared to those of the authentic standards for identification. Prior to HPLC analysis, the diluted extracts with ascorbic acid added and the standard calibration mixtures were filtered using 0.22 µm pore-size Millex-HV hydrophilic polyvinylidene difluoride syringe filter devices (Merck Millipore) with 33 and 4 mm diameters, respectively. An injection volume of 10 µL was used for all HPLC analyses.

3.3.7. Gravimetric determination of soluble solids content of extract

The soluble solids (SS) contents of all extract filtrates were determined in duplicate by gravimetric analysis. An aliquot (10 mL) of the extract filtrate were transferred to pre-weighed nickel moisture dishes on a Merck Model 402 steam-bath and evaporated until visibly dry. Final drying occurred in a forced-air laboratory drying oven set at 100 °C for 60 min, whereafter the samples were cooled under desiccation, re-weighed and the resulting difference in mass calculated. The theoretical extract yield was calculated based on the total solvent volume and mass of plant material that was used, and expressed in terms of g.100 g^{-1} plant material (%; m.m^{-1}).

3.3.8. Total polyphenol content and total antioxidant capacity

The TPC and TAC of the FDEs, reconstituted in deionised water, were determined in triplicate by using the 96-well plate format of the Folin-Ciocalteau method and α,α-diphenyl-β-picrylhydrazyl (DPPH) radical scavenging assay, respectively, as described by Arthur *et al.* (2011). The TPC and TAC results were expressed in terms of g gallic acid equivalents (GAE) per 100 g FDE and µmol Trolox equivalents (TE) per g FDE, respectively. The Trolox equivalent antioxidant capacity (TEAC)

of aspalathin, iso-orientin and orientin were determined by analysing a range of concentrations (2–16 µM in the reaction volume) for each compound. The % DPPH radical inhibition was plotted against concentration and the slope of each linear regression model was divided by the corresponding slope for Trolox. The concentration of each compound in the FDE and its TEAC value were subsequently used to determine the contribution of the compound to the TAC of the extract.

3.3.9. Statistical analysis

Univariate analysis of variance (ANOVA) was carried out on all OFAT experiment data using SAS® software (Version 9.2, SAS Institute Inc., Cary, NC, USA) to determine whether differences between treatment means were significant. Least significant difference (LSD) of the Student's t-test ($P = 0.05$) was calculated to compare treatment means where significant differences were found ($P < 0.05$) (Ott & Longnecker, 2010). Levene's test was used to test for treatment homogeneity of variance. In instances where variances were not equal a weighted analysis of variance was used for the combined analyses. The Shapiro-Wilk test was performed on the standardised residuals from the models to assess for normal distribution of the data (Shapiro & Wilk, 1965). Statistica 12.0 (Statsoft Southern Africa, Sandton, South Africa) was used to analyse all data generated by RSM. The statistical significance and suitability of the regression model, its factors and their interactions were determined at the 5% probability level ($P < 0.05$) using ANOVA. Standardised Pareto charts were used to illustrate the significant effects obtained for the different response values by ANOVA. The fitting efficiency of the data to the model was evaluated by calculating the correlation coefficient (R^2), the adjusted correlation coefficient (R^2_{adj}) and the significance of lack of fit (LOF). The regression equation that was generated for each response was illustrated as two-dimensional contour plots and three-dimensional response surface plots. The intra-class correlation coefficient (ICC) was used to assess the predictive ability of the models. The hot water extraction parameters were optimised by the application of multiple desirability profiling. Post-hoc agglomerative hierarchical clustering (AHC) was applied to the validation experiment data using XLStat (version 2014, Addinsoft, New York, USA) in order to identify different batch classes. GR production batch clusters were identified based on their particle size distributions as determined by sieving. Univariate box-and-whisker diagrams were generated using XLStat (version 2014, Addinsoft, New York, USA) to present the distribution of the content values for each rooibos compound in the commercial GR sample and their extracts. Regression analysis was performed using MS Excel 2016 (Microsoft, Redmond, WA, USA).

3.4. Results and discussion

Rooibos extracts have in recent years been utilised in various consumer products in the food, nutraceuticals and cosmetics categories (Biénabe *et al.*, 2009; Joubert & De Beer, 2011). One of the most recent applications by the South African food industry is its inclusion in a new variety of "health-promoting" whole-wheat bread (Anon., 2015). These uses are largely linked to the antioxidant activity of rooibos (Joubert & De Beer, 2011). Unfermented rooibos plant material is the preferred raw material for the production of rooibos extracts with high polyphenol content (specifically aspalathin) (Joubert & De Beer, 2014). Minimum acceptable levels of total polyphenols and aspalathin in the plant material intended for extract production have not yet been defined, as this would depend on the intended final application of the extract and determined by the extract manufacturer. Harvesting the plant material when aspalathin levels are optimal would be a logical first step to producing a rooibos nutraceutical extract with high aspalathin content.

Various botanical extracts have been proven to be valuable renewable sources of health-promoting bioactive compounds, and extract of unfermented *Aspalathus linearis* containing high levels of aspalathin is an example of one with potential for application in a nutraceutical product. Plant materials are complex by nature, and the extraction of compounds they contain is influenced by process parameters like temperature, solvent type, extraction time, mechanical action (e.g. shaking or ultrasonication) and the solubility of the target compounds (Azmir *et al.*, 2013). Furthermore, the distribution of the target compounds may differ between different types or batches of plant material (Takeuchi *et al.*, 2009).

Aspalathin is a water-soluble, hydrophilic compound (Huang *et al.,* 2008), and hot water extraction is a safe and energy-efficient method for rooibos extraction particularly if it is for the production of food-grade extracts. Other considerations when selecting a solvent is that it should have "generally recognized as safe" (GRAS) status. Whilst an aqueous organic solvent extract of GR would potentially deliver an extract with higher bioactive content, it would also entail the input of additional energy and unit operations to remove and recover the solvents for downstream processing. In the interest of conserving energy and adhering to "green chemistry" principles, the use of water is therefore advantageous (Chemat *et al.*, 2012). It is additionally suitable in that hot water infusions of *Aspalathus linearis* have traditionally been consumed as a beverage and is an established commercial product with no reported health hazards (Joubert & De Beer, 2011).

Previous studies on the extraction of rooibos focussed on fermented rooibos and applied OFAT analysis to study the effect of extraction temperature, water-to-leaf ratio and flow rate, using a fixed-bed flow-through batch extraction system, on soluble solids recovery and polyphenol content of extracts (Joubert, 1988b; 1990b; 1990c; Joubert & Hansmann, 1990). Higher extraction temperatures, and higher water-to-leaf ratios as well as longer extraction times led to more effective

extraction of soluble matter and polyphenols. For these experiments no individual phenolic compounds were quantified and only colourimetric methods were used to determine total polyphenol, flavonoid and non-flavonoid content of extracts.

3.4.1. Characterisation of phenolic content of different batches of green rooibos plant material

The aspalathin content of commercial GR, the raw material used in this study for investigation of aspalathin extraction, has not been quantified to date. For this reason, a large number of production batches (n = 47), sourced from a major commercial GR producer, have been sampled and analysed for their aspalathin content, as well as the content of three other flavonoids, nothofagin, orientin and iso-orientin. The aspalathin content of these production batches (Batches A1–A47) varied between 2.50–4.49%, while their nothofagin content varied between 0.22–0.51% (Fig. 3.1), despite the plant material having originated from the same plantation over a time period of just 48 days. The mean aspalathin and nothofagin content of the various batches of plant material, sorted by harvest date, are depicted in Fig. 3.2. There was no clearly identifiable trend regarding dihydrochalcone content and harvest time over this period. Various factors would have potentially affected the dihydrochalcone content of the various batches, with genetic variation being one of the primary factors. As per normal industry practice, the plantation was established using seedlings from randomly collected seeds originating from open-pollinated plants. Joubert & De Beer (2011) have previously demonstrated that the aspalathin content of rooibos leaves of individual plants shows significant variation, with similar variation likely to be observed for nothofagin. Minor differences in processing conditions between batches, i.e. time delays between harvesting, shredding and drying, could also contribute to variation in dihydrochalcone content of the dried product. Both the aspalathin and nothofagin content of rooibos decreased rapidly when the plant material is shredded, due to oxidation (Joubert, 1996). Iso-orientin and orientin, the flavone derivatives of aspalathin, were also present in the plant material in low quantities (<0.5%; Fig. 3.1). The iso-orientin and orientin contents were very similar in all instances, with the highest difference between iso-orientin and orientin seen in any individual batch being 0.019 g.100 g^{-1} plant material. The iso-orientin content was slightly higher than orientin in some cases, and *vice versa* in other cases (Data included in Addendum A; Table 6.1).

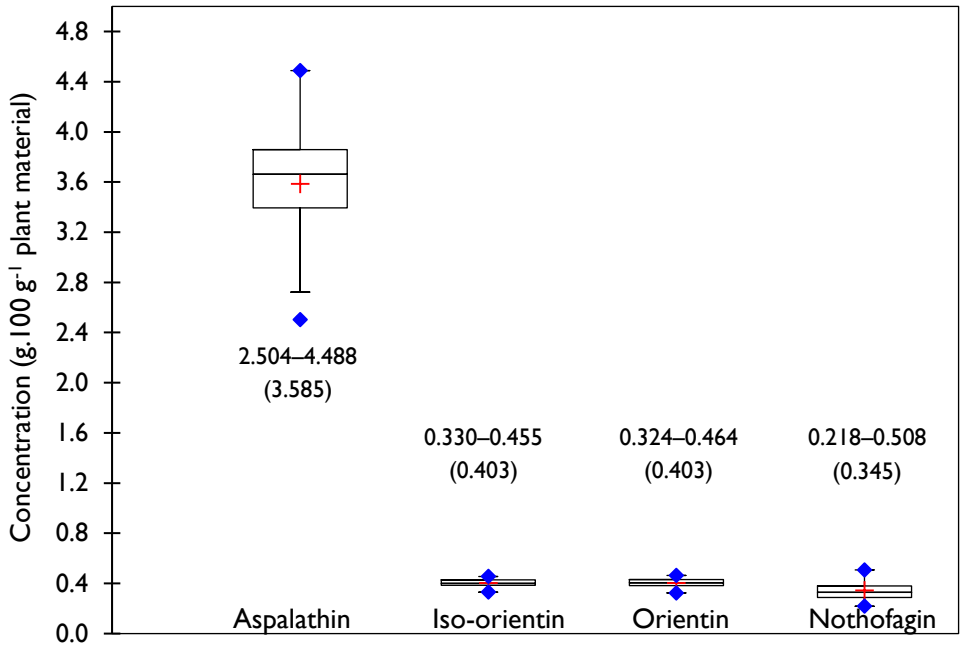

Figure 3.1 Box-and-whisker plots of aspalathin, iso-orientin, orientin and nothofagin contents of green *Aspalathus linearis* plant material (g.100 g^{-1}), indicating mean (cross markers), standard deviation (whiskers), 25th, 50th (median) and 75th percentiles (box) and outliers (diamond markers).

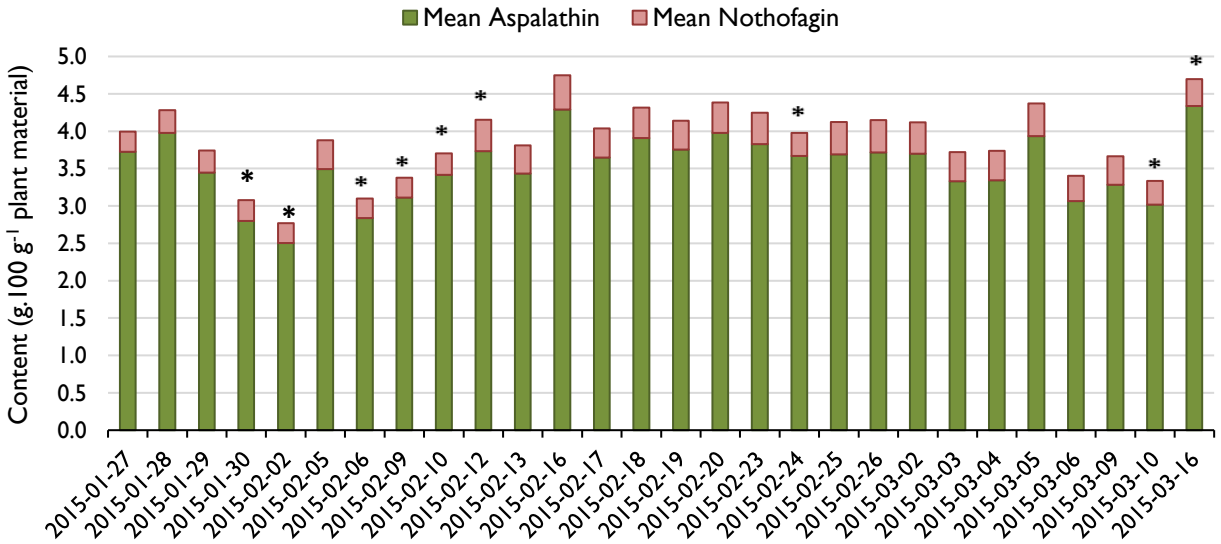

Figure 3.2 Stacked column graph depicting the mean aspalathin and nothofagin content of commercial green rooibos production batches, with plant material harvested and processed over 48-day period in early summer 2015. Values are mean of two production batches processed on the same day except those indicated with an asterisk, where only one production batch was processed on the given day.

3.4.2. Risk assessment for extraction unit operation

A risk analysis was performed to determine which process parameters and material attributes would most likely have a significant effect on the extraction efficiency (Fig. 3.3), using an Ishikawa diagram

adapted from Gong *et al.* (2014). Some of the input factors, e.g. target compound content in the plant material, particle size distribution and plant material composition, are not directly controllable by the operator of the extraction process. These factors were therefore not considered for further investigation at this stage. Environmental factors (e.g. humidity and pressure) were considered low-priority in terms of potential effect on extraction efficiency. The solvent type would be a significant input factor in any extraction optimisation, but since the express aim of the current study was to optimise the hot water extraction of green *Aspalathus linearis*, this factor, as well as solvent concentration was not applicable for further investigation. Solvent: plant material ratio, extraction time and extraction temperature were identified as critical process parameters (CPPs) in the extraction process. All are under direct control of the process operator and can be measured using standard laboratory equipment, which make them appropriate candidates for use in optimisation studies and quality assessment.

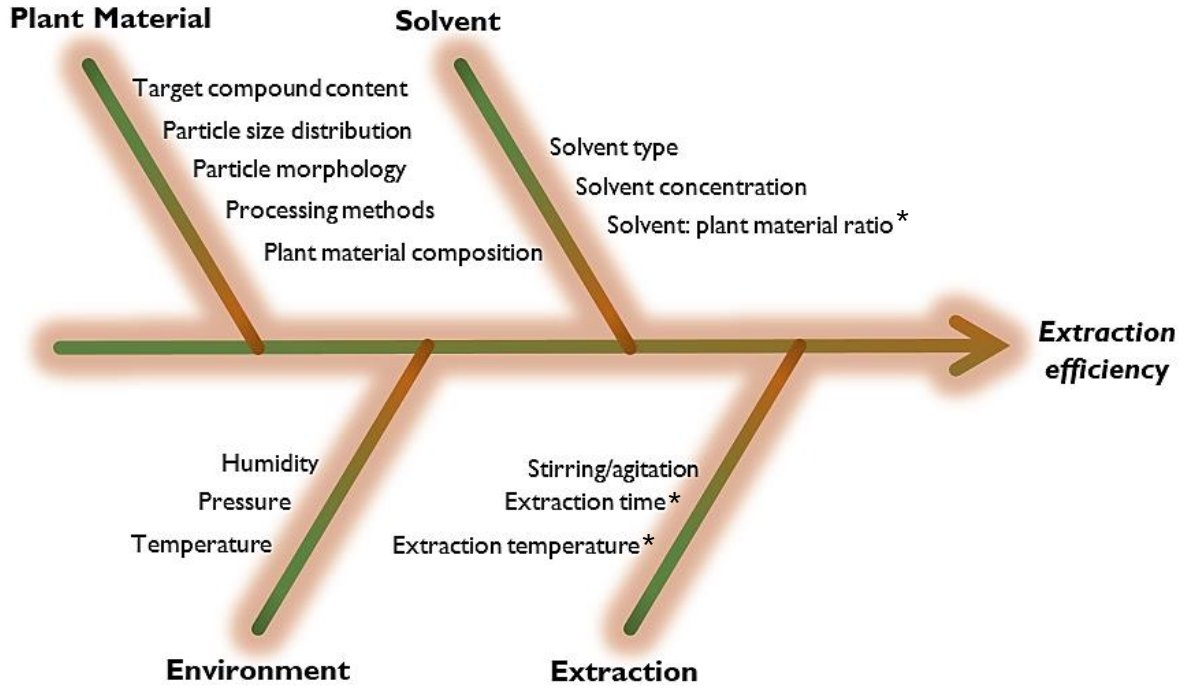

Figure 3.3 Ishikawa (fishbone) diagram showing potentially significant input factors identified in extraction process which may affect process output (extraction efficiency) (adapted from Gong *et al.*, 2014). Asterisks indicate input factors optimised by central composite design.

3.4.3. One-factor-at-a-time (OFAT) extraction

A series of OFAT hot water extraction experiments were carried out to determine the individual effects of the selected CPPs, as well as feasible ranges of treatment levels within which an optimal response would potentially be located. Aliquots of commercial GR plant material (Batch B) were

used in all the OFAT extraction experiments. The aspalathin, iso-orientin, orientin and nothofagin contents of this batch of plant material as determined by water-acetonitrile extraction are shown in Table 3.3. The aspalathin content of this batch was lower than that of the other production batches (Fig. 3.1). These values represent the amounts of the four major flavonoids which are potentially available for extraction from the plant material. The extraction efficiency of the hot water extraction process can therefore be quantified by expressing the amount of the target compound obtained by extraction as a percentage of its content in the plant material as determined by water-acetonitrile extraction. Fig. 3.4 shows the particle size distribution of Batch B in terms of four size fractions (from largest to smallest: >12 mesh, 16<x<12 mesh, 20<x<16 mesh and <20 mesh). Nearly 70% ($m.m^{-1}$) of the plant material was <16 mesh, with the remaining ca. 30% comprised of larger particle sizes (>16 mesh).

Table 3.3 Content of major flavonoid compounds ($g.100\ g^{-1}$ plant material) in commercial green rooibos (Batch B).

Compound	Unrefined ("as-is") plant material	Size fractions			
		>12 mesh	16<x<12 mesh	20<x<16 mesh	<20 mesh
Aspalathin	2.438	0.303	1.590	3.223	3.628
Iso-orientin	0.349	0.042	0.177	0.355	0.443
Orientin	0.208	0.031	0.129	0.256	0.314
Nothofagin	0.246	0.025	0.164	0.328	0.367

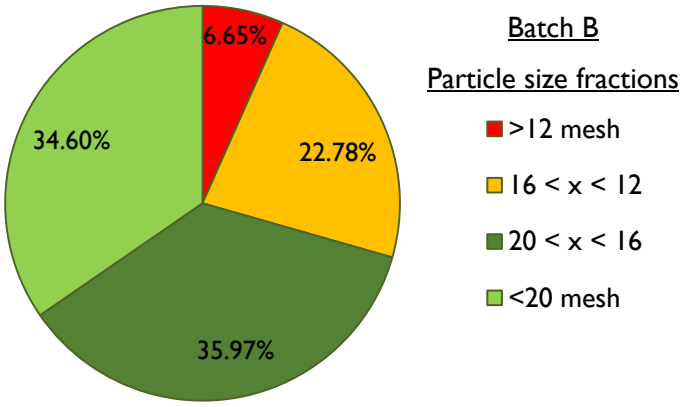

Figure 3.4 Particle size distribution of commercial green rooibos production Batch B.

Since the extract and aspalathin yield were of greater importance to the present study and the optimisation of the extraction process, only these responses will be discussed here in the interest of brevity. Additional data are presented in the addendum for the nothofagin, iso-orientin and orientin yields from the plant material and contents in the extract (Addendum A; Figs. 6.1–6.8).

3.4.3.1. Effect of extraction time on extraction efficiency

The effect of different extraction times (10, 20, 30, 40, 50 and 60 min) on the extraction efficiency of the four major rooibos flavonoids was investigated at a fixed extraction temperature (93 °C) and fixed water-to-plant material ratio of 10:1 ($v.m^{-1}$). Unrefined plant material sampled from Batch B was used, i.e. the plant material was not sieved or milled prior to extraction. Extract yield (%; $g.100\ g^{-1}$ plant material) did not differ significantly between the 10, 20 and 30 min extraction times (Fig. 3.5), but significantly higher yields, compared to 30 min extraction, were obtained at 40, 50 and 60 min. No significant differences were observed between the extract yields for 40, 50 and 60 min extraction time ($P < 0.05$). Considering that the extract yields at 10 and 50 min were 15.91 and 17.44%, respectively, the major portion of the hot water-soluble solids had already been extracted after just 10 min. Joubert & Hansmann (1990) showed that approximately 50% of the hot water-soluble solids of fermented rooibos was extracted after 5 min when using 90 °C and a flow-through batch system. Jaganyi & Wheeler (2003) demonstrated that approximately 50% of the aspalathin in fermented rooibos is extracted within 5 min in water at 80 °C, with a steady state reached after ca. 60 min.

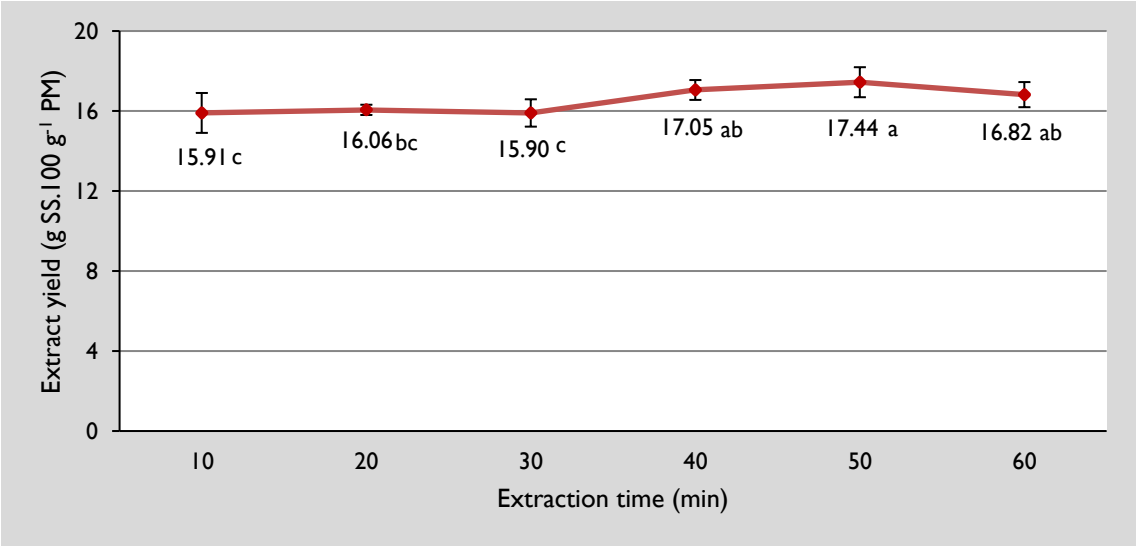

Figure 3.5 Effect of extraction time on extract yield of unrefined green rooibos (extraction temperature = 93 °C; water-to-plant material ratio = 10:1; $v.m^{-1}$). Values with the same letter are not significantly different ($P < 0.05$). SS, soluble solids; PM, plant material.

The aspalathin yield or recovery from the plant material and its corresponding content in the extract did not increase significantly with longer extraction times (Fig. 3.6). However, the aspalathin content in the extract marginally decreased from 10 min onwards, with the extract containing significantly less aspalathin only after 60 min. Oxidative degradation of aspalathin due to

the high temperature (Joubert *et al*., 2010) and/or the increased co-extraction of other water-soluble compounds may be responsible.

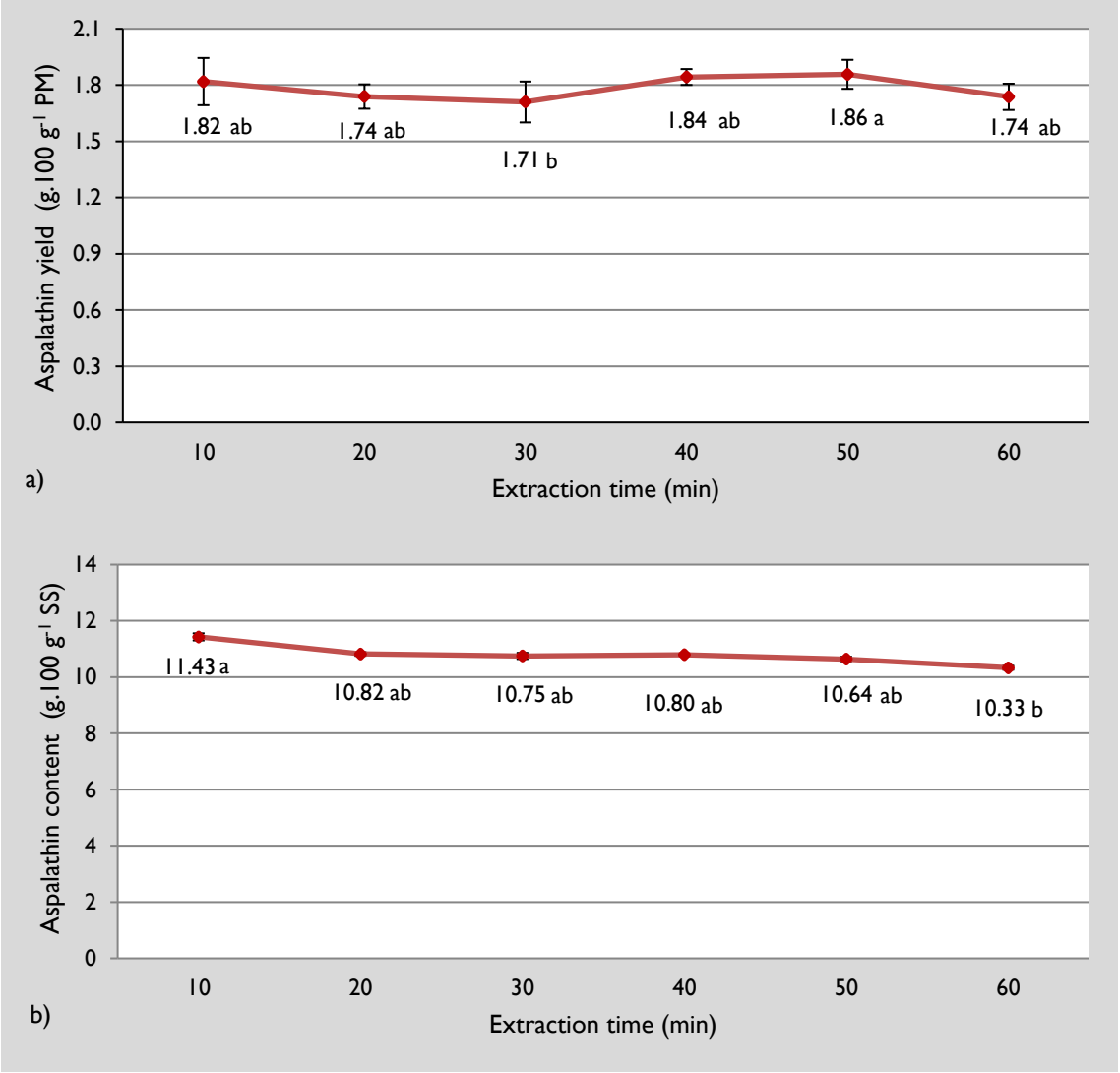

Figure 3.6 Effect of extraction time on (a) aspalathin yield and (b) aspalathin content of unrefined green rooibos extract (extraction temperature = 93 °C; water-to-plant material ratio = 10:1; v.m^{-1}). Values with the same letter are not significantly different ($P < 0.05$). SS, soluble solids; PM, plant material.

A GREwas subsequently heated for 60 min at 41, 67 and 93 °C and sampled over time at 10 min intervals to determine to what extent the four major flavonoids would degrade due to the application of heat in the extraction process (Addendum A; Fig. 6.9). Higher extraction temperature was associated with a greater decrease in the aspalathin content after 60 min (18% decrease at 93 °C vs. 7% at 41 °C). At 93 °C, the sharpest decrease in the aspalathin content occurred within the first 10 min (10%), with a less pronounced decrease seen after an extraction time of 20 min and longer. Additional data depicting the effect of heat treatment on the iso-orientin, orientin and nothofagin contents of the extract are also presented in Addendum A (Figs. 6.10–6.12). In the

interest of maximising the extract yield it would be unfeasible to employ an extraction time of 10 min or less, and an inevitable degree of thermal degradation should therefore be assumed when producing an extract by these means. The range in which an optimal extraction time in terms of overall process desirability might likely be located was identified as 10–40 min, and a fixed extraction time of 20 min was chosen for the subsequent OFAT experiments.

3.4.3.2. Effect of extraction temperature on extraction efficiency

The second OFAT experiment investigated the effect of different extraction temperatures (30, 45, 60, 75 and 90 °C) on the extraction efficiency of the water-soluble solids and aspalathin, using unrefined plant material sampled from Batch B. The extraction time and water-to-plant material ratio were fixed at 20 min and 10:1 ($v.m^{-1}$), respectively. Given the boiling point of water and the experimental setup, an upper limit of 90 °C was used. The extract yield increased significantly ($P < 0.05$) with each increasing increment of extraction temperature tested. No plateau was thus attained within the temperature range tested (Fig. 3.7).

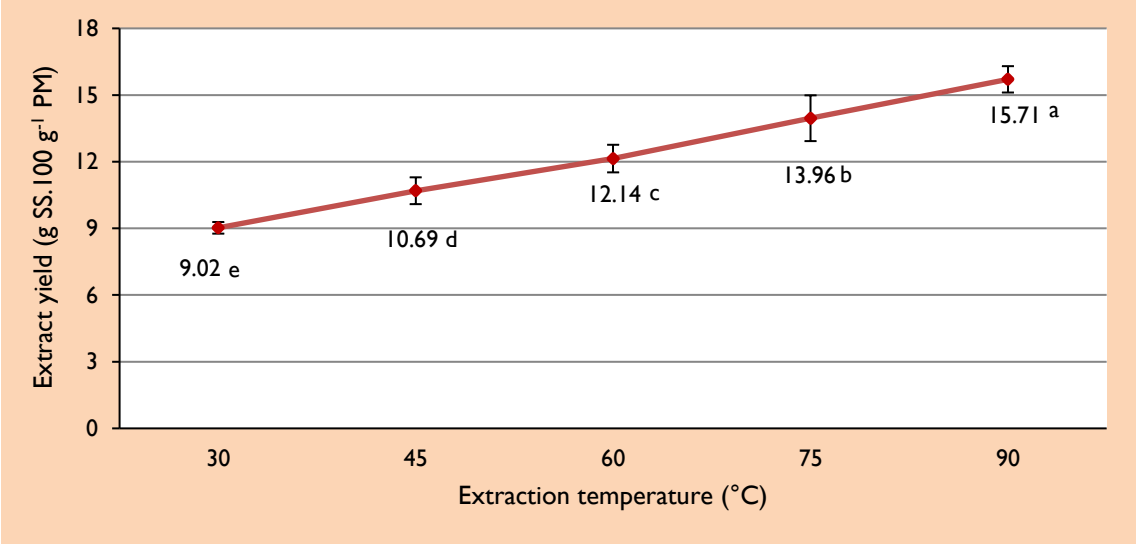

Figure 3.7 Effect of extraction temperature on extract yield of unrefined green rooibos (extraction time = 20 min; water-to-plant material ratio = 10:1; $v.m^{-1}$). Values with the same letter are not significantly different ($P < 0.05$). SS, soluble solids; PM, plant material.

A similar trend was observed for aspalathin yield (Fig. 3.8a). However, the aspalathin content of the extract was not greatly affected by temperature (Fig. 3.8b), with only extract obtained at 90 °C, having a significantly higher aspalathin content than extract obtained at 30 °C. This indicates that the extraction of other compounds such as polysaccharides was more or less affected to the same extent as aspalathin.

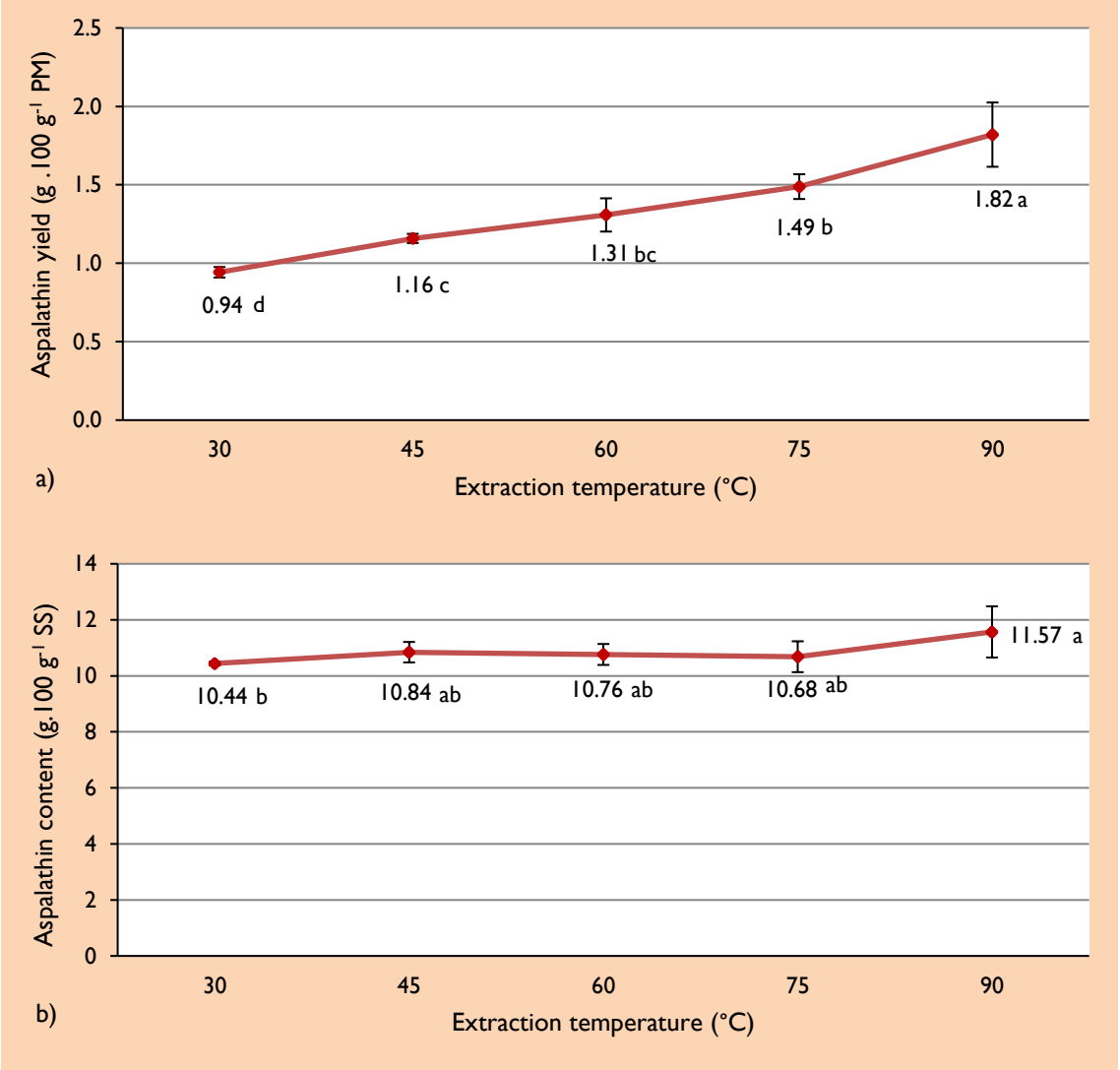

Figure 3.8 Effect of extraction temperature on (a) aspalathin yield and (b) aspalathin content of green rooibos hot water extract (extraction time = 20 min; water-to-plant material ratio = 10:1; $v.m^{-1}$). Values with the same letter are not significantly different ($P < 0.05$). SS, soluble solids. PM, plant material.

3.4.3.3. Effect of water-to-plant material ratio on extraction efficiency

The third OFAT experiment investigated the effect of using different water-to-plant material ratios (20:1, 15:1, 10:1 and 5:1; $v.m^{-1}$) on the extraction efficiency. The extraction time and temperature were fixed at 20 min and 60 °C, respectively, and unrefined plant material from Batch B was used. Extraction at 60 °C was selected as it represented the middle point of the temperature range under investigation. Soluble solids were optimally extracted with a 15:1 ratio, but the extract yield was not significantly different ($P < 0.05$) from those obtained with ratios of 10:1 and 20:1 (Fig. 3.9). It was, however, significantly higher ($P < 0.05$) than the yield obtained with a 5:1 ratio.

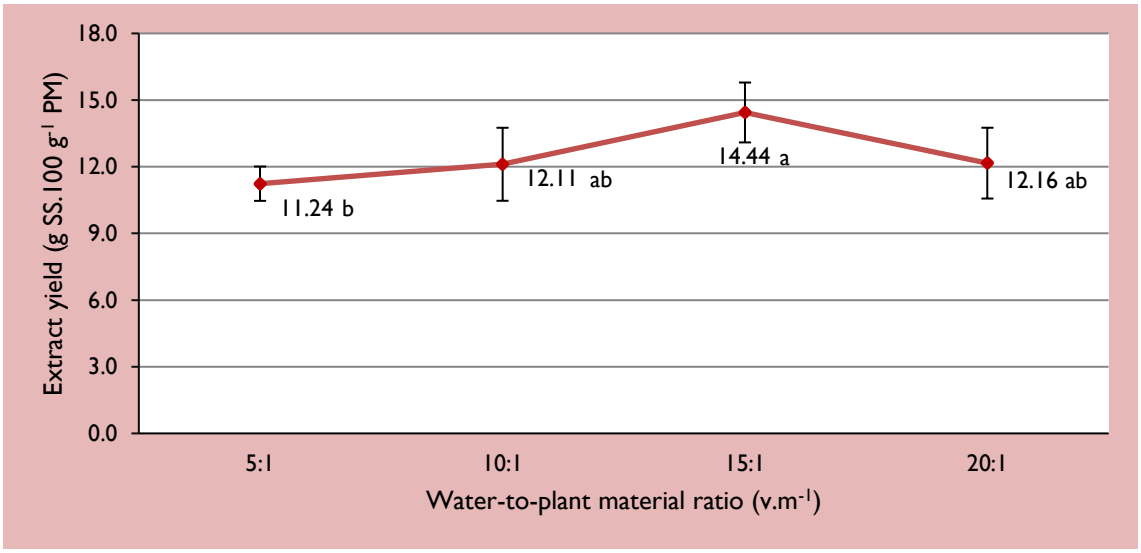

Figure 3.9 Effect of water-to-plant material ratio on extract yield of unrefined green rooibos (extraction time = 20 min; extraction temperature = 60 °C). Values with the same letter are not significantly different ($P < 0.05$). SS, soluble solids; PM, plant material.

The aspalathin yield increased significantly from a 5:1 to a 15:1 ratio, but there was no significant difference ($P < 0.05$) between the aspalathin yield at 15:1 and 20:1 (Fig. 3.10a). Such results have been observed for other plant extracts and compounds, i.e. the yield of theanine from green *Camellia sinensis* increased with higher water-to-tea ratios up to 20:1, beyond which point a plateau was reached (Vuong *et al.*, 2011). The principles of mass transfer dictate that the driving force of the extraction process is the concentration gradient of the solute between the solid and the bulk of the solvent. This concentration gradient is steeper when a higher solvent-to-solid ratio is employed, regardless of the type of solvent used (Takeuchi *et al.*, 2009). In a study similarly utilising a single factor experiment phase followed by RSM, Yang *et al.* (2010) observed a significant increase in flavonoid yields from *Citrus auranthium* when the ratio of the solvent (50% aqueous ethanol) to the plant material was increased from 10:1 to 40:1.

Despite the improved extraction efficiency, the increase in solvent consumption may have a direct impact on the cost-efficiency of the process and should be carefully considered when an optimal set of process parameters are selected. The highest aspalathin content in the extract (Fig. 3.10b) was obtained with a 20:1 ratio, but it did not differ significantly ($P < 0.05$) from the aspalathin contents obtained with a 10:1 and 15:1 ratio, indicating that similar aspalathin content could be achieved in the rooibos extract by using as little as half the amount of water required for a 20:1 water-to-rooibos ratio. This should be borne in mind when practical optimum extraction parameters are identified. Based on these results, for the subsequent preliminary OFAT experiment, a fixed water-to-plant material ratio of 15:1 was chosen.

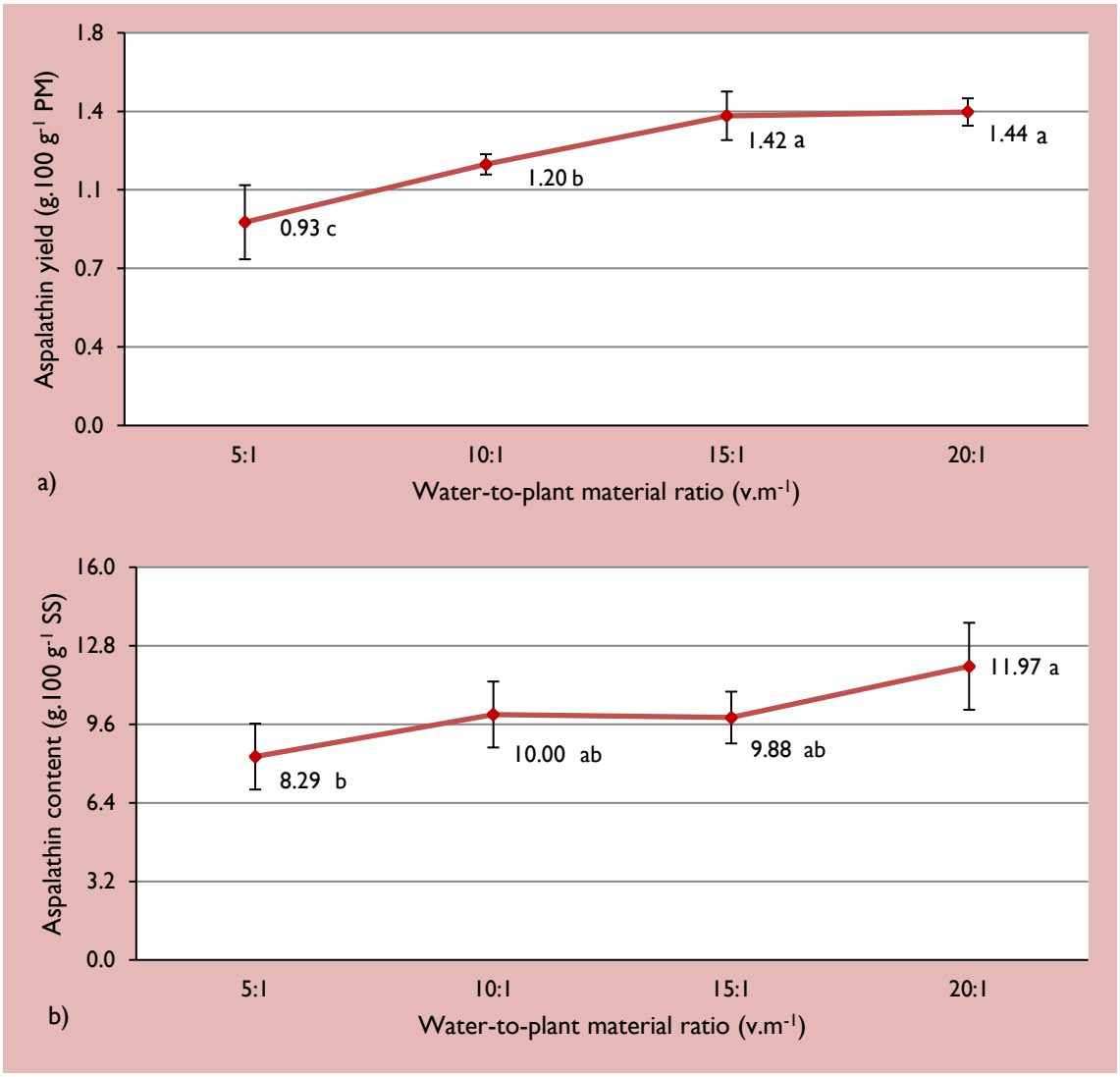

Figure 3.10 Effect of water-to-plant material ratio (v.m^{-1}) on (a) aspalathin yield and (b) aspalathin content of unrefined green rooibos extract (extraction time = 20 min; extraction temperature = 60 °C). Values with the same letter are not significantly different ($P < 0.05$). SS, soluble solids; PM, plant material.

3.4.3.4. Effect of particle size on extraction efficiency

The fourth and final OFAT experiment investigated the effect of using different particle size fractions of green rooibos plant material on the extraction efficiency. Unlike the previous three OFAT extractions, the plant material was not used as received, but it was separated into four particle size fractions, including the fraction collected in the pan (<20 mesh). Higher mesh numbers represent smaller particle sizes. Each size fraction was extracted at 60 °C for 20 min and a 15:1 water-to-plant material ratio.

The extract yield increased significantly as the particle size decreased, with an almost 3-fold increase in the yield between the largest size fraction (>12 mesh) and the smallest (<20 mesh) (Fig 3.11). This indicates that the larger particle sizes resulted in less efficient extractions due to greater

diffusion distances. However, the larger amount of woody material and stems in the >16 mesh size fractions is also expected to have a major impact on extract yield. Studies conducted with *Cyclopia subternata*, also a fynbos plant from the Fabaceae family, showed that its stems contained 51% of the hot water soluble solids of the leaves (De Beer *et al.*, 2012).

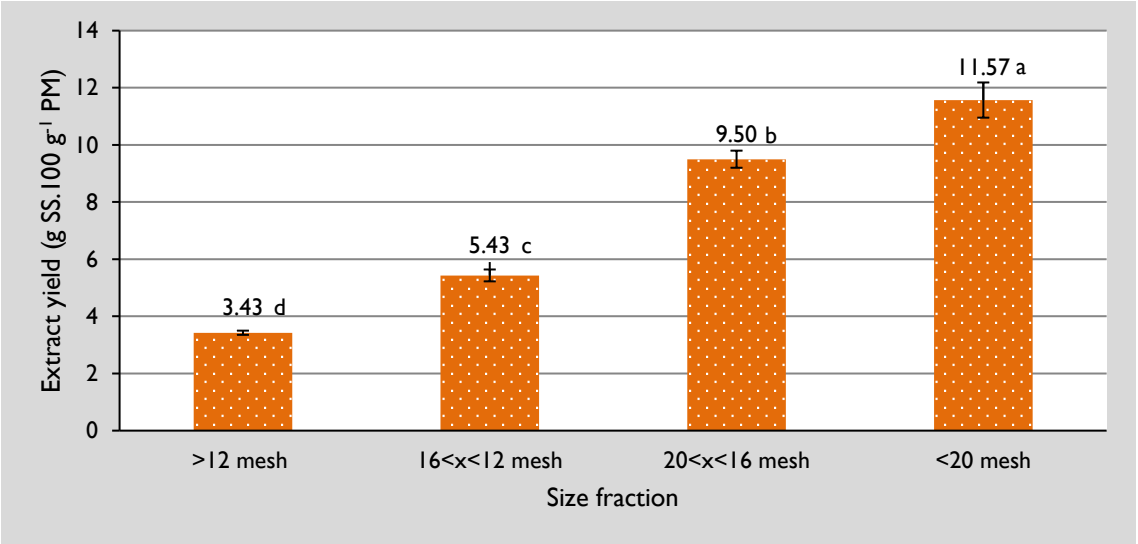

Figure 3.11 Effect of particle size on extract yield of green rooibos (extraction temperature = 60 °C; extraction time = 20 min; water-to-plant material ratio = 15:1; $v.m^{-1}$). Values with the same letter are not significantly different ($P < 0.05$). SS, soluble solids; PM, plant material.

The aspalathin yield and content in the extract both showed a similar trend, increasing significantly with each level of increase in the particle size ($P < 0.05$) (Fig. 3.12). A nearly four-fold increase in the aspalathin content of the extract was achieved with the smallest particle size fraction (18.55%) compared with the largest size fraction (4.64%). As previously noted for extract yield, not only size, but the plant material composition in terms of leaf and stem content is important. When having plant material with the same composition, smaller particles sizes were also associated with significantly higher extraction yields of soluble solids and target compounds from grape seed (Bucić-Kojić *et al.*, 2007), berry pomace (Laroze *et al.*, 2010), ground maize (Naidu *et al.*, 2007), ground pomegranate peel (Wang *et al.*, 2011), green tea (Vuong *et al.*, 2011) and *Sophora japonica* (Liu *et al.*, 2016). The effect of particle size is attributed to the diffusion rate limiting step of extraction (Schwartzberg & Chao, 1982). Reduction of the particle size also increases the contact area between the solvent and the plant matrix, enhancing extraction (Azmir *et al.*, 2013).

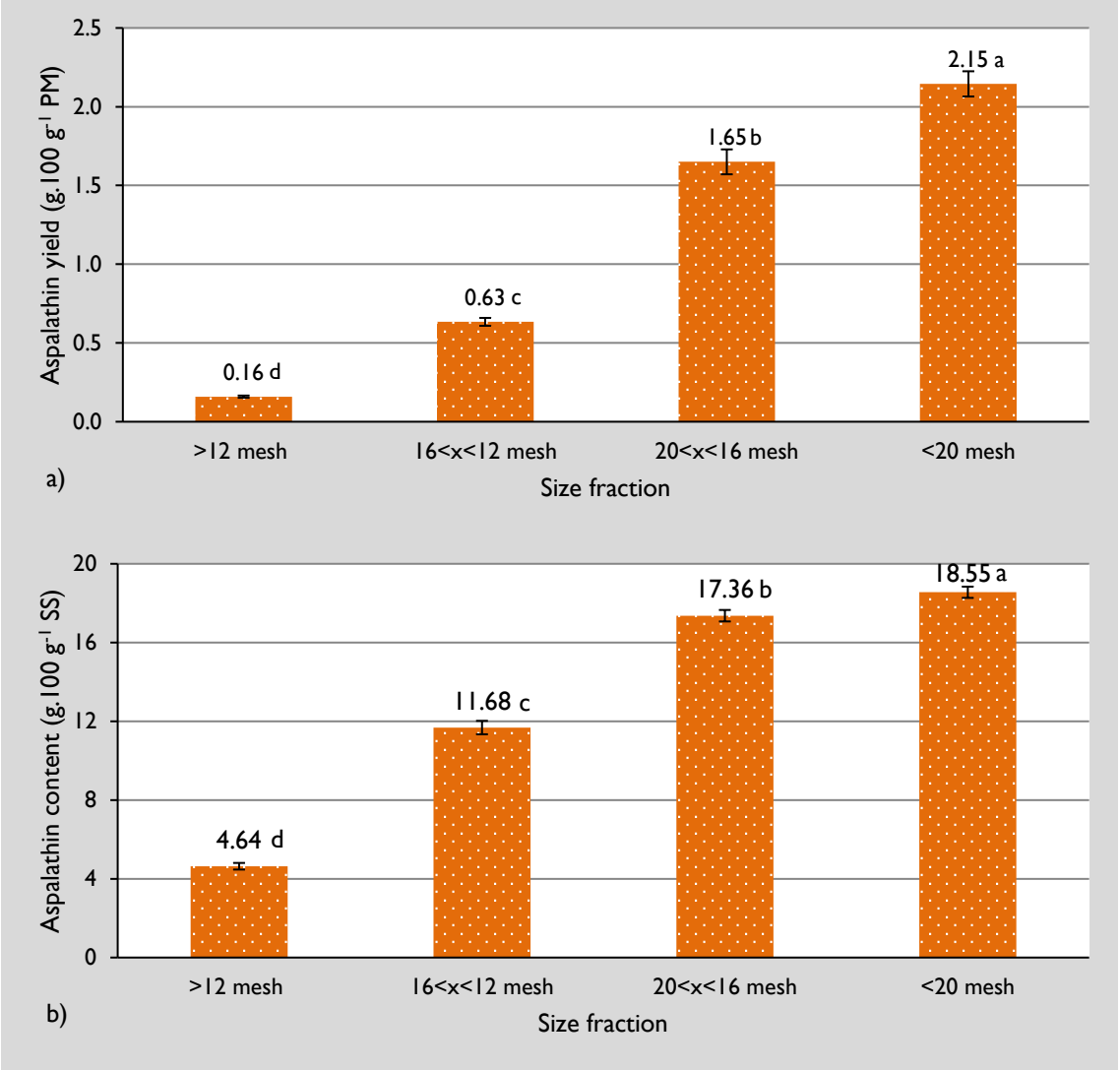

Figure 3.12 Effect of particle size on (a) aspalathin yield and (b) aspalathin content of aqueous green rooibos extract (extraction temperature = 60 °C; extraction time = 20 min; water-to-plant material ratio = 15:1; $v.m^{-1}$). Values with the same letter are not significantly different ($P < 0.05$). SS, soluble solids. PM, plant material.

Joubert & De Beer (2012) investigated the composition of 74 batches of unrefined (i.e. comminuted but not sieved) fermented rooibos plant material in terms of three particle size fractions (>10 mesh, coarse tea; 40<x<10 mesh, refined tea and <40 mesh, dust), and found a weak (r = 0.300) but significant (P = 0.009) negative correlation between the size of the coarse fraction and the extract yield. Joubert (1984) previously reported that rooibos waste material (mainly coarse stems) had a low soluble solids content (8.9%) compared with the unrefined fraction (20.4%) consisting of leaves and stems. Although reduction in plant material size affects extraction yields, excessively fine plant material could complicate filtering of the extract or cause blockage of extraction equipment. Very fine plant material may also tend to agglomerate and thus negatively affect the mass transfer kinetics by forming preferential flow channels, preventing effective penetration of the solvent in the solid matrix (Pinelo *et al.*, 2005).

3.4.4. Application of response surface methodology (RSM)

The results of the OFAT experiments indicated the ranges of levels of the independent variables within which the optimum extraction efficiency would most likely be located given process limitations. The extraction temperature, time and water-to-plant material ratio were selected for inclusion in the CCD. Although the particle size did have a major effect on the extraction efficiency, this variable was not included in the CCD, since the particle size distribution and stem/leaf contents of Batch B could not reasonably be assumed to be representative of that of all production batches of commercial GR. The larger particle size fractions of one production batch of GR might contain a higher proportion of stems than another, or the average dimensions of the cut leaves may vary significantly between batches. A shorter cut length is employed when plant material is intended for tea bags as opposed to loose-format packaging.

The process parameters were investigated and prediction models were generated using the three independent variables: extraction time (X_1 = 10–40 min), extraction temperature (X_2 = 41–93 °C) and water-to-plant material ratio (X_3 = 6.59:1–23.41:1; v.m^{-1}). The CCD comprising 16 experimental runs was carried out in triplicate, amounting to a total of 48 runs. It was decided that the optimal parameters would be validated using different batches of plant material selected from the sample set A1–A47, and that the effect of reducing the mean particle size of these validation batches would be simultaneously investigated (see section 3.4.5.).

3.4.4.1. Analysis of RSM data

The data obtained from the RSM experiments are shown in Table 3.4. The following ranges of response values were obtained: extract yield, 9.754–17.827 g.100 g^{-1} plant material; aspalathin yield, 1.073–2.497 g.100 g^{-1} plant material; aspalathin extraction efficiency, 43.982–100%; and aspalathin content of the extract, 10.506–14.005 g.100 g^{-1} soluble solids.

Table 3.4 Layout of central composite design (CCD), performed in triplicate, for optimisation of green rooibos hot water extraction.

Treatment combination	CCD Run No.[1]	X_1 Time (min)	X_2 Temperature (°C)	X_3 Water: PM[2] ($v.m^{-1}$)	Extract yield (%)[3]	Asp yield (%)[4]	Asp_HWE (%)[5]	Asp_EE (%)[6]
1	1(F)	16 (-1)	51 (-1)	10:1 (-1)	9.754	1.073	11.003	43.982
	17(F)	16 (-1)	51 (-1)	10:1 (-1)	10.414	1.176	11.294	48.204
	33(F)	16 (-1)	51 (-1)	10:1 (-1)	12.334	1.331	10.791	54.551
2	2(F)	16 (-1)	51 (-1)	20:1 (+1)	10.943	1.266	11.567	51.875
	18(F)	16 (-1)	51 (-1)	20:1 (+1)	10.718	1.221	11.390	50.031
	34(F)	16 (-1)	51 (-1)	20:1 (+1)	11.297	1.269	11.233	52.006
3	3(F)	16 (-1)	82 (+1)	10:1 (-1)	14.038	1.559	11.106	63.898
	19(F)	16 (-1)	82 (+1)	10:1 (-1)	15.662	1.916	12.236	78.543
	35(F)	16 (-1)	82 (+1)	10:1 (-1)	14.851	1.746	11.758	71.564
4	4(F)	16 (-1)	82 (+1)	20:1 (+1)	16.131	1.878	11.645	76.987
	20(F)	16 (-1)	82 (+1)	20:1 (+1)	15.938	1.876	11.768	76.866
	36(F)	16 (-1)	82 (+1)	20:1 (+1)	16.048	1.793	11.172	73.477
5	5(F)	34 (+1)	51 (-1)	10:1 (-1)	11.787	1.337	11.346	54.808
	21(F)	34 (+1)	51 (-1)	10:1 (-1)	11.889	1.511	12.709	61.924
	37(F)	34 (+1)	51 (-1)	10:1 (-1)	12.456	1.370	11.000	56.154
6	6(F)	34 (+1)	51 (-1)	20:1 (+1)	12.420	1.509	12.150	61.849
	22(F)	34 (+1)	51 (-1)	20:1 (+1)	13.229	1.517	11.465	62.162
	38(F)	34 (+1)	51 (-1)	20:1 (+1)	13.397	1.563	11.665	64.048
7	7(F)	34 (+1)	82 (+1)	10:1 (-1)	16.299	1.827	11.210	74.885
	23(F)	34 (+1)	82 (+1)	10:1 (-1)	16.011	1.981	12.374	81.917
	39(F)	34 (+1)	82 (+1)	10:1 (-1)	17.203	1.883	10.943	77.152
8	8(F)	34 (+1)	82 (+1)	20:1 (+1)	17.608	2.167	12.308	88.822
	24(F)	34 (+1)	82 (+1)	20:1 (+1)	16.949	2.046	12.072	83.852
	40(F)	34 (+1)	82 (+1)	20:1 (+1)	16.355	1.941	11.868	79.550

9	9(A)	10 (-α)	67 (0)	15:1 (0)	11.145	1.215	10.898	49.777
	25(A)	10 (-α)	67 (0)	15:1 (0)	12.999	1.623	12.483	66.503
	41(A)	10 (-α)	67 (0)	15:1 (0)	12.269	1.462	11.914	59.910
10	10 (A)	40 (+α)	67 (0)	15:1 (0)	15.857	1.846	11.642	75.659
	26 (A)	40 (+α)	67 (0)	15:1 (0)	15.682	1.977	12.606	81.020
	42(A)	40 (+α)	67 (0)	15:1 (0)	14.702	1.772	12.052	72.616
11	11(A)	25 (0)	41 (-α)	15:1 (0)	11.274	1.308	11.602	53.609
	27(A)	25 (0)	41 (-α)	15:1 (0)	11.331	1.328	11.722	54.435
	43(A)	25 (0)	41 (-α)	15:1 (0)	11.027	1.200	10.880	49.168
12	12(A)	25 (0)	93 (+α)	15:1 (0)	17.010	1.998	11.748	81.896
	28(A)	25 (0)	93 (+α)	15:1 (0)	17.827	2.497	14.005	100.00
	44(A)	25 (0)	93 (+α)	15:1 (0)	17.479	2.148	12.287	88.024
13	13(A)	25 (0)	67 (0)	6.6:1(-α)	13.014	1.385	10.643	56.765
	29(A)	25 (0)	67 (0)	6.6:1 (-α)	14.613	1.621	11.092	66.428
	45(A)	25 (0)	67 (0)	6.6:1 (-α)	15.647	1.644	10.506	67.369
14	14(A)	25 (0)	67 (0)	23.4:1 (+α)	15.016	1.854	12.344	75.967
	30(A)	25 (0)	67 (0)	23.4:1 (+α)	14.551	1.838	12.635	75.357
	46(A)	25 (0)	67 (0)	23.4:1 (+α)	14.323	1.714	11.967	70.245
15	15(C)	25 (0)	67 (0)	15:1 (0)	14.012	1.608	11.479	65.921
	16(C)	25 (0)	67 (0)	15:1 (0)	14.290	1.751	12.252	71.755
	31(C)	25 (0)	67 (0)	15:1 (0)	15.048	1.832	12.174	75.083
	32(C)	25 (0)	67 (0)	15:1 (0)	14.510	1.805	12.438	73.968
	47(C)	25 (0)	67 (0)	15:1 (0)	15.424	1.734	11.243	71.073
	48(C)	25 (0)	67 (0)	15:1 (0)	14.198	1.704	12.000	69.825

[1] (F) = factorial design point; (A) = axial point; (C) = central point; [2] PM = plant material; [3] g.100 g^{-1} PM; [4] Aspalathin yield = g.100 g^{-1} PM; [5] Aspalathin content of hot water extract = g.100 g^{-1} soluble solids; [6] Aspalathin extraction efficiency = g.100 g^{-1} aspalathin in PM

Regression analysis and ANOVA were carried out to determine the suitability of the generated models. Standardised Pareto charts were used to evaluate the significance of the linear, quadratic and interaction effects of the independent variables on each response. Desirability profiling was employed to determine the optimal extraction conditions for maximum response values. The predictive ability of the models was then assessed by conducting a set of verification experiments.

The statistical significance of the independent variables and their interactions, as well as the fit of the model to the data, was estimated by performing ANOVA, which compares the variance between different combinations of independent variables (treatments) and the variance due to random errors. The response values for extract yield (EY), aspalathin extraction efficiency (Asp_EE) and aspalathin content of the extract (Asp_HWE) were fitted as a function of the three independent variables X_1, X_2 and X_3. The regression coefficients that were generated by the ANOVA were used to generate quadratic regression equations with which the values of the responses can be predicted. The ANOVA results, with estimated linear, quadratic and interaction regression coefficients for all three responses, are presented in Tables 3.5–3.7. For EY, extraction time showed both a significant linear and quadratic effect ($P < 0.05$), while temperature and water-to-plant material ratio had only a significant linear effect ($P < 0.05$) (Table 3.5). Extraction time, temperature and water-to-plant material ratio had significant linear effects ($P < 0.05$) on Asp_EE (Table 3.6). For Asp_HWE, significant linear effects ($P < 0.05$) were demonstrated for extraction temperature and water-to-plant material ratio (Table 3.7).

The suitability of the models can be evaluated in terms of R^2_{adj} or lack-of-fit (LOF). R^2 represents the amount of variation around the mean that is explained by the quadratic model, and R^2_{adj} is the same term adjusted to account for the number of terms in the model, allowing for direct comparison of models with different amounts of independent variables. R^2_{adj} is usually lower in value than R^2, which should preferably be at least 0.8 for a model with a good fit. The LOF test compares the variability between observations of different replications of the independent variables with the variability of the model residuals. It makes use of the mean square (MS) pure error as the error term and is considered a more sensitive test of model fit than R^2_{adj}. A model is considered to have a good fit to the data if there is significant regression and non-significant LOF. No significant LOF was present for any of the responses under investigation, indicating suitability of the respective models. For both EY and Asp_EE, R^2_{adj} was >0.8 (Tables 3.5 & 3.6), which, together with a non-significant LOF value, indicates good predictive ability for the respective models. The polynomial model for prediction of the aspalathin content of the extract, however, had a low R^2_{adj}value (0.188; Table 3.7). Table 3.8 provides the full prediction equations for these dependent variables.

Table 3.5 ANOVA of experimental results for the polynomial regression equation for extract yield (EY; g.100 g^{-1} plant material).

Parameter[1]	Regr. Coeff.[2]	SS[3]	DF[4]	MS[5]	F	P
Intercept	-3.25911					
(1) Time (min) (L)	0.33417	28.289	1	28.289	59.701	0.000
Time (min) (Q)	-0.00417	3.172	1	3.172	6.693	0.014
(2) Temperature (°C) (L)	0.21631	172.582	1	172.582	364.215	0.000
Temperature (Q)	-0.00062	0.610	1	0.610	1.286	0.265
(3) Water:PM (v.m^{-1}) (L)	0.07155	2.128	1	2.128	4.490	0.042
Water:PM (v.m^{-1}) (Q)	-0.00288	0.144	1	0.144	0.305	0.589
1L x 2L	-0.00056	0.148	1	0.148	0.312	0.580
1L x 3L	0.00027	0.004	1	0.004	0.008	0.931
2L x 3L	0.00081	0.094	1	0.094	0.199	0.659
Lack of fit		3.822	5	0.764	1.613	0.184
Pure error		15.637	33	0.474		
Total SS		225.739	47			
R^2						0.914
R^2_{adj}						0.884

[1] L = linear coefficient; Q = quadratic coefficient; L x L = interaction coefficient; PM = Plant material; [2] Regression coefficients; [3] Sum of squares; [4] Degrees of freedom; [5] Mean square

Table 3.6 ANOVA of experimental results for the polynomial regression equation for aspalathin extraction efficiency (Asp_EE; %; g.100 g^{-1} aspalathin in plant material).

Parameter[1]	Regr. Coeff.[2]	SS[3]	DF[4]	MS[5]	F	P
Intercept	-33.12033					
(1) Time (min) (L)	1.83101	919.205	1	919.205	36.785	0.000
Time (min) (Q)	-0.02358	101.419	1	101.419	4.059	0.052
(2) Temperature (°C) (L)	1.03315	5162.649	1	5162.649	206.602	0.000
Temperature (Q)	-0.00205	6.751	1	6.751	0.270	0.607
(3) Water:PM (v.m^{-1}) (L)	1.66153	277.075	1	277.075	11.088	0.002
Water:PM (v.m^{-1}) (Q)	-0.06077	64.152	1	64.152	2.567	0.119
1L x 2L	-0.00474	10.505	1	10.505	0.420	0.52
1L x 3L	0.01265	7.777	1	7.777	0.311	0.581
2L x 3L	0.00549	4.354	1	4.354	0.174	0.679
Lack of fit		81.718	5	16.344	0.654	0.661
Pure error		824.618	33	24.988		
Total SS		7416.420	47			
R^2						0.878
R^2_{adj}						0.849

[1] L = linear coefficient; Q = quadratic coefficient; L x L = interaction coefficient; PM = plant material; [2] Regression coefficients; [3] Sum of squares; [4] Degrees of freedom; [5] Mean square

Table 3.7 ANOVA of experimental results for the polynomial regression equation for aspalathin content of the extract (Asp_HWE; g.100 g^{-1} soluble solids).

Parameter[1]	Regr. Coeff.[2]	SS[3]	DF[4]	MS[5]	F	P
Intercept	6.94526					
(1) Time (min) (L)	0.06851	0.844	1	0.844	2.620	0.115
Time (min) (Q)	-0.00064	0.074	1	0.074	0.231	0.634
(2) Temperature (°C) (L)	0.03521	2.148	1	2.148	6.671	0.014
Temperature (Q)	-0.00004	0.003	1	0.003	0.009	0.927
(3) Water:PM ($v.m^{-1}$) (L)	0.25220	2.662	1	2.662	8.266	0.007
Water:PM ($v.m^{-1}$) (Q)	-0.00775	1.043	1	1.043	3.239	0.081
1L x 2L	-0.00059	0.165	1	0.165	0.512	0.479
1L x 3L	0.00126	0.077	1	0.077	0.239	0.628
2L x 3L	-0.00000	0.000	1	0.000	0.000	0.998
Lack of fit		2.959	5	0.592	1.838	0.133
Pure error		10.627	33	0.322		
Total SS		20.698	47			
R^2						0.344
R^2_{adj}						0.188

[1] L = linear coefficient; Q = quadratic coefficient; L x L = interaction coefficient; PM = plant material; [2] Regression coefficients; [3] Sum of squares; [4] Degrees of freedom; [5] Mean square

Table 3.8 Polynomial prediction equations for three dependent variables[1] in green rooibos hot water extraction.

Dependent variable	Prediction equation
Extract yield	$\hat{Y} = -3.25911 + 0.33417X_1 + 0.21631X_2 + 0.07155X_3 - 0.00417X_1^2 - 0.00062X_2^2 - 0.00288X_3^2 - 0.00056X_1X_2 - 0.00027X_1X_3 + 0.00081X_2X_3$
Aspalathin extraction efficiency	$\hat{Y} = -33.12033 + 1.83101X_1 + 1.03315X_2 + 1.66153X_3 - 0.02358X_1^2 - 0.00205X_2^2 - 0.06077X_3^2 - 0.00474X_1X_2 + 0.01265X_1X_3 - 0.00549X_2X_3$
Aspalathin content of extract	$\hat{Y} = 6.94526 + 0.06851X_1 + 0.03521X_2 + 0.25220X_3 - 0.00064X_1^2 + 0.00004X_2^2 - 0.00775X_3^2 - 0.00059X_1X_2 + 0.00126X_1X_3 + 0.00001X_2X_3$

[1] X_1 = extraction time (min); X_2 = extraction temperature (°C); X_3 = water-to-plant material ratio ($v.m^{-1}$)

Standardised Pareto charts for the dependent variables provide further insight into the relative effect of independent variables and their interaction (Figs. 3.13–3.15). Linear, quadratic and interaction effects of the independent variables are graphically depicted as rectangular bars, with the length of each bar being proportional to the absolute scale of the standard estimated effects. The effect of a given parameter is significant if its bar crosses the vertical line which represents the P = 0.05 confidence level.

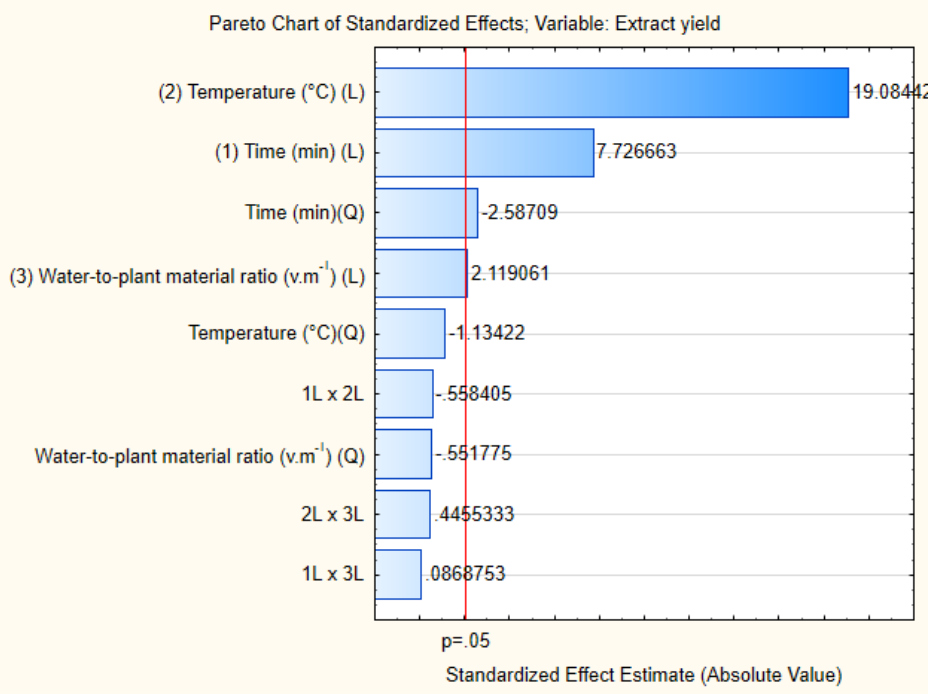

Figure 3.13 Standardised Pareto chart showing linear, quadratic and interaction effects for extract yield (g.100 g^{-1} plant material). L = linear effect; Q = quadratic effect; LxL = interaction effect.

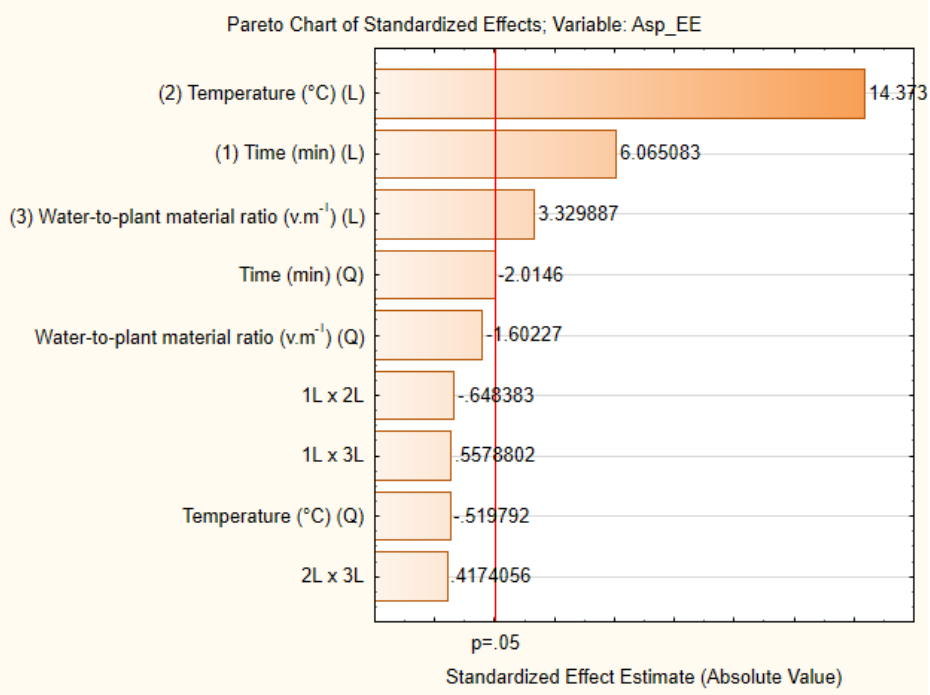

Figure 3.14 Standardised Pareto chart showing linear, quadratic and interaction effects for aspalathin extraction efficiency (Asp_EE; g.100 g^{-1} aspalathin in plant material). L = linear effect; Q = quadratic effect; LxL = interaction effect.

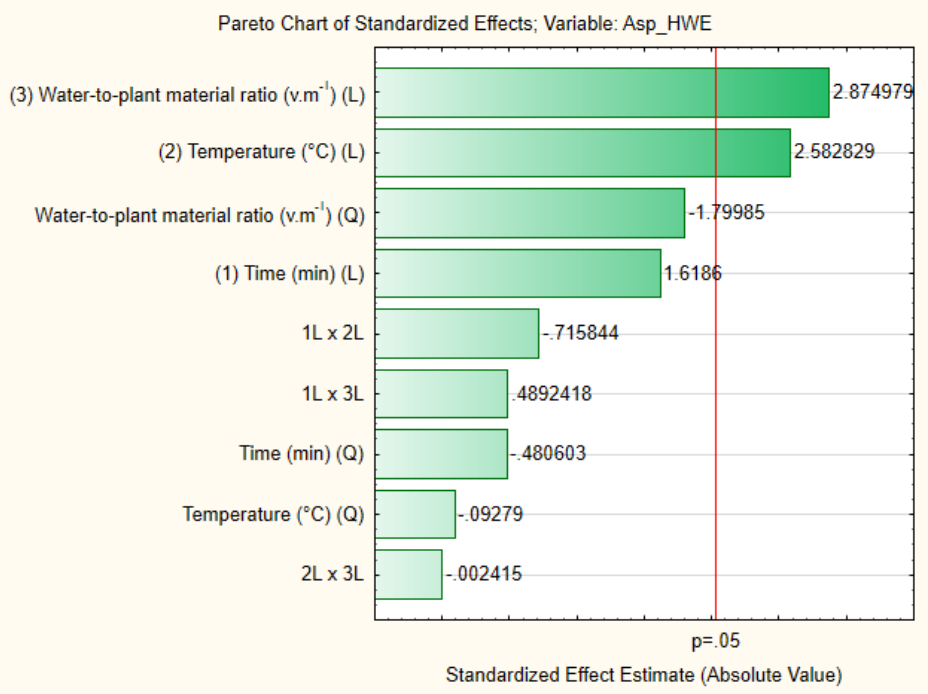

Figure 3.15 Standardised Pareto chart showing linear, quadratic and interaction effects for aspalathin content of extract (Asp_HWE; g.100 g^{-1} soluble solids). L = linear effect; Q = quadratic effect; LxL = interaction effect.

The standardised Pareto chart for EY indicates that the linear effects of extraction temperature, time and water-to-plant material ratio had a significant effect on this response (Fig. 3.13), with extraction temperature having the greatest effect. This is in agreement with the results of the OFAT extractions, demonstrating that extraction temperature has the greatest individual effect on the EY. Response surface plots for EY (Figs. 3.16a–c) further illustrate this matter. The yield increases linearly with increasing temperature and fixed extraction time up to 100 °C, and an optimal response (considering the practical limitations of water as solvent) is located between 25 to 35 min and 85 to 100 °C. The lesser effect of extraction time on extract yield is apparent from the less steep gradient of the response surface in the direction of increasing extraction time. The relatively small effect of the water-to-plant material ratio on extract yield is demonstrated by the shapes of the response surfaces in Fig. 3.16b & 3.16c, where changes in this variable are accompanied by minor changes in extract yield. The effect of the water-to-plant material ratio was greater at the shorter extraction times, as evident from the steeper gradient of the response surface at extraction time <25 min (Fig. 3.16b).

The aspalathin extraction efficiency was also most affected by the linear effect of extraction temperature, followed by the linear effect of extraction time. The linear effect of the water-to-plant material ratio was more prominent for aspalathin extraction efficiency than for extract yield, as illustrated by the relative sizes of their horizontal bars on the Pareto charts (Figs. 3.13 & 3.14). Fig. 3.16d depicts the response surface for aspalathin extraction efficiency as affected by extraction

temperature and time. It is similar in shape to the corresponding plot for extract yield (Fig. 3.18a), indicating an optimal response between 25–35 min and 85–100 °C. Figs. 3.16e & 3.16f show that an increase in the water-to-plant material ratio improved the aspalathin extraction efficiency, although this effect was not as pronounced as those of the extraction temperature and time (as reflected in the Pareto Chart (Fig. 3.14).

Asp_HWE was most affected by the linear effect of the water-to-plant material ratio (Fig. 3.15) and was not affected by the linear effect of the extraction temperature as much as EY and Asp_EE, although there was a significant positive effect. The OFAT experiments also demonstrated that extract with a higher aspalathin content could be obtained with a higher water-to-plant material ratio. Fig. 3.17a shows that the combined effects of the extraction temperature and extraction time on Asp_HWE were greater at the lower levels of these factors. The optimal response for combined effects of water-to-plant material ratio and extraction time on the aspalathin content in the extract is evident from Fig. 3.17b. An optimal response is located within the ranges 25–40 min and 16:1–26:1, respectively. Fig. 3.17c shows the combined effects of the water-to-plant material ratio and extraction temperature on the aspalathin content in the extract. At the lower water-to-plant material ratios and extraction temperatures, aspalathin content increased linearly, but this effect was less pronounced at higher extraction temperatures. The response surfaces for Asp_HWE all demonstrate that the optimal levels of the independent variables for achieving the highest aspalathin content are most likely located within the ranges 25–40 min (extraction time), 85–100 °C (extraction temperature) and 16:1–26:1 ($v.m^{-1}$) water-to-plant material ratio.

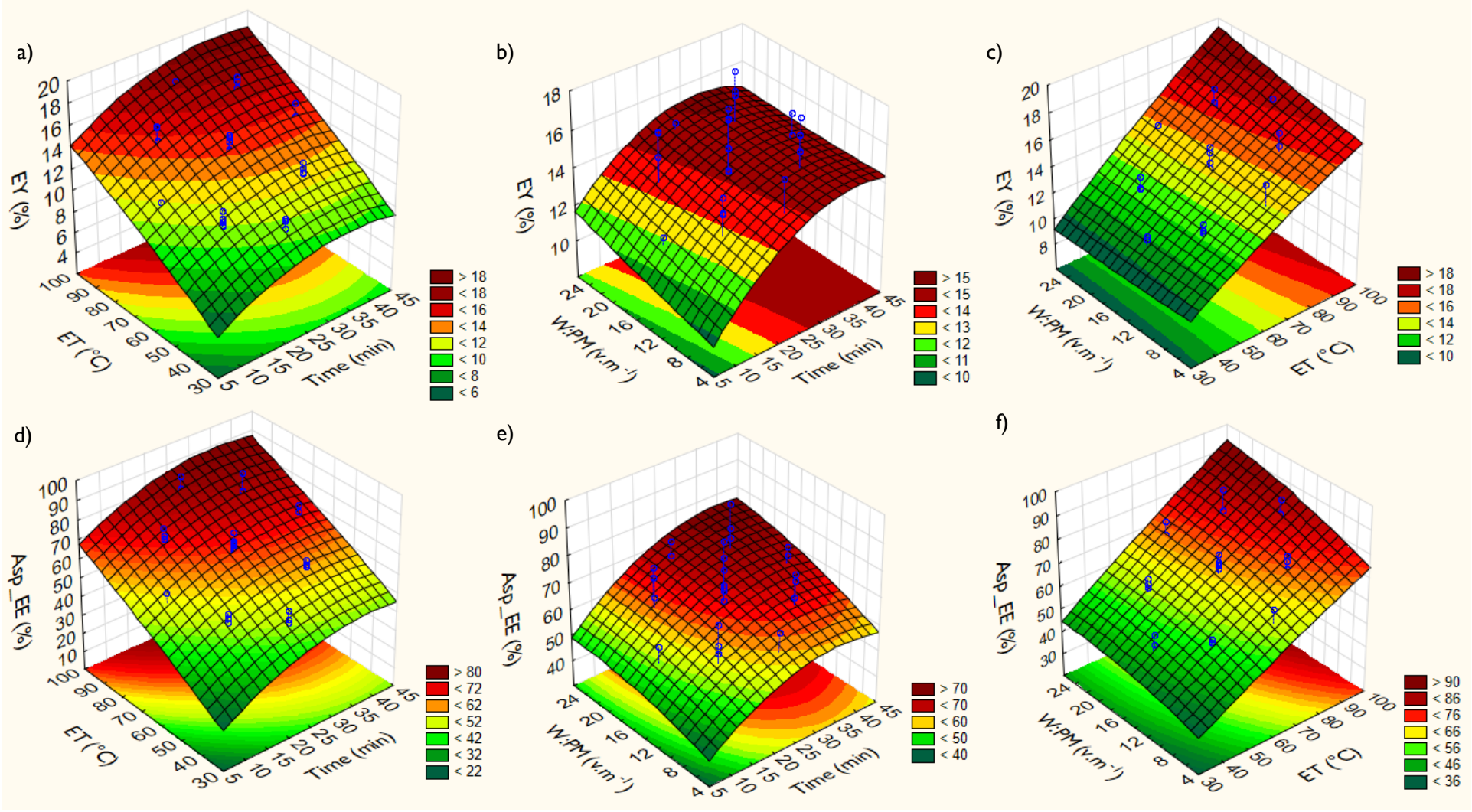

Figure 3.16 Response surface plots for extract yield (EY; %, g.100 g^{-1} plant material) and aspalathin extraction efficiency (Asp_EE; %, g.100 g^{-1} aspalathin in plant material), showing effects of (a & d) extraction temperature (ET; °C) and time (min) at fixed water-to-plant material ratio (W:PM) of 15:1 ($v.m^{-1}$), (b & e) W:PM and extraction time at fixed ET of 67 °C, and (c & f) W:PM and ET at fixed extraction time of 25 min.

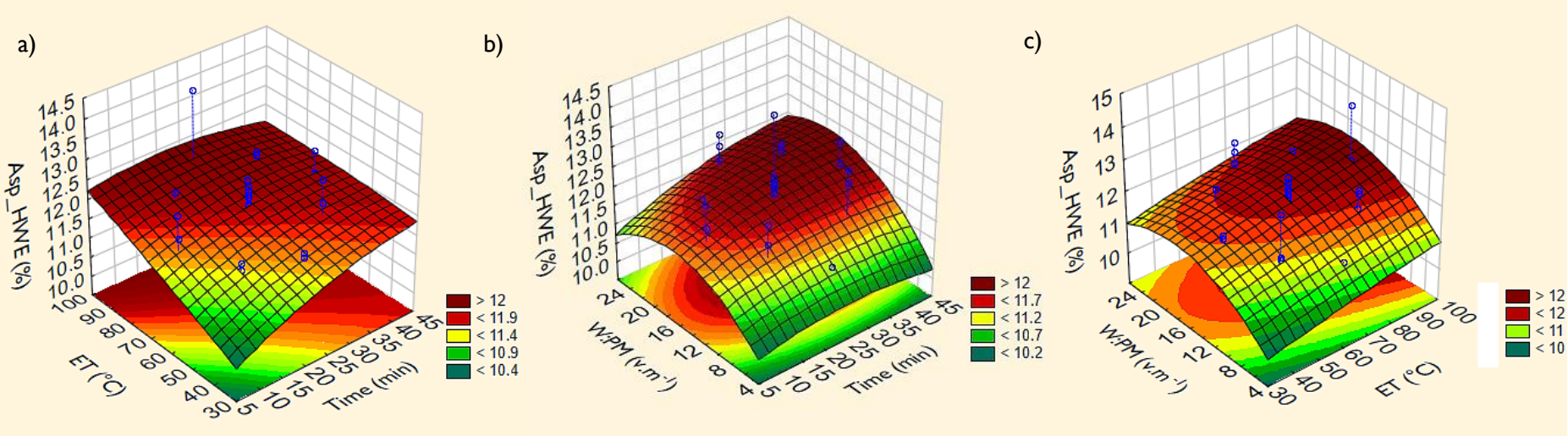

Figure 3.17 Response surface plots for aspalathin content of the hot water extract (Asp_HWE; g.100 g^{-1} soluble solids) showing effects of (a) extraction temperature (°C) and time (min) at fixed water-to-plant material ratio of 15:1 ($v.m^{-1}$), (b) water-to-plant material ratio ($v.m^{-1}$) and extraction time (min) at fixed extraction temperature of 67 °C, and (c) water-to-plant material ratio ($v.m^{-1}$) and extraction temperature (°C) at fixed extraction time of 25 min. SS, soluble solids. PM, plant material.

3.4.4.2. Verification of prediction models

Verification of the prediction models is required in order to assess how well the experimental results would agree with values predicted using these models. One additional replication of the central composite design, was carried out as a verification experiment. The predicted and experimentally observed response values. as well as the over/underestimation obtained for all 16 standard runs in the verification experiment are presented in Table 3.9.

The intraclass correlation coefficient (ICC) was used to assess how well the experimental data fits the model. It is an indication of the reliability of quantitative measurements, with reliability referring to the reproducibility of the measurement when repeated randomly. ICC values range between 0 and 1, with values closer to 1 indicating a better model fit and a greater reliability of the model to predict response values. ICC(agreement) is a subclass of the ICC which accounts for any bias that may have occurred by incorporating the standard error of measurement (SEM), whereas ICC(consistency) excludes the SEM but is less sensitive as a result. Predicted response values and the observed results from the verification experiments are presented as scatter plots to demonstrate the distribution of the data (Figs. 3.18–3.20).

Table 3.9 Verification of prediction models for extract yield, aspalathin extraction efficiency (Asp_EE) and aspalathin content of extract (Asp_HWE).

Std. Run	X_1 Time (min)	X_2 Temp (°C)	X_3 Water: PM[1] (v.m^{-1})	Extract yield (%)[2]			Asp_EE (%)[3]			Asp_HWE (%)[4]		
				Obs[5]	*Pred*[6]	Δ[7]	*Obs*	*Pred*	Δ	*Obs*	*Pred*	Δ
1	16	51	10:1	10.985	10.874	0.111	43.549	48.993	-5.444	9.673	11.028	-1.355
2	16	51	20:1	11.654	11.180	0.474	50.073	52.205	-2.132	10.483	11.425	-0.942
3	16	82	10:1	14.023	15.011	-0.988	61.043	71.920	-10.877	10.622	11.652	-1.030
4	16	82	20:1	14.793	15.568	-0.775	66.041	76.835	-10.794	10.893	12.048	-1.155
5	34	51	10:1	12.946	12.668	0.278	55.983	58.652	-2.669	10.552	11.367	-0.815
6	34	51	20:1	12.577	13.023	-0.446	60.313	64.141	-3.828	11.701	11.991	-0.290
7	34	82	10:1	15.474	16.492	-1.018	68.591	78.933	-10.342	10.816	11.660	-0.844
8	34	82	20:1	16.591	17.097	-0.506	76.120	86.125	-10.005	11.195	12.282	-1.087
9	10	67	15:1	11.074	12.264	-1.190	48.744	58.175	-9.431	10.740	11.561	-0.821
10	40	67	15:1	14.165	15.051	-0.886	64.663	74.038	-9.375	11.139	12.035	-0.896
11	25	41	15:1	10.322	10.758	-0.436	47.537	51.287	-3.750	11.238	11.532	-0.294
12	25	93	15:1	16.930	17.631	-0.701	77.777	88.945	-11.168	11.209	12.300	-1.091
13	25	67	6.6:1	13.286	14.022	-0.736	56.124	62.815	-6.691	10.307	10.968	-0.661
14	25	67	23.4:1	14.254	14.796	-0.542	66.701	71.609	-4.908	11.418	11.825	-0.407
15	25	67	15:1	13.966	14.613	-0.647	59.743	71.509	-11.766	10.438	11.944	-1.506
16	25	67	15:1	13.746	14.613	-0.867	61.481	71.509	-10.028	10.913	11.944	-1.031

[1] PM = plant material; [2] g.100 g^{-1} PM; [3] g.100 g^{-1} aspalathin in PM; [4] g.100 g^{-1} soluble solids; [5] Observed; [6] Predicted; [7] Δ = (Observed – Predicted)

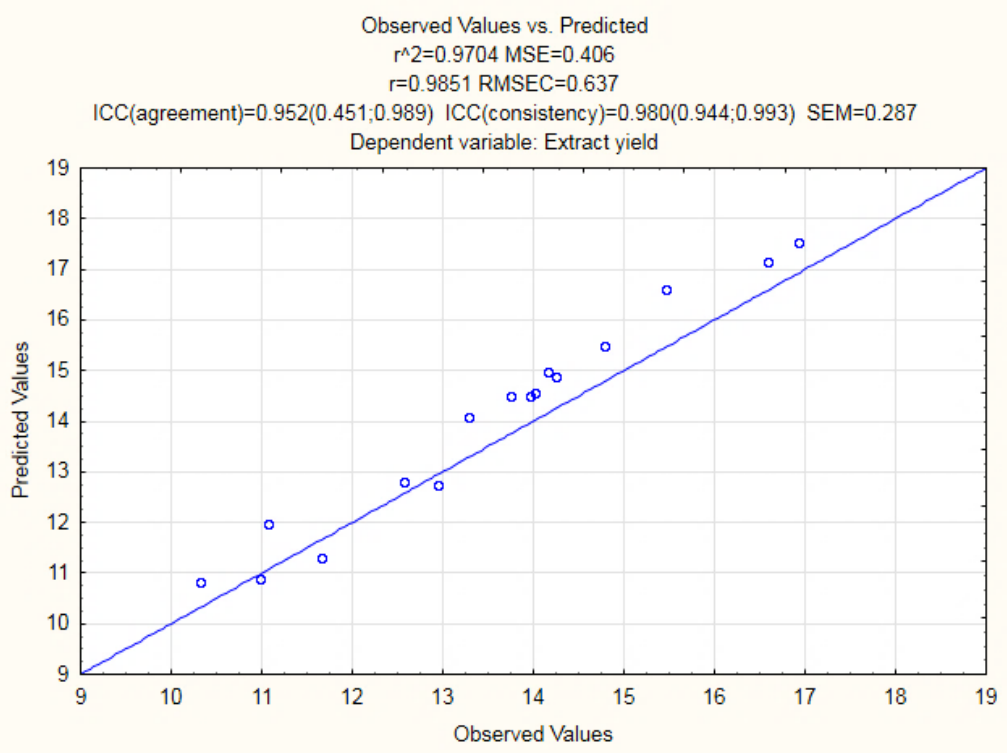

Figure 3.18 Correlation of predicted and observed values for extract yield (EY) model verification.

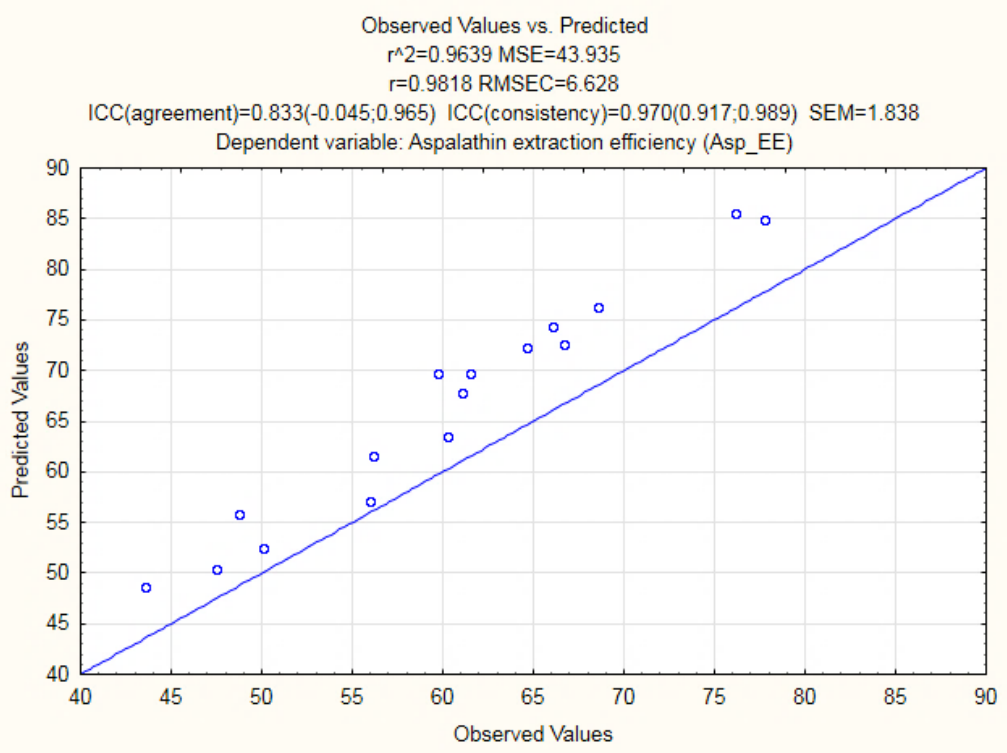

Figure 3.19 Correlation of predicted and observed values for aspalathin extraction efficiency (Asp_EE) model verification.

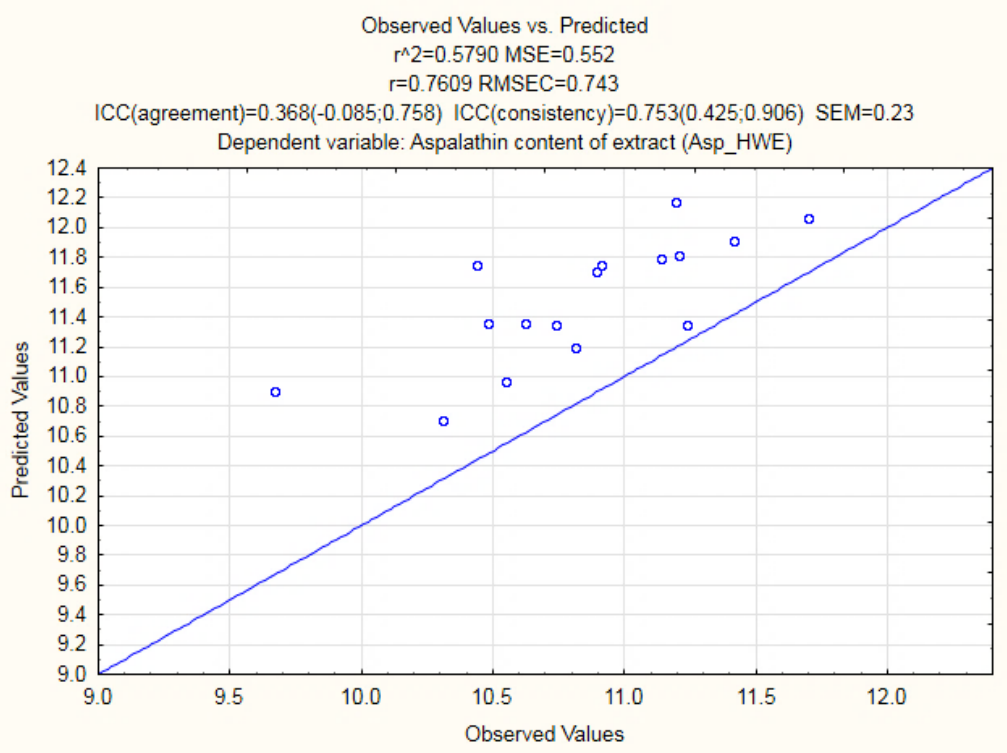

Figure 3.20 Correlation of predicted and observed values for aspalathin content of extract (Asp_HWE) model verification.

The two dependent variables, EY (g.100 g^{-1} plant material) and Asp_EE (g.100 g^{-1} aspalathin in plant material), displayed high ICC values. For EY, ICC(agreement) and ICC(consistency) values of 0.952 and 0.980 were obtained, respectively, while for Asp_EE, the corresponding values were 0.833 and 0.970, respectively. These values indicate a satisfactory predictive ability for application in quality assessment. For large-scale cost and profit predictions, it is required that ICC values be as close to 1.0 as possible.

The ICC(agreement) and ICC(consistency) values of the remaining dependent variable, Asp_HWE (g.100 g^{-1} soluble solids), were 0.368 and 0.753, respectively. This is not surprising, given that the poor predictive ability of the polynomial model for this response, based on R^2_{adj} (0.188; Table 3.7). This suggests that the generated model would not be acceptable for use in quality assessment, as it would not provide consistent predictions regarding the aspalathin content of the green rooibos extract when the levels of independent variables i.e. the extraction conditions are known. This could lead to the rejection of product which has an aspalathin content outside of the predicted ranges defined for this critical quality attribute.

For further evaluation of the predictive ability of the model, Bland-Altman plots (Fig. 3.21) were used to assess the agreement between observed and predicted values and to analyse for the presence of bias within the data. The means of the observed and predicted values are plotted on the *x*-axis, and the differences between the observed and predicted values are displayed on the *y*-axis. The experimental data should ideally be scattered closely around the mean and within the 95%

limits of agreement. This would represent a small difference between the predicted and observed results. If no bias is present in the experimental data, then the mean lies at 0 on the *y*-axis.

The Bland-Altman plots for extract yield, aspalathin content of the extract and aspalathin extraction efficiency show, with the exception of one point in Fig. 3.21a, that the experimental points were scattered between the 95% limits of agreement on both sides of the mean. This indicates a small difference between the experimental and predicted results and satisfactory predictive ability. For all three responses the means were slightly below 0, indicating a slight bias due to random variation and subsequent overestimation. Given consideration to all the parameters to evaluate the predictive ability of the models, it is therefore suggested that EY and Asp_EE should be considered when quality assessment of GR hot water extracts is conducted.

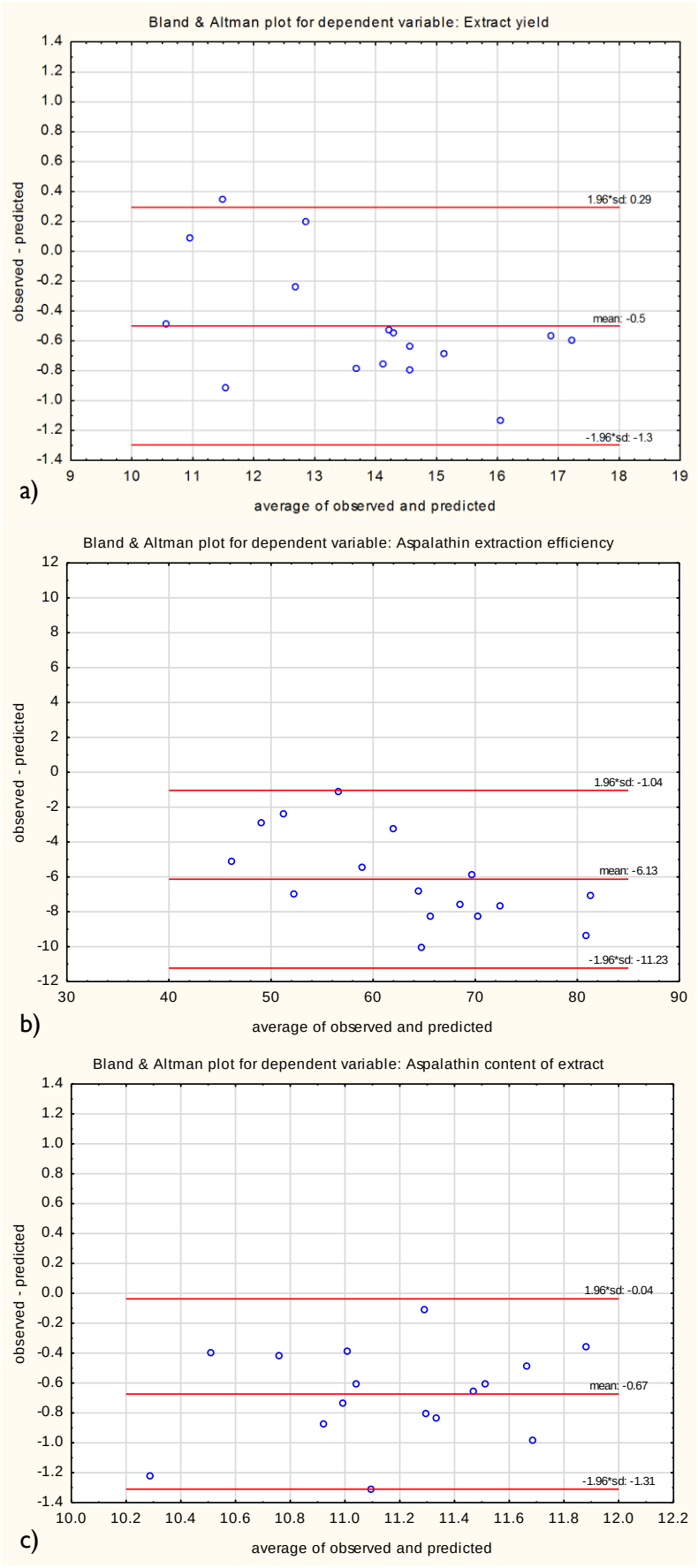

Figure 3.21 Bland-Altman plots for (a) extract yield, (b) aspalathin extraction efficiency and (c) aspalathin content of extract model verification.

3.4.4.3. Desirability profiling

The concept of desirability profiling in RSM refers to the identification of a desirability function for the given dependent variable(s) under investigation. Response values are then predicted using these functions and are assigned scores ranging from 0 (most undesirable) to 1 (most desirable). A series of graphs, profiling the desirability of each response are generated for each of the independent variables. Responses may be maximised, minimised or kept at constant values. When the desirability scores for a given parameter are plotted, the remaining parameters are fixed at constant values. The desirability profile which is finally obtained gives an indication of the levels of the independent variables that would produce the most desirable predicted response values.

Figs. 3.22–3.24 show the desirability profiles for EY, Asp_EE and Asp_HWE, all optimised for a maximum response value. The 95% confidence intervals (blue lines) are used to aid in the assessment of the reliability of the predicted responses. The gradients of the various desirability curves (green) are a reflection of the magnitude of the effect on the response value. The desirability plots mirror the Pareto charts in that they clearly indicate that the extraction temperature had a strongly positive effect on the extract and aspalathin yield, followed by extraction time and water-to-plant material ratio. The greater effect of the latter on Asp_EE than on EY is also clear from the respective gradients of the desirability curves for these responses. The less pronounced effect of the extraction temperature on increasing Asp_HWE, as opposed to EY and Asp_EE, is reflected by the more gradual incline of the desirability curve for extraction temperature in Fig. 3.24.

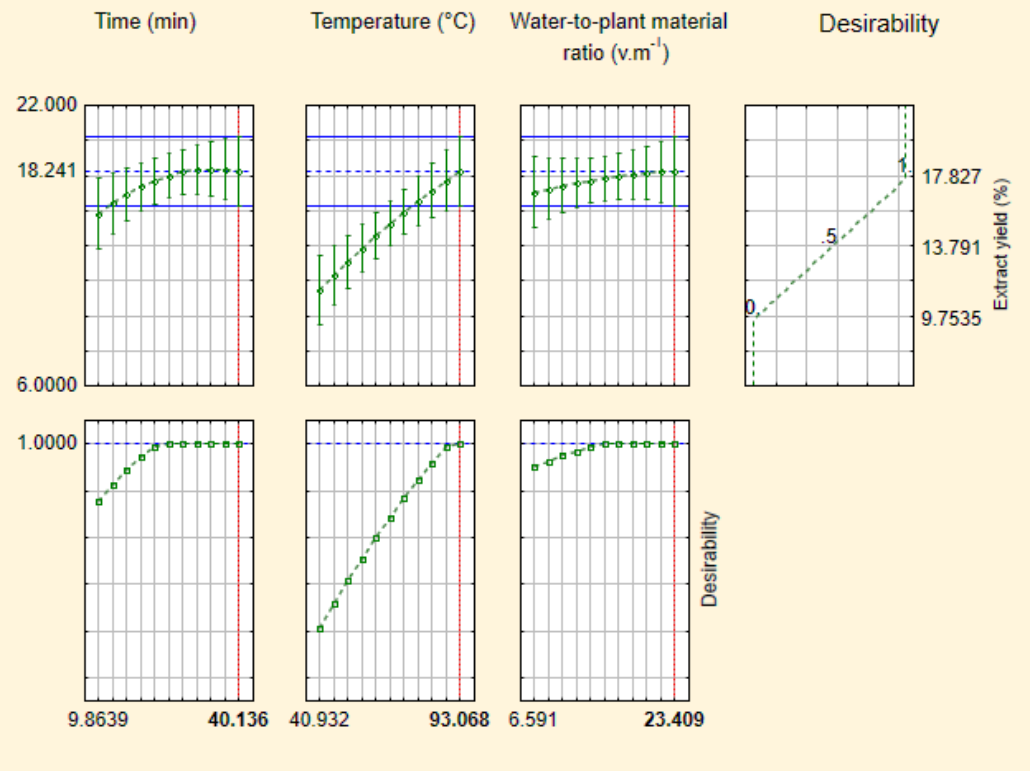

Figure 3.22 Desirability profiles for extract yield. Optimal values for each independent variable are indicated in bold at the bottom.

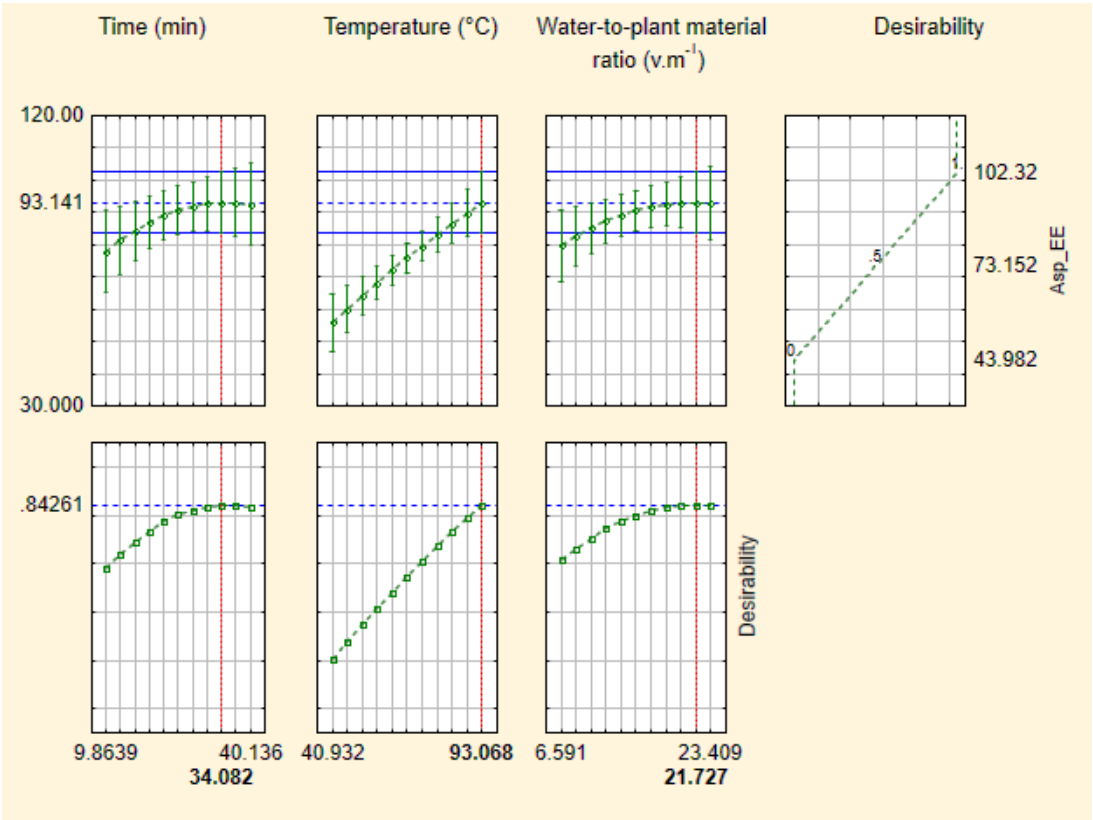

Figure 3.23 Desirability profiles for aspalathin extraction efficiency (Asp_EE). Optimal values for each independent variable are indicated in bold at the bottom.

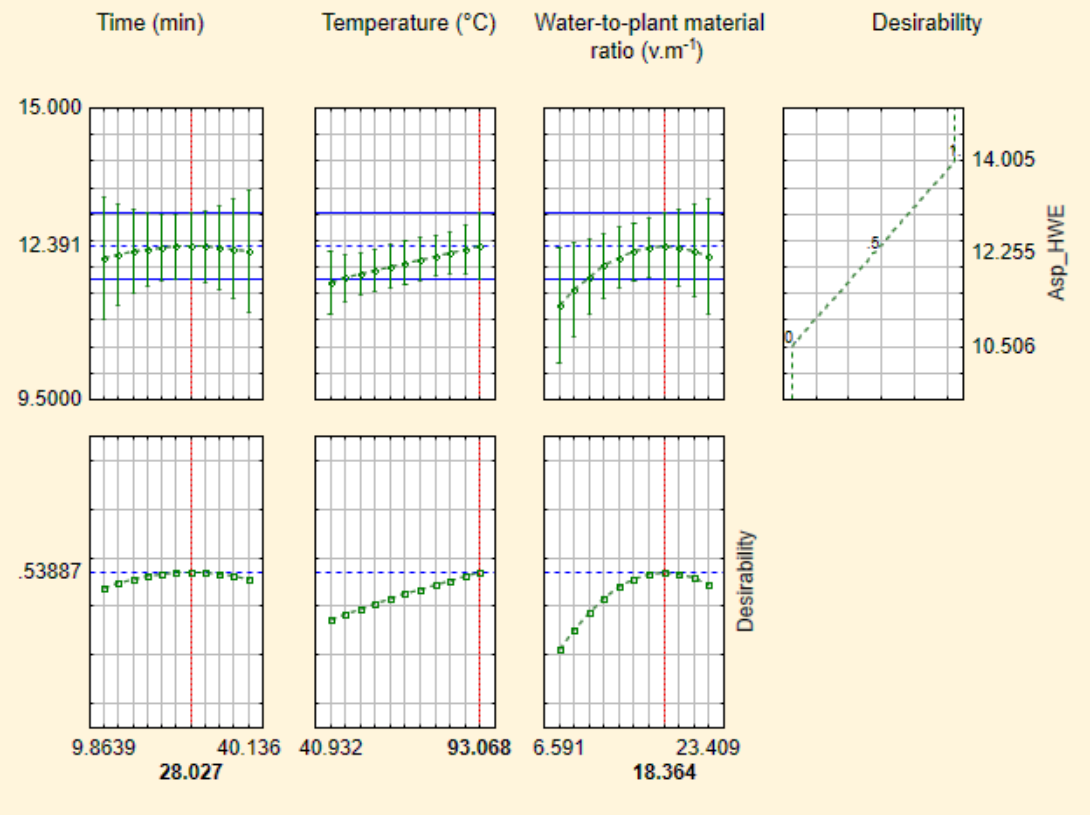

Figure 3.24 Desirability profiles for aspalathin content of extract (Asp_HWE). Optimal values for each independent variable are indicated in bold at the bottom.

Multi-response optimisation was carried out to obtain the optimal values of the three parameters which would simultaneously maximise the extract yield and aspalathin extraction efficiency (Fig. 3.25). The response, Asp_HWE, was not included in the multiple desirability profiling due to the poor predictive ability of its prediction model. The optimal values for all three independent variables are at the upper limit of the experimental ranges, i.e. 40 min, 93 °C and 23.4:1 water-to-plant material ratio. This is in agreement with the general responses obtained from the Pareto charts, response surface plots and individual desirability profiles, i.e. that extract yield and aspalathin extraction efficiency were significantly increased by increasing levels of these parameters.

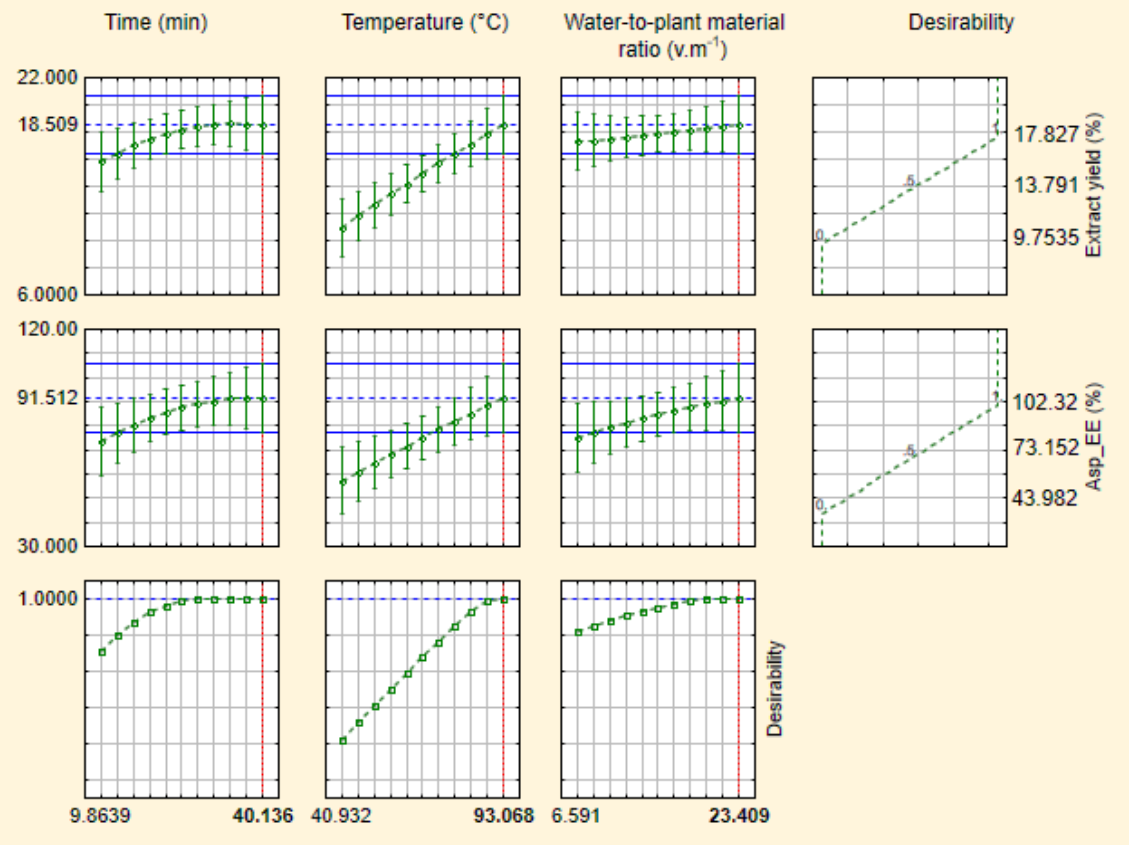

Figure 3.25 Desirability profiles for multi-response optimisation of extract yield and aspalathin extraction efficiency. Optimal values for each independent variable are indicated in bold at the bottom.

3.4.4.4. Practical optimum extraction parameters

Even though RSM is a useful tool to establish statistical models for the optimisation of the extraction process, the theoretical optimum conditions predicted by these models may not always be practically or economically feasible. Fig. 3.25 shows that the effect of increasing the extraction temperature stayed constant up to 93 °C, thus not reaching an optimum, whereas the desirability curves of extraction time and water-to-plant material ratio reached plateaus as they approached the upper limits of their experimental ranges (more so for the extraction time). Despite 40 min being indicated as the optimum extraction time, the increase in desirability from 30 min to 40 min is too slight to justify a 40 min extraction time from a practical viewpoint. The proposed optimal water-to-plant material ratio of 23.4:1 would provide a higher extraction yield (18.5 vs. 17.24%) and aspalathin extraction efficiency (89.96 vs. 79.27%) than a lower ratio of 10:1, but this increase is also not large enough to justify the higher solvent and energy consumption this would entail. The optimal water-to-plant material ratio was therefore set at 10:1. The proposed optimal extraction temperature of 93 °C was accepted. The final optimum hot water extraction conditions, otherwise referred to as the critical process parameters (CPP) for the extraction process, are summarised in Table 3.10. The

optimal conditions are presented as ranges of values in order to allow for minor deviations in operations.

Table 3.10 Critical process parameters for optimised hot water extraction of green rooibos.

Parameter	Range
Extraction time (min)	29–31
Extraction temperature (°C)	90–95
Water-to-plant material ratio ($v.m^{-1}$)	9–11

3.4.5. Validation of optimum hot water extraction process

By substituting the lower and upper values of the CPPs into the polynomial models for extraction yield and aspalathin extraction efficiency (Table 3.8), the CQAs of the hot water extraction process were determined (Table 3.11). The minimum EY and Asp_EE one could expect by adhering to these CPPs are 17.071% and 81.933%, respectively. This would most likely only hold true for batches with aspalathin content, particle size distribution and stem content similar to that of production batch B. The lowest expected values are particularly important since the aim is to ensure that minimally acceptable quality levels are attained, whereas overestimation of the yields or extraction efficiency would not compromise quality or safety.

Table 3.11 Predicted **r**anges of critical quality attributes (CQAs) for hot water extraction of green rooibos using practical optimum extraction parameters[1].

CQA	Range
Extract yield (%) ($g.100\ g^{-1}$ plant material)	17.071–17.601
Aspalathin extraction efficiency (Asp_EE; %) ($g.100\ g^{-1}$ in plant material)	81.933–87.642
Aspalathin content of extract (Asp_HWE; %) ($g.100\ g^{-1}$ soluble solids)	11.620–11.911

[1] Extraction temperature = 93 °C; extraction time = 30 min; water-to-plant material ratio = 10:1 ($v.m^{-1}$)

The predictive ability of the regression models for extract yield and aspalathin extraction efficiency was investigated by carrying out 10 additional extractions using the optimal extraction conditions and the same plant material production batch (Batch B) that was used in the CCD experiments. Table 3.12 shows that the minimum predicted yield of 17.071% was obtained in all instances, and that the maximum predicted yield of 17.601% was surpassed in six out of ten

instances. The minimum predicted Asp_EE (81.933%) was obtained three out of ten cases, with some of the remaining values nearly reaching the target, e. g. 81.443 and 81.293%. This could be attributed to variations in the composition of the different aliquots of plant material, despite their originating from the same plant material production batch. Higher relative stem content in any given aliquot of plant material could result in less efficient extraction of aspalathin, as opposed to an aliquot with a relatively higher leaf content. The Asp_HWE was >10% in all instances, but the minimum predicted value of 11.620 was not obtained in any of the replications.

Table 3.13 shows 95% confidence intervals for the three dependent variables, EY, Asp_EE and Asp_HWE. These intervals represent the range of response values, based on the actual experimental data. to be expected (with 95% confidence) if a future extraction is conducted using the practical optimum parameters with green rooibos batches similar to batch B (Kidd, M., 2016, Centre for Statistical Consultation, Stellenbosch, personal communication, 11 August).

Table 3.12 Results of validation experiments for optimum extraction conditions using green rooibos production batch B.

Replication	Extract yield (%)[1]	Asp_EE (%)[2]	Asp_HWE (%)[3]
1	18.505	85.566	11.273
2	17.355	71.673	10.068
3	17.520	81.293	11.312
4	17.475	80.142	11.180
5	18.885	87.094	11.244
6	17.770	80.712	11.073
7	18.180	80.127	10.745
8	17.490	78.806	10.985
9	17.990	81.443	11.037
10	18.370	84.811	11.256

[1] soluble solids, g.100 g^{-1} plant material; [2] Aspalathin extraction efficiency = g.100 g^{-1} aspalathin in plant material; [3] Aspalathin content of hot water extract = g.100 g^{-1} soluble solids

Table 3.13 Confidence intervals (95%) for critical quality attributes (CQAs) in hot water extraction of green rooibos carried out using practical optimum extraction parameters[1].

CQA	Range
Extract yield (%) (g.100 g^{-1} plant material)	17.355–18.885
Aspalathin extraction efficiency (Asp_EE; %) (g.100 g^{-1} in plant material)	71.673–87.094
Aspalathin content of extract (Asp_HWE; %) (g.100 g^{-1} soluble solids)	10.068–11.312

[1] Extraction temperature = 93 °C; extraction time = 30 min; water-to-plant material ratio = 10:1 ($v.m^{-1}$)

In order to validate the practical optimal extraction parameters using different plant material to that which was used to obtain data for the models, 47 production batches of commercial green rooibos (A1–A47), previously characterised in terms of major rooibos flavonoid content with water-acetonitrile extractions (refer to section 3.4.1.), were used to prepare extracts (in duplicate) using an extraction temperature of 93 °C for 30 min and a water-to-plant material ratio of 10:1 ($v.m^{-1}$) (Table 3.14).

Table 3.14 Extract yield, aspalathin extraction efficiency (Asp_EE) and aspalathin content (Asp_HWE) of optimised green rooibos hot water extracts (n = 47). Bold italic script indicates minimum and maximum values for each response.

Batch	Extract yield (%)[1]	Asp_EE (%)[2]	Asp_HWE (%)[3]	Batch	Extract yield (%)[1]	Asp_EE (%)[2]	Asp_HWE (%)[3]
A1	20.840	65.941	11.987	**A25**	19.551	57.175	9.708
A2	22.051	64.944	10.782	**A26**	19.901	64.205	12.053
A3	21.783	62.420	12.156	**A27**	20.425	60.890	11.695
A4	21.145	65.419	11.488	**A28**	18.918	56.127	11.200
A5	21.408	66.184	10.727	**A29**	19.260	55.386	10.698
A6	21.554	***72.295***	11.460	**A30**	19.600	57.334	11.659
A7	16.337	52.044	8.944	**A31**	19.764	52.589	10.932
A8	***15.411***	49.916	***8.108***	**A32**	22.069	55.039	10.125
A9	17.594	53.967	10.743	**A33**	22.109	58.742	10.126
A10	17.536	52.557	10.439	**A34**	***22.892***	55.784	10.569
A11	15.070	52.112	9.810	**A35**	20.392	68.446	***12.330***
A12	15.779	49.886	9.841	**A36**	21.218	57.928	9.742
A13	17.237	54.332	10.108	**A37**	21.184	56.739	10.220
A14	19.944	66.390	9.713	**A38**	20.962	59.034	9.951
A15	17.236	50.750	10.068	**A39**	21.310	58.836	10.737
A16	17.115	***40.758***	9.157	**A40**	20.759	56.654	10.322
A17	17.072	55.496	8.843	**A41**	20.946	60.019	10.362
A18	16.468	48.154	10.915	**A42**	21.978	69.032	9.552
A19	17.513	52.774	9.108	**A43**	22.043	64.842	10.656
A20	16.667	54.877	11.560	**A44**	16.710	51.376	10.109
A21	16.231	47.866	9.751	**A45**	17.963	49.172	9.293
A22	18.195	48.530	11.879	**A46**	18.017	47.373	9.846
A23	18.125	46.686	10.595	**A47**	18.715	47.403	10.433
A24	20.594	61.416	11.409	**Mean**	19.268	56.507	10.466

[1] g.100 g^{-1} plant material; [2] Aspalathin extraction efficiency = g.100 g^{-1} aspalathin in plant material; [3] Aspalathin content of hot water extract = g.100 g^{-1} soluble solids

The mean EY was 19.27%. The minimum predicted EY of 17.07% was obtained in 40 out of the 47 batches, with the lowest and highest yields attained being 15.07% and 22.89%, respectively. The minimum predicted Asp_EE of 81.93% was not attained in any of the 47 batches. The range of Asp_EE values attained was 40.76% to 72.31%, with the mean value of 56.51% falling considerably

short of the predicted minimum response. The highest Asp_EE value attained (72.295%) did not meet the predicted minimum response value.

Large variation was observed in the TPC and TAC_{DPPH} of the extracts (Table 3.15). The mean values for TAC_{DPPH} (3440 µmol TE.g^{-1}) and TPC (34.8 g GAE.100 g^{-1}) of GR FDEs were significantly higher than those of fermented rooibos FDEs with mean TAC_{DPPH} and TPC values of 2180 µmol TE.g^{-1} and 27.09 g GAE.100 g^{-1}, respectively (Joubert & De Beer, 2012).

Table 3.15 Total polyphenol content (TPC, g gallic acid equivalents.100 g^{-1}), total antioxidant capacity (TAC, µmol Trolox equivalents.g^{-1}) and % contribution[1] of aspalathin, iso-orientin and orientin to the TAC of green rooibos (GR) extracts (n = 47).

Parameter	Range	Mean	Standard deviation
TP	29.7–43.5	34.8	3.3
TAC	2873–4286	3440	307
% contribution to TAC (aspalathin)	13.1–22.8	18.5	2.7
% contribution to TAC (iso-orientin)	1.3–2.1	1.7	0.2
% contribution to TAC (orientin)	1.2–1.9	1.6	0.2
% contribution to TAC (aspalathin, iso-orientin and orientin)	16.0–26.7	21.7	3.1

[1] % contribution of the compounds to the TAC of GR extracts was calculated using concentration in the extracts and their TEAC values (aspalathin = 2.721; iso-orientin = 2.439; orientin = 2.161)

The aspalathin content of the extract (%; g.100 g^{-1} soluble solids) varied between 8.11 and 12.33% (Table 3.14), and contributed between 13.1% and 22.8% to the TAC_{DPPH} (Table 3.15). The individual iso-orientin and orientin contents of the extracts were <1.2% in all instances (Addendum A; Table 6.1). These compounds also contributed significantly less to the TAC_{DPPH} than aspalathin. The combined content of these flavonoids in the FDEs ranged between 10.22% and 14.88% (mean = 12.63%) and contributed between 16.0% and 26.7% to its TAC_{DPPH}. Fermented rooibos hot water extract contained 2.27% of these compounds on average (Joubert & De Beer, 2012).

The correlations between the flavone and dihydrochalcone content of the plant material and those of the FDEs are depicted in Fig. 3.26. For the dihydrochalcone content, a linear relationship was established but large variation was evident (Fig. 3.26a; R^2 = 0.483). The flavone content of the plant material showed a weak correlation with that in the corresponding FDE (Fig. 3.26b; R^2 = 0.119). The variation in the total hot water soluble solids content of the plant material (as reflected in the theoretical extract yield) indicates that other constituents are likely contributing to the variation in the total phenolic content of the FDEs.

The potential of UV spectrophotometry as a screening method to determine the flavonoid content of the optimised extracts was investigated in an additional experiment (Data included in Addendum A; section 6.3). The total dihydrochalcone (aspalathin and nothofagin) content of the extract showed a significant ($P < 0.001$) but weak correlation (R^2 = 0.429) with the absorbance at

290 nm wavelength (Fig. 6.13). Similarly, the total flavone (iso-orientin and orientin) content of the extract correlated significantly ($P < 0.001$) but weakly ($R^2 = 0.397$) with the absorbance at 350 nm. Joubert *et al.* (2008) also investigated the potential of UV spectrophotometry as a quick screening method as alternative to HPLC to quantify the dihydrochalcone content of unfermented rooibos. The dihydrochalcone content of the aqueous green rooibos extracts, determined with UV spectroscopy, correlated strongly with the sum of the aspalathin and nothofagin contents as quantified by HPLC ($r = 0.97$). A linear model generated using the correlation data was used to predict the dihydrochalcone content of extracts based on spectrophotometric measurements with reasonable accuracy ($R^2 = 0.92$). The weak correlation between UV and HPLC measurements in the present study compared with Joubert *et al.* (2008) could be ascribed to the smaller sample set used (n = 47 vs. n = 73), as well as a more limited range of values used to generate the linear models. The presence of compounds other than the target compounds under investigation which also absorb UV radiation at the tested wavelengths is also likely to contribute to the weak correlation.

Differences in the water solubility of the flavones and dihydrochalcones may also contribute to the variation observed. The conversion of aspalathin to iso-orientin and orientin is also a likely contributing factor. This conversion is accelerated under conditions favourable for oxidation, e.g. during hot water extraction in the presence of oxygen (Joubert & De Beer, 2014). It has been demonstrated that iso-orientin is formed in larger quantities than orientin in solution (Krafczyk & Glomb, 2008). This was confirmed by the iso-orientin contents of the individual FDEs, which were all consistently higher than that of orientin (Data included in Addendum A; section 6.2, Table 6.1). In the plant material, the iso-orientin content was not always higher than the orientin content, which suggests that some conversion of aspalathin to iso-orientin occurs during hot water extraction. Nothofagin would be less susceptible to oxidative degradation during the relatively short extraction time due to the catechol arrangement on the B-ring (Krafczyk & Glomb, 2008).

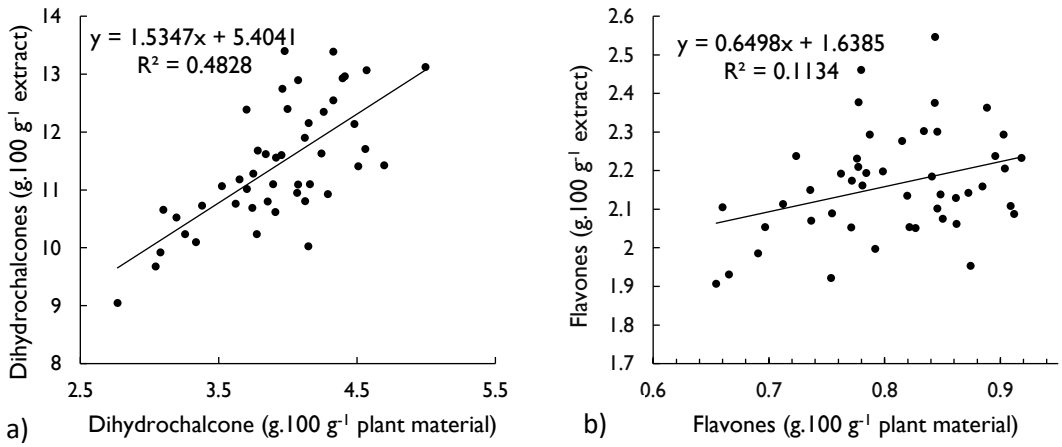

Figure 3.26 Relationship between (a) dihydrochalcone and (b) flavone content of batches of commercial green rooibos plant material (n = 47) and their corresponding content in hot water green rooibos extract.

Since there is expected to be inherent variation present in the aspalathin content and extractable soluble solids content of different batches of commercial green rooibos plant material, it would be difficult to reliably predict a guaranteed amount of aspalathin in the extracted rooibos solids. The outcome would most likely be affected by the specific attributes of the plant material used in a given instance. The relative amounts of aspalathin present in different production batches, which typically consist of processed material from various individual plants which are pooled together at a certain point in the production process. These heterogeneous blends of processed plant material may also contain varying levels of different material types (e.g. leaf, stem or flower) due to the often uncontrollable differences in individual processing methods by human operators. The mean plant material particles sizes may vary from batch to batch, for instance, due to the tendency of one operator to cut on average a larger leaf size. The stem content of some production batches may be significantly higher than those of similar quality grade batches due to the less discerning eye of a different quality controller or operator at the processing level.

The extraction efficiency of the process could be improved by carrying out additional processing on the plant material before extraction commences. It was noted during the preparation for the validation experiments, as the plant material was unpacked and visually inspected, that the different batches of plant material bore distinct differences in their average particle sizes and "white stick"/stem content. Some batches contained negligible amounts of stem material, while others had an almost excessive amount of stems. The average leaf sizes in some batches were relatively large. It was to be expected, therefore, that aspalathin would be extracted more efficiently from some batches than from others simply due to the visible differences in the plant material. Specifically, it was proposed that the removal of the largest and coarsest particle fractions, which would include significant amounts of aspalathin-poor stems, could improve the aspalathin extraction efficiency by reducing the mean particle size and increasing the leaf-to-stem ratio of the plant material.

In order to obtain the different size fractions of plant material, the ten validation batches of sieved using a SMC Mini-Sifter (J.M. Quality Control Services, , South Africa) fitted with three mesh screens (12, 16 and 20 mesh). An aliquot of plant material (300 g; in duplicate) from each batch was sieved for 90 s and the various size fractions were collected and weighed to determine the relative contribution of each to the mass of the bulk plant material as received from the supplier. Fig. 3.27 shows the relative amounts of each of the four size fractions in the ten batches under investigation. The two larger particle size fractions are represented by red bars and the two smaller particle size fractions are represented by green bars. The red bars thus represent the fraction of plant material which, if discarded, would potentially enhance the extraction efficiency by reducing the mean particle size of the entire batch. Fig. 3.27 demonstrates that there were great differences between the amounts of the various size fractions in the ten selected batches. Five of the batches (B7, B8, B23,

B44 and B48) were made up almost entirely of large Fraction 1 and Fraction 2 particles, whereas two batches (B3 and B31) contained less than 5% large particles. Discarding the large particle size fractions would therefore be unlikely to enhance the extraction efficiency in some instances (e.g. B3), and it would be undesirable in many cases (e.g. B7 and B48) since it would mean discarding the majority of the plant material received. Each of the ten validation batches was subjected to two different particle size reduction treatments (SRTs) (Table 3.13).

Table 3.16 Particle size reduction treatment (SRT) groups.

Treatment	Description
SRT1	Size fraction 1 (>12 mesh) removed
SRT2	Size fractions 1 and 2 (>16 mesh) removed

The hot water extractions were carried out at the optimal extraction conditions again but using the size-reduced plant material. There was no consistency in the effect of the particle size reduction treatments on the extract yields and aspalathin extraction efficiencies of the various batches (Table 3.17). In some instances, major improvements in both the yield and aspalathin extraction efficiency were observed when the larger particles were removed, but in other instances they remained constant or even decreased. Post-hoc agglomerative hierarchical clustering was carried out in order to identify groups of batches which were similar in their particle size distribution. Three clusters were identified (Table 3.18), as shown in the accompanying dendrogram (Fig. 3.28).

Table 3.17 Extract yields and aspalathin extraction efficiency obtained for ten validation batches of green rooibos subjected to particle size reduction treatments.

Batch	Aspalathin content[1]	Extract yield (%)[2]			Aspalathin extraction efficiency (%)[3]		
		Validation run	SRT 1 >12 mesh removed	SRT 2 >16 mesh removed	Validation run	SRT 1 >12 mesh removed	SRT 2 >16 mesh removed
A1	3.788	21.282	22.348	22.644	67.621	75.264	75.019
A2	3.661	20.156	19.780	21.905	63.492	62.971	73.896
A3	4.246	24.252	22.074	23.908	69.883	65.889	69.051
A7	2.800	16.345	19.788	23.169	63.034	80.802	100.000
A13	3.210	17.689	21.978	25.562	61.792	85.933	100.000
A23	4.095	19.487	19.868	23.044	56.752	58.874	70.151
A31	4.007	20.877	19.443	19.432	66.848	60.422	62.595
A38	3.539	19.048	20.959	23.244	54.654	59.313	68.264
A42	3.040	20.980	22.575	23.170	71.762	79.077	83.792
A44	3.290	20.639	22.954	25.711	68.822	78.963	92.384

[1] g.100 g^{-1} plant material; [2] g.100 g^{-1} plant material; [3] g.100 g^{-1} aspalathin in plant material

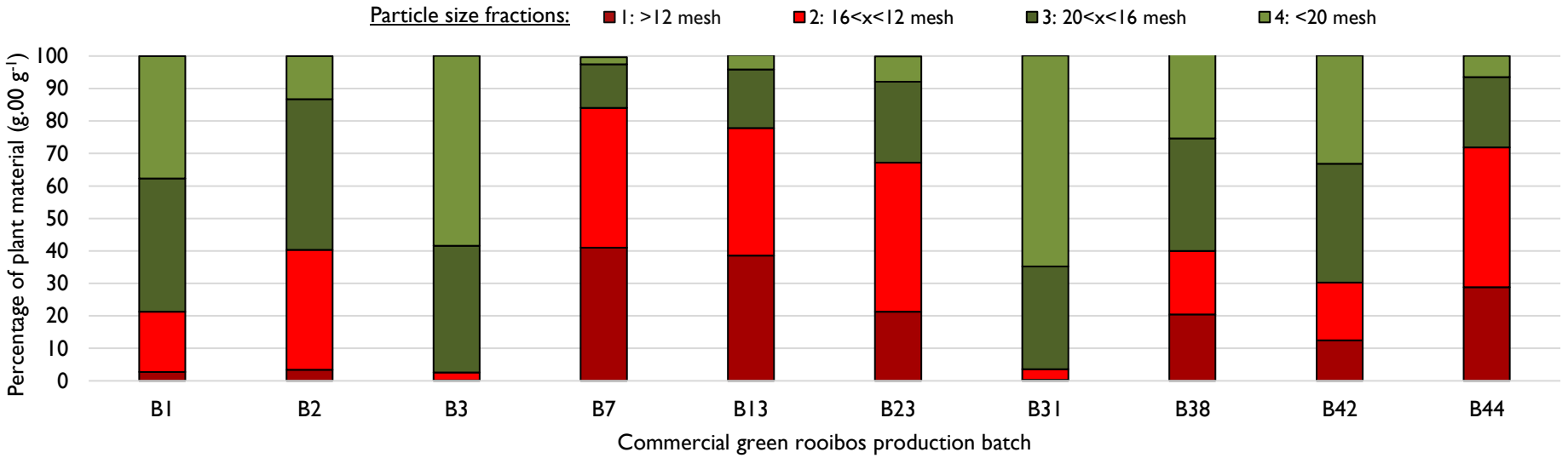

Figure 3.27 Particle size distribution of ten commercial green rooibos production batches.

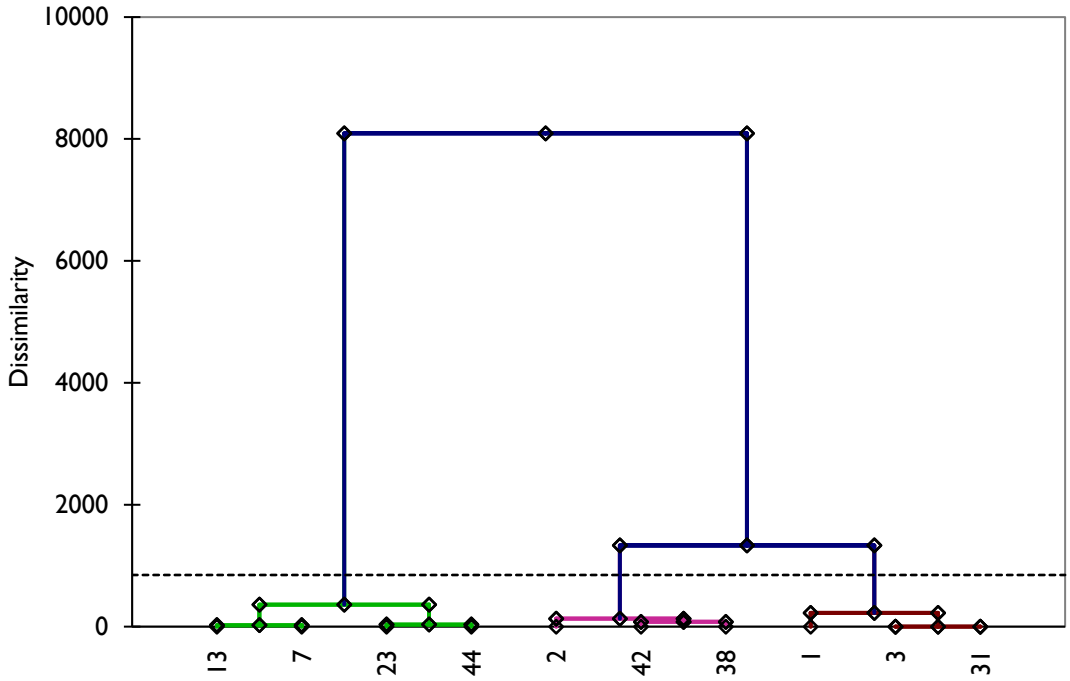

Figure 3.28 Dendrogram depicting clusters of commercial green rooibos production batches grouped according to similar particle size distribution by agglomerative hierarchical clustering.

Table 3.18 Batch classes of green rooibos as identified by agglomerative hierarchical clustering (AHC).

Batch cluster description	Production batches
Fine	A1, A3, A31
Medium	A2, A38, A42
Coarse	A7, A13, A23, A44

Figs. 3.29–3.31 show examples of plant material from all three batch classes: fine (A1), medium (A2) and coarse (A23). The plant material in Fig. 3.29 (Batch A1 – fine) contained a greater proportion of stems and woody material, which appear white or off-white, whereas that in Fig. 3.31 (A23 – coarse) contained almost no such material and consisted almost entirely of leaf cuttings of various shades of green or dark-brown. The average size of the leaf particles in batch A23 was also greater than that in other production batches, which explains why its particle size distribution showed that the majority of the plant material consisted of large particles (>16 mesh) (Fig. 3.27). It would be unfeasible to remove the large particle fraction in this case, since it would mean discarding the leaf material. Instead, only plant material batches containing leaves cut to below a specified size and minimal stem and wood contents should be used as the raw material for the extract production. The plant material should be sieved prior to extraction to obtain only particle of below size 16 mesh and remove as many residual stems or coarse particles still present.

Figure 3.29 Commercial green rooibos plant material from Batch A1 (AHC Batch Class 1; fine) as received from supplier.

Figure 3.30 Commercial green rooibos plant material from Batch A2 (AHC Batch Class 2; medium) as received from supplier.

Figure 3.31 Commercial green rooibos plant material from Batch A23 (AHC Batch Class 3; coarse) as received from supplier.

Means plots of the three different batch size classes for extract yield and aspalathin extraction efficiency are shown in Fig. 3.32. A sharp increase in the extract yield was observed when coarse batches were subjected to particle size reduction treatments (Fig. 3.32a). The aspalathin extraction efficiency also improved with particle size reduction in coarse batches, although to a lesser degree than the extract yield (Fig. 3.32b). The batches with fine plant material were either negatively affected or not significantly affected by particle size reduction treatments, since they typically contained smaller amounts of coarse, woody particles (Fig. 3.33). Isolated leaf cuttings collected from the same production batch (A7) are shown in Fig. 3.34, demonstrating the range of leaf cut sizes and degree of oxidative colour changes which may be observed in commercial green rooibos.

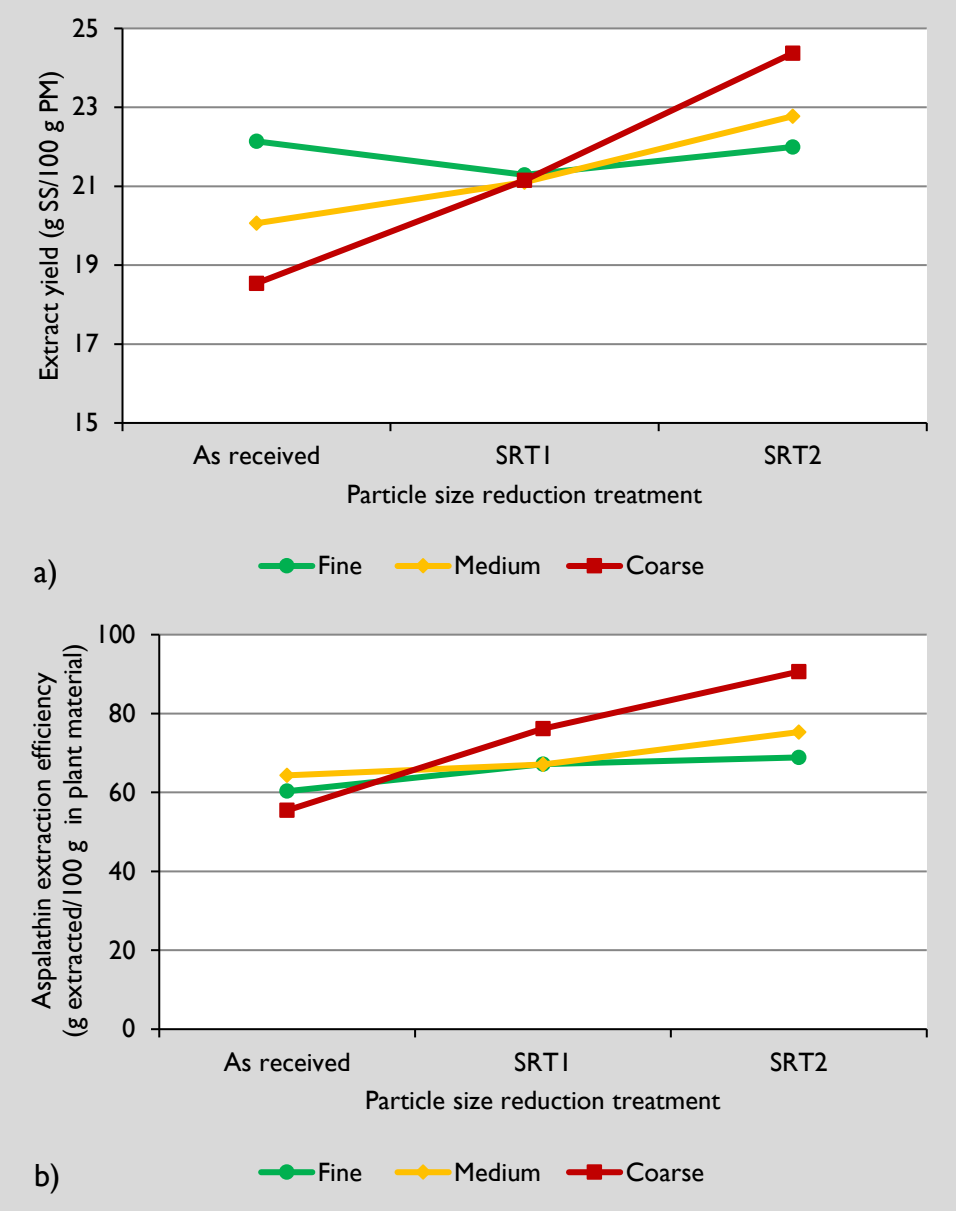

Figure 3.32 Effect of particle size reduction treatments on (a) extract yield and (b) aspalathin extraction efficiency for different batch size classes (Fine, Medium, Coarse) of commercial green rooibos plant material.

Figure 3.33 Coarse, non-leaf material found in commercial green rooibos production batches.

Figure 3.34 Rooibos leaf cuttings isolated from a single production batch showing variable dimensions and degrees of oxidative colour changes.

3.5. Conclusion

A large variation in the composition of the green rooibos plant material, originating from the same plantation and harvested over a relatively short time period, was observed as demonstrated by the batch-to-batch variation in the theoretical extract yield, TPC and TAC_{DPPH}, as well as the content of the major flavonoids, aspalathin, nothofagin, orientin and iso-orientin. The dihydrochalcone content

of green rooibos only moderately predicted the dihydrochalcone content of the corresponding freeze-dried extract, which is an obstacle to the manufacturer intent on producing a green rooibos extract with a specified dihydrochalcone content. Specifying minimum dihydrochalcone values for green rooibos extract to ensure efficacy as an antidiabetic nutraceutical is not yet possible. Additional research is required to gain insight into the therapeutic dose needed for bioactivity.

Single factor experiments showed that extraction time, extraction temperature, water-to-plant material ratio and particle size significantly affect extraction efficiency. Since the particle size distribution may differ between individual production batches of green rooibos, only the parameters extraction time, temperature and the water-to-plant material ratio were optimised using response surface methodology and multiple desirability profiling. Optimal hot water extraction conditions (critical process parameters) were identified based on statistical analyses and informed by considerations of cost-efficiency. Validation of the prediction models for aspalathin extraction efficiency and extract yield showed that predicted values were not always achievable with batches of plant material different from that used to generate the model data. The most likely cause for this is the heterogeneous distribution of aspalathin in the plant material, as well as major differences in the cut leaf sizes and composition of the various batches.

Standardisation of the batches in terms of particle size could be achieved to a certain degree by sieving out particles above a specified size (e.g. 16 mesh), but the inherent variation in the aspalathin content of individual leaf particles would still result in variable aspalathin content in the final extract. It is therefore clear that the plant material to be used for extraction should have a small particle size (<16 mesh) and minimal stem content. The length of leaf particles should be as short as possible, since this enhances the rate of diffusion of the target compound from the leaf interior to the solvent and therefore ensures that more of the target compound (i.e. aspalathin) would be extracted within the 30 min extraction time period. Plant material intended specifically for the production of aspalathin-enriched extracts should be virtually free of stem material and the length of leaf particles should be as short as possible (≈ 5–10 mm). To ensure optimal extraction of aspalathin from green rooibos plant material, quality-by-design methodology should ideally be applied to the processing steps at the harvesting and cutting stage. This would most likely ensure that a more consistent set of quality attributes are obtained in the extract.

3.6. References

Aherne, S.A. & O'Brien, N.M. (2002). Dietary flavonoids: chemistry, food content and metabolism. *Nutrition*, **18**, 75-81.

Anonymous (2015). Albany Ultima health range. [Internet document]. URL http://www.albany.co.za/ultima.php. 09/11/2015.

Arthur, H., Joubert, E., De Beer, D., Malherbe, C.J. & Witthuhn, R.C. (2011). Phenylethanoid glycosides as major antioxidants in *Lippia multiflora* herbal infusion and their stability during steam pasteurisation of plant material. *Food Chemistry*, **127**, 581–588.

Astill, C., Birch, M.R., Dacombe, C., Humphrey, P.G. & Martin, P.T. (2001). Factors affecting the caffeine and polyphenol contents of black and green tea infusions. *Journal of Agricultural and Food Chemistry*, **49**, 965–977.

Azmir, J., Zaidul, I.S.M., Rahman, M.M., Sharif, K.M., Mohamed, A., Sahena, F., Jahurul, M.H.A., Ghafoor, K., Norulaini, N.A.N. & Omar, A.K.M. (2013). Techniques for extraction of bioactive compounds from plant materials: a review. *Journal of Food Engineering*, **117**, 426–436.

Bezerra, M.A., Santelli, R.E., Oliveira, E.P., Villar, L.S. & Escaleira, L.A. (2008). Response surface methodology (RSM) as a tool for optimisation in analytical chemistry. *Talanta*, **76**, 965–977.

Biénabe, E., Bramley, C. & Kirsten, J. (2009). An economic analysis of the evolution in intellectual property strategies in the South African agricultural sector: the rooibos industry. In: *The Economics of Intellectual Property in South Africa* (edited by E. Burrone & P. Rai). Pp. 56–83. Geneva: World Intellectual Property Organisation.

Bucić-Kojić, A., Planinić, M., Tomas, S., Bilić, M., & Velić, D. (2007). Study of solid–liquid extraction kinetics of total polyphenols from grape seeds. *Journal of Food Engineering*, **81**, 236–242.

Chemat, F., Vian, M.A. & Cravotto, G. (2012). Green extraction of natural products: concept and principles. *International Journal of Molecular Sciences,* **13**, 8615–8627.

Chen, S., Xing, X.H., Huang, J.J. & Xu, M.S. (2011). Enzyme-assisted extraction of flavonoids from *Ginkgo biloba* leaves: improvement effect of flavonol transglycosylation catalyzed by *Penicillium decumbens* cellulase. *Enzyme and Microbial Technology*, **48**, 100–105.

Cossuta, D., Vatai, T., Báthori, M., Hohmann, J., Keve, T. & Simándi, B. (2012). Extraction of hyperforin and hypericin from St. John's Wort (*Hypericum perforatum*) with different solvents. *Journal of Food Process Engineering*, **35**, 222–235.

Das, A.K., Mandal, S.C., Mandal, V., Beg, S. & Singh, B. (2014). QbD as an emerging paradigm in extraction technology for developing optimized bioactives. *Pharma Times*, **46**, 50–56.

De Beer, D., Malherbe, C.J., Beelders, T., Willenburg, E.L., Brand, D.J. & Joubert, E. (2015). Isolation of aspalathin and nothofagin from rooibos (*Aspalathus linearis*) using high-performance countercurrent chromatography: sample loading and compound stability considerations. *Journal of Chromatography A*, **1381**, 29–36.

De Beer, D., Schulze, A.E., Joubert, E., De Villiers, A., Malherbe, C.J. & Stander, M.A. (2012). Food ingredient extracts of *Cyclopia subternata* (Honeybush): variation in phenolic composition and antioxidant capacity. *Molecules*, **17**, 14602–14624.

Dejaegher, B. & Vander Heyden, Y. (2011). Experimental designs and their recent advances in set-up, data interpretation, and analytical applications. *Journal of Pharmaceutical and Biomedical Analysis*, **56**, 141–158.

Di Ferdinando, M., Brunetti, C., Fini, A. & Tattini, M. (2013). Flavonoids as antioxidants in plants under abiotic stresses. In: *Abiotic Stress Responses in Plants: Metabolism, Productivity and Sustainability* (edited by P. Ahmad & M.N.V. Prasads). Pp. 159–179. New York: Springer Science & Business Media.

Fischer, R., Vasilev, N., Twyman, R.M. & Schillberg, S. (2015). High-value products from plants: the challenges of process optimization. *Current Opinion in Biotechnology*, **32**, 156–162.

Gong, X., Chen, H., Chen, T & Qu, H. (2014). Unit operation optimization for the manufacturing of botanical injections using a design space approach: a case study of water precipitation. *PLoS one*, **9**, doi: 10.1371/journal.pone.0104493.

Granato, D. & De Araújo Calado, V.M. (2014). The use and importance of design of experiments (DOE) in process modelling in food science and technology. In: *Mathematical and Statistical Methods in Food Science and Technology* (1st ed.) (edited by D. Granato & G. Ares). Pp. 3–18. New York, USA: John Wiley & Sons.

Hernández-Jiménez, A., Kennedy, J.A., Bautista-Ortín, A.B. & Gómez-Plaza, E. (2012). Effect of ethanol on grape seed proanthocyanidin extraction. *American Journal of Enology and Viticulture*, **63**, 57–61.

Huang, M., Du Plessis, J., Du Preez, J., Hamman, J. & Viljoen, A. (2008). Transport of aspalathin, a rooibos tea flavonoid, across the skin and intestinal epithelium. *Phytotherapy Research*, **22**, 699–704.

Huang, J., Kaul, G., Cai, C., Chatlapalli, R., Hernandez-Abad, P., Ghosh, K. & Nagi, A. (2009). Quality by design case study: an integrated multivariate approach to drug product and process development. *International Journal of Pharmaceutics*, **382**, 23–32.

ICH (2009). ICH Harmonised Tripartite Guideline: Pharmaceutical Development Q8(R2). [Internet document]. URL http://www.ich.org/fileadmin/Public_Web_Site/ICH_Products/Guidelines/Quality/Q8_R1/Step4/Q8_R2_Guideline.pdf. 18/08/2016.

Jaganyi, D. & Wheeler, P.J. (2003). Rooibos tea: equilibrium and extraction kinetics of aspalathin. *Food Chemistry*, **83**, 121–126.

Joubert, E. (1984). Studies in verband met verkitsing van rooibos tee (*Aspalathus linearis*). MSc Food Science Thesis, Stellenbosch University, South Africa.

Joubert, E. (1988a). Technical note: effect of agglomeration on the properties of spray-dried rooibos tea. *International Journal of Food Science and Technology*, **23**, 203–207.

Joubert, E. (1988b). Effect of batch extraction conditions on yield of soluble solids from rooibos tea. *International Journal of Food Science and Technology*, **23**, 43–47.

Joubert, E. (1990a). Chemical and sensory analyses of spray- and freeze-dried extracts of rooibos tea (*Aspalathus linearis*). *International Journal of Food Science and Technology*, **25**, 344–349.

Joubert, E. (1990b). Effect of batch extraction conditions on yield of polyphenols from rooibos tea (*Aspalathus linearis*). *International Journal of Food Science and Technology*, **25**, 339–343.

Joubert, E. (1990c). Effect of time on fixed-bed extraction of polyphenols from rooibos tea (*Aspalathus linearis*). *LWT – Food Science and Technology,* **23**, 181–183.

Joubert, E. (1996). HPLC quantification of the dihydrochalcones, aspalathin and nothofagin in rooibos tea (*Aspalathus linearis*) as affected by processing. *Food Chemistry*, **55**, 403–411.

Joubert, E. & De Beer, D. (2011). Rooibos (*Aspalathus linearis*) beyond the farm gate: from herbal tea to potential phytopharmaceutical. *South African Journal of Botany*, **77**, 869–886.

Joubert, E. & De Beer, D. (2012). Phenolic content and antioxidant activity of rooibos food ingredient extracts. *Journal of Food Composition and Analysis*, **27**, 45–51.

Joubert, E. & De Beer, D. (2014). Antioxidants of rooibos beverages: role of plant composition and processing. In: *Processing and Impact on Antioxidants in Beverages* (edited by V. Preedy). Academic Press, San Diego. Pp. 131–144.

Joubert, E., De Beer, D., Hernández, I. & Munné-Bosch, S. (2014). Accumulation of mangiferin, isomangiferin, iriflophenone-3-C-ß-glucoside and hesperidin in honeybush leaves (*Cyclopia genistoides* Vent.) in response to harvest time, harvest interval and seed source. *Industrial Crops and Products,* **56***,* 74–82.

Joubert, E., Gelderblom, W.C.A., Louw, A. & De Beer, D. (2008). South African herbal teas: *Aspalathus linearis*, *Cyclopia* spp. and *Athrixia phylicoides*. A review. *Journal of Ethnopharmacology*, **119**, 376–412.

Joubert, E. & Hansmann, C.F. (1990). Effect of time on fixed-bed extraction of soluble solids from rooibos tea (*Aspalathus linearis*). *LWT – Food Science and Technology*, **23**, 178–180.

Joubert, E., Viljoen, M., De Beer, D., Malherbe, C.J., Brand, D.J. & Manley, M. (2010). Use of green rooibos (*Aspalathus linearis*) extract and water-soluble nanomicelles of green rooibos extract encapsulated with ascorbic acid for enhanced aspalathin content in ready-to-drink iced teas. *Journal of Agricultural and Food Chemistry*, **58**, 10965–10971.

Kamakura, R., Son, M.J., De Beer, D., Joubert, E., Miura, Y. & Yagasaki, K. (2015). Antidiabetic effect of green rooibos (*Aspalathus linearis)* extract in cultured cells and type 2 diabetic model KK-Ay mice. *Cytotechnology*, **67**, 699–710.

Karakashov, B, Grigorakis, S., Loupassaki, S. & Makris, D.P. (2015). Optimisation of polyphenol extraction from *Hypericum perforatum* (St. John's Wort) using aqueous glycerol and response surface methodology. *Journal of Applied Research on Medicinal and Aromatic Plants*, **2**, 1–8.

Kawano, A., Nakamura, H., Hata, S., Minakawa, M., Miura, Y. & Yagasaki, K. (2009). Hypoglycemic effect of aspalathin, a rooibos tea component from *Aspalathus linearis*, in type 2 diabetic model db/db mice. *Phytomedicine*, **16**, 437–443.

Krafczyk, N. & Glomb, M.A. (2008). Characterization of phenolic compounds in rooibos tea. *Journal of Agricultural and Food Chemistry*, **56**, 3368–3376.

Laroze, L.E., Díaz-Reinoso, B., Moure, A., Zúñiga, M.E. & Domínguez, H. (2010). Extraction of antioxidants from several berries pressing wastes using conventional and supercritical solvents. *European Food Research and Technology*, **231**, 669–677.

Leardi, R. (2009). Experimental design in chemistry: a tutorial. *Analytica Chimica Acta*, **652**, 161–172.

Liu, J.L., Li, L.Y. & He, G.H. (2016). Optimization of microwave-assisted extraction conditions for five major bioactive compounds from Flos Sophorae Immaturus (Cultivars of *Sophora japonica* L.) using response surface methodology. *Molecules*, **21**, 296–323.

Mazibuko, S.E., Muller, C.J.F., Joubert, E., De Beer, D., Johnson, R., Opoku, A.R. & Louw, J. (2013). Amelioration of palmitate-induced insulin resistance in C2C12 muscle cells by rooibos (*Aspalathus linearis*). *Phytomedicine*, **20**, 813–819.

Mazibuko, S.E. Joubert, E. Johnson, R., Louw, J., Opoku, A.R. & Muller, C.J.F. (2015). Aspalathin improves glucose and lipid metabolism in 3T3-L1 adipocytes exposed to palmitate. *Molecular Nutrition & Food Research*, **59**, 2199–2208.

Moloughney, S. (2016). Sustaining both people & planet. [Internet document]. URL http://www.nutraceuticalsworld.com. 02/05/2016.

Muller, C.J.F., Joubert, E., De Beer, D., Sanderson, M., Malherbe, C.J., Fey, S.J. & Louw, J. (2012). Acute assessment of aspalathin-enriched green rooibos (*Aspalathus linearis)* extract with hypoglycaemic potential. *Phytomedicine*, **20**, 32–39.

Naidu, K., Singh, V., Johnston, D.B., Rausch, K.R. & Tumbleson, M.E. (2007). Effects of ground corn particle size on ethanol yield and thin stillage soluble solids. *Cereal Chemistry*, **84**, 6–9.

Ng, T.B. (2006). Pharmacological activity of sanchi ginseng (*Panax notoginseng*). *Journal of Pharmacy and Pharmacology*, **58**, 1007–1019.

Ott, R.L. & Longnecker, M. (2010). *An Introduction to Statistical Methods and Data Analysis*, 6th ed. Belmont, California: Duxbury Press.

Pinelo, M., Rubilar, M., Jerez, M., Sineiro, J. & Nuñez, M.J. (2005). Effect of solvent, temperature, and solvent-to-solid ratio on the total phenolic content and antiradical activity of extracts from different components of grape pomace. *Journal of Agricultural and Food Chemistry*, **53**, 2111–2117.

Rathore, A.S. & Winkle, H. (2009). Quality by design for biopharmaceuticals. *Nature Biotechnology*, **27**, 26–34.

Saraph, J.V., Benson, P.G. & Schroeder, R.G. (1989). An instrument for measuring the critical factors of quality management. *Decision Sciences*, **20**, 810–829.

Schwartzberg, H.G. & Chao, R.Y. (1982). Solute diffusivities in leaching processes. *Food Technology*, **36**, 73–86.

Shapiro, S.S. & Wilk, M.B. (1965). An analysis of variance test for normality (complete samples). *Biometrika*, **52**, 591–611.

Shi, J., Nawaz, H., Pohorly, J., Mittal, G., Kakuda, Y. & Jiang, Y. (2005). Extraction of polyphenolics from plant material for functional foods — engineering and technology. *Food Reviews International*, **21**, 139–166.

Son, M.J., Minikawa, M., Miura, Y. & Yagasaki, K. (2013). Aspalathin improves hyperglycaemia and glucose intolerance in obese diabetic *ob/ob* mice. *European Journal of Nutrition*, **52**, 1607–1619.

Takeuchi, T.M., Pereira, C.G., Braga, M.E.M., Maróstica, M.R., Leal, P.F. & Meireles, M.A.A. (2009). Low-pressure solvent extraction (solid-liquid extraction, microwave assisted, and ultrasound assisted) from condimentary plants. In: *Extracting Bioactive Compounds for Food Products: Theory and Applications* (edited by Meireles, M.A.A.). Pp 138–211. New York, USA: Taylor & Francis Group, LLC.

Uzayisenga, R., Ayeka, P.A. & Wang, Y. (2014). Anti-diabetic potential of *Panax notoginseng* saponins (PNS): a review. *Phytotherapy Research*, **28**, 510–516.

Vuong, Q.V., Golding, J.B., Stathopoulos, C.E., Nguyen, M.H. & Roach, P.D. (2011). Optimizing conditions for the extraction of catechins from green tea using hot water. *Journal of Separation Science*, **34**, 3099–3106.

Wang, Z., Pan, Z., Ma, H. & Atungulu, G.G. (2011). Extract of phenolics from pomegranate peels. *The Open Food Science Journal*, **5**, 17–25.

Wijngaard, H., Hossain, M.B., Rai, D.K. & Brunton, N. (2012). Techniques to extract bioactive compounds from food by-products of plant origin. *Food Research International*, **46**, 505–513.

Yang, L., Cao, Y.L., Jiang, J.G., Lin, Q.S., Chen, J. & Zhu, L. (2010). Response surface optimization of ultrasound-assisted flavonoids extraction from the flower of *Citrus aurantium* L. var. amara Engl. *Journal of Separation Science*, **33**, 1349–1355.

Yao, L., Caffin, N., D'Arcy, B., Jiang, Y., Shi, J., Singanusong, R., Liu, X., Datta, N., Kakuda, Y. & Xu, Y. (2005). Seasonal variations of phenolic compounds in Australia-grown tea (*Camellia sinensis*). *Journal of Agricultural and Food Chemistry*, **53**, 6477–6483.

Zimmerman, B.F. & Gleichenhagen, M. (2011). The effect of ascorbic acid, citric acid and low pH on the extraction of green tea: how to get most out of it. *Food Chemistry*, **124**, 1543–1548.

4. Optimisation of spray-drying of green rooibos extract using quality-by-design methodology

4.1. Abstract

Spray-drying is a commonly applied technique for the production of dried plant extracts containing bioactive compounds. Green rooibos extract (GRE), optimised for high aspalathin content, could be commercialised as a nutraceutical or functional food ingredient, and spray-drying would provide the dual benefit of preserving the extract by removing moisture, as well as converting it to powdered form for ease of distribution, handling and storage. Spray-drying of rooibos extracts have not previously been optimised. Quality-by-design (QbD) methodology including risk assessment, one-factor-at-a-time (OFAT) and response surface methodology (RSM) analyses was applied to optimise the spray-drying process of aqueous GRE. OFAT analysis was carried out to established a set of basic operating parameters to be kept at fixed levels for the subsequent multivariate optimisation of the three important independent variables (inlet air temperature, feed concentration and feed flow rate) by central composite design. The process yield was the only response for which a significant regression model (R^2_{adj} = 0.88) was generated. The inlet air temperature had the most significant effect on the process yield, with higher temperatures resulting in greater yields. Verification of the polynomial regression model for the process yield confirmed its satisfactory predictive ability. Using desirability profiling, optimal levels of the independent variables for maximum powder yield were identified: inlet air temperature, 210–230 °C; feed concentration, 9–11% ($m.m^{-1}$) and feed flow rate, 0.62–0.67 $L.h^{-1}$. The optimum process parameters were applied to spray-drying feed formulations containing no carrier, maltodextrin and inulin, respectively. Validation experiments conducted according to the optimum process parameters demonstrated that yields for the powder/spray-dried extracts (SDEs) fall within the predicted range as determined by the regression model. The addition of a carrier did not result in improved yields, but improved bulk flow properties of the powder and a lesser degree of particle aggregation were observed for the inulin-containing formulation compared with the maltodextrin-containing formulation and the pure SDE. X-ray powder diffraction studies demonstrated the amorphous nature of all SDEs, produced under optimum process conditions. Their low moisture content and water activity (<2.2% and <0.13), indicate efficient drying and good potential for extended storage stability under appropriate conditions. The addition of carrier material in the SDE formulation did not affect the dry basis moisture content, but did significantly ($P < 0.05$) lower the water activity. Carrier materials like inulin or maltodextrin could thus confer additional storage stability to the SDE by reducing the amount of water available for undesirable chemical reactions or physical state changes to take place. Moisture sorption analysis confirmed that all the SDEs were moderately hygroscopic and contained surface adsorbed moisture, as evidenced by hysteresis. Storage below 25 °C and 40% relative humidity is recommended for the optimised SDEs in order to maintain optimal quality. Isothermal microcalorimetry studies demonstrated that no interactions were present between the carriers and the extract, another indication that both

inulin and maltodextrin would be suitable carriers. Inulin would be the more suitable carrier for an antidiabetic nutraceutical formulation by virtue of its lower glycaemic index, reported stimulant effect on the growth of beneficial intestinal flora, as well as its generally more favourable effects on the physicochemical characteristics (wettability and flow properties) of the SDE. These results represent another step towards the establishment of a robust manufacturing process for an aspalathin-enriched GRE.

4.2. Introduction

Plant extracts, irrespective of the process used to extract the desired constituents, must be converted into a shelf-stable product that can be utilised in various applications, e.g. as a food ingredient or a nutraceutical. Such extracts are generally available in the form of free-flowing powders with sufficiently low moisture content and water activity to promote storage stability for a long shelf-life and to facilitate easier handling of the extract (Shah & Rohit, 2005; Azmir *et al.*, 2013). The moisture content (MC) of herbal extracts may be reduced by a variety of methods of which spray-drying is one of the most widely used (Costa *et al.*, 2015). Spray-drying converts liquid plant extracts into a fine powder by rapidly removing the moisture from atomised particles in a heated gas stream, after which said particles are recovered from the gas stream and collected as a powdered, spray-dried extract (SDE) (Ré, 1998). The physicochemical attributes of the SDE may be affected by a number of process parameters, e.g. inlet air temperature, feed concentration, feed flow rate and air flow rate, which should be set at optimal levels for good process efficiency (Gharsallaoui *et al.*, 2007; Patel *et al.*, 2015). Spray-drying efficiency can be assessed in terms of a set of critical quality attributes (CQAs) as identified and defined for the particular unit operation, e.g. to achieve a minimum acceptable yield, particular powder flow properties and/or maximum retention of bioactive compounds.

Spray-drying conditions may expose labile extract constituents to high operating temperatures resulting in their thermal degradation or in unwanted physicochemical attributes of the SDE. Carrier materials or excipients are frequently added to extracts prior to spray-drying to protect desired constituents from significant degradation and also to enhance the physicochemical properties of the powdered extract (Sollohub & Cal, 2010; Woo & Bhandari, 2013). Maltodextrins of various dextrose equivalents are frequently used as carrier materials in the spray-drying of plant extracts due to their widespread availability, low cost, versatility and food-safe status (Costa *et al.*, 2015). Since maltodextrin is metabolised as glucose by the human gastrointestinal system, its glycaemic index (GI) of 100 might prevent it from being applicable in a nutraceutical preparation with proposed antidiabetic applications (Englyst *et al.*, 1996). Gross *et al.* (2004) linked increasing intakes of refined carbohydrate (corn syrup) concomitant with decreasing intakes of fiber to the upward trend in the prevalence of type 2 diabetes mellitus. Inulin, a polysaccharide derived from the chicory

root, has also been successfully used as an excipient in spray-drying of plant extracts (Saénz *et al.*, 2009; Bakowska-Barczak & Kolodziejczyk, 2011; Hashemiravan *et al.*, 2013). Its lower caloric content of 6.3 $kJ.g^{-1}$ (vs. 16.4 $kJ.g^{-1}$ for glucose) and its negligible effect on blood glucose concentration could make it a feasible alternative carrier for a case such as the present, in which the promotion of normoglycaemia is a desired target product attribute (Gargari *et al.*, 2013; Mensink *et al.*, 2015a; 2015b). Additionally, inulin is considered a prebiotic and natural dietary fibre which stimulates the growth of beneficial intestinal flora (Kolida *et al.*, 2002). The increased consumption of non-digestable dietary fiber, like inulin, has been linked to a lower risk for cardiovascular and metabolic diseases, lower body mass index and improved gastrointestinal health (Slavin, 2013).

To date, no research has been published on the optimisation of spray-drying of rooibos extracts. The main objectives of the present study were to optimise and validate the spray-drying conditions for aqueous green rooibos extract (GRE). Carriers investigated were maltodextrin and inulin. Quality-by-design (QbD) principles used for extract optimisation were again applied to the spray-drying unit operation to maintain the concept downstream in the production process of powdered extract. This included a preliminary risk assessment step, followed by application of response surface methodology (RSM) in a "design of experiment" approach and finally the definition of a control space. Physicochemical analyses of the SDEs carried out, included compatibility testing of the encapsulating/carrier agents with the extract and determination of colour, moisture sorption isotherms, solid-state phase and flow characteristics of the powders. Stability of the extract during spray-drying was assessed in term of the retention of the major green rooibos (GR) flavonoid, aspalathin. Optimal spray-drying process parameters, intended to maximise the process yield, whilst maintaining an acceptable quality standard, were identified and a control space for production of spray-dried GRE was defined.

4.3. Materials and methods

4.3.1. Chemicals and reagents

All chemicals and reagents, used in the spray-drying experiments and subsequent analyses of the SDEs, are identical to those described in the previous chapter (section 3.3.1.).

4.3.2. Preparation of freeze-dried extract for spray-drying feed formulations

Commercial GR (≈ 4.5 kg) was sampled from a large sample set (n = 47) of production batches (1.5 kg per batch), obtained from Rooibos Ltd. (Clanwilliam, South Africa; harvested and processed between 27 Jan and 16 March 2015). A large volume (≈30 L) of aqueous GRE was prepared by extracting the plant material using deionised water at 93 °C for 30 min at a 10:1 ($v.m^{-1}$) water-to-

plant material ratio according the "optimum" conditions previously determined (Chapter 3). Briefly, extraction was carried out in separate closed glass vessels (150 g plant material per vessel) with manual agitation carried out every 5 min for 5 s. The extract was filtered warm through Whatman No 4 filter paper (GE Life Sciences, Buckinghamshire, United Kingdom) using a Büchner filter with Vacuubrand ME2C vacuum pump (Vacuubrand GmbH & Co. KG, Wertheim, Germany). The recovered filtrates were pooled, mixed thoroughly and freeze-dried in stainless steel trays, using a VirTis Genesis 35ES Lyophiliser (S.P. Scientific, Warminster, PA, USA). The freeze-dried extract (FDE) was collected, thoroughly blended and sealed in glass jars. These were stored in a plastic container containing silica gel beads as drying agent, until reconstitution with deionised water for spray-drying.

4.3.3. Carriers

Orafti HP (high-performance) inulin with a 21–26 degree of polymerisation (DP), extracted from chicory root (*Cichorium intybus* var. *sativum*), was obtained from Savannah Fine Chemicals (Pty) Ltd (Gardenview, South Africa). Maltodextrin with a dextrose equivalent (DE) of 9, derived from maize starch, was kindly provided by Tongaat Hulett Starch (Germiston, Gauteng, South Africa) and sourced from the Qinhuanglao Lihau Starch Co., Ltd (Qinhuanglao, Hebei, China). Inulin was used as the carrier material in all preliminary experiments and in the 16 experimental runs of the central composite design. Two formulations containing maltodextrin and inulin, respectively, were both compared with a pure SDE (i.e. no carrier) in validation experiments performed at the optimised spray-drying process parameters.

4.3.4. Spray-drying

Spray-drying was carried out using a Büchi B-290 Mini spray-dryer (Büchi Labortechnik AG, Flawil, Switzerland) (Fig. 4.1). Pressurised and dehumidified air, generated using a Haug SO45-E2-ASY oil-free air compressor (Haug Kompressoren AG, St. Gallen, Switzerland) and a Büchi B-296 dehumidifier, was used as drying medium. The dehumidifier standardises the drying air by removing moisture with a <5 °C cold trap, thus providing reproducible results in spite of variations in ambient humidity (Büchi, 2009). The powdered SDE was recovered in a glass vessel after separation from the drying air by a cyclone separator system. At the end of each experimental run, once the total volume of the extract feed preparation had been converted to powder, heating of the inlet air was terminated and the system was allowed to run until the inlet temperature had fallen below 80 °C, at which point the system was shut off and the SDE recovered from the collection vessel. The mean outlet temperature of each spray-drying run was continuously measured by the in-line temperature

probe of the spray-dryer situated between the spray-cylinder outlet and the cyclone system inlet (between point 4 and 5 on Fig. 4.1). The outlet air temperature (T_{OA}) of each experimental run was recorded after the spraying process had been running for at least 5 min to ensure that it had stabilised, and the value was expressed as the mean of three measurements taken 5 min apart.

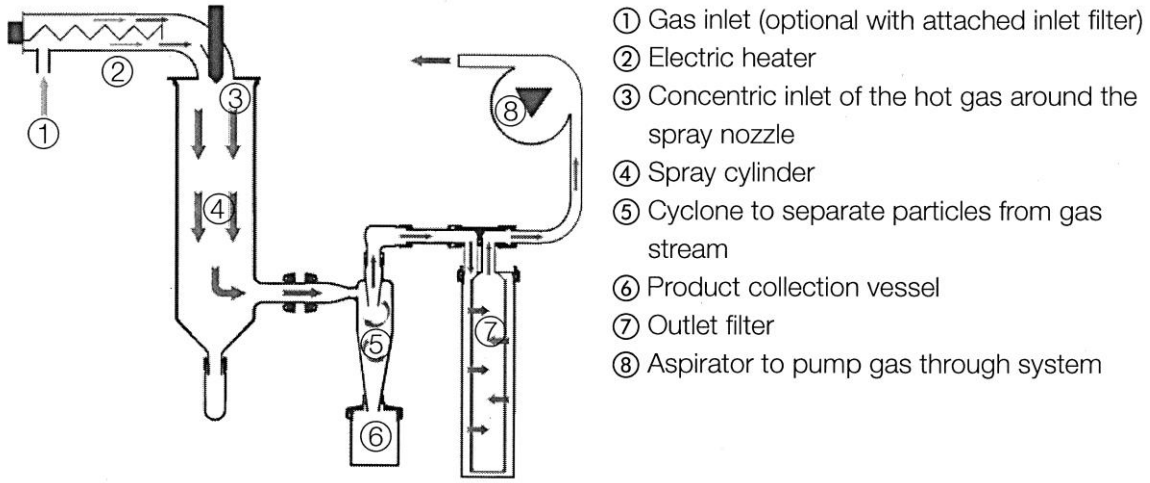

Figure 4.1 Functional principles and components of spray-drying system (Büchi, 2009).

4.3.4.1. Spray-drying yield determination

The mass of recovered SDE was recorded to the nearest three decimals after each spray-drying run using a Sartorius L420P balance (Sartorius AG, Göttingen, Germany). The process yield was then calculated by using the following equation:

$$\%Yield = \frac{m_{SDE}}{m_{SFP}} \times 100$$

where m_{SDE} represents the mass of SDE recovered and m_{SFP} represents the mass of solids in the feed preparation. The mass of the product ("as-is", i.e. not recalculated to dry basis) was used to express yield except when noted otherwise.

4.3.4.2. Gravimetric determination of total solids content of spray-drying feed preparation

The total solids content of all spray-drying feed preparations was determined (in duplicate) by gravimetric analysis. An unfiltered aliquot (10 mL) of feed preparation was transferred to a pre-weighed nickel moisture dish placed on a Merck Model 402 steam-bath (MSD Pty., Ltd, Midrand, South Africa) and evaporated until visibly dry. Final drying occurred in a forced-air laboratory drying oven set at 100 °C for 60 min. The samples were cooled under desiccation, re-weighed and the resulting difference in mass expressed as the total solids content ($m.v^{-1}$).

4.3.4.3. Preliminary risk assessment for spray-drying unit operation

Prior to conducting any experiments on the effect of process input factors on the spray-drying efficiency, a risk assessment step was carried out to identify the various factors which should be taken into consideration in a spray-drying optimisation study. An Ishikawa diagram was constructed to group together process parameters and material attributes most likely to have a significant effect on the spray-drying process efficiency (Saraph *et al.*, 1989). The process efficiency in this case refers to the capacity of the process to produce a maximum yield of powdered extract with sufficiently low moisture content and retention of target compounds. Previous practical experience with spray-drying of fermented rooibos extracts (Joubert, 1988; Joubert *et al.*, 2009) and examples drawn from literature (Ré, 1998; Baldinger *et al.*, 2012; Costa *et al.*, 2015) were considered in the selection of suitable input factors for further investigation.

4.3.4.4. One-factor-at-a-time (OFAT) experiments

The high number of potential independent variables of spray-drying system required that a series of six preliminary experiments (Table 4.1) be carried out to determine the basic operational settings (aspirator performance, air flow rate, inlet air dehumidification and nozzle cleaning frequency) to be used prior to multivariate optimisation of the spray-drying process according to central composite experimental design. In these preliminary experiments, parameters were evaluated one-factor-at-a-time (OFAT) while the remaining parameters were kept at a fixed level. The process yields and the moisture content of the recovered SDEs were determined and taken into consideration for the selection of the basic operating parameters.

Table 4.1 Operating parameters for six preliminary OFAT spray-drying experiments[1] using Büchi B-290 Mini spray-dryer.

Parameter	Preliminary experiment					
	1	**2**	**3**	**4**	**5**	**6**
Feed concentration (%)[2]	10	10	10	20	30	20
Air flow rotameter (mm)	45	45	60	60	60	60
Feed flow rate (% PPP)[3]	30	30	30	30	30	20
Dehumidification of drying air	On	Off	On	On	On	On

[1] Fixed parameters: 100% aspirator performance, 4 nozzle cleaning pulses per min, 1:1 inulin to extract ratio ($m.m^{-1}$), inlet air temperature = 200 °C; [2] g total solids per 100 g H_2O; [3] PPP = peristaltic pump performance

4.3.4.5. Optimisation of spray-drying by response surface methodology

A central composite design (CCD) consisting of 16 experimental runs was used to optimise the spray-drying process in terms of three operating parameters. The independent variables under investigation were inlet air temperature (T_{IA}; °C), feed concentration (FC, %; $m.m^{-1}$) and feed flow rate (FFR; % peristaltic pump performance, PPP). PPP refers to a setting on the control panel of the Büchi Mini B-290 spray-dryer, and represents the rate at which the feed preparation is pumped into the drying chamber (expressed as a percentage of the maximum peristaltic pump performance). The percentage value can be roughly converted to a volumetric flow rate by means of technical data provided by the manufacturer (Fig. 4.2). Since the device control panel requires that the FFR be specified in terms of % PPP, this measure was used instead of a volumetric flow rate. The final, optimised level for the FFR can then be converted to an estimated volumetric flow rate using the linear plot.

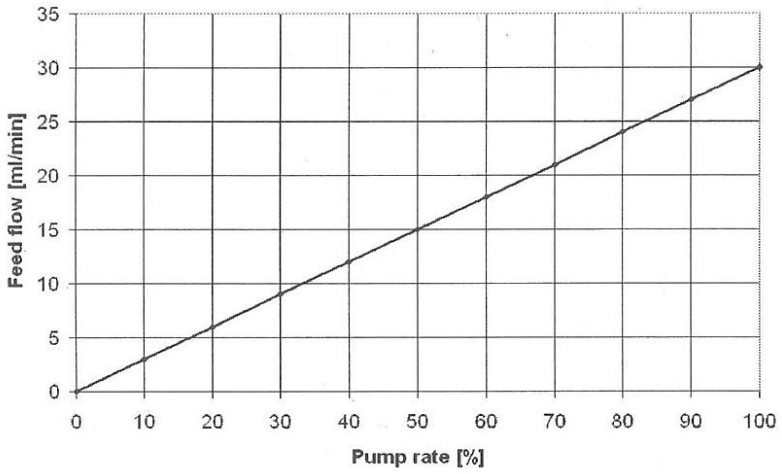

Figure 4.2 Plot showing relationship between pump rate (% peristaltic pump performance) and volumetric feed flow rate for Büchi B-290 Mini spray-dryer using standard silicone tube (2 mm ID, 4 mm OD) and water (Büchi, 2009).

The ranges of treatment levels for the independent variables (Table 4.2) in the CCD were chosen based on the results of the preliminary experiments. The 16 experimental runs of the CCD were performed in a completely randomised order. Statistical analysis was applied to the data in order to establish optimal spray-drying process parameters. The optimal process parameters were validated by spray-drying three different formulations of the feed preparation, viz. pure extract (no carrier), extract with inulin (1:1; $m.m^{-1}$) and extract with maltodextrin (1:1; $m.m^{-1}$).

Table 4.2 Three independent variables and their coded levels used in central composite design for optimisation of spray-drying of green rooibos extract.

Independent variable	Symbol	Levels				
		-α (-1.68)	-1	0	+1	+α (1.68)
Inlet air temperature (°C)	X_1	150	164	185	206	220
Feed concentration (%; m.m^{-1})	X_2	5	10	17.5	25	35
Feed flow rate (% PPP)[1]	X_3	15	19	25	31	35

[1] PPP = peristaltic pump performance

Table 4.3 Layout of central composite design for spray-drying optimisation.

Standard run[1]	Independent variable		
	Inlet air temperature (°C)	Feed concentration (%; m.m^{-1})[2]	Feed flow rate (% PPP)[3]
1(F)	164	10.0	19
2(F)	164	10.0	31
3(F)	164	25.0	19
4(F)	164	25.0	31
5(F)	206	10.0	19
6(F)	206	10.0	31
7(F)	206	25.0	19
8(F)	206	25.0	31
9(A)	150	17.5	25
10(A)	220	17.5	25
11(A)	185	5.0	25
12(A)	185	30.0	25
13(A)	185	17.5	15
14(A)	185	17.5	35
15(C)	185	17.5	25
16(C)	185	17.5	25

[1] (F) = factorial design point, (A) = axial point, (C) = center point; [2] g total solids per 100 g H_2O; [3] PPP = peristaltic pump performance

4.3.5. Physicochemical analyses of spray-dried extracts

4.3.5.1. High-performance liquid chromatography

Reverse-phase high performance liquid chromatography with diode array detection (RP-HPLC-DAD) was performed to quantify the four major rooibos flavonoids in the spray-drying feed preparations and in the SDEs, using the rapid screening method (16 min) of De Beer *et al.* (2015) and equipment as described in Chapter 3. For analysis of each SDE, approximately 4.5 mg powder was weighed off using a Precisa 262SMA-FR 5-decimal balance (Precisa Gravimetrics AG, Dietikon, Switzerland) and dissolved in 1000 µL of deionised water. The spray-drying feed preparations were diluted to approximately 3.5 $mg.mL^{-1}$ using deionised water. Hundred µL of 10% ascorbic acid was subsequently added to each diluted working solution to prevent degradation of the target compounds during analysis. The results were expressed as a percentage of the SDE (dry basis) or the total solids content of the feed preparations (g per 100 g = %; $m.m^{-1}$). An injection volume of 5 µL (in duplicate) was used for all HPLC analyses.

4.3.5.2. Retention of target compound

The retention of the main target compound of interest, aspalathin, following spray-drying, was determined by using the following equation:

$$Aspalathin\ retention\ (\%) = \frac{[Asp]_{SDE}}{[Asp]_{FS}} \times 100$$

where $[Asp]_{SDE}$ refers to the concentration of aspalathin in the spray-dried extract and $[Asp]_{FS}$ refers to the concentration of aspalathin in the feed preparation, both expressed as $g.100\ g^{-1}$ solids (dry basis). A value of 100 represents complete retention of the target compound with no quantifiable degradation having been caused by the spray-drying process.

4.3.5.3. Water activity and moisture content

The water activity (a_w) of the SDEs was determined using a LabMASTER-Aw electric hygrometer (Novasina AG, Lachen, Switzerland), calibrated using a 11% saline standard according to the manufacturer's instructions. The MC of the SDEs was determined gravimetrically using an HR73 Halogen Moisture Analyser (Mettler-Toledo, Greifensee, Switzerland). Approximately 2 g of the sample was placed on an aluminium dish and desiccated for 60 min at 100 °C. The MC was automatically calculated as a percentage of the total mass of the sample (wet basis), and was then manually converted to percentage dry basis using the equation:

$$MC_{db} = \frac{MC_{wb}}{(100 - MC_{wb})} \times 100$$

where MC_{db} is the percentage moisture content (dry basis) and MC_{wb} is the percentage moisture content (wet basis).

4.3.5.4. Objective colour measurement

The colour attributes of the optimised SDEs were described in terms of the CIE$L^*a^*b^*$ colour space and measured in reflectance mode, using a CM-5 spectrophotometer (Konica Minolta, Inc., Tokyo, Japan) and a 152 mm integrating sphere. Auto-calibration of the equipment was conducted using a built-in standard white calibration plate. Manual zero calibration was carried out using a zero calibration box (black inverted cone cylinder) before taking measurements. Conditions were standardised on Illuminant D65 and diffuse illumination using 8° and 10° viewing and observer angles, respectively, and a measurement area of 30 mm diameter. The SDE sample was illuminated through the base of an optical glass tube cell cup (CR-A502, 40 mm depth, 60 mm diameter, Konica Minolta) during analysis. All colour measurements were carried out in triplicate. This entailed the use of a clean cuvette for each replication and thorough mixing of the sample between measurements. Chroma (C^*) and hue (h) values were automatically calculated by the SpectraMagic NX Procolour data software (Konica Minolta, Inc.). The difference in colour (ΔE) between the control and treatment samples was calculated using the following equation:

$$\Delta E = \sqrt{\Delta a^{*2} + \Delta b^{*2} + \Delta L^{*2}}$$

4.3.5.5. Isothermal microcalorimetry

A 2277 Thermal Activity Monitor (TAMIII) (TA Instruments, New Castle, Delaware, USA) equipped with an oil bath (stability of ±100 µK over 24 h) was used to analyse the three different SDEs produced at the optimised spray-drying conditions. The temperature of the calorimeter was maintained at 30 °C. Heat flow was measured for the single components (inulin, maltodextrin and extract), as well as for the combinations of extract and carrier. The calorimetric outputs observed for individual components are summed to give a theoretical response. This calculated theoretical response represents a calorimetric output that would be expected if the components comprising the mixture do not interact with each other. If the components do interact, the measured calorimetric

response will differ from the calculated theoretical response. Heat flow measurements were expressed in terms of μW per g of sample.

4.3.5.6. Thermal analyses

A Shimadzu (Shimadzu Corporation, Kyoto, Japan) DSC-60 instrument was used to produce thermograms of the SDEs produced using the optimised spray-drying parameters. Approximately 3–5 mg of each sample was accurately weighed and sealed in an aluminium crimp cell. A heating program of 25–250 °C with a heating rate of 10 °C.min^{-1} and nitrogen gas purge of 35 mL.min^{-1}. A Shimadzu DTG-60 instrument (Shimadzu Corporation, Kyoto, Japan) was used to record differential thermal analysis (DTA) and thermogravimetric analysis (TGA) simultaneously. DTA measures the heat flux (μV) of the powders during heating and is suited for the determination of characteristic phase transition temperatures, while TGA measures mass loss (mg) during a fixed period of heating. Samples (3–5 mg) were accurately weighed in open aluminium cells and then heated from 25–300 °C at a heating rate of 10 °C.min^{-1} under nitrogen gas purge of 35 mL.min^{-1}. The three SDEs, produced at the optimised spray-drying conditions, were compared to pure inulin and maltodextrin samples. The onset, midpoint and end temperatures of all relevant thermal events are reported.

4.3.5.7. Moisture sorption isotherms

Moisture sorption analyses of the three SDEs were performed utilising a VTI-SA moisture sorption analyser (TA Instruments, New Castle, DE, USA). The microbalance was calibrated prior to each moisture sorption run using a 100 mg standard weight. The microbalance was set to zero prior to weighing of the sample into the quartz sample container. The sample was carefully placed into the sample holder and care was taken to evenly distribute the sample. The percentage relative humidity (% RH) was set using TA Instruments Isotherm software. The % RH ramp was initially set from 5 to 95% RH, followed by a decrease from 95 to 5% RH, but deliquescence of all samples at ≈60% RH precluded testing over the entire range. The last absorption phase was set to also ramp from 5 to 95% RH. The temperature was set at a constant 25 °C throughout the % RH ramp phase. The program criteria were set to 0.0001% weight change or 2-min stability of weight gained or lost before the program would continue to the next set parameter. The experimental data were fitted to the Brunauer, Emmett and Teller (BET) sorption isotherm by using the following equation:

$$\frac{MC_{db}}{M_{0B}} = \frac{C_B a_w}{(1-a_w)(1-a_w+C_B a_w)}$$

where MC_{db} is the moisture content (dry basis) in g.100 g^{-1} solids at a_w (a_w = equilibrium RH (%)/100), M_{0B} is the BET monolayer moisture content value expressed in the same units, and C_B is the BET surface heat constant. The experimental data were also fitted to the Guggenheim, Anderson & De Boer (GAB) equation:

$$\frac{MC_{db}}{M_{0G}} = \frac{C_G K a_w}{(1 - K a_w)(1 - K a_w + C_G K a_w)}$$

where M_{0G} is the GAB monolayer moisture content value, K is a constant related to the GAB equation and C_G is the GAB surface heat constant. GAB and BET parameters were calculated according to methodology previously described by Blahovec & Yanniotis (2008).

4.3.5.8. X-ray powder diffraction

X-ray powder diffraction (XRPD) measurements were performed to confirm the crystalline or amorphous nature of the optimised spray-dried samples. A PANalytical (Almelo, Netherlands) Empyrean X-ray diffractometer with a PIXcel3D detector was used to record XRPD patterns at 25 °C. Samples were evenly distributed on a zero background sample holder. The measurement parameters for all the scans were set as follows: target, Cu; voltage, 40 kV; current, 40 mA; divergence slit, 2 mm; anti-scatter slit, 0.6 mm; detector slit, 0.2 mm; scanning speed, 2° min^{-1} (step size, 0.02°; step time, 1.0 s).

4.3.5.9. Wettability (Contact angle measurement)

Contact angle measurements were carried out using a Krüss DSA100 (A. Krüss Optronic GmbH, Hamburg, Germany) drop analyser. The static sessile drop method was used and the solvent was deionised water. Samples were prepared by lightly pressing the powders between two glass slides in order to obtain a uniform and level powder bed. A single drop of water was deposited on the powder bed and an image was captured by video. The first frame to feature a well-defined vibration-free drop was analysed to determine the contact angle. The Krüss DSA4 software was used to analyse the shape and angle of the deposited water drop. The contact angle was measured in triplicate for each sample. The contact angle is measured through the liquid phase and is inversely proportional to the degree of wettability (Yuan & Lee, 2013).

4.3.5.10. Determination of powder bulk properties

The poured bulk density (ρ_B) of the three SDEs was calculated as the ratio between the sample mass and its volume occupied after gently pouring ca. 20 g of powder into a 100 mL graduated measuring cylinder. Their tapped bulk density (ρ_T) was determined in the same way after tapping the cylinder until no measurable change in the volume was noticed (ca. 100 times). All measurements were conducted in triplicate. These values were used to calculate the Hausner ratio (HR) and Carr's compressibility index (CCI) (Carr, 1965; Fitzpatrick, 2013) according to the following formulae:

$$HR = \frac{\rho_T}{\rho_B}$$

$$CCI = 100(1 - \frac{\rho_B}{\rho_T})$$

4.3.5.11. Scanning electron microscopy

Images of the three SDEs were obtained using a Zeiss MERLIN field emission scanning electron microscope and Zeiss SmartSEM software (Carl Zeiss AG, Oberkochen, Germany). The samples were mounted on a small stub using carbon tape and then sputter coated with a thin (10 nm) layer of gold, using an Edwards S150A Gold Sputter Coater (Edwards, Crawley, England) to make the sample conductive prior to imaging. Secondary electron images of the sample were captured using a Zeiss inlens (SE1 – Secondary Electron type 1) detector. The beam conditions during the image analysis were: 5 kV acceleration voltage (extra-high tension target), 250 pA beam current (I-Probe), 3–5.5 mm working distance, and a high resolution column configuration (Column mode).

4.3.6. Statistical analysis

Univariate analysis of variance (ANOVA) was carried out on all single factor experiment data using SAS® software (Version 9.2, SAS Institute Inc., Cary, NC, USA) to determine whether differences between treatment means were significant. Least significant difference (LSD) of the Student's t-test ($P = 0.05$) was calculated to compare treatment means where significant differences were found ($P < 0.05$) (Ott & Longnecker, 2010). Levene's test was used to test for treatment homogeneity of variance. In instances where variances were not equal a weighted analysis of variance was used for the combined analyses. The Shapiro-Wilk test was performed on the standardised residuals from the models to assess for normal distribution of the data (Shapiro & Wilk, 1965). Statistica 12.0 (Statsoft® Southern Africa, Sandton, South Africa) was used to analyse all data generated by response surface methodology. The statistical significance and suitability of the regression model, its factors and their interactions were determined at the 5% probability level ($P < 0.05$) using analysis of

variance (ANOVA). Standardised Pareto charts were used to illustrate the significant effects obtained for the different response values by ANOVA. The fitting efficiency of the data to the model was evaluated by calculating the correlation coefficient (R^2), the adjusted correlation coefficient (R^2_{adj}) and the significance of lack-of-fit (LOF). The regression equation that was generated for each response was illustrated as two-dimensional contour plots and three-dimensional response surface plots. Optimal levels of the independent variables were identified by applying desirability profiling. The intra-class correlation coefficient (ICC) and Bland-Altman plots were used to assess the predictive ability of the model.

4.4. Results and discussion

4.4.1. Risk assessment for spray-drying unit operation

A risk analysis was performed to determine which process parameters and/or material attributes would most likely have a significant effect on the efficiency of the spray-drying process (Fig. 4.3). An Ishikawa ("fishbone") diagram, adapted from Baldinger *et al.* (2012), was used to identify three major categories of input factors: spray-dryer (equipment-related), feed material and spray-drying air/gas.

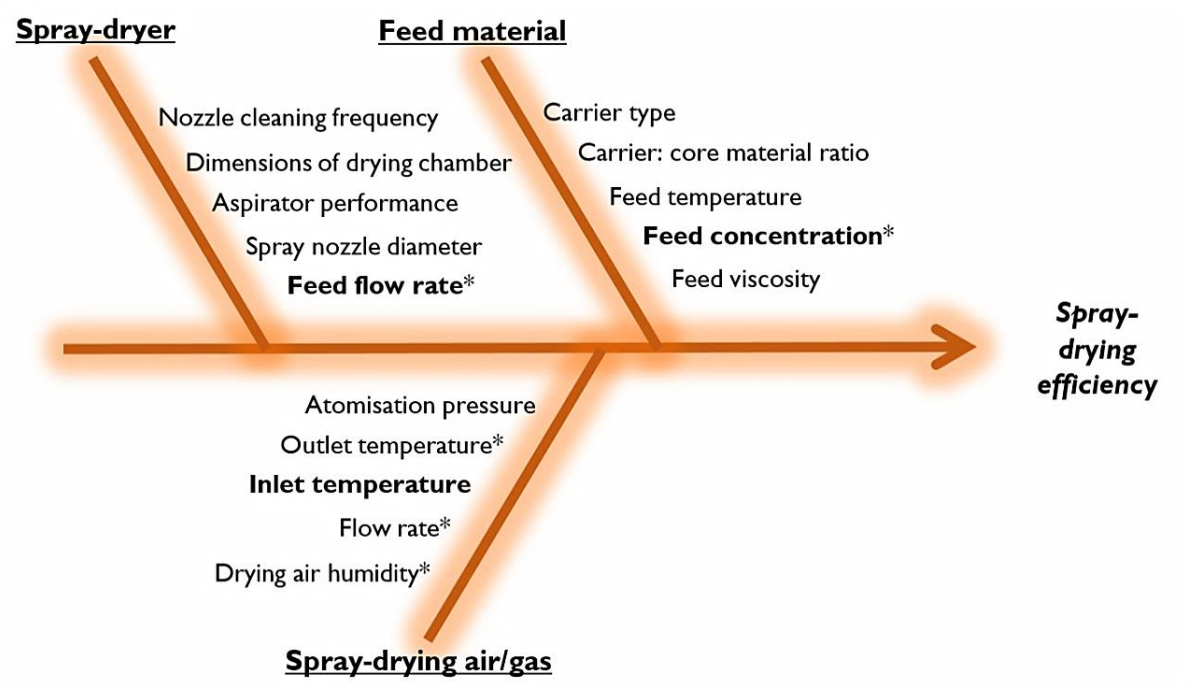

Figure 4.3 Ishikawa diagram for identification of critical process parameters and /or material attributes in a spray-drying process. Asterisks indicate parameters investigated in preliminary experiments performed for spray-drying of an aqueous green rooibos extract. Parameters in bold script were included in the central composite design for process optimisation (adapted from Baldinger et al., 2012).

The spray-dryer used in the present study features a number of possible settings which are directly controllable, e.g. nozzle cleaning frequency, aspirator performance, FFR and T_{IA}. Some of the other factors, like the drying chamber dimensions and spray nozzle diameter, are dependent on the type of equipment being used and would not be appropriate for inclusion in an experimental design for process optimisation. The standard spray nozzle included with the equipment (tip diameter = 0.7 mm) was used in all experiments. The spray-dryer also features a nozzle cleaning system which utilises compressed air to force a thin probe through the nozzle aperture at a rate specified by the operator (0–10 pulses per min). While nozzle cleaning is necessary to prevent clogging of the spray nozzle, each intermittent pulse of compressed air will momentarily interrupt the stream of drying air and, therefore, the atomisation process. The efficiency of the process could be adversely affected, especially if an excessively high rate of nozzle cleaning frequency is selected. The nozzle cleaning frequency was set at four pulses.min^{-1} for all spray-drying experiments and was therefore not considered for further investigation. The "performance" of the aspirator pump at the distal end of the system, expressed as a percentage of its maximum air flow rate (approximately 35 m^3.h^{-1}), is also under direct control of the operator. For the purposes of this study, the aspirator performance was set at 100% throughout, as per the manufacturer's recommendations for optimal performance (Büchi, 2009).

It was decided that a comparison between carrier materials would be made once the optimised spray-drying parameters had been established, and the effects of using different carrier materials were, therefore, not investigated in the preliminary phase or as variable in the CCD. Inulin was consequently used as the carrier material in all the preliminary experiments and in the 16 experimental runs of the CCD. The mass ratio of inulin to GRE was fixed at 1:1 for all experiments, and not selected for further investigation. The feed preparations were maintained at ambient temperature (≈23 °C) and stirred continuously with a magnetic stirrer to prevent any settling and to maintain homogeneity. The concentration of solids in the feed preparation could have a major impact on the process efficiency (Cal & Sollohub, 2010; Costa *et al.*, 2015), and was selected for further investigation in the preliminary experiments.

The effect of the atomisation air pressure, automatically maintained at a level of ≈6 kPa by the air compressor system, was not investigated and was kept at this fixed level. The T_{OA} cannot be considered as a true process input factor, since its value is a function of a number of other parameters, e.g. T_{IA}, air flow rate and aspirator performance. It should rather be considered a process output or response. The T_{OA} represents the highest temperature to which the spray-dried particles are exposed before being recovered by the cyclone separator system, and could be a useful indicator of process efficiency (Ameri & Maa, 2006; Büchi, 2009). The T_{IA} is consistently cited as one of the most important factors affecting spray-drying process efficiency (Ré, 1998; Gharsallaoui *et*

al., 2007; Cal & Sollohub, 2010), and was therefore selected for inclusion as variable in the CCD without conducting any preliminary investigations regarding its effects.

Excessive humidity of the drying air could affect the quality of the final product by imparting higher MC to the SDE (Patel *et al.*, 2015). The Büchi B-290 spray-dryer features an optional dehumidifying attachment (Model B-296), the use of which was investigated in the preliminary experiments. The flow rate of the drying air can be directly controlled by the operator by means of an adjustable rotameter, and the effect of using two different air flow rates was also selected for investigation in the preliminary experiments.

4.4.2. Preliminary experiments

The results of the preliminary experiments (PEs), conducted prior to the optimisation of the spray-drying process, are shown in Table 4.4. The MC of all the recovered SDEs were <5%, indicating efficient drying irrespective of the particular operating parameters. PE1 and PE2 investigated the effect of connecting the dehumidifier unit to the system. The MC_{db} of the SDE was higher when the dehumidifier was disconnected (3.50% vs. 1.79%), indicating that dehumidification of the drying air would enhance the process efficiency. The dehumidifier was therefore used for all subsequent experiments.

Direct comparison of PE1 and PE3 indicated that a higher air flow rate was associated with a higher yield even when the difference in the MC_{db} of the powder was taken into account. The mean T_{OA} was lower when the air flow rotameter was set at 60 mm as opposed to 45 mm (94 vs. 115.5 °C). This can be explained by the higher rate of atomisation and energy consumption associated with a higher air flow rate (Woo & Bhandari, 2013). The higher mean T_{OA} measured for PE1 could also explain the lower yield at these conditions, since the particles would be more prone to stickiness when exposed to a higher temperature at the drying chamber outlet, resulting in decreased recovery of product in the collection vessel (Ameri & Maa, 2006; Costa *et al.*, 2015). Therefore, the highest possible rotameter setting for the air flow rate was selected for all subsequent experiments. The rotameter setting of 60 mm corresponds to an actual air flow rate of approximately 1744 $L.h^{-1}$, derived from conversion tables provided by the manufacturer (Büchi, 2009).

Direct comparison of PE3, PE4 and PE5 indicated that the use of different FCs (10, 20 and 30%, respectively) had a noticeable effect on the MC_{db} of the SDE, with a higher FC having resulted in powder with a lower MC_{db}. This can be explained by the lower solvent-to-solids ratio of the feed preparation fed into the system per time unit, thus allowing for more efficient dehydration. Direct comparison of PE4 and PE6 showed that a lower FFR (20 vs. 30 % PPP) did not have a substantial effect on the MC_{db} of the SDE, but that it did result in a higher mean T_{OA} (104°C vs. 93.5 °C). This

is an indication of increased energy consumption required for drying as a greater volume of feed preparation delivered to the system per time unit. Based on the results of the risk assessment and preliminary investigations, three factors were selected for inclusion in the optimisation study, viz. T_{IA}, FC and FFR.

The basic operating parameters used in PE6 was selected for all subsequent spray-drying experiments in the optimisation study, i.e. 100% aspirator performance; dehumidifier connected; 1:1 carrier-to-extract ratio ($m.m^{-1}$); air flow rotameter setting of 60 mm and four nozzle cleaning pulses per min.

Table 4.4 Results of preliminary spray-drying experiments.

Parameter	Preliminary experiment					
	1	**2**	**3**	**4**	**5**	**6**
Aspirator (%)	100	100	100	100	100	100
Inlet air temperature (T_{IA}; °C)	200	200	200	200	200	200
Feed concentration (FC; %)[1]	10	10	10	20	30	20
Carrier: extract ($m.m^{-1}$)	1:1	1:1	1:1	1:1	1:1	1:1
Air flow rotameter (mm)	45	45	60	60	60	60
Feed flow rate (FFF; % PPP)[2]	30	30	30	30	30	20
Nozzle cleaner (pulses per min)	4	4	4	4	4	4
Dehumidification of drying air	On	Off	On	On	On	On
Mean outlet air temperature (T_{OA}; °C)	115.5	97	94	93.5	94	104
Moisture content (dry basis) (%)	1.79	3.50	4.32	2.75	1.97	2.23
Yield (%)[3]	72.10	70.05	79.80	82.40	82.55	80.86
Yield (dry basis) (%)[3]	70.81	67.60	76.35	80.34	80.92	78.98

[1] g solids/100 g H_2O; [2] PPP = peristaltic pump performance; [3] g SDE recovered per 100 g solids in feed preparation

4.4.3. Optimisation of spray-drying by response surface methodology

4.4.3.1. Analysis of experimental data

The results of the process optimisation experiments, conducted according to a CCD, are shown in Table 4.5. The process yield, i.e. the percentage of total solids in the feed preparation recovered as SDE, was considered as one of the major critical process attributes for this unit operation as it would directly affect the economic feasibility of a scaled-up spray-drying process (Ameri & Maa, 2006). MC and a_w of the SDEs were also major indicators of process efficiency, since the fundamental principle behind the process is to reduce the MC (and therefore the a_w) to acceptable levels for optimal quality and stability (Ré, 1998). The process efficiency also extends to the retention of aspalathin in the SDE. Aspalathin retention values were expressed as the aspalathin content of the SDE as a percentage of the aspalathin content in the corresponding solids in the feed preparation. Not only is retention of aspalathin important in terms of its bioactivity, but it is one of

the most thermo-labile constituents of rooibos extract (Joubert *et al.*, 2010) and therefore a good indicator of extract stability under processing conditions. The mean T_{OA} was investigated as a response, since its value is dependent on the interaction between other independent variables and cannot be directly controlled by the operator.

Table 4.5 Central composite design for spray-drying optimisation.

	Independent variables			Responses					
Standard run[1]	X_1 **T_{IA} (°C)**[2]	X_2 **FC (%)**[3]	X_3 **FFR (%PPP)**[4]	**Yield (%)**[5]	**Yield$_{(db)}$ (%)**[6]	**MC$_{db}$ (%)**[7]	**a_w**[8]	**Asp ret (%)**[9]	**T_{OA} (°C)**
1(F)	164	10.0	19	72.852	70.537	3.178	0.124	95.1	82.5
2(F)	164	10.0	31	69.933	67.374	3.659	0.147	92.2	70.0
3(F)	164	25.0	19	69.351	67.755	2.302	0.127	97.5	99.5
4(F)	164	25.0	31	55.624	54.338	2.312	0.124	91.7	90.5
5(F)	206	10.0	19	76.376	75.126	1.636	0.123	96.4	102.5
6(F)	206	10.0	31	75.160	73.177	2.638	0.116	93.0	100.5
7(F)	206	25.0	19	74.378	72.427	2.623	0.132	92.9	118.0
8(F)	206	25.0	31	73.865	71.815	2.775	0.169	94.7	117.0
9(A)	150	17.5	25	59.978	58.014	3.274	0.150	94.2	76.0
10(A)	220	17.5	25	77.565	76.143	1.833	0.100	93.3	112.5
11(A)	185	5.0	25	76.107	73.802	3.029	0.145	90.1	85.0
12(A)	185	30.0	25	66.700	65.519	1.771	0.117	98.6	103.5
13(A)	185	17.5	15	76.031	74.653	1.812	0.124	97.2	98.0
14(A)	185	17.5	35	65.983	64.416	2.375	0.144	97.6	93.0
15(C)	185	17.5	25	72.187	70.925	1.748	0.120	94.7	105.5
16(C)	185	17.5	25	73.276	71.583	2.310	0.114	89.8	101.0

[1] (F) = factorial design point; (A) = axial point; (C) = center point; [2] Inlet air temperature; [3] FC, feed concentration, g solids per 100 g H_2O; [4] FFR, feed flow rate, PPP, peristaltic pump performance; [5] g powder recovered per 100 g total solids in feed preparation; [6] Yield calculated on dry basis; [7] moisture content (dry basis); [8] Water activity; [9] Aspalathin retention = g aspalathin.100 g^{-1} powder(dry basis) ÷ g aspalathin in 100 g feed preparation; [10] Outlet air temperature.

Regression analysis and ANOVA were carried out to determine the suitability of the generated prediction models for the responses under investigation. Standardised Pareto charts were generated for all dependent variables under investigation, but the only statistically significant effects observed were for the powder yield (Fig. 4.4). A significant, positive effect ($P < 0.05$) was observed for the linear effect of T_{IA}, whereas the linear effects of FC and FFR were similar in their negative values, but with only the former showing borderline statistical significance ($P < 0.05$). Toneli *et al.* (2010) used a Büchi B-191 spray-dryer to produce an inulin powder, and also reported that T_{IA} had a significant effect on the yield, more so than any other tested factor. They also found

that an increasing FFR had a significant negative effect on the yield, and this was ascribed to increased clogging of the atomisation nozzle at a higher peristaltic pump performance.

No statistically significant effects were observed on the Pareto charts for the dependent variables MC_{db}, a_w and aspalathin retention. The linear effect of T_{IA} had a statistically significant effect on the mean T_{OA}, as might be expected. However, it was decided that the latter response would not be included as a critical process parameter (CPP) for the unit operation (Addendum B; Fig. 7.1).

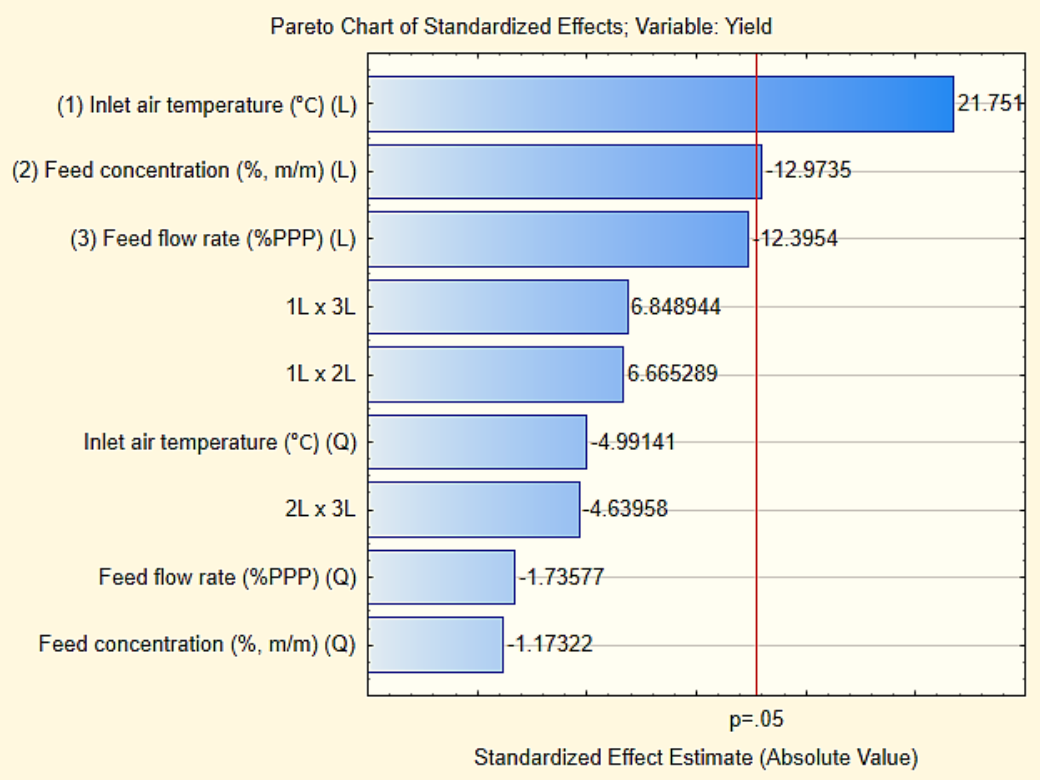

Figure 4.4 Standardised Pareto chart showing linear, quadratic and interaction effects for spray-drying yield. L = linear effect; Q = quadratic effect; LxL = interaction effect; PPP = peristaltic pump performance.

The statistical significance of the independent variables and their interactions, as well as the fit of the model to the data, was estimated by performing ANOVA, which compares the variance between different combinations of independent variables (treatments) and the variance due to random errors. Table 4.6 summarises the ANOVA results for the powder yield model. The suitability of a model can be evaluated in terms of R^2_{adj} or LOF. R^2 represents the amount of variation around the mean that is explained by the quadratic model, and R^2_{adj} is the same term adjusted to account for the number of terms in the model, allowing for direct comparison of models with a different number of independent variables. R^2_{adj} is usually lower than R^2, which should preferably be at least 0.8 for a model with a good fit. The LOF test compares the variability between observations of different replications of the independent variables with the variability of the model residuals. It makes use of the mean square (MS) pure error as the error term and is

considered a more sensitive test of model fit than R^2_{adj}. A model is considered to have a good fit to the data if there is significant regression and non-significant LOF. For the model under investigation LOF was non-significant (P = 0.254), while R^2_{adj} was 0.88, thus indicating good predictive ability of the model. The response values were fitted as a function of the three independent variables (represented by X_1, X_2 and X_3). The regression coefficients that were generated by the ANOVA were used to formulate a quadratic regression equation which could be used to predict the values of the response when the levels of the independent variables are known (Table 4.7).

Table 4.6 ANOVA of experimental results for the polynomial regression equation for spray-drying yield (g powder recovered per 100 g total solids in feed preparation).

Parameter[1]	Regr. coeff.[2]	SS[3]	DF[4]	MS[5]	F	P
Intercept	36.205					
(1) Inlet air temperature (°C) (L)	0.702	280.558	1	280.558	473.148	0.029
Inlet air temperature (°C) (Q)	-0.003	14.773	1	14.773	24.914	0.126
(2) Feed concentration (%, m m^{-1}) (L)	-1.604	99.802	1	99.802	168.311	0.049
Feed concentration (%, m m^{-1}) (Q)	-0.005	0.816	1	0.816	1.377	0.449
(3) Feed flow rate (% PPP) (L)	-2.068	91.107	1	91.107	153.647	0.051
Feed flow rate (% PPP) (Q)	-0.012	1.787	1	1.787	3.013	0.333
1L x 2L	0.012	26.343	1	26.343	44.426	0.094
1L x 3L	0.014	27.815	1	27.815	46.908	0.092
2L x 3L	-0.028	12.764	1	12.764	21.526	0.135
Lack of fit		25.364	5	5.073	8.555	0.254
Pure error		0.593	1	0.593		
Total SS		579.720	15			
R^2						0.955
R^2_{adj}						0.888

[1] L = linear coefficient; Q = quadratic coefficient; L x L = interaction coefficient; [2] Regression coefficients; [3] Sum of squares; [4] Degrees of freedom; [5] Mean square

Table 4.7 Polynomial prediction equation for powder yield.

Dependent variable	Prediction equation
Powder yield (%; g powder recovered per 100 g total solids in feed preparation)	$\hat{Y} = 36.20537 + 0.70184X_1 - 1.60426X_2 - 2.06818X_3 - 0.00286X_1^2 - 0.00535X_2^2 - 0.01218X_3^2 + 0.01152X_1X_2 + 0.01480X_1X_3 - 0.02807X_2X_3$

Combined response surface plots for powder yield provide further visual evidence of the significant effects as indicated on the Pareto chart. Figs. 4.5a & 4.5b show that higher T_{IA} was associated with higher yields. Increasing the FFR at a fixed, low T_{IA} (140 °C) resulted in a sharp

decrease in the yield, but this effect was less pronounced at the upper end of the T_{IA} range (220 °C). As with the FFR, the effect of changing the FC was more pronounced at a low T_{IA}, but T_{IA} >200 °C was associated with high yields regardless of the FC.

Fig. 4.5c depicts the effects of the FFR and FC on the powder yield at the fixed central point of the tested T_{IA} range (185 °C). The effect of the FC on the yield was more pronounced at the upper limit of the tested FFR range, and in turn the effect of the FFR on the yield was more noticeable at the upper limit of the tested FC range. The increase in the rate of feed delivery into the drying chamber increases the amount of solvent to be removed within a given time interval, placing a greater demand for drying energy on the system and may subsequently result in less efficient drying of the aerosolised droplets, as well as unwanted accumulation of residual moisture within the drying chamber (Costa *et al.*, 2015; Patel *et al.*, 2015). The use of lower T_{IA} was associated with excess moisture in the drying chamber. Visual evidence pointing towards decreased yields were often quite apparent (Fig. 4.6), with the clear glass walls of the laboratory-scale spray-dryer allowing for observation into the spraying cylinder throughout the entire process. When all the other operating parameters were kept at a fixed level and an inlet air temperature of 206 °C was used, less particles and moisture droplets were seen accumulating within the drying chamber (Fig. 4.6b) as compared with drying at a lower inlet air temperature (164 °C) (Fig. 4.6a).

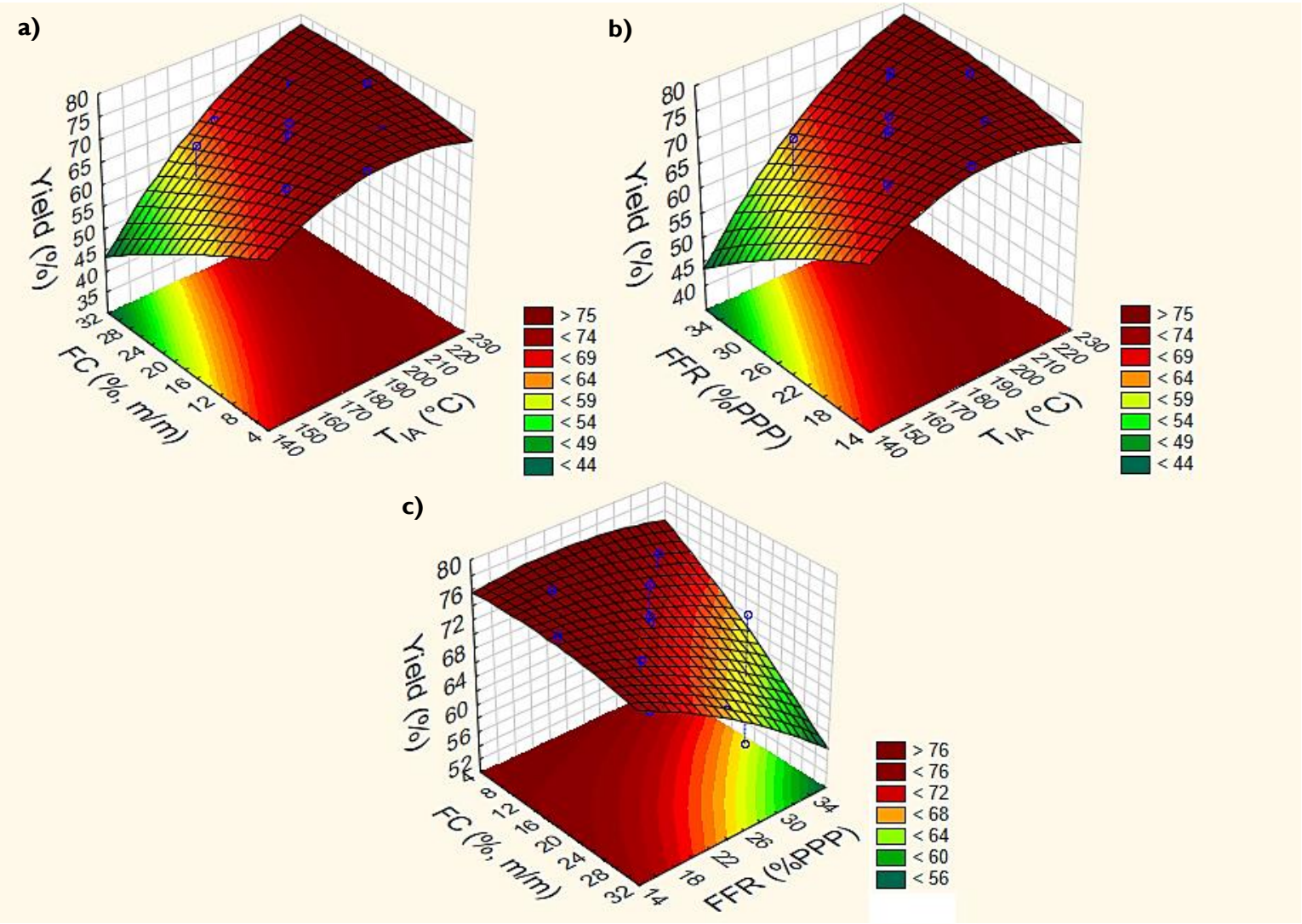

Figure 4.5 Combined response surface plots showing effects of (a) feed concentration (FC; %, m m^{-1}) and inlet air temperature (T_{IA}; °C), (b) feed flow rate (FFR; % peristaltic pump performance, PPP) and T_{IA}, and (c) FC and FFR on spray-drying yield (%; g powder recovered per 100 g total solids in feed preparation).

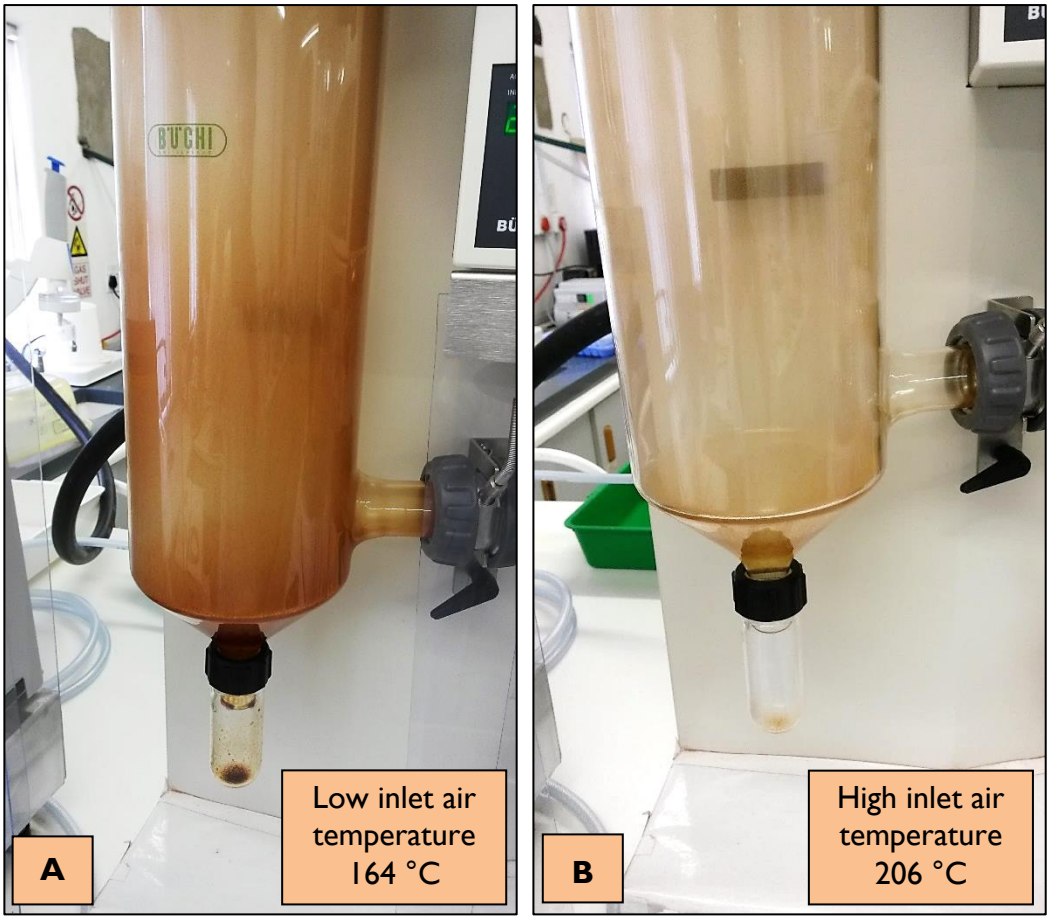

Figure 4.6 Accumulation of moisture and sticky spray-dried particles in drying chamber at (a) low inlet air temperature (164 °C) and (b) high inlet air temperature (206 °C). All other parameters were at fixed levels: feed flow rate = 19% peristaltic pump performance; feed concentration = 10%; m m^{-1}.

4.4.3.2. Verification of prediction models

Verification of a prediction model is required in order to assess how well the experimental results would agree with values predicted using such model. Six points of the CCD were replicated as verification runs. The predicted and experimentally observed response values. as well as the over/underestimation obtained for all six verification experiments are presented in Table 4.8.

The intraclass correlation coefficient (ICC) was used to assess how well the experimental data fits the model. It is an indication of the reliability of quantitative measurements, with reliability referring to the reproducibility of the measurement when repeated randomly. ICC values range between 0 and 1, with values closer to 1 indicating a better model fit and a greater reliability of the model to predict response values. ICC(agreement) is a subclass of the ICC accounting for any bias that may have occurred by incorporating the standard error of measurement (SEM), whereas ICC(consistency) excludes the SEM, but is less sensitive as a result. Predicted response values and

the observed results from the verification experiments are presented as scatter plots to demonstrate the distribution of the data (Fig. 4.7).

Table 4.8 Verification experiments for spray-drying yield prediction model according to central composite design.

Verification run	Independent variables			Response		
	Inlet temperature (°C)	Feed concentration (%)[1]	Feed flow rate (% PPP)[2]	Observed yield (%)[3]	Predicted yield (%)[3]	Δ[4]
Vr1	164	17.5	25	70.834	66.861	3.973
Vr2	206	17.5	25	80.116	75.926	4.190
Vr3	185	10.0	25	73.807	75.067	-1.260
Vr4	185	25.0	25	66.853	69.640	-2.787
Vr5	185	17.5	19	77.941	74.799	3.142
Vr6	185	17.5	31	73.828	69.633	4.195

[1] g total solids per 100 g H_2O; [2] PPP = peristaltic pump performance; [3] g powder recovered per 100 g solids in feed preparation; [4] Δ = (Observed yield – Predicted yield)

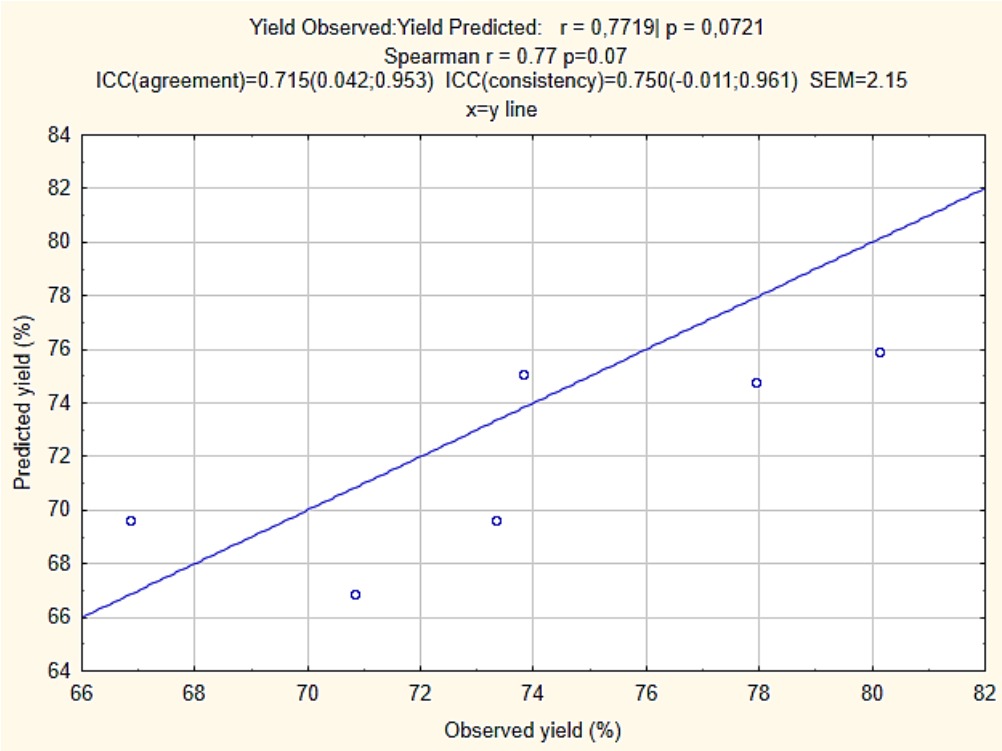

Figure 4.7 Correlation of predicted and observed values for spray-drying yield model verification.

The ICC(agreement) and ICC(consistency) values of the dependent variable, powder yield, were 0.715 and 0.750, respectively. These values indicate a satisfactory predictive ability, however for large-scale cost and profit predictions, it is required that ICC values be as close to 1.0 as possible.

For further evaluation of the predictive ability of the model, a Bland-Altman plot (Fig. 4.8) was used to assess the agreement between observed and predicted values and to analyse for the presence of bias within the data. The means of the observed and predicted values are plotted on the *x*-axis, and the differences between the observed and predicted values are displayed on the *y*-axis. The experimental data should ideally be scattered closely around the mean and within the 95% limits of agreement. This would represent a small difference between the predicted and observed results. If no bias is present in the experimental data, then the mean lies at 0 on the *y*-axis.

The Bland-Altman plots for spray-drying yield shows that the experimental points were scattered between the 95% limits of agreement on both sides of the mean. This indicates a small difference between the experimental and predicted results and satisfactory predictive ability. The mean is above 0, indicating a slight bias due to random variation and subsequent underestimation. This is reflected in the Δ values listed in Table 4.8, which were positive in four out of six cases, indicating observed yields which were generally higher than the predicted yield. Small variations in moisture content of the recovered powder would contribute to this variation. Furthermore, the recovery of the powder from the collection vessel in such a laboratory-scale set-up is not automated and relies entirely on the actions of the operator. This means that the amount of powder recovered in a small-scale set-up could differ substantially, but this would most likely be less of an issue in a scaled-up, industrial setting, where larger volumes of product are processed.

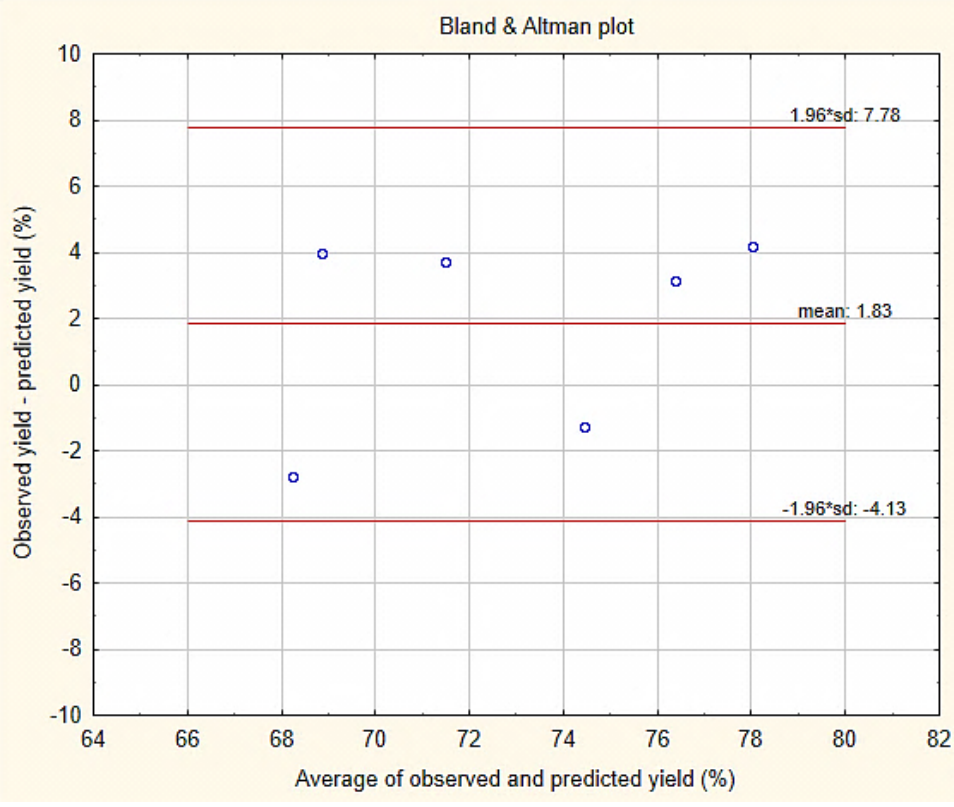

Figure 4.8 Bland-Altman plot for spray-drying yield model verification.

4.4.3.3. Desirability profiling

The concept of desirability profiling in RSM has been previously discussed in section 3.4.4.3. Desirability profiles gives an indication of the levels of the independent variables that would produce the most desirable response values. Fig. 4.9 shows the desirability profiles for powder yield, optimised for a maximum response value. The 95% confidence intervals (blue lines) are used to aid in the assessment of the reliability of the predicted responses. The gradients of the various desirability curves (green) are a reflection of the magnitude of the effect on the response value.

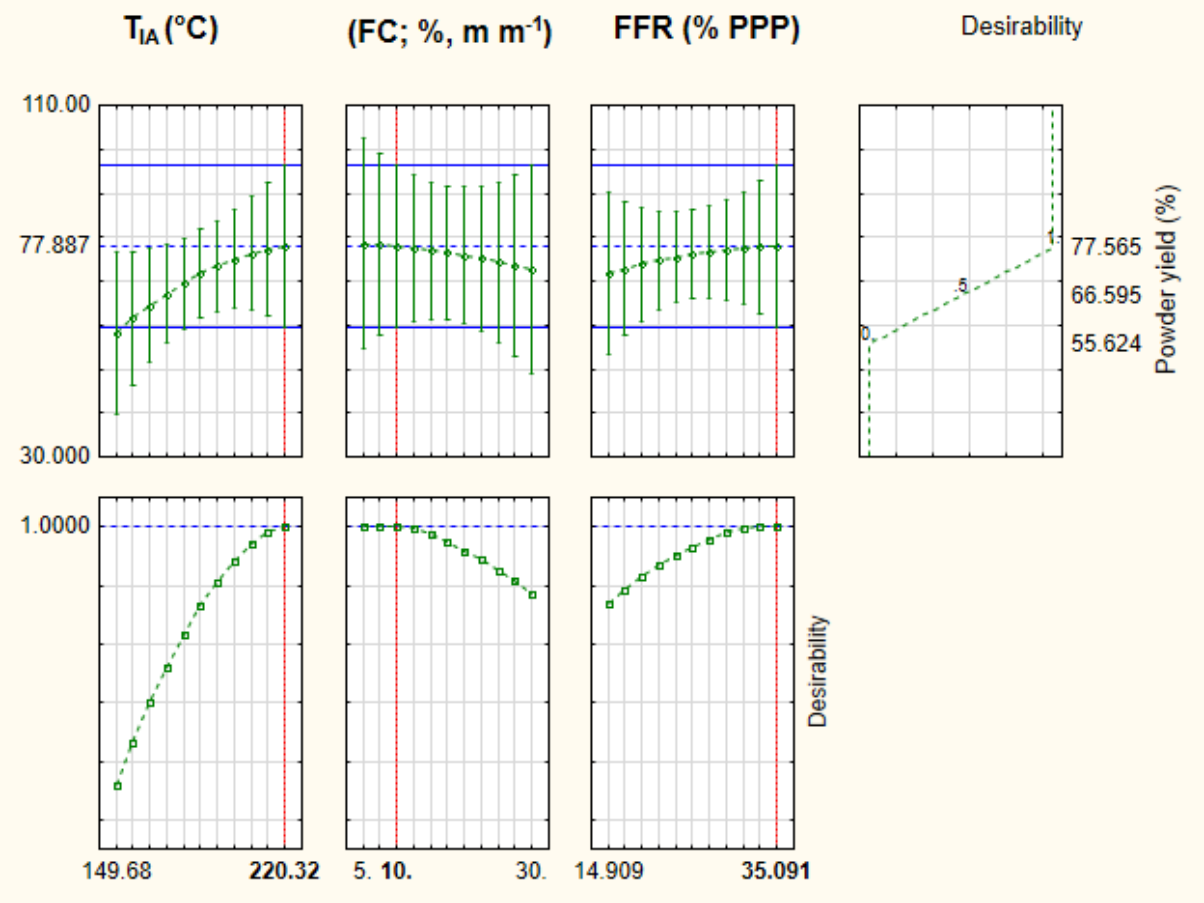

Figure 4.9 Desirability profiles for powder yield. Optimal values for each independent variable are indicated in bold at the bottom.

The steep gradient of the desirability plot for T_{IA} confirms its effect on the powder yield, with the desirability steadily increasing as the temperature is increased. The optimal T_{IA} was identified as 220 °C, the upper limit of the tested range. The desirability plot for FC indicates an optimal level of 10%, with the desirability gradually decreasing from 12.5% and higher, but the effect is not as pronounced as that of T_{IA}. The desirability plot for FFR shows a steady increase in desirability with increasing FFR, reaching a plateau at ≈33%. The optimal level for this independent variable was identified as 35% PPP, the upper limit of the tested range. This is an indication that the

actual optimum may lie outside the experimental domain. The latter was determined to a large extent by operation limitations of the equipment. No multi-response optimisation was performed for the spray-drying process since the powder yield was the only response for which a significant prediction model could be determined.

4.4.3.4. Practical optimum spray-drying parameters

The final optimum spray-drying conditions, otherwise referred to as the critical process parameters (CPP) for the spray-drying process, are summarised in Table 4.9. The optimal conditions are presented as ranges of values in order to allow for minor deviations in operations. The highest temperature setting possible using the Büchi B-290 Mini spray-dryer was 220 °C, but this upper limit may be higher in a different system. Laboratory-scale spray-drying with T_{IA} above 220 °C is not frequently encountered in literature, however. An optimal range of T_{IA} was therefore identified as 210–230 °C. The optimal range for the FC was identified as 9–11%.

The optimal level of the FFR, identified by desirability profiling and expressed as the % PPP, corresponds roughly to a volumetric flow rate of 10.67 $mL.min^{-1}$ or 0.64 $L.h^{-1}$ (Fig 4.2; Büchi, 2009). An optimal range for the peristaltic pump performance (34–36%) translates roughly to a volumetric flow rate of 10.3–11.2 $mL.min^{-1}$ (≈0.62–0.67 $L.h^{-1}$).

Previously, Joubert (1988) used T_{IA} maintained at 200±10 °C, a T_{OA} of ca. 90°C and a concentrate feed rate of 20 kg/hr (water evaporation rate 13 kg/hr) for the spray-drying of fermented rooibos extract-maltodextrin mixture (1:1) of 36% solids content. In this case a pilot-plant spray-dryer, equipped with a centrifugal disk atomiser, was used. The moisture content of the powder was 3.3%. The percentage recovery of powder was not determined due to relative scale (quantity of feed vs. dimensions of the drying chamber and cyclone system; Joubert, E., 2016, ARC, Stellenbosch, personal communication, 18 August).

Table 4.9 Critical process parameters for hot water extraction of green rooibos.

Parameter	Range
Inlet air temperature (°C)	210–230
Feed concentration (%; g solids per 100 g H_2O)	9–11
Feed flow rate (% peristaltic pump performance)	34–36

4.4.4. Powder yield and mean outlet air temperature

By substituting the lower and upper values of the CPPs into the polynomial prediction model for powder yield (Table 4.7), this CQA of the spray-drying process could be predicted (Table 4.10).

The minimum powder yield predicted by adhering to these CPPs is 77.120%. The lowest expected value is particularly important since the aim is to ensure that a minimally acceptable efficiency level is attained, whereas excess yields would not compromise product quality or safety.

Table 4.10 Range of predicted spray-drying yield using selected range of critical process parameters.

Critical quality attribute (CQA)	Range
Spray-drying yield (%) (g powder recovered per 100 g solids in feed preparation)	77.120–78.601

In order to validate the optimal CPPs, three different formulations of SDE were produced using the optimal process parameters: extract (100% extract; 0% carrier) and two extract-carrier mixtures containing maltodextrin and inulin as carriers, respectively. The carriers were added to the extract in a 1:1 ratio ($m.m^{-1}$) whilst maintaining a FC of 10% solids. Table 4.11 lists the yields and mean T_{OA} that were recorded for each of the three validation formulations. The powder yields obtained for the different formulations were all within the range that was predicted using the polynomial model (Table 4.10) and they did not differ significantly between treatments ($P > 0.05$) (Table 4.11). No improvement in yield was therefore noted when a carrier was used instead of pure extract. The mean T_{OA} was slightly lower when a carrier was used. This could be attributed to a greater energy requirement for the removal of moisture bound to the carbohydrate structure of the carrier materials.

Table 4.11 Powder yield, mean outlet temperature and aspalathin retention obtained for three different experiments using practical optimum spray-drying parameters.

Sample	Yield (%)[1]	Mean outlet air temperature (°C)	Aspalathin retention (%)[2]
Pure extract	78.28 ± 0.27 a	109.11 ± 1.35 a	95.71 ± 0.55 a
Extract: inulin (1:1; $m.m^{-1}$)	77.92 ± 0.09 a	105.11 ± 0.51 b	95.13 ± 0.23 a
Extract: maltodextrin (1:1; $m.m^{-1}$)	78.39 ± 0.46 a	105.22 ± 0.51 b	97.27 ± 1.00 a

[1] g powder recovered per 100 g total solids in feed preparation; [2] Aspalathin retention = g aspalathin in 100 g SDE (dry basis) ÷ g aspalathin in 100 g feed preparation. Values given as average of three measurements ± standard deviation. Values with same letters in each column are not significantly different ($P > 0.05$).

These results indicate that the optimal spray-drying process parameters, identified by response surface methodology and desirability profiling, gave the desired yields as predicted by the polynomial model. The powder yields in the present study are higher than those reported by Couto *et al.* (2011; 62.85–68.72%) for an SDE of *Eugenia dysenterica* encapsulated with maltodextrin (12.5–25% $m.m^{-1}$) at an inlet air temperature of 180 °C. Similarly, the present powder yields were higher

than those obtained by Pauck (2016) in the spray-drying of green honeybush extracts, whether pure (i.e. no carrier, 62.2%) or encapsulated with inulin or corn syrup solids in a 1:1 mass ratio (63.5 and 61.4%, respectively). The latter study, which was conducted using the same Büchi B-290 spray-dryer, utilised a T_{IA} of 180 °C and a drying air rotameter setting of 40 mm. Higher yields could possibly have been obtained for the honeybush powder if the maximum levels of these parameters had been used, as they were in the present study. Spray-drying generally provides favourable yields if the process is carried out optimally, but what is considered acceptable varies amongst investigators. Even yields as low as 45% have been cited as acceptable when sugar-rich products were spray-dried (Sollohub & Cal, 2010). Table 4.12 presents the 95% confidence interval for the powder yields reported in Table 4.11. This indicates the range of powder yields that might be expected for GRE (with or without carrier), spray-dried at laboratory-scale using the optimum parameters identified by RSM and basic operating conditions described in section 4.4.2 (Kidd, M., 2016, Centre for Statistical Consultation, Stellenbosch, personal communication, 11 August). Larger drying chambers used in up-scaled industrial spray-drying operations would most likely reduce the degree of wall deposition by setting the drying chamber walls out of the range of most particle trajectories, thus improving the process yield further (Oakley, 1994; Keshani *et al.*, 2015).

Table 4.12 Confidence intervals (95%) for powder yield obtained using optimum spray-drying parameters[1].

CQA	Range
Powder yield (%) (g per 100 g total solids in feed)	77.824–78.900

[1] Inlet air temperature = 220 °C; feed concentration = 10%; feed flow rate = 35% peristaltic pump performance

4.4.5. Physicochemical properties of optimised spray-dried extracts

4.4.5.1. Water activity, moisture content and moisture sorption characteristics

Moisture content (MC) and water activity (a_w) are two significant factors which may affect the stability and various quality parameters of spray-dried powders (Ré, 1998). Moisture sorption isotherms (MSIs) are useful to describe the relationship between MC and a_w, and to predict how powders might react if exposed to conditions of high relative humidity (RH) (Al-Muhtaseb *et al.*, 2002). Moisture sorption isotherms can also be useful for the prediction of adequate storage conditions for a particular product, e.g. avoiding exposure to RH higher than that corresponding to the monolayer moisture content (M_0) (Gabas *et al.*, 2007). The SDEs recovered from the collection vessel directly after spray-drying were free-flowing, but exposure to conditions of high relative humidity and subsequent sorption of moisture could result in a decrease of the glass transition

temperature (T_G), resulting in stickiness, caking and loss of its free-flowing properties (Bhandari & Howes, 1999). The MC_{db} and a_w of the three different SDE formulations, produced at the optimum spray-drying conditions, are given in Table 4.13. All the SDEs had MC_{db} <2.3%, and the addition of carrier did not show a significant effect on the MC. However, the a_w of the SDEs containing carriers was significantly lower ($P < 0.05$) than that of the pure extract. This is attributed to binding of water (with reduction in vapour pressure) by the hydrophilic polymer structure of the carriers, which would account for their lower a_w values. Fig. 4.10 shows the MSIs of the SDEs, displaying a weak sigmoidal shape, a typical curve characteristic of type II isotherms (Al-Muhtaseb *et al.*, 2002). Moisture sorption data which were derived from the BET and GAB models for each treatment are summarised in Table 4.14.

Table 4.13 Moisture content (% dry basis; MC_{db}) and water activity (a_w) of three different optimised spray-dried extract formulations[1].

Sample	MC_{db} (%)	a_w
Pure extract	2.155 ± 0.04 a	0.122 ± 0.007 a
Extract: inulin (1:1; $m.m^{-1}$)	2.154 ± 0.06 a	0.071 ± 0.009 b
Extract: maltodextrin (1:1; $m.m^{-1}$)	2.055 ± 0.0.58 a	0.067 ± 0.005 b

[1] Values given as average of three measurements ± standard deviation. Values in columns with same letters are not significantly different ($P < 0.05$).

Table 4.14 BET and GAB moisture sorption data obtained at 25 °C for spray-dried pure green rooibos extract and extract in combination with inulin and maltodextrin, respectively.

Sample	BET Model			GAB Model			
	C_B[1]	M_0[2]	$M_{0.5}$[3]	C_G[4]	M_0[2]	$M_{0.5}$[3]	K
Pure extract	8.516	3.464	6.200	4.940	4.063	8.104	1.132
Extract: inulin (1:1; $m.m^{-1}$)	14.672	3.098	5.801	9.511	3.069	7.981	1.274
Extract: maltodextrin (1:1; $m.m^{-1}$)	7.087	3.852	6.870	7.767	3.363	8.002	1.223

[1] C = constant in BET sorption model; [2] M_0 = monolayer moisture content (% dry basis); [3] $M_{0.5}$ = moisture content (% dry basis) at 50% relative humidity

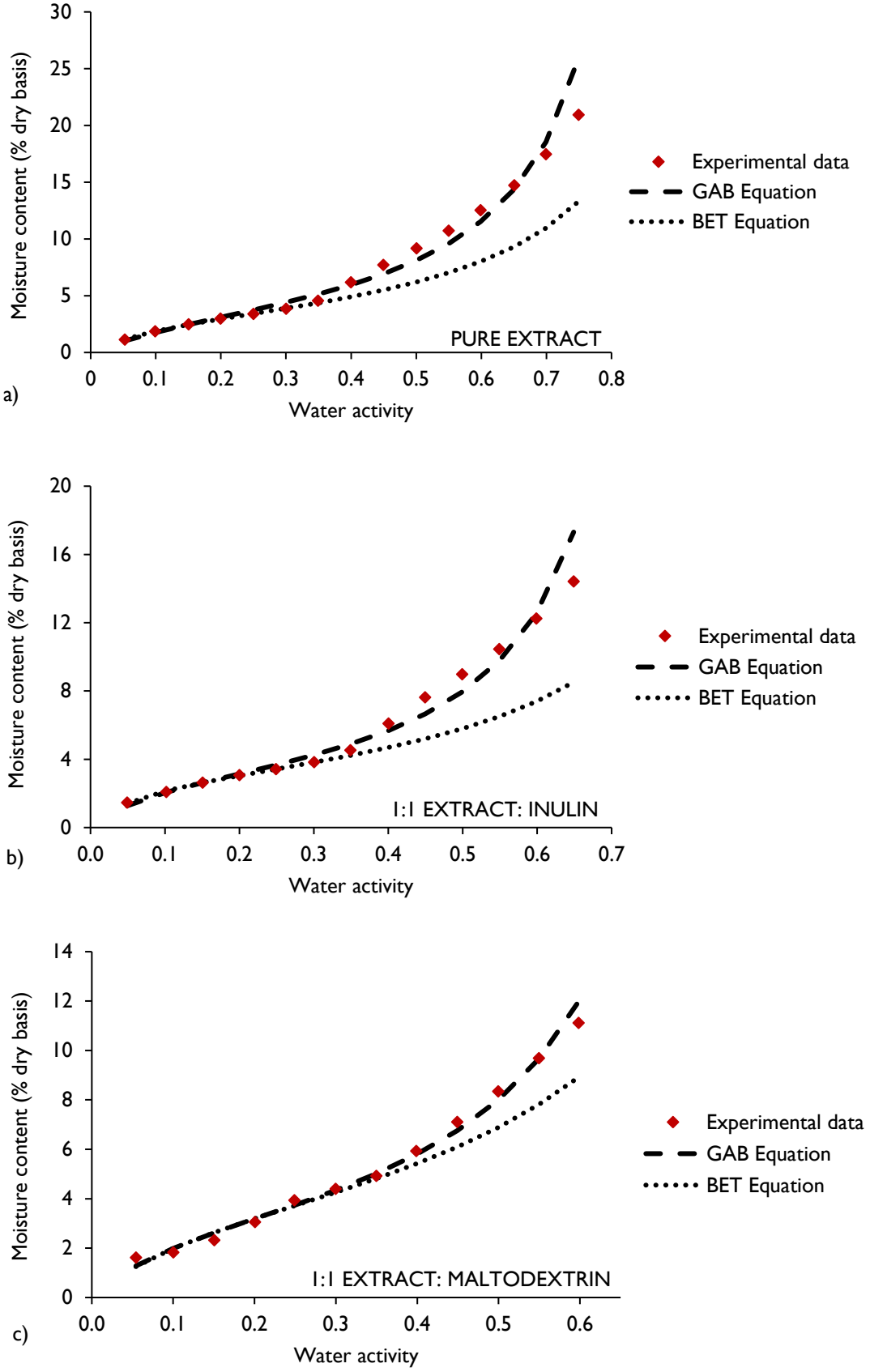

Figure 4.10 Moisture sorption isotherms obtained at 25 °C of spray-dried (a) pure green rooibos (GR) extract, (b) GR extract with inulin (1:1; $m.m^{-1}$) and (c) GR extract with maltodextrin (1:1; $m.m^{-1}$) fitted with the GAB and BET sorption models.

The BET models displayed good fit to the experimental data only at a_w < 0.4, but the GAB model displayed a better fit for the higher a_w values. This is in accordance with published literature which often highlights the limitations of the BET model at higher ranges of a_w (Timmermann *et al.*, 2001; Timmermann, 2003; Blahovec & Yanniotis, 2008). A particularly useful feature of using the BET and GAB models is the ability to determine the monolayer moisture content (M_0) of a sample. The M_0 refers to the maximum amount of water which can be strongly absorbed to specific sites on the surface of the material (Labuza & Altunakar, 2007). It is considered to be a critical value above which water is more available for taking part in chemical reactions, and is temperature-dependent, decreasing with increasing temperature (Al-Muhtaseb *et al.*, 2002). Table 4.14 shows the M_0 value of each of the mixtures and the pure extract as calculated using the BET and GAB models. All the M_0 values (3.069–4.063%) fall within the range of 0.2–0.3 a_w (Fig. 4.10). For each formulation, the MC_{db} was lower than the corresponding M_0 values (GAB or BET). These results indicate that the MC_{db} and a_w of the SDEs fall within the range of the monolayer value and the powder can thus be considered shelf-stable if stored under appropriate conditions which prohibit further moisture uptake (Al-Muhtaseb *et al.*, 2002). The relationship between the M_0 and the glass transition temperature (T_G) greatly affects the stability of low-moisture, amorphous products like food powders, specifically the transition from a glassy to a rubbery state. In powdered foods this typically occurs in the range of 0.35–0.45 a_w (Al-Muhtaseb *et al.*, 2002).

The monolayer values of the pure GRE are similar to that determined for spray-dried Assam green tea extract (4.2%; Donlao & Siriwattanayotin, 2012). Interestingly, the M_0 values for a spray-dried green honeybush tea extract is 5.1% (Pauck, 2015). Considering that blends containing these two South African teas are sold in teabag form, spray-dried blends sold as "instant teas" may in future find a market. The similar M_0 values of the spray-dried green honeybush and rooibos powders indicate that such blends would be feasible, since storage conditions for the individual powders could be applicable to the blend.

It is recommended that the SDEs are to be stored below 40% RH at <25 °C. Higher humidity levels than this will result in the increased absorption of moisture, leading to higher a_w and the risk of physical state changes and quality deterioration. Ortiz *et al.* (2008) found that catechins in spray-dried green tea powder, stored for 12 weeks at 22 °C, were most shelf-stable at <42% RH, whereas storage at higher RH resulted in significant catechin degradation, increased moisture sorption and caking of the powders.

The full moisture sorption analysis (at 25 °C) included two adsorption phases and one desorption phase. The first adsorption phase was carried out by ramping the RH from 0 to ≈65%. This was followed by a desorption phase in which the RH was ramped back to 0%. Finally, the second adsorption phase was carried out in the same way as the first. Fig. 4.11 shows the adsorption and desorption curves for the SDE formulations. The moisture sorption data showed

that the samples can absorb a substantial amount of moisture, with two out of the three samples only tested with a % RH ramp of up to 60% due to deliquescence of the samples.

Many dried food products, especially sugar-rich products, are known to exhibit marked hysteresis in moisture sorption studies. This is characterised by higher MC during desorption than during adsorption, i.e. the desorption curve lies above the adsorption curve. The hysteresis phenomenon may be related to the availability of polar sites for the bonding of water molecules. "Plasticising" of an amorphous material in the glass transition range, swelling of the biopolymer and increasing availability of the number of hydroxyl groups have been suggested as explanation of this phenomenon for starch (Al-Muhtaseb *et al*., 2002). Water acts as a plasticiser by depressing the T_G, thus accelerating the transition of a glass to an amorphous rubber, a state in which the diffusion of water to the bulk of the solids is enhanced (Jadhav *et al*., 2009). Hysteresis is not yet fully understood, but the favoured theory is that in the initial adsorption phase, the polar sites in the molecular structure of the biopolymer will be almost completely occupied by adsorbed water, and the subsequent drying step draws the water-holding sites closely together to the point of possible interaction. Thus, the water holding capacity of the material is reduced in the subsequent adsorption phase (Al-Muhtaseb *et al*., 2002), as clearly evident for the desorption 1 and adsorption 2 curves of the extract-inulin mixture (Fig. 4.11). The occurrence of hysteresis is apparent from the adsorption-desorption curves of all three SDEs (Fig. 4.11), however the a_w range where hysteresis occurs differ. For the pure extract hysteresis is evident at $a_w > 0.5$, for the extract-inulin mixture at $0.05 < a_w > 0.55$, and for the extract-maltodextrin mixture at $a_w > 0.35$.

Newman *et al.* (2008) defined the hygroscopicity of a material as its tendency to take up moisture, at increasing levels of relative humidity and a constant temperature. They identified three broad categories of moisture uptake, viz. (1) surface adsorption without penetration into the solid bulk, (2) surface liquefaction and (3) absorption into the bulk portions of the solid. Surface adsorption (1) of moisture can promote particle agglomeration and adversely affect flow properties, (Newman *et al*., 2008). Absorption of moisture into the deeper layers affects the thermodynamic properties of the solid, most notably though an increase in the free volume and molecular mobility (Al-Muhtaseb *et al*., 2002). Hygroscopicity testing is considered an important preformulation step since it can provide an early indication of physicochemical stability and the effect of moisture uptake on surface or bulk properties. Hygroscopicity characteristics of the SDEs were derived from the MSI data. Since deliquescence of some samples in the present study occurred above 60% RH (where RH = a_w x 100), hygroscopicity was defined as the % moisture uptake which occurred at 25 °C/60% RH (Table 4.15)

Table 4.15 Hygroscopicity of three different formulations of spray-dried green rooibos extract at 25 °C/60% relative humidity.

Sample	Hygroscopicity (%)[1]
Pure extract	12.538
Extract: inulin (1:1; $m.m^{-1}$)	12.245
Extract: maltodextrin (1:1; $m.m^{-1}$)	11.116

[1] Expressed as % moisture (g per 100 g solids; dry basis)

All three samples had similar hygroscopicity values falling within the range of 11–12.6% moisture. This corresponds with the MC_{db} values, which did not differ significantly between treatments (Table 4.13). According to an adapted European Pharmacopeia classification system for hygroscopicity of active pharmaceutical ingredients, as described by Callahan *et al.* (1982), all three formulations could be described as "moderately hygroscopic". This emphasises the importance of preventing exposure of the product to high environmental humidity as it would most likely result in substantial uptake of moisture and subsequent quality deterioration.

4.4.5.2. Objective colour measurement

Table 4.16 presents the CIE$L^*a^*b^*$ colour data for the three SDEs produced using the optimised operating conditions. Data for the carriers, inulin and maltodextrin, are included to illustrate their contribution to the change in colour when added to the pure extract. The carriers both had L^* values close to 100, and a^* and b^* values close to 0, indicating colours approximating absolute whiteness. Addition of the carriers to the pure extract resulted in an increase in the L^* value, i.e. an increase in the lightness towards absolute white ($L^* = 100$). Şahin-Nadeem *et al.* (2001) and Caliskan & Dirim (2013) also reported that the addition of maltodextrin to spray-dried plant extracts resulted in significantly higher L^* values. The positive a^* and b^* values of the three SDE samples indicate that their colour falls within the red to yellow quadrant. The overall differences in the objective colour between the three different treatments is represented by the ΔE values, which were significantly different between all three formulations. Fig. 4.12 shows the actual spray-dried powders for comparison. The image supports the objective data in that a darker shade of orange is apparent when observing the pure extract as opposed to the lighter shade of orange of the carrier-containing formulations. Studies by Rhim & Hong (2011) and Addala *et al.* (2015) reported that the colour of red pepper (*Capsicum annuum*) powder changed significantly with increasing a_w and temperature towards dark brown, which was attributed to oxidative degradation and the formation of browning compounds which are detrimental to the product quality, and storage at <25 °C and $a_w < 0.4$ was subsequently recommended for the optimal retention of the desired powder quality characteristics.

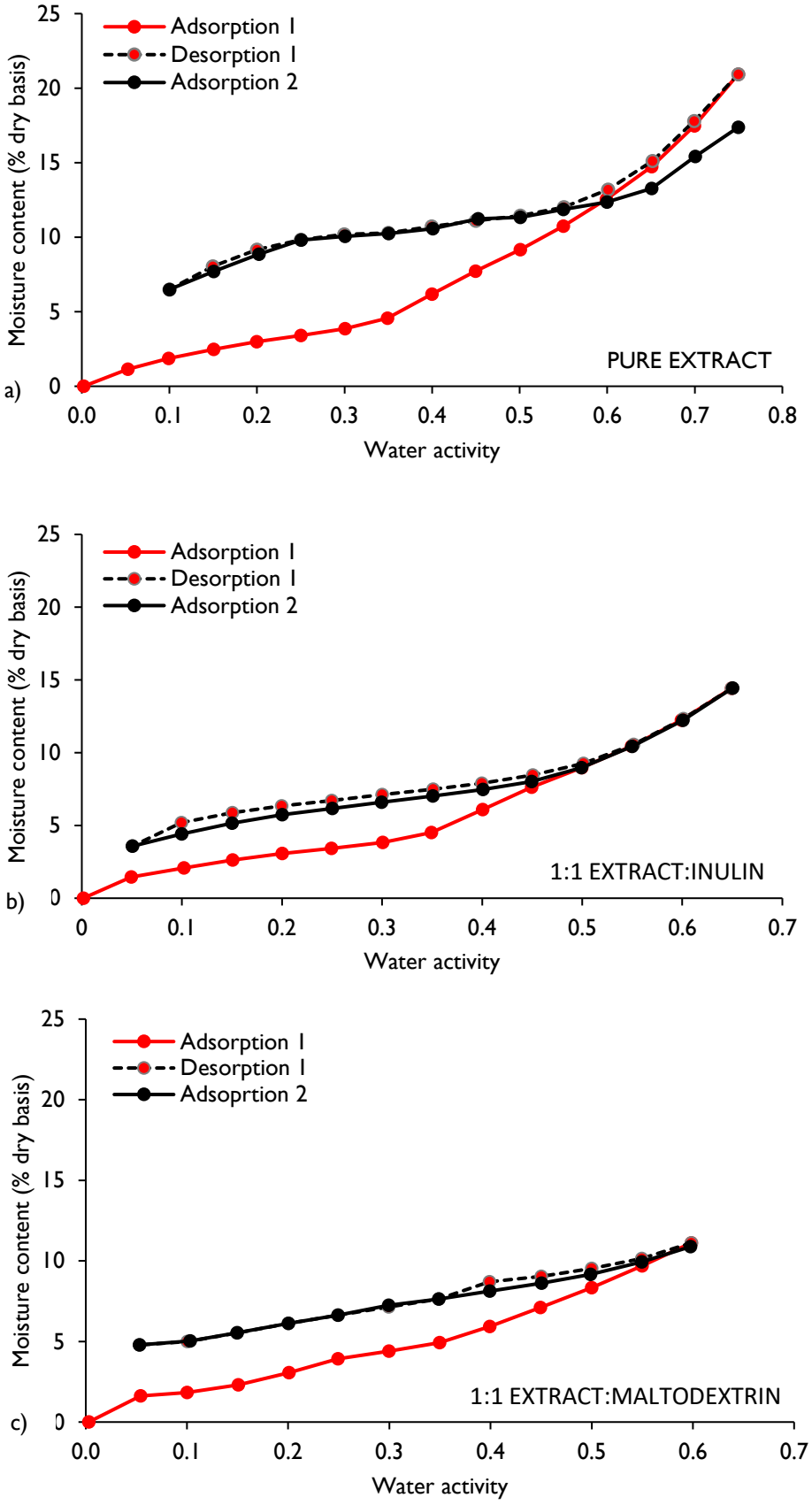

Figure 4.11 Moisture sorption isotherms for spray-dried (a) pure green rooibos (GR) extract, b) GR extract with inulin (1:1; m.m^{-1}) and (c) GR extract with maltodextrin (1:1; m.m^{-1}), showing first adsorption, desorption and second adsorption at 25 °C.

Table 4.16 Objective colour measurement data (mean ± standard deviation) for carriers and three different treatments of optimised spray-dried extracts (SDEs) of green rooibos.

Sample	Colour parameters					
	L*	***a****	***b****	***C****	***h***	ΔE [1]
Inulin	98.152 ± 0.658	-0.211 ± 0.024	2.547 ± 0.171	3.478 ± 0.642	94.983 ± 0.544	-
Maltodextrin	97.954 ± 1.008	-0.224 ± 0.044	4.117 ± 0.491	4.214 ± 0.483	96.167 ± 0.741	-
Pure extract	64.420 ± 0.781 c	19.540 ± 0.425 a	34.007 ± 0.185 a	39.223 ± 0.370 a	60.120 ± 0.398 c	0.000 c
Extract: inulin (1:1; $m.m^{-1}$)	68.913 ± 2.495 b	17.480 ± 1.077 b	32.737 ± 0.566 b	37.110 ± 1.016 b	61.900 ± 1.010 b	5.104 b
Extract: maltodextrin (1:1; $m.m^{-1}$)	72.227 ± 2.330 a	15.033 ± 1.030 c	29.507 ± 0.641 c	33.120 ± 1.056 c	63.003 ± 0.918 a	10.868 a

[1] $\Delta E = \sqrt{(\Delta a^{*2} + \Delta b^{*2} + \Delta L^{*2})}$ = Difference in colour between control (pure extract) and SDEs with carrier. Values with different letters are significantly different ($P < 0.05$). Inulin and maltodextrin values for reference only.

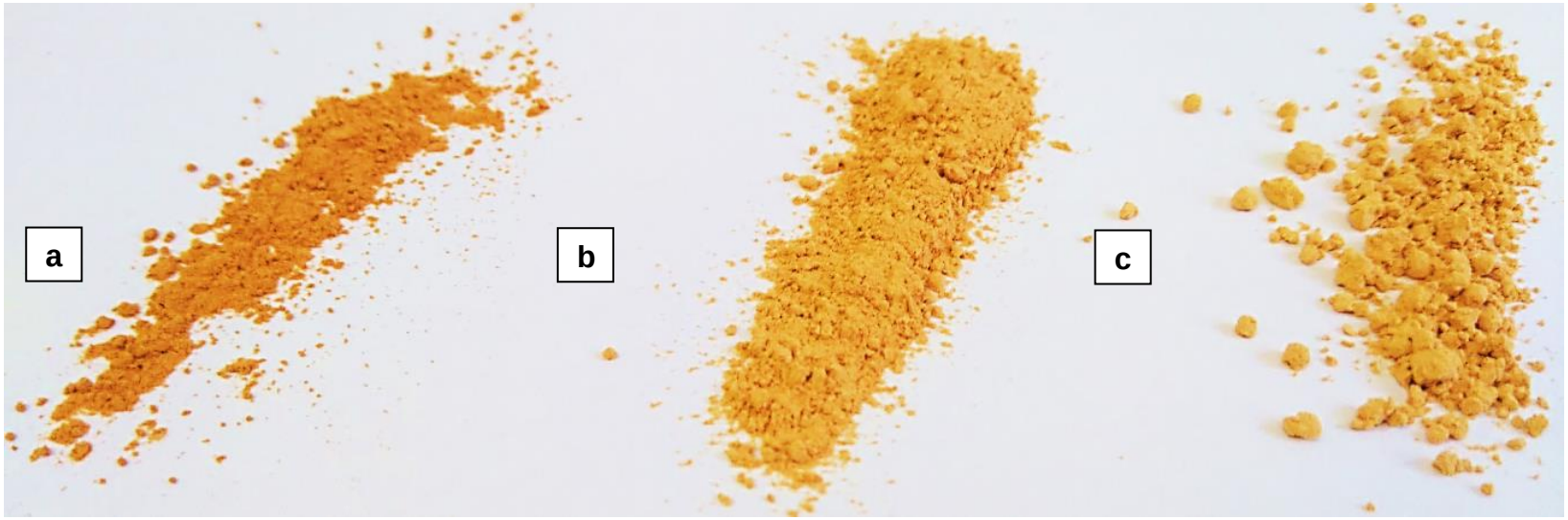

Figure 4.12 Three different treatments of optimised spray-dried extract of green rooibos: (a) pure extract, (b) extract with inulin (1:1; $m.m^{-1}$) and (c) extract with maltodextrin (1:1; $m.m^{-1}$).

4.4.5.3. Scanning electron microscopy

Scanning electron microscopy (SEM) micrographs of the three different SDE formulations are presented in Fig. 4.13. Polydisperse particles with pronounced morphological differences were obtained. Most of the particles exhibited a spherical shape with irregular surfaces and a range of diameters which generally did not exceed 10 µm. The particles of pure spray-dried extract (Figs. 4.13a & 4.13d), and extract encapsulated with maltodextrin (Figs. 4.13c & 4.13f) appeared more shrivelled and fissured than those of the extract encapsulated with inulin (Figs. 4.13b & 4.13e). Surface dents and fissures are indicative of solidification of the walls prior to the onset of expansion (De Barros-Fernandes *et al.*, 2013), as well as shrinkage during the drying process (Rosenberg *et al.*, 1985). Ré (1998) stated that surface roughness, cracks and fissures may be attributed to a slow rate of film formation during the drying of the atomised droplets, and that increasing the drying temperature will result in faster film formation at the droplet surface and, therefore, smoother particles with more favourable flow characteristics. Surface roughness is commonly encountered in spray-drying of polymeric substances, but can be minimised by adhering to optimal process parameters.

Nunes *et al.* (2015) when using a Büchi B-290 spray-dryer found that spray-dried particles of pure yerba mate (*Ilex paraguariensis*) extract were more deformed, dented and extensively wrinkled than spray-dried particles encapsulated with maltodextrin. In the present study, the inulin-containing formulation had particles with smoother surfaces than those containing maltodextrin, but also displayed some visible cracks and disintegration. Fig. 4.13e shows detail of an inulin containing microsphere with an exposed interior and a smooth spherical wall surrounding a number of smaller microspheres, demonstrating the encapsulating effect of the spray-drying process. The inulin-containing formulation also displayed less surface aggregation or fusion of multiple particles than the other two formulations, which, together with smoother surfaces of the individual particles, might explain its generally more favourable flow properties as discussed in the previous section. Belščak-Cvitanović *et al.* (2015) obtained SEM micrographs of pure spray-dried green tea (*Camellia sinensis*) extract, and described similar irregularly shaped spheroid particles with pronounced surface aggregation and fissuring, which was improved with the addition of a number of encapsulating agents (modified corn starch, pectin, alginate and carrageenan).

Toneli *et al.* (2010) used SEM to characterise the particle size and morphology of inulin powders which were spray-dried with a Büchi B-191 at T_{IA} of 130–210 °C and exposed to mean outlet air temperatures of 42.40–108.56 °C. They obtained polydisperse spherical particles of varying surface roughness and size (mean ø = 0.60–25.31 µm), with a general trend of agglomeration of smaller particles around larger particles. Spray-drying of the inulin at 210 °C, which was identified as the optimal inlet air temperature, resulted in the smoothest particle surfaces.

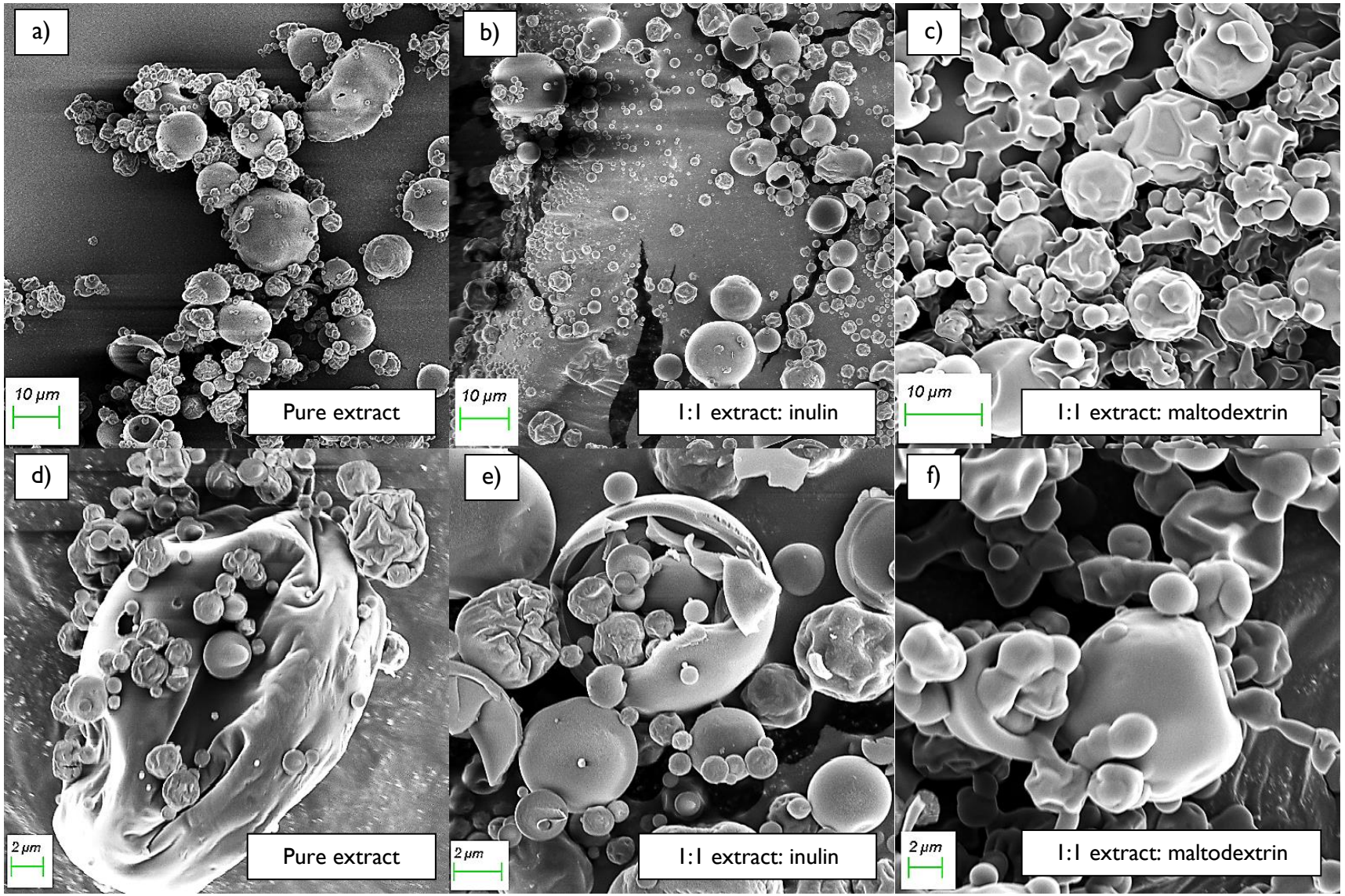

Figure 4.13 Scanning electron micrographs of three different formulations of optimised green rooibos spray-dried extracts. Spray-drying was carried out using an inlet air temperature of 220 °C, feed flow rate of 10 mL.min^{-1} (35% peristaltic pump performance) and feed concentration of 10% (m.m^{-1}).

4.4.5.4. Isothermal microcalorimetry

Calorimetry refers to measuring techniques that are used for direct determination of the rate of heat production, heat and heat capacity as a function of temperature and time. Microcalorimetry is a powerful tool for detecting incompatibilities and instabilities between active pharmaceutical ingredients and excipients. The method of microcalorimetry is a reliable way of detecting incompatibilities due to the fact that practically all physical and chemical processes are accompanied by detectable heat exchange (Chadha & Bhandari, 2014) and thus, microcalorimetry is sensitive to all physical and chemical processes associated with heat flow. The high sensitivity of this method makes it possible to carry out measurements at temperatures close to real conditions and to detect very slow reactions (Aucamp, M., 2016, Department of Pharmaceutical Sciences, North West University, personal communication, 8 March).

Figure 4.14a depicts the heat flow *versus* time data obtained for green rooibos extract in combination with inulin in a ratio of 1:1 ($m.m^{-1}$). No incompatibility or interaction between the green rooibos extract and inulin was identified at 30 °C. The interaction heat flow was calculated to be -3.681 ± 5.233 $\mu W.g^{-1}$. This results in an average interaction heat flow of close to 0.00 $\mu W.g^{-1}$, indicating that there was no incompatibility between the green rooibos extract and inulin in a 1:1 mass ratio. Similarly, no incompatibility or interaction between the extract and maltodextrin in a 1:1 mass ratio were observed (Figure 4.1.4b). With the interaction heat flow calculated to be -4.172 ± 5.895 μWg^{-1} and an average interaction heat flow of close to 0.00 $\mu W.g^{-1}$, the two compounds are compatible with one another in a 1:1 mass ratio.

These results indicate that inulin and maltodextrin would be suitable carrier materials for a green rooibos nutraceutical produced by spray-drying.

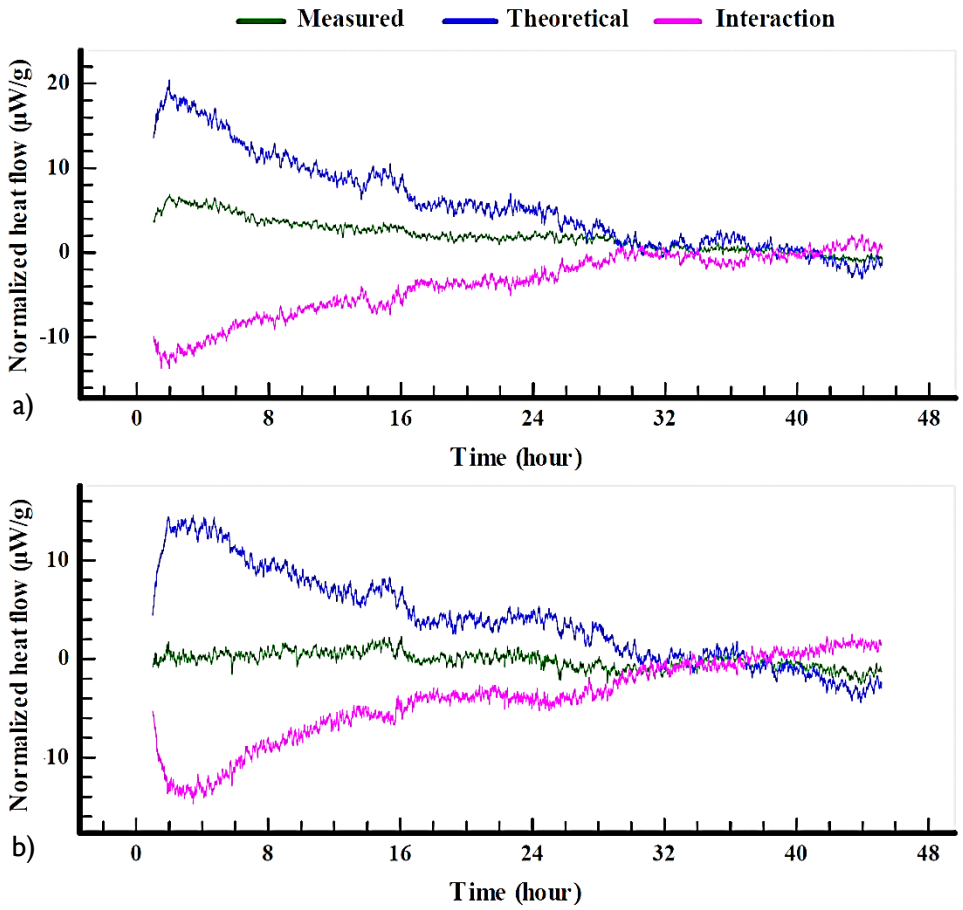

Figure 4.14 Heat flow versus time for green rooibos extract in combination with (a) inulin (1:1; $m.m^{-1}$) and (b) maltodextrin (1:1; $m.m^{-1}$) at 30 °C.

4.4.5.5. X-ray powder diffraction

XRPD directly measures the crystal structure of a powdered solid, and is typically presented as a plot of intensity vs. diffraction angle (2Θ) (Chadha & Bhandari, 2014). Spray-dried food products typically exist in an amorphous state due to the limited time for crystallisation to occur during the drying process (Bhandari & Howes, 1999). For formation of an ordered crystalline structure time is required for the molecules to move to an energetically preferred point. As temperature falls during evaporation, molecular motion slows down and the substance enters dynamic arrest, forming disordered glass at a specific temperature equalling the T_G (Jadhav *et al.*, 2009). A proportion of the spray-dried product may be in crystalline form, but this will depend on the drying rate, as well as the composition and property of the individual ingredients present (Roos *et al.*, 1996).

Fig. 4.15 shows the diffractograms of the three SDE formulations, all of which display the characteristic fuzzy/"halo" appearance of an amorphous material, with no distinct intensity peaks. Amorphous materials are not at thermodynamic equilibrium, and are therefore unstable relative to the corresponding crystalline forms. Ronkart *et al.* (2009) demonstrated that inulin which was spray-

dried at an inlet air temperature of 230 °C, similar to the present study, had a more amorphous structure than its counterpart spray-dried at 120 °C. This was attributed to partial melting of the crystalline structure at higher temperatures. Diffractograms of the inulin and maltodextrin are included in Addendum B (Figs. 7.2c & 7.3c), and they display similar evidence of an amorphous nature with the typical halo appearance. Amorphous glass will tend to convert to the crystal form eventually due to this inherent instability, and the rate of crystallisation will be dependent on the temperature and moisture content (Slade *et al.*, 1993; Bhandari & Howes, 1999). Crystallisation will lead to a release of water due to the organised molecular structure, accelerating chemical changes (Sablani *et al.*, 2007). The current data which confirms the amorphous, i.e. inherently unstable, nature of the GR SDEs further emphasises the need for stricter environmental control during their storage, with lower RH and temperature conditions recommended to prevent crystallisation.

4.4.5.6. Thermal analyses

With the amorphous nature of the SDE powders having been established by XRPD, thermal analysis by differential scanning calorimetry (DSC) was applied in order to characterise the T_G for the temperature (or temperature range) at which an amorphous solid (glass) will undergo a transition to an amorphous rubber (Le Meste *et al.*, 2002) or viscous liquid form (Jadhav *et al.*, 2009). Each amorphous solid has its own T_G which is affected by a number of material-specific factors, e.g. chemical structure, molecular weight (MW), degree of branching and cross-linking, and the amount of moisture present (Schaller-Povolny *et al.*, 2000; Jadhav *et al.*, 2009). An amorphous solid in a rubbery state will be more prone to crystallisation, with the rate increasing significantly as the product temperature is elevated above its T_G. As the rate of nucleation and crystallisation increases, so does the release of water of hydration to the surrounding matrix, which results in continuation of the process at new nucleation sites (Schaller-Povolny *et al.*, 2000). Thus, it is useful to investigate thermodynamic and glass transition characteristics of spray-dried powders in order to determine which storage conditions would be most favourable in terms of preventing crystallisation and quality deterioration. The thermal analysis results for the pure extract (no carrier) are shown in Fig. 4.16. The DSC thermogram depicts a very broad endothermic event, starting at 69.36 °C and ending at 120.92 °C (Fig. 4.16a). This could be an indication of surface adsorbed moisture. The rooibos extract starts to degrade at ≈190 °C. In order to confirm that the broad endothermic event from 69.36–120.92 °C can be attributed to surface adsorbed moisture, thermogravimetric analysis (TGA) was performed. The simultaneous TGA/DTA analysis is depicted in Fig. 4.16b. This trace showed that in the region of 25–120 °C approximately 2.48% mass was lost, which corresponds with the endothermic event in the corresponding DSC thermogram. Complete mass loss over the temperature range of 120–250 °C was 26.34%, confirming the partial degradation of the extract.

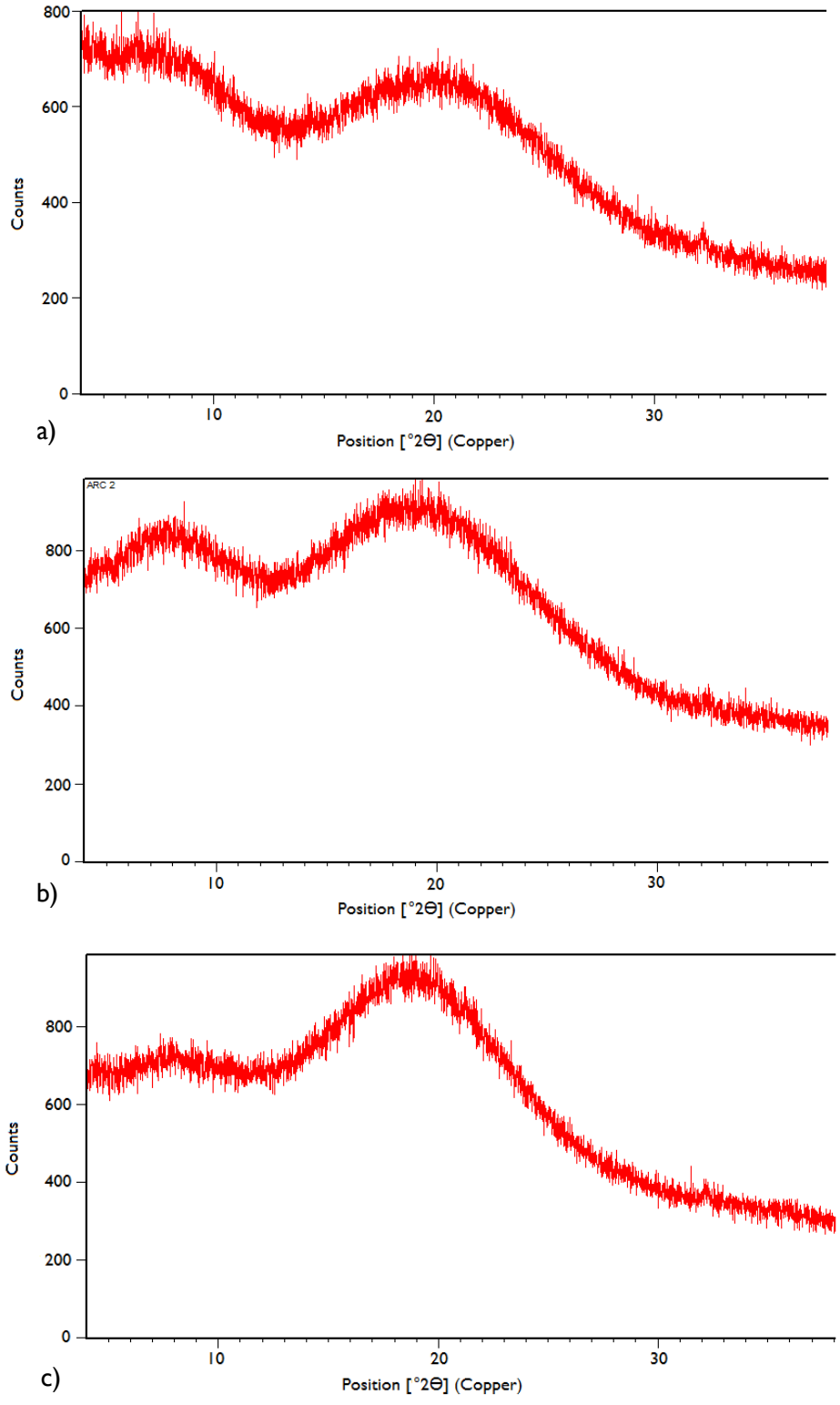

Figure 4.15 X-ray diffractograms of spray-dried (a) pure green rooibos (GR) extract, (b) GR extract with inulin (1:1; $m.m^{-1}$) and (c) GR extract with maltodextrin (1:1; $m.m^{-1}$) at 25 °C.

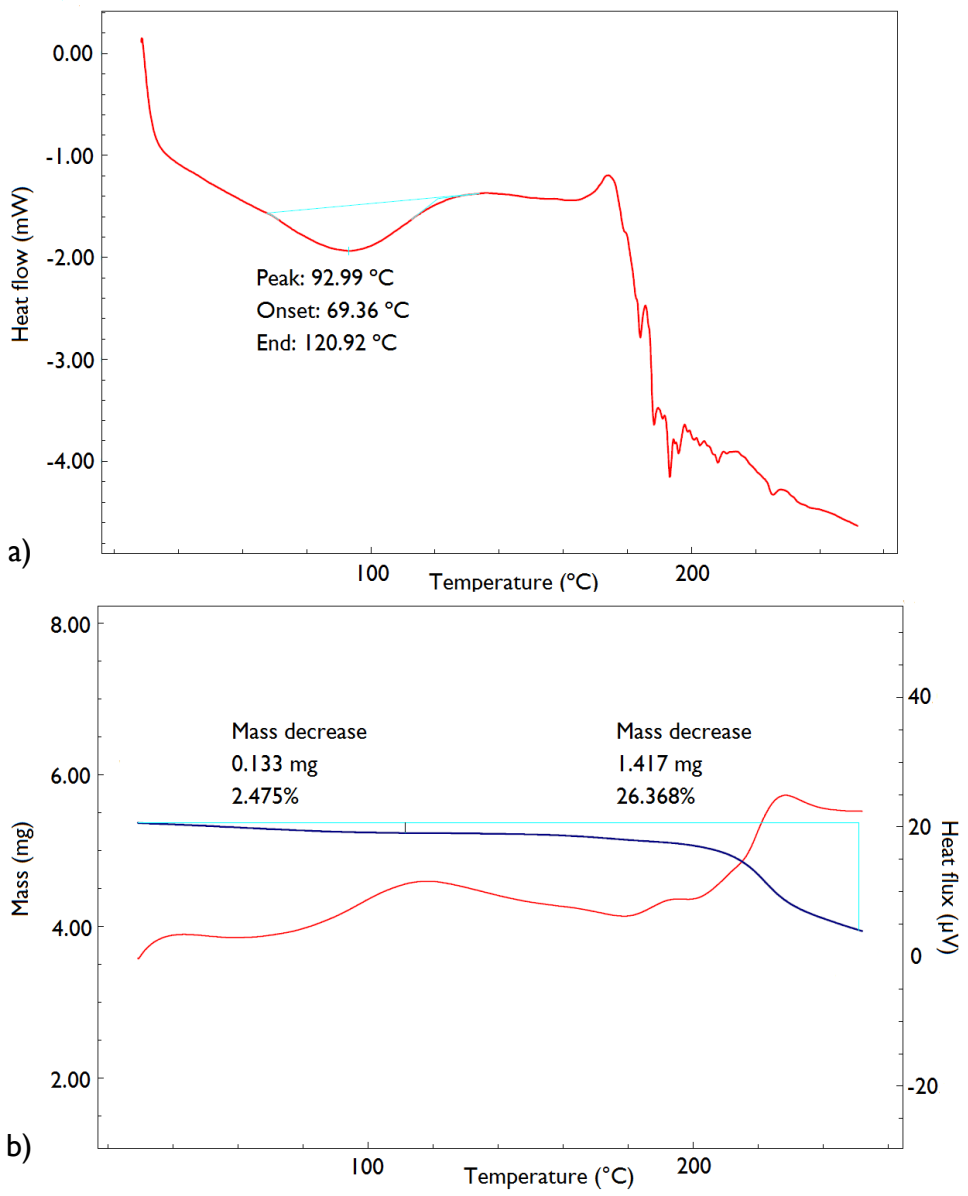

Figure 4.16 (a) Differential scanning calorimetry (DSC) thermogram and (b) thermogravimetric analysis trace (blue) with a simultaneous differential thermal analysis (DTA) trace (red) for spray-dried pure green rooibos extract.

From the DSC thermogram in Fig. 4.17a it is evident that no interactions between the rooibos extract and the inulin were present, confirming isothermal microcalorimetry results (Fig. 4.14a). If this were to be the case, different endo- or exotherms not otherwise visible on the thermograms of the pure extract and pure inulin (Addendum B; Fig. 7.2) would have been present on the thermogram of the extract-inulin mixture. The degradation of the rooibos extract above 200 °C is still clearly visible, as is the broad endotherm between 50–110 °C, which is an attribute of both the rooibos extract and the inulin. From the TGA, a moisture loss of 1.97% was observed over the range of 25–100°C (Fig. 4.17b). The T_G was not clear on either the pure DSC thermogram (Fig. 4.17a) or the DTA trace obtained from the simultaneous TGA/DTA trace (Fig. 4.17b), however it

was possible to identify an endothermic event at 173.46 °C, which could represent a point of glass transition. This roughly corresponds with a glass transition which was observed for the inulin powder at ≈135 °C (Addendum B; Fig. 7.2a). Dan *et al.* (2009) and Van Drooge *et al.* (2009) have previously detected T_G of inulin at ≈165 °C and 155 °C. The T_G of a mixture of various compatible components is a non-linear function of the individual components (Bhandari & Howes, 1999). This could partially explain the higher temperature range at which the endothermic event took place in the extract-inulin mixture.

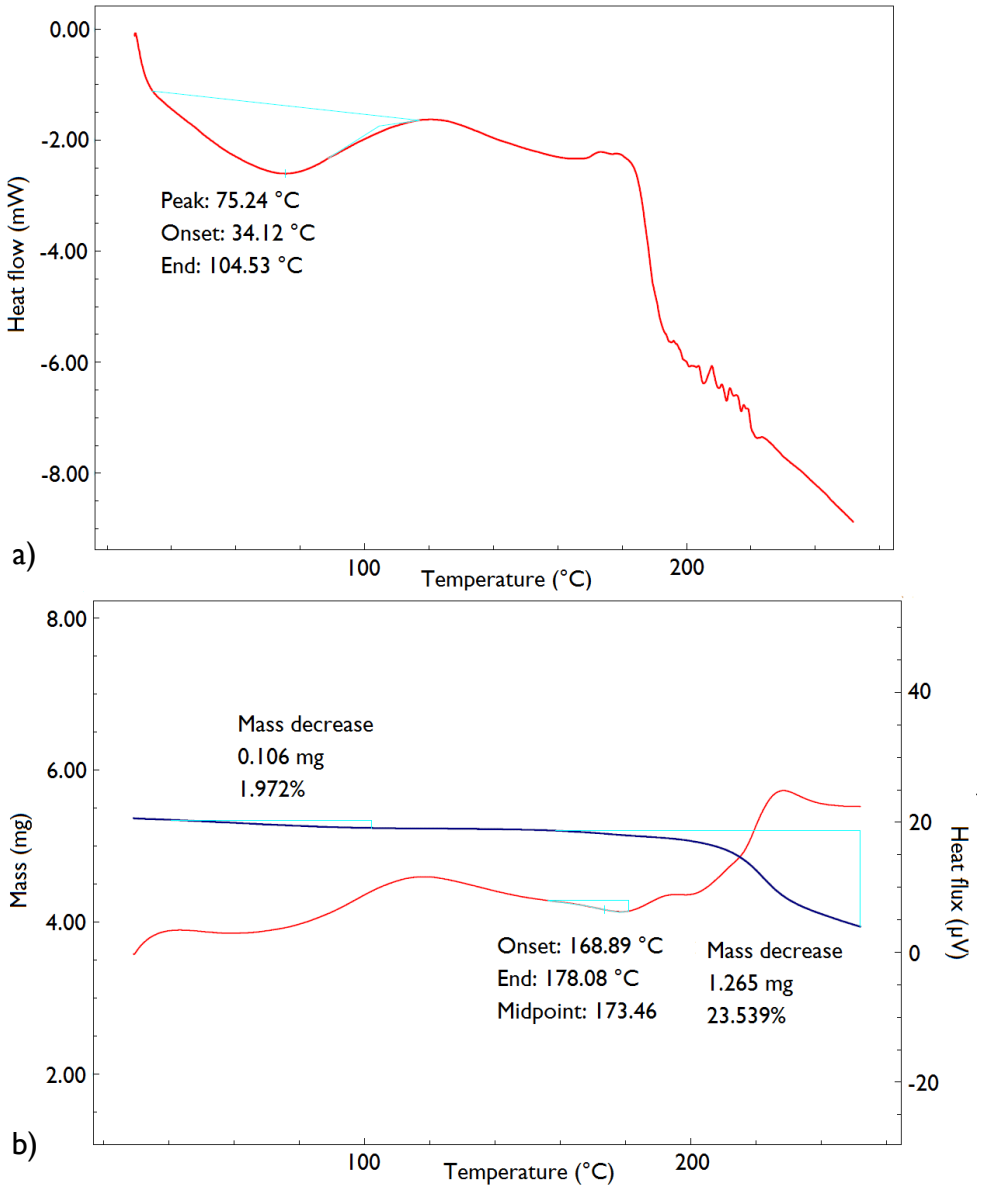

Figure 4.17 (a) Differential scanning calorimetry (DSC) thermogram and (b) thermogravimetric analysis trace (blue) with a simultaneous differential thermal analysis (DTA) trace (red) obtained for spray-dried green rooibos extract with inulin (1:1; $m.m^{-1}$).

Fig. 4.18a shows the DSC thermogram obtained for the formulation containing rooibos extract and maltodextrin. A very pronounced endotherm was visible in the temperature region of 35–115 °C, ascribed to the surface adsorbed moisture as discussed previously. The resulting thermogram of the rooibos-maltodextrin mixture does not differ from the thermograms of the individual components, therefore it can be concluded that there no interactions between the GRE and maltodextrin (Addendum B; Fig. 7.3).

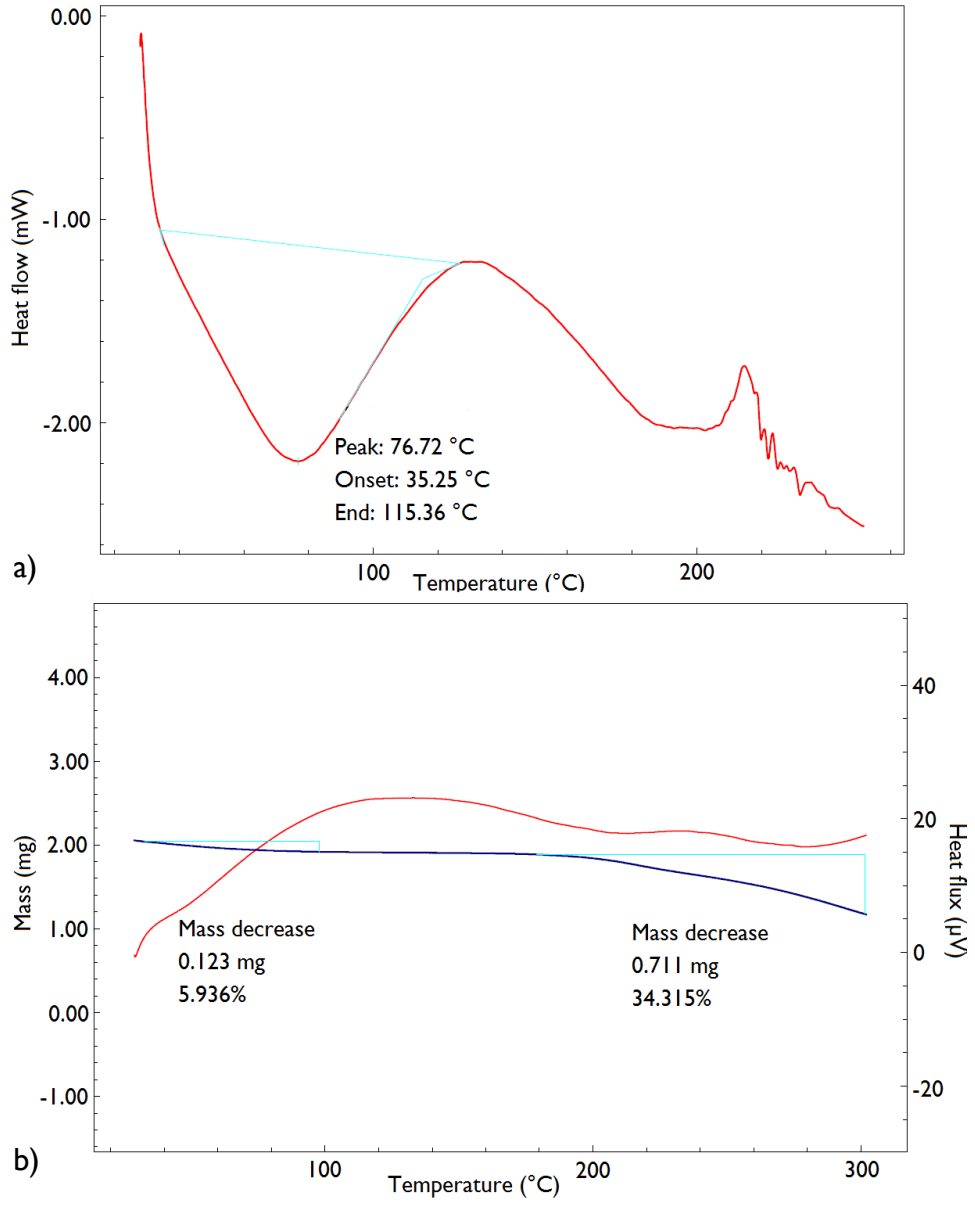

Figure 4.18 (a) Differential scanning calorimetry (DSC) thermogram and (b) thermogravimetric analysis trace (blue) with a simultaneous differential thermal analysis (DTA) trace (red) obtained for spray-dried green rooibos extract with maltodextrin (1:1; $m.m^{-1}$).

From data obtained for thermal analysis it could be concluded that the GRE is compatible with both inulin and maltodextrin, confirming the results obtained with isothermal microcalorimetry. The thermogravimetric analyses additionally showed that all the samples contained adsorbed surface moisture to some extent. Stojanovic *et al.* (2012) used simultaneous TGA/DTA analysis to investigate the thermal behaviour of calcium alginate encapsulated thyme extract, and also found that dehydration of the polymer network resulted in a significant mass decrease in the range 50–150 °C, followed by a second mass decrease from 220 °C, which was attributed to degradation of the major phenolic compounds present in the aqueous thyme extract.

Sugars that are commonly found in food products, such as fructose, glucose and sucrose, typically have low T_G (5, 31 and 62 °C), and their effect on reducing the T_G is very notable in sugar-rich products which tend to crystallise more readily when exposed to increasing storage temperatures and relative humidity (Bhandari & Howes, 1999). Spray-drying of sugar-rich products are generally not economically feasible unless high molecular weight carrier materials are added to increase the T_G. If the product temperature is above the T_G, the amorphous material exists in a rubbery state characterised by greater molecular mobility and a tendency to become excessively sticky. It has been recommended that spray-drying processes should be designed in such a manner as to avoid exposing particle surfaces to a temperature 10–20 °C above the T_G, thus reducing stickiness and improving solids recovery (Roos & Karel, 1991; Woo *et al.*, 2009; Keshani *et al.*, 2015). In practice, this would include ensuring that the mean T_{OA} of the spray-dryer remains below the T_G. While it was not possible to reliably identify exact T_Gs for the three different SDEs in the present study, the high powder yields obtained in all the validation experiments (>77 %) suggest that their T_G value were higher than the mean outlet temperatures to which they were subjected during the drying process (105–109 °C).

While it is important to consider glass transition phenomena during the drying process, it is also crucial to ensure that the dried product is properly stored afterwards. Moisture can depress the T_G of spray-dried powders significantly, since water has a very low T_G of ≈-135 °C (Johari *et al.*, 1987). Additional moisture uptake should be minimised and/or prevented by using water-impermeable packaging material, e.g. aluminium foil (Newman *et al.*, 2008). Even small amounts of moisture uptake could result in significant quality deterioration. A localised area of moisture uptake, e.g. due to damaged or inadequate packaging, could result in accelerated, localised crystallisation reactions. The tightly packed crystalline structure will tend to expel adsorbed water, and this moisture will be absorbed at the surface of neighbouring particles, forming interparticulate liquid bridges in the process. This undesirable phenomenon is referred to as "caking" (Peleg & Hollenbach, 1984; Bhandari & Howes, 1999). Furthermore, the expelled moisture could initiate crystallisation in new sites, resulting in a "domino effect" of detrimental crystal formation. The development of caking is time-dependent, with longer exposure to adverse storage conditions resulting in more

extensive caking, whereas stickiness is a relatively instantaneous phenomenon (Bhandari & Howes, 1999). The spray-dried product should be cooled to an appropriately low temperature ($<T_G$) before packaging to minimise any further physical changes.

Kawai *et al.* (2011) investigated the thermal behaviour of commercial inulin powder of different molecular weights (MW). High-performance (HP) inulin (DP = 27), specifically designed to remove low molecular weight fractions, was compared with low-MW and native inulin (DP = 7 and 13, respectively). The authors confirmed that the T_G of high-performance inulin (145.1 °C) was higher than that of low-MW and native inulin (111.4 and 125 °C, respectively). Low-MW and native inulin also exhibited substantially greater moisture sorption tendencies at >60% RH. Schaller-Povolny *et al.* (2000) demonstrated that the use of high-MW Raftiline HP inulin (DP = 23) was preferable over low-MW inulin since it showed less tendency to cake at high RH, and retained its desirable characteristics over the greatest range of a_w. The authors recommended the use of HP inulin for the formulation of a more stable dried product. This reinforces the recommendation that HP, high-MW inulin, similar to the kind used in the present study, is the preferred form of inulin to be used as carrier material for a high-value nutraceutical powder.

4.4.5.7. Wettability (Contact angle measurement)

As wettability is inversely proportional to the contact angle value, the formulation with the lowest contact angle value, i.e. the inulin-containing formulation, displayed the most favourable wettability properties (Table 4.17). The pure GRE and the maltodextrin-containing formulation had contact angle values of >90°, which classifies these SDEs as hydrophobic, whereas the extract-inulin formulation had a contact angle <90°, indicating hydrophilicity and the ability to readily form a common interface with water molecules (Anderson, 1986; Yuan & Lee, 2013). Fig. 4.19, showing images captured during the wettability analyses, supports these findings, as the extract-inulin powder can clearly be seen to coalesce with the water droplet (Fig. 4.19b), whereas the droplets were repelled by surfaces of the powdered extract and extract-maltodextrin mixture (Figs. 4.19a & C, respectively). The wettability of a powder will have a substantial effect on its overall solubility, since wetting is a precursor to dissolution (Anderson, 1986). Based on the present findings, inulin would be the preferred encapsulant for a spray-dried green rooibos extract with intended nutraceutical applications, since a poorly soluble SDE may present a major obstacle. Many potential new pharmaceutical preparations prove ineligible for further development due to poor dissolution profiles, since they are typically marked by low intestinal absorption and bioavailability (Behera *et al.*, 2010).

Table 4.17 Contact angle measurements for three different green rooibos spray-dried extract formulations.

Sample	Mean contact angle (°) ± standard deviation
Pure extract	94.90 ± 2.93
Extract: inulin (1:1; $m.m^{-1}$)	81.15 ± 1.11
Extract: maltodextrin (1:1; $m.m^{-1}$)	97.75 ± 5.23

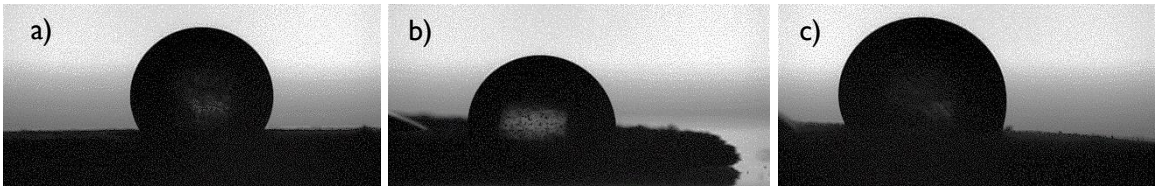

Figure 4.19 Photographs showing detail of distilled water droplet on compressed powder bed for contact angle measurement of spray-dried (a) pure green rooibos (GR) extract, (b) GR extract with inulin (1:1 mass ratio) and (c) GR extract with maltodextrin (1:1 mass ratio).

4.4.5.8. Density and flow characteristics

Density and flow characteristics are important quality attributes to consider in the development of a powdered extract, since it may affect handling, distribution and storage, especially in a scaled-up production setting (Tenou *et al.*, 1999; Prescott & Barnum, 2000). Carr's compressibility index (CCI) and the Hausner ratio, both derived from the poured and tapped bulk density values, are frequently used to broadly classify the flow characteristics of powders (Table 4.18).

Table 4.18 Powder flow characteristics based on Carr's compressibility index (CCI) and Hausner ratio (Carr, 1965; Fitzpatrick, 2013).

Flow character	CCI (%)	Hausner ratio[1]
Very, very poor	> 38	> 1.60
Very poor	32–37	1.46–1.59
Poor	26–31	1.35–1.45
Passable	21–25	1.26–1.34
Fair	16–20	1.19–1.25
Good	11–15	1.12–1.18
Excellent	0–10	1.00–1.11

[1] tapped ÷ poured bulk density

The flow characteristics of spray-dried pure green rooibos extract was not improved by the addition of maltodextrin in terms of its Hausner ratio, but it did result in a very slight worsening of

the flow characteristics according to the CCI (Table 4.19). Lumping, affecting flowability, was visually evident for the extract-maltodextrin mixture (Fig. 4.12c). The addition of inulin resulted in improved flow characteristics as both the CCI and Hausner ratio classifications changed from "fair" to "good". This provides further evidence that inulin, aside from its potential health benefits, would be an ideal carrier material for the nutraceutical formulation in terms of optimising process efficiency.

Table 4.19 Density and flow characteristics of optimised spray-dried green rooibos extracts according to Carr's compressibility index (CC1) and the Hausner ratio.

Sample	Poured bulk density ($g.mL^{-1}$)	Tapped bulk density ($g.mL^{-1}$)	CCI (%)	Hausner ratio[1]
Pure extract	0.243	0.288	16.0 (fair)	1.2 (fair)
Extract: inulin (1:1; $m.m^{-1}$)	0.269	0.309	12.7 (good)	1.1 (good)
Extract: maltodextrin (1:1; $m.m^{-1}$)	0.232	0.279	16.7 (fair)	1.2 (fair)

[1] tapped ÷ poured bulk density

4.5. Conclusion

Laboratory-scale spray-drying of aqueous green rooibos extracts, optimised by a quality-by-design approach, was effective in producing free-flowing amorphous powders with low moisture content and water activity immediately after drying. The very brief period of exposure of the spray-dried particles to the heated drying air (≈1 s), which typically does not exceed ≈110 °C in temperature, ensured that the heat-labile bioactive compound, aspalathin, was well retained within the dried product immediately after drying (>89%). In validation experiments which compared a carrier-free powder formulation with formulations containing inulin and maltodextrin, respectively, it was noted that aspalathin retention was not improved by the addition of a carrier. The addition of carrier materials did reduce the a_w of the powders, however, which would improve storage stability by limiting the amount of water available for degradative chemical reactions. Maltodextrin or inulin could provide the additional benefit of raising the T_G of the amorphous powders, which would prevent the transition to a less stable rubbery state characterised by stickiness and, eventually, caking. The moderately hygroscopic nature of the powders, as well as their tendency to deliquesce at high levels of RH, emphasises the importance of using appropriate storage conditions (<25 °C and

<40% RH) and packaging material to prevent deterioration of quality throughout the subsequent processing steps leading to the manufacture of a commercially viable end-product

4.6. References

Addala, R., Vasavada, M., Dong, J. & Subramanian, S. (2015). Effect of storage conditions on rate of color degradation of paprika based products. *Journal of Food Processing & Technology*, **6**, doi: 10.4172/2157-7110.1000423.

Al-Muhtaseb, A.H., McMinn, W.A.M. & Magee, T.R.A. (2002). Moisture sorption isotherm characteristics of food products: a review. *Food and Bioproducts Processing*, **80**, 118–128.

Ameri, M. & Maa, Y.F. (2006). Spray drying of biopharmaceuticals: stability and process considerations. *Drying Technology*, **24**, 763–768.

Anderson, W.G. (1986). Wettability literature survey — part 2: wettability measurement. *Journal of Petroleum Technology*, **38**, 1246–1261.

Azmir, J., Zaidul, I.S.M., Rahman, M.M., Sharif, K.M., Mohamed, A., Sahena, F., Jahurul, M.H.A., Ghafoor, K., Norulaini, N.A.N. & Omar, A.K.M. (2013). Techniques for extraction of bioactive compounds from plant materials: a review. *Journal of Food Engineering*, **117**, 426–436.

Bakowska-Barczak, A.M & Kolodziejczyk, P.P. (2011). Black currant polyphenols: their storage stability and microencapsulation. *Industrial Crops and Products*, **34**, 1301–1309.

Baldinger, A., Clerdent, L., Rantanen, J., Yang, M. & Groghanz, H. (2012). Quality by design approach in the optimization of the spray drying process. *Pharmaceutical Development and Technology*, **17**, 389–397.

Behera, A.L., Sahoo, S.K. & Patil, S.V. (2010). Enhancement of solubility: a pharmaceutical overview. *Der Pharmacia Lettre*, **2**, 310–318.

Belščak-Cvitanović, A., Lević, S. Kalušević, A., Špoljarić, I., Đorđević, V., Komes, D., Mršić, G. & Nedović, V. (2015). Efficiency assessment of natural biopolymers as encapsulants of green tea (*Camellia sinensis* L.) bioactive compounds by spray drying. *Food and Bioprocess Technology*, **8**, 2444–2460.

Bhandari, B.R. & Howes, T. (1999). Implication of glass transition for the drying and stability of dried foods. *Journal of Food Engineering*, **40**, 71–79.

Blahovec, J. & Yanniotis, S. (2008). GAB generalized equation for sorption phenomena. *Food and Bioprocess Technology*, **1**, 82–90.

Büchi (2009). *B-290 Operation Manual Version H.* Flawil, Switzerland: Büchi Labortechnik AG.

Cal, K. & Sollohub, K. (2010). Spray drying technique. I: Hardware and process parameters. *Journal of Pharmaceutical Sciences*, **99**, 575–586.

Callahan, J.C., Cleary, G.W., Elefant, M., Kaplan, G., Kensler, T. & Nash, R.A. (1982). Equilibrium moisture content of pharmaceutical excipients. *Drug Development and Industrial Pharmacy*, **8**, 355–369.

Caliskan, G. & Dirim, S.N. (2013). The effects of the different drying conditions and the amounts of maltodextrin addition during spray drying of sumac extract. *Food and Bioproducts Processing*, **91**, 539–548.

Carr, R.L. (1965). Classifying flow properties of solids. *Chemical Engineering*, **72**, 69–72.

Chadha, R. & Bhandari, S. (2014). Drug–excipient compatibility screening — role of thermoanalytical and spectroscopic techniques. *Journal of Pharmaceutical and Biomedical Analysis*, **87**, 82–97.

Costa, S.S., Machado, B.A.S., Martin, A.R., Bagnara, F, Ragadalli, S.A. & Alves, A.R.C. (2015). Drying by spray drying in the food industry: micro-encapsulation, process parameters and main carriers used. *African Journal of Food Science*, **9**, 462–470.

Dan, A., Ghosh, S. & Moulik, S.P. (2009). Physicochemical studies on the biopolymer inulin: a critical evaluation of its self-aggregation, aggregate-morphology, interaction with water, and thermal stability. *Biopolymers*, **91**, 687–699.

De Barros Fernandes, R.V., Borges, S.V., Botrel, D.A, Silva, E.K., Da Costa, J.M.G. & Queioz, F. (2013). Microencapsulation of rosemary essential oil: characterization of particles. *Drying Technology*, **31**, 1245–1254.

De Beer, D., Malherbe, C.J., Beelders, T., Willenburg, E.L., Brand, D.J. & Joubert, E. (2015). Isolation of aspalathin and nothofagin from rooibos (*Aspalathus linearis*) using high-performance countercurrent chromatography: sample loading and compound stability considerations. *Journal of Chromatography A*, **1381**, 29–36.

Donlao, N. & Siriwattanayotin, S. (2012). Moisture adsorption isotherms of assam green tea powder. In: 1st Mae Fah Luang University International Conference. Pp. 1–9. November 2012. Muang, Thailand.

Englyst, H.N., Veenstra, J. & Hudson, G.J. (1996). Measurement of rapidly available glucose (RAG) in plant foods: a potential *in vitro* predictor of the glycaemic response. *British Journal of Nutrition*, **75**, 327–337.

Fitzpatrick, J. (2013). Powder properties in food production systems. In: *Handbook of Food Powders: Processes and Properties* (edited by B. Bhandari). Pp. 285–308. Cambridge: Woodhead Publishing.

Gabas, A.L., Telis, V.R.N., Sobral, P.J.A. & Telis-Romero, J. (2007). Effect of maltodextrin and arabic gum in water vapor sorption thermodynamic properties of vacuum dried pineapple pulp powder. *Journal of Food Engineering*, **82**, 246–252.

Gargari, B.P, Dehghan, P., Aliasgharzadeh, A. & Jafar-abadi, M.A. (2013). Effects of high-performance inulin supplementation on glycemic control and antioxidant status in women with type 2 diabetes. *Diabetes & Metabolism Journal*, **37**, 140–148.

Gharsallaoui, A., Roudaut, G., Chambin, O., Voilley, A. & Saurel, R. (2007). Applications of spray drying in microencapsulation of food ingredients: an overview. *Food Research International*, **40**, 1107–1121.

Gross, L.S., Li, L., Ford, E.S. & Liu, S. (2004). Increased consumption of refined carbohydrates and the epidemic of type 2 diabetes in the United States: an ecologic assessment. *The American Journal of Clinical Nutrition*, **79**, 774–779.

Hashemiravan, M., Mazloom, A.S. & Farhaydar, N. (2013). Nano particles of blueberry in inulin and β-cyclodextrin microcapsules. *International Journal of Nanoscience and Nanotechnology*, **9**, 185–192.

Jadhav, N., Gaikwad, V., Nair, K. & Kadam, H. (2009). Glass transition temperature: basics and application in pharmaceutical sector. *Asian Journal of Pharmaceutics*, **3**, 82–89.

Johari, G.P., Hallbruker, A., & Mayer, E. (1987). The glass liquid transition of hyperquenched water. *Nature*, **330**, 552–553.

Joubert, E. (1988). Technical note: effect of agglomeration on the properties of spray-dried rooibos tea. *International Journal of Food Science and Technology*, **23**, 20–207.

Joubert, E. & Ferreira, D. (1996). Antioxidants of rooibos tea — a possible explanation for its health promoting properties?. *The South African Journal of Food Science and Nutrition*, **8**, 79–83.

Joubert, E., Viljoen, M., De Beer, D., Malherbe, C.J., Brand, D.J. & Manley, M. (2010). Use of green rooibos (*Aspalathus linearis*) extract and water-soluble nanomicelles of green rooibos extract encapsulated with ascorbic acid for enhanced aspalathin content in ready-to-drink iced teas. *Journal of Agricultural and Food Chemistry*, **58**, 10965–10971.

Joubert, E., Viljoen, M., De Beer, D. & Manley, M. (2009). Effect of heat on aspalathin, iso-orientin, and orientin contents and color of fermented rooibos (*Aspalathus linearis*) iced tea. *Journal of Agricultural and Food Chemistry*, **57**, 4204–4211.

Kawai, K., Fukami, K., Thanatuksorn, P., Viriyarattanasak, C. & Kajiwara, K. (2011). Effects of moisture content, molecular weight, and crystallinity on the glass transition temperature of inulin. *Carbohydrate Polymers*, **83**, 934–939.

Keshani, S., Daud, W.R.W., Nourouzi, M.M., Namvar, F. & Ghasemi, M. (2015). Spray drying: an overview on wall deposition, process and modeling. *Journal of Food Engineering*, **146**, 152–162.

Kolida, S., Tuohy, K. & Gibson, G.R. (2002). Prebiotic effects of inulin and oligofructose. *British Journal of Nutrition*, 87, S193–S197.

Labuza, T.P. & Altunakar, B. (2007). Water activity and moisture sorption isotherms. In: *Water Activity in Foods: Fundamentals and Applications* (edited by G.V. Barbosa-Cánovas, A.J. Fontana, S.J. Schmidt & T.P. Labuza). Pp. 109–154. Ames: Blackwell Publishing, Ltd.

Le Meste, M., Champion, D., Roudaut, G., Blond, G. & Simatos, D. (2002). Glass transition and food technology: a critical appraisal. *Journal of Food Science*, **67**, 2444–2458.

Mensink, M.A., Frijlink, H.W., Van der Voort Maarschalk, K. & Hinrichs, W.L.J. (2015a). Inulin, a flexible oligosaccharide I: Review of its physicochemical characteristics. *Carbohydrate Polymers*, **130**, 405–419.

Mensink, M.A., Frijlink, H.W., Van der Voort Maarschalk, K. & Hinrichs, W.L.J. (2015b). Inulin, a flexible oligosaccharide II: Review of its pharmaceutical applications. *Carbohydrate Polymers*, **134**, 418–428.

Newman, A.W., Reutzel-Edens, S.M. & Zografi, G. (2008). Characterization of the "hygroscopic" properties of active pharmaceutical ingredients. *Journal of Pharmaceutical Sciences*, **97**, 1047–1059.

Nunes, G.L., Boaventura, B.C.B., Pinto, S.S., Verruck, S., Murakami, F.S., Prudêncio, E.S. & Amboni, R.D.D.M.C. (2015). Microencapsulation of freeze concentrated *Ilex paraguariensis* extract by spray drying. *Journal of Food Engineering*, **151**, 60–68.

Oakley, D., 1994. Scale-up of spray dryers with the aid of computational fluid dynamics. *Drying Technology*, **12**, 217–233.

Ortiz, J., Ferruzzi, M.G., Taylor, L.S. & Mauer, L.J. (2008). Interaction of environmental moisture with powdered green tea formulations: effect on catechin chemical stability. *Journal of Agricultural and Food Chemistry*, **56**, 4068–4077.

Ott, R.L. & Longnecker, M. (2010). *An Introduction to Statistical Methods and Data Analysis*, 6th ed. Belmont, California: Duxbury Press.

Patel, B.B., Patel, J.K., Chakraborty, S. & Shukla, D. (2015). Revealing facts behind spray dried solid dispersion technology used for solubility enhancement. *Saudi Pharmaceutical Journal*, **23**, 352–365.

Pauck, C.E. (2016). Effects of formulation on the stability of green *Cyclopia subternata* extract during spray-drying and storage. MSc Food Science Thesis, Stellenbosch University, South Africa.

Peleg, M., & Hollenbach, A. M. (1984). Flow conditioners and anticaking agents. *Food Technology*, **38**, 93–99.

Prescott, J.K. & Barnum, R.A. (2000). On powder flowability. *Pharmaceutical Technology*, **23**, 60–84.

Ré, M.I. (1998). Microencapsulation by spray drying. *Drying Technology*, **16**, 1195–1236.

Rhim, J.W. & Hong, S.I. (2011). Effect of water activity and temperature on the color change of red pepper (*Capsicum annuum* L.) powder. *Food Science and Biotechnology*, **20**, 215–222.

Ronkart, S.N., Paquot, M., Blecker, C.S., Fougnies, C., Doran, L., Lambrechts, J.C., Norberg, B. & Deroanne, C. (2009). Impact of the crystallinity on the physical properties of inulin during water sorption. *Food Biophysics*, **4**, 49–58.

Rosenberg, M., Kopelman, I.J. & Talmon, Y. (1985). A scanning electron microscopy study of microencapsulation. *Journal of Food Science*, **50**, 139–144.

Roos, Y., & Karel, M. (1991). Plasticizing effect of water on thermal behavior and crystallization of amorphous food models. *Journal of Food Science*, **56**, 38–43.

Roos, Y. H., Karel, M., & Kokini, J. L. (1996). Glass transitions in low moisture and frozen foods: effect on shelf life and quality. *Food Technology*, **50**, 95–108.

Sablani, S.S., Kasapis, S. & Rahman, M.S. (2007). Evaluating water activity and glass transition concepts for food stability. *Journal of Food Engineering*, **78**, 266–271.

Saénz, C., Tapia, S., Chávez, J. & Robert, P. (2009). Microencapsulation by spray drying of bioactive compounds from cactus pear (*Opuntia ficus-indica*). *Food Chemistry*, **114**, 616–622.

Şahin-Nadeem, H., Torun, M. & Özdemir, F. (2011). Spray drying of the mountain tea (*Sideritis stricta*) water extract by using different hydrocolloid carriers. *LWT – Food Science and Technology*, **44**, 1626–1635.

Saraph, J.V., Benson, P.G. & Schroeder, R.G. (1989). An instrument for measuring the critical factors of quality management. *Decision Sciences*, **20**, 810–829.

Schaller-Povolny, L.A., Smith, D.E. & Labuza, T.P. (2000). Effect of water content and molecular weight on the moisture isotherms and glass transition properties of inulin. *International Journal of Food Properties*, **3**, 173–192.

Shah, M.V. & Rohit, M.C. (2013). Novel techniques for isolation and extraction of phyto-constituents from herbal plants. *American Journal of Phytomedicine and Clinical Therapeutics*, **1**, 338–350.

Shapiro, S.S. & Wilk, M.B. (1965). An analysis of variance test for normality (complete samples). *Biometrika*, **52**, 591–611.

Slade, L., Levine, H., Ievolella, J., & Wang, M. (1993). The glassy state phenomenon in applications for the food industry: application of the food polymer science approach to structure — function relationships of sucrose in cookie and cracker systems. *Journal of the Science of Food and Agriculture*, **63**, 133–176.

Slavin, J. (2013). Fiber and prebiotics: mechanism and health benefits. *Nutrients*, **5**, 1417–1435.

Sollohub, K. & Cal, K. (2010). Spray drying technique. II. Current applications in pharmaceutical technology. *Journal of Pharmaceutical Sciences*, **99**, 587–597.

Stojanovic, R., Belscak-Cvitanovic, A., Manojlovic, V., Komes, D., Nedovic, V. & Bugarski, B. (2012). Encapsulation of thyme (*Thymus serpyllum* L.) aqueous extract in calcium alginate beads. *Journal of the Science of Food and Agriculture*, **92**, 685–696.

Tenou, E., Fitzpatrick, J.J. & Synnot, E.C. (1999). Characterisation of food powder flowability. *Journal of Food Engineering*, **39**, 31–37.

Timmermann, E.O. (2003). Multilayer sorption parameters: BET or GAB values?. *Colloids and Surfaces A: Physicochemical and Engineering Aspects*, **220**, 235–260.

Timmermann, E.O., Chirife, J. & Iglesias, H.A. (2001). Water sorption isotherms of foods and foodstuffs: BET and GAB parameters. *Journal of Food Engineering*, **48**, 19–31.

Toneli, J., Park, K., Negreiros, A. & Murr, F. (2010). Spray-drying process optimization of chicory root inulin. *Drying Technology*, **28**, 369–379.

Van Drooge, D.J., Hinrichs, W.L.J., Visser, M.R. & Frijlink, H.W. (2006). Characterization of the molecular distribution of drugs in glassy solid dispersions at the nano-meter scale, using differential scanning calorimetry and gravimetric water vapour sorption techniques. *International Journal of Pharmaceutics*, **310**, 220–229.

Woo, M.W. & Bhandari, B. (2013). Spray drying for food powder production. In: *Handbook of Food Powders: Processes and Properties* (edited by B. Bhandari). Pp. 29–56. Cambridge: Woodhead Publishing.

Woo, M., Daud, W.R.W., Tasirin, S.M. & Talib, M.Z.M. (2009). Controlling food powder deposition in spray dryers: wall surface energy manipulation as an alternative. *Journal of Food Engineering*, **94**, 192–198.

Yuan, Y. & Lee, T.R. (2013). Contact angle and wetting properties. In: *Surface Science Techniques* (edited by G. Bracco and B. Holst). Pp. 3–34. Berlin: Springer-Verlag, GmbH.

5. General Discussion and Conclusions

In view of the growing global epidemic of lifestyle-related chronic illnesses, including obesity and type 2 diabetes mellitus (T2D) (Guarigata *et al.*, 2014; Ng *et al.*, 2014; IDF, 2016), the development of a nutraceutical or functional food ingredient with health-promoting attributes against metabolic disease could be a meaningful pursuit. Such a condition-specific nutraceutical has a greater chance in the market place, given the many nutraceutical products that are put on the market every year. Manufacturers have moved on from antioxidant plant extracts and are seeking either novel ingredients and/or extracts that can be marketed with specific health conditions in mind (Dormán *et al.*, 2016). The bioactivity of aspalathin and green rooibos extracts (GREs) containing significant amounts of aspalathin (as previously discussed in Chapter 2), in particular their antidiabetic effects, motivated the development of a nutraceutical extract from green rooibos (GR), creating a need for the current research on the optimisation of a production process for GRE. Specifying minimum aspalathin values for GRE to ensure efficacy as an anti-diabetic nutraceutical is not yet possible, as additional research is required to determine the minimum therapeutic dose needed for bioactivity. However, the maximum recovery of aspalathin from the plant material is an important precursor to such considerations as it would have an impact on the formulation and product cost.

Analysis of 47 production batches of GR, sampled from a major producer during a short period of just 48 days during summer and early autumn, confirmed substantial variation in the composition of the plant material, even though all the batches originated from the same plantation. The plantation was established using seedlings from randomly collected seeds produced by open-pollinated plants, as per normal industry practice. Batch-to-batch variations in the theoretical extract yield, total polyphenol content and total antioxidant capacity, as well as the content of the major flavonoids, aspalathin, nothofagin, orientin and iso-orientin were indicated. The aspalathin content of the large sample set (Batches A1–47) of GR ranged between 2.5 and 4.5% of the dried plant material, and the aspalathin content of Batch B (harvested 20 August 2014), used for extract optimisation, was 2.4%. This is quite low compared with some reported results for GR, which also showed that the aspalathin content of GR plant material varies significantly. Joubert & Schulz (2006) found that whole, dried shoots of GR (n = 97), originating from 24 plantations, contained between 3.80 and 9.70% of aspalathin (mean = 6.60%). Joubert *et al.* (2013) reported aspalathin content of GR leaves varying from 5.97–13.48 (mean = 9.68%) for 54 plants sampled from two plantations. As these results indicate, problematic variation in the raw materials could be expected in the production of a standardised GRE, especially if the production batches are sourced from different geographical areas and are subject to different quality assurance protocols or post-harvest processing methods. Minor discrepancies between the processing conditions for the different production batches, e.g. time delays between the harvesting, shredding and drying steps, could also have contributed to the variation. The aspalathin content of rooibos decreases rapidly due to oxidation once the plant material is bruised and shredded, as reported in a study by Joubert (1996).

After 15 min of oxidation, <80% of the initial aspalathin content of the leaf remained, and after 210 min just a third of the initial aspalathin content was still present. This emphasises the need for strict control of the handling of the fresh material and the drying unit operation for GR intended as raw material for a high-value GRE, so that maximal retention of the target compound can be facilitated from the earliest possible stage.

Risk assessment and preliminary "one-factor-at-a-time" (OFAT) experiments showed that the extraction time, extraction temperature, water-to-plant material ratio and particle size all had significant effects ($P < 0.05$) on the yields of aspalathin and extract (hot water soluble solids), as well as on the content of aspalathin in the extract. Particle size distribution may differ between individual production batches of GR and, therefore, only the extraction time, temperature and the water-to-plant material ratio were optimised using a batch of "fine cut" green rooibos with optimisation techniques employing central composite design and response surface methodology (RSM). Multi-response desirability profiling was used to identify optimal extraction conditions, and critical process parameters (CPPs) were identified based on statistical analyses and informed by considerations of cost-efficiency (Table 5.1)

Table 5.1 Critical process parameters for optimised hot water extraction and spray-drying of green rooibos.

Unit operation	Parameter (unit)	Range
Hot water extraction	Extraction time (min)	29–31
	Extraction temperature (°C)	90–95
	Water-to-plant material ratio ($v.m^{-1}$)	9–11
Spray-drying	Inlet air temperature (°C)	210–230
	Feed concentration (%; g solids per 100 g H_2O)	9–11
	Feed flow rate (% peristaltic pump performance)	34–36[1]

[1] Translates to a volumetric flow rate of 10.3–11.2 $mL.min^{-1}$ (≈0.62–0.67 $L.h^{-1}$) (Büchi, 2009).

Validation of the polynomial prediction models for aspalathin extraction efficiency (Asp_EE; %, g extracted per 100 g aspalathin in plant material) and extract yield (g soluble solids per 100 g plant material) showed that predicted values were not always achievable when producing extracts with batches of plant material different from that which was used to generate the model data. Batch B was used to generate the prediction model data in the present study. When the "optimal" extraction parameters of 93 °C, 30 min and 10:1 water-to-plant material ratio ($v.m^{-1}$) were applied to batches A1–47, the minimum predicted extract yield of 16.79% was not obtained in seven instances, and the predicted minimum Asp_EE of 76.35% was not reached in *any* of the hot water

extractions. The most likely cause for this was the heterogeneous distribution of aspalathin in the plant material, particularly in the stems and leaves, as well as major differences in the leaf particle sizes and amount of coarse, woody material in the respective batches.

From the results it was evident that it would be difficult to reliably predict a guaranteed amount of aspalathin in the extract. This was reflected in the weak linear correlation (R^2 = 0.483) between the total dihydrochalcone content in the extracts and their corresponding plant material (GR production batches A1–A47), as well as the poor predictive ability of the polynomial prediction model for this response generated by RSM. The extraction rates of aspalathin and soluble solids are both enhanced, to various degrees, by higher temperatures and water-to-plant material ratios, as well as longer extraction times. The aspalathin content of the extract (Asp_HWE) is a function of both of these variables, represented by the formula

$$Asp_{HWE} = \frac{Aspalathin\ yield}{Extract\ yield} \times 100$$

This could explain why regression analysis revealed no significant effect of the extraction temperature on Asp_HWE, and why verification of the polynomial prediction model for this response showed poor predictive ability. The aspalathin and extract yields both increased significantly ($P < 0.05$) with increasing temperature, with the result that only minor increases in Asp_HWE were observed. The Asp_HWE remained within a relatively narrow range (10–14%) even with large differences in temperature, unlike the extract yield.

Despite not having obtained the predicted minimum response according to the polynomial model, a minimum of 15% water soluble solids yield was achieved in all optimised hot water extractions (mean ± SD = 19.26 ± 2.16) using the commercial GR batches "as-is", i.e. without a preliminary sieving step. Similarly, a minimum Asp_HWE of 8.1% (mean ± SD = 10.67 ± 0.96) was obtained. This suggests that, theoretically, one could expect at least 15% soluble solids recovery and 8% aspalathin in the hot water extract obtained from most GR production batches with at least 2.5% aspalathin content and when operating within the CPP's. Manley *et al.* (2006) reported that a minimum level of 4% aspalathin in dried GR plant material has been specified in the past by a major extract manufacturer in order to produce extracts containing at least 15% aspalathin.

Quantification of individual phenolic compounds in plant material is often achieved by high performance liquid chromatography (HPLC) analysis due to its high selectivity and accuracy, but it typically requires additional sample preparation. Such comprehensive and time-consuming analyses are usually not required in an industrial setting, and rapid screening methods for raw plant materials at an early stage of production could be of great practical benefit. It would enable the identification of batches of plant material which meet the minimum quality criteria in terms of the target compound content. Examples of potential screening tools which have been investigated for GR

include near-infrared spectroscopy (Schulz *et al.*, 2003; Manley *et al.*, 2006), Fourier transmission (FT)-Raman spectroscopy (Baranska *et al.*, 2006) and ultraviolet (UV) spectroscopy and colourimetric methods (Joubert *et al.*, 2008).

Extracting specific secondary plant metabolites, like aspalathin, from botanical raw materials for extract production is complicated by the heterogeneous distribution of these compounds within the plant material. The accumulation of secondary metabolites is thought to be part of an evolved natural defence mechanism in plants which helps repair oxidative stress damage and deter predation, and this accumulation may not occur at the same rate or to the same extent in different parts of the plant matrix (Petrussa *et al.*, 1996). Flavonoid glycosides, like aspalathin, are thought to play a major role in the protection of plants against UV light-induced oxidative damage (Aherne & O'Brien, 2002). Consequently, they tend to occur predominantly in the leaves, stems, flowers and other peripheral parts of plants (e.g. fruit skins or peels), and typically decrease in concentration towards the core of the plant matrix (Winkel-Shirley, 2002; Lattanzio *et al.*, 2008). Kotina *et al.* (2012) reported that the coarser wood and bark fragments of fermented rooibos contained mostly colourless phloem and xylem upon investigation of microscopic cross sections. Using FT-Raman spectroscopy, Baranska *et al.* (2006) observed heterogeneous distribution of aspalathin in GR leaves, with the highest concentrations noted in the central part of the leaf.

Joubert (1984) showed that rooibos waste material provided a low yield of water soluble solids (8.9%) compared with a refined fraction containing mostly leaves (20.4%). Joubert & De Beer (2012) described the composition of 74 batches of unrefined (i.e. comminuted but not sieved) fermented rooibos plant material in terms of three particle size fractions: >10 (coarse), 10>x>40 (refined tea) and <40 mesh (dust). A weak (r = 0.300), but significant (P = 0.009) negative correlation was observed between the size of the coarse fraction and the yield of soluble solids from the unrefined tea. It was reported previously that the coarse, woody particles were considered useful for the production of extracts since the appearance of the plant material is not as important. However, this would only hold true for the production of a rooibos extract in which the aspalathin content is not of main concern, e.g. for flavour applications. For the production of a GRE high in aspalathin or total phenolic content, the use of waste material would be contra-indicated, and only the most highly refined and virtually wood-free plant material batches should be selected. In the present study, a nearly four-fold increase in the Asp_HWE of Batch B was achieved using the smallest particle size fraction (<20 mesh; 18.55%) compared with only the largest particle size fraction (>12 mesh; 4.64%).

Laboratory-scale spray-drying of the GRE, preceded by risk assessment and preliminary OFAT experiments to establish basic operating parameters, produced amorphous powders with low moisture content (<4%, dry basis; MC_{db}) and water activity (<0.17; a_w) immediately after drying.

The very brief period of exposure of the spray-dried particles to the heated drying air (≈1 s), which typically does not exceed ≈110 °C in temperature, ensured that the heat-labile bioactive compound, aspalathin (Joubert *et al.*, 2009; De Beer *et al.*, 2012; De Beer *et al.*, 2015), was well retained within the dried product immediately after drying (>89%). RSM optimisation and regression analysis showed that only the powder yield could be predicted accurately by a polynomial model, and this response was therefore selected as the primary indicator of the spray-drying process efficiency.

Despite the statistical analyses indicating that optimal powder yields will be obtained with a 10% feed concentration, this may not be the optimal setting in terms of overall process efficiency if energy consumption is taken into account. The energy consumption is directly proportional to the drying rate which, in turn, is proportional to the differential between the inlet and outlet air temperatures of the drying chamber (Filkova & Mujumdar, 1995). At a fixed drying rate, the energy consumption will be determined mainly by the feed concentration. An increase in feed solids content from 10 to 25% can result in a 66.6% reduction in energy consumption (Filkova & Mujumdar, 1995). Joubert (1988) spray-dried a 1:1 mixture fermented rooibos hot water soluble solids and maltodextrin at a feed concentration of >30%, using an industrial type pilot-plant spray dryer. Scale-up of the spray-drying unit operation to an industrial setting may involve the use of a two or three-stage spray-drying system. This refers to a system in which an additional drying step(s) is added, after and/or before the spray-drying step, in order to further reduce energy consumption. Filkova & Mujumdar (1995) recommended that as much water should be removed from the feed as possible before spray-drying, whilst still ensuring a pumpable feed. Such a preconcentration step, which may be carried out using membrane processes or vacuum evaporation, could result in significant energy savings (Table 5.2).

Table 5.2 Spray-drying energy consumption for various feed concentrations at fixed drying rate (Filkova & Mujumdar, 1995).

Feed concentration (%)[1]	Approximate energy consumption[2]
10	23.65×10^3
20	10.46×10^3
30	6.17×10^3
40	3.97×10^3
50	2.68×10^3

[1] g total solids per 100 g water; [2] $kJ.kg^{-1}$ powder yield

In validation experiments which compared a carrier-free extract powder with formulations containing extract with inulin or maltodextrin, respectively, it was noted that aspalathin retention was not improved by the addition of a carrier. The addition of carrier materials did reduce the a_w of the powders, however, which would improve storage stability by limiting the amount of water available for degradative chemical reactions. X-ray powder diffraction confirmed the amorphous nature of all the powders. Maltodextrin or inulin could provide the additional benefit of raising the glass transition temperature of the amorphous extract powder, which would prevent the transition to a less stable rubbery state characterised by stickiness and, eventually, caking (Bhandari & Howes, 1999). Monolayer moisture content values (M_0), falling within the range of 0.2–0.3 a_w, were determined for all the SDEs using the BET and GAB sorption models. For each SDE, the a_w was <0.2 and the MC_{db} was lower than the corresponding M_0 values (GAB or BET), indicating that the powders can thus be considered shelf-stable if stored under appropriate conditions which would prohibit further moisture uptake (Al-Muhtaseb *et al.*, 2002). The moderately hygroscopic nature of the powders, as well as their tendency to deliquesce at high relative humidity (RH) levels, emphasises the importance of using appropriate storage conditions (<25 °C and <40% RH) and packaging material to prevent deterioration of quality throughout the subsequent processing steps leading to the manufacture of a commercially viable end-product. Deliquescence of the powders, i.e. transformation from a solid to a saturated solution above a threshold environmental moisture content, occurred at ≈60% RH. Deliquescence is of particular importance in food products, since the presence of different chemical compounds with unique deliquescent behaviour in a complex blend, such as a powdered herbal extract, leads to lowering of the deliquescence point (Mauer & Taylor, 2010). Deliquescence promotes the degradation of labile compounds (since reactions occur more readily in solution), as well as the tendency of the powdered mixture to agglomerate and cake (Salameh *et al.*, 2007). If the powders remain dry, no interaction should occur between its constituents since no incompatibilities were detected using isothermal microcalorimetry.

Genetic factors aside, in the production of herbal nutraceutical extracts, batch-to-batch variation starts from the collection of the raw material, and these variations may be magnified during storage and further processing of the intermediate products, e.g. spray-dried powders. Therefore, standardisation of this type of product should encompass the entire production process, from cultivation to distribution and storage (Calixto *et al.*, 2000; Kunle *et al.*, 2012). From the earliest stages, it is crucial to establish good agricultural practices (GAP) for any herbal raw material in order to avoid contamination by foreign matter or microorganisms, which may also lead to deterioration and rejection of the plant material (World Health Organization, 1992). Recently, analysis of rooibos herbal tea has demonstrated the presence of pyrrolizidine alkaloids (PAs) (Bodi *et al.*, 2014; Huybrechts & Callebaut; 2015; Shimshoni *et al.*, 2015). PAs are a class of secondary plant

metabolites with species dependent carcinogenic, hepatotoxic, genotoxic and pneumotoxic risks (Huybrechts & Callebaut, 2015), and their presence in rooibos tea strongly suggests contamination of the plant material with weeds (Joubert, E., 2016, ARC Infruitec-Nietvoorbij, Stellenbosch, personal communication, 30 August).

To ensure that the optimal extraction of aspalathin from GR plant material is achieved, quality-by-design (QbD) methodology should ideally be applied to the "upstream" processing steps at the harvesting, cutting, drying and raw material storage steps since they have a direct impact on the quality of the input material for the hot water extraction unit operation (Fig. 5.1). This would most likely ensure that a more consistent set of quality attributes are obtained in the GRE, which can then be carried over to the next unit operation to become an input material with its own set of criteria.

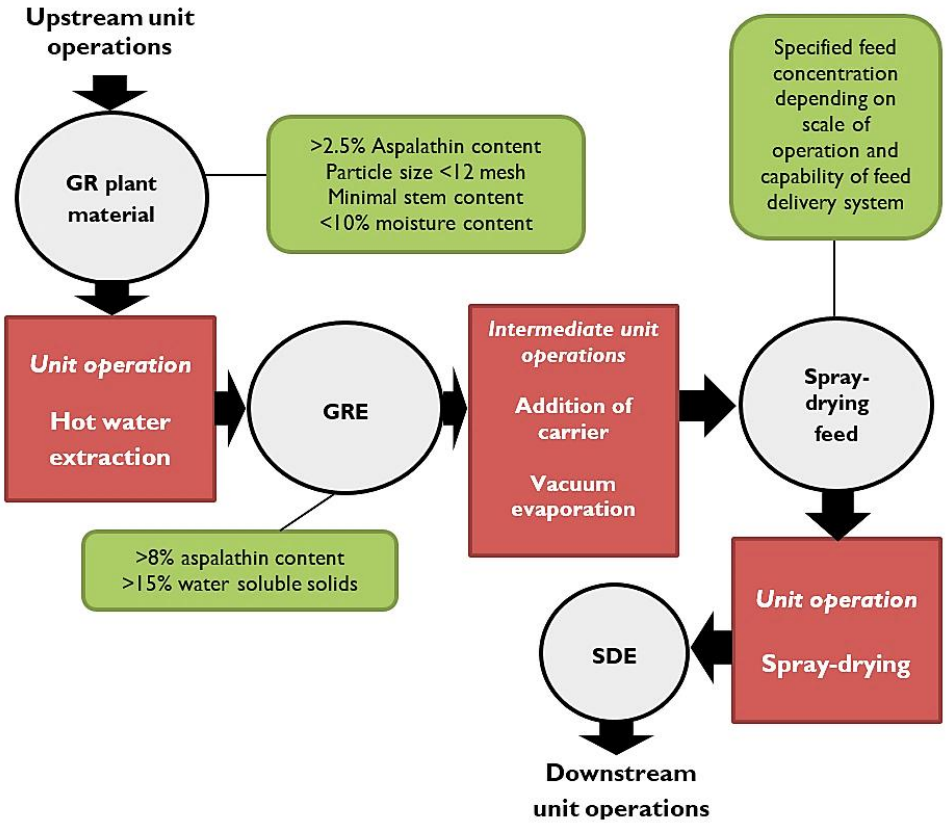

Figure 5.1 Diagram of a hypothetical production process for a green rooibos (GR) nutraceutical showing a series of unit operations and their inputs/outputs. GRE, green rooibos extract. SDE, spray-dried extract.

As demonstrated by the results of the RSM extractions, the efficiency of the HWE unit operation would most likely be affected by the specific attributes of the plant material used in a given instance. The amount of aspalathin different GR production batches, which typically consist of processed material from various individual plants which are pooled together at a certain point in the production process, may differ. The plant material particles sizes may vary from batch to batch, for

instance, due to the tendency of one operator to cut a larger average leaf size than another. The stem content of some production batches may be higher than those of others due to less stringent control of particle size at the processing level. Standardisation of the GR production batches in terms of particle size could possibly be achieved to a certain degree by sieving out particles above a specified size (e.g. 12 mesh), but the inherent variation in the aspalathin content of individual leaf particles would still most likely result in variability in the aspalathin content of the final extract, albeit perhaps to a lesser degree.

For the manufacturer intent on maximising profit, the maximum amount of product should be obtained from each kg of raw material. Discarding coarse or "unwanted" material would therefore be advantageous in terms of maximising soluble solids recovery from the raw material, but that would mean discarding a sometimes significant fraction of the bulk material which has been purchased. Therefore, manufacturers should ensure that, when purchasing batches of GR for GRE production, it contains only "useable" plant material.

It is therefore clear that the plant material to be used for extraction should have a small particle size (<12 mesh) and minimal stem content. The length of the needle-like leaf particles should be as short as possible, since this enhances the rate of diffusion of the target compound from the leaf interior to the solvent and therefore ensures that more of the target compound (i.e. aspalathin) would be extracted within the 30 min extraction time period. Plant material intended specifically for the production of aspalathin-enriched extracts should preferably be virtually free of stem material to achieve extracts with high aspalathin content values and the length of leaf particles should be as short as possible (≈5–10 mm). Milling of the material to obtain smaller particle size would reduce the limitations of mass transfer and increase the extraction rate due to a shorter diffusion distance for solutes within the plant matrix (Azmir *et al.*, 2013). However, excessively fine plant material could complicate filtration of the extract by passing through coarse mesh screens or by causing blockages of bag filters.

Standardisation of herbal pharmaceuticals or nutraceuticals to a specific bioactive or marker compound is often achieved with the aid of excipients, i.e. inert substances added for their functional properties (Staniforth, 1993; Kunle *et al.*, 2012). The challenges of predicting an exact concentration of aspalathin in the SDE may thus be ameliorated by the addition of varying amounts of an excipient to the final product in order to achieve a standardised aspalathin content. Herbal extracts are often prone to undergoing quality deterioration during storage due to ongoing chemical reactions between the different constituents, which could lead to a reduction in the bioactive compound and possibly even the formation of toxic metabolites (Thakur *et al.*, 2011). Shelf-stability testing of the GR SDE should be carried out in the future in order to ascertain whether its critical quality attributes are retained over a long storage period and after exposure to adverse environmental conditions.

Additional compatibility testing would have to be carried out for the extract and any other excipient which may be added further along the production line.

The potential of the GRE as a functional food ingredient could be explored further. Possible applications include the formulation and development of value-added baked goods containing GRE, similar to what has been described by Wang *et al.* (2007) and Pasrija *et al.* (2015) for bread incorporating green tea (*Camellia sinensis*) extract. The high antioxidant activity of green tea extracts has prompted investigation into their use as a preservative in a number of products, particularly meat products which are prone to lipid oxidation and colour instability (Senanayake, 2013). Lavelli *et al.* (2010) investigated the fortification of a dried apple product with green tea extract and found that it improved the antioxidant activity of the apple product 3–5 fold. Similar applications could be found for GRE with high levels of aspalathin, a potent antioxidant (Von Gadow *et al.*, 1997; Snijman *et al.*, 2009). Recent investigations have shown that rooibos extract delayed lipid oxidation in ostrich meat (Cullere *et al.*, 2013; Hoffman *et al.*, 2014; Jones *et al.*, 2015). The findings of this study would be largely applicable to a production process utilising fermented rooibos as well, although changes in the extract composition may affect physicochemical properties of the spray-dried powder.

In summary, the primary objectives of this study were realised, pointing the way towards further research aimed at the production of a health-promoting, value-added extract of green *Aspalathus linearis*.

References

Aherne, S.A. & O'Brien, N.M. (2002). Dietary flavonoids: chemistry, food content and metabolism. *Nutrition*, **18**, 75–81.

Al-Muhtaseb, A.H., McMinn, W.A.M. & Magee, T.R.A. (2002). Moisture sorption isotherm characteristics of food products: a review. *Food and Bioproducts Processing*, **80**, 118–128.

Azmir, J., Zaidul, I.S.M., Rahman, M.M., Sharif, K.M., Mohamed, A., Sahena, F., Jahurul, M.H.A., Ghafoor, K., Norulaini, N.A.N. & Omar, A.K.M. (2013). Techniques for extraction of bioactive compounds from plant materials: a review. *Journal of Food Engineering*, **117**, 426–436.

Baranska, M., Schulz, H., Joubert, E. & Manley, M. (2006). In situ flavonoid analysis by FT-Raman spectroscopy: identification, distribution, and quantification of aspalathin in green rooibos (*Aspalathus linearis*). *Analytical Chemistry*, **78**, 7716–7721.

Bhandari, B.R. & Howes, T. (1999). Implication of glass transition for the drying and stability of dried foods. *Journal of Food Engineering*, **40**, 71–79.

Bodi, D., Ronczka, S., Gottschalk, C., Behr, N., Skibba, A., Wagner, M., Lahrssen-Wiederholt, M., Preiss-Weigert, A. & These, A. (2014). Determination of pyrrolizidine alkaloids in tea, herbal drugs and honey. *Food Additives & Contaminants: Part A*, **31**, 1886–1895.

Büchi (2009). *B-290 Operation Manual Version H.* Flawil, Switzerland: Büchi Labortechnik AG.

Calixto, J.B. (2000). Efficacy, safety, quality control, marketing and regulatory guidelines for herbal medicines (phytotherapeutic agents). *Brazilian Journal of Medical and Biological Research*, **33**, 179–189.

Cullere, M., Hoffman, L.C. & Dalle Zotte, A. (2013). First evaluation of unfermented and fermented rooibos (*Aspalathus linearis*) in preventing lipid oxidation in meat products. *Meat Science*, **95**, 72–77.

De Beer, D., Joubert, E., Viljoen, M. & Manley, M. (2012). Enhancing aspalathin stability in rooibos (*Aspalathus linearis*) ready-to-drink iced teas during storage: the role of nano-emulsification and beverage ingredients, citric and ascorbic acids. *Journal of the Science of Food and Agriculture*, **94**, 272–284.

De Beer, D., Malherbe, C.J., Beelders, T., Willenburg, E.L., Brand, D.J. & Joubert, E. (2015). Isolation of aspalathin and nothofagin from rooibos (As*palathus linearis*) using high-performance countercurrent chromatography: sample loading and compound stability considerations. *Journal of Chromatography A*, **1381**, 29–36.

Dormán, G., Flachner, B., Hajdú, I. & András, C.D. (2016). Target identification and polypharmacology of nutraceuticals. In: *Nutraceuticals: Efficacy, Safety and Toxicity* (edited by R.C. Gupta). Pp. 263–286. Cambridge: Academic Press.

Filkova, I. & Mujumdar, A.S. (1995). Industrial spray drying systems. In: *Handbook of Industrial Drying*, 2nd ed., Vol. 1. (edited by S. Mujumdar). Pp. 263–308. Florida: CRC Press.

Guarigata, L., Whiting, D.R., Hambleton, I., Beagley, J., Linnenkamp, U. & Shaw, J.E. (2014). Global estimates of diabetes prevalence for 2013 and projections for 2035. *Diabetes Research and Clinical Practice*, **103**, 137–149.

Hoffman, L.C., Jones, M., Muller, N., Joubert, E. & Sadie, A. (2014). Lipid and protein stability and sensory evaluation of ostrich (*Struthio camelus*) droëwors with the addition of rooibos tea extract (*Aspalathus linearis*) as a natural antioxidant. *Meat Science*, **96**, 1289–1296.

Huybrechts, B. & Callebaut, A. (2015). Pyrrolizidine alkaloids in food and feed on the Belgian market. *Food Additives & Contaminants: Part A*, **32**, 1939–1951.

IDF (2016). International Diabetes Federation — South Africa. [Internet document]. URL http://www.idf.org/membership/afr/south-africa. 07/12/2016.

Jones, M., Hoffman, L.C. & Muller, M. (2015). Effect of rooibos extract (*Aspalathus linearis*) on lipid oxidation over time and the sensory analysis of blesbok (*Damaliscus pygargus phillipsi*) and springbok (*Antidorcas marsupialis*) droëwors. *Meat Science*, **103**, 54–60.

Joubert, E. (1984). Studies in verband met verkitsing van rooibos tee (*Aspalathus linearis*). MSc Food Science Thesis, Stellenbosch University, South Africa.

Joubert, E. (1988). Effect of batch extraction conditions on yield of soluble solids from rooibos tea. *International Journal of Food Science and Technology*, **23**, 43–47.

Joubert, E. (1996). HPLC quantification of the dihydrochalcones, aspalathin and nothofagin in rooibos tea (*Aspalathus linearis*) as affected by processing. *Food Chemistry*, **55**, 403–411.

Joubert, E. & De Beer, D. (2012). Phenolic content and antioxidant activity of rooibos food ingredient extracts. *Journal of Food Composition and Analysis*, **27**, 45–51.

Joubert, E., De Beer, D., Malherbe, C.J., Muller, N., Bonnet, S.L., Van der Westhuizen, J.H. & Ferreira, D. (2013). Occurrence and sensory perception of *Z*-2-(ß-D-glucopyranosyloxy)-3-phenylpropenoic acid in rooibos (*Aspalathus linearis)*. *Food Chemistry*, **136**, 1078–1085.

Joubert, E., Manley, M. & Botha, M. (2008). Evaluation of spectroscopic methods for screening of green rooibos (*Aspalathus linearis*) and green honeybush (*Cyclopia genistoides*) extracts for high levels of bio-active compounds. *Phytochemical Analysis*, **19**, 169–178.

Joubert, E. & Schulz, H. (2006). Production and quality aspects of rooibos tea and quality products. A review. *Journal of Applied Botany and Food Quality*, **80**, 138–144.

Joubert, E., Viljoen, M., De Beer, D. & Manley, M. (2009). Effect of heat on aspalathin, iso-orientin, and orientin contents and color of fermented rooibos (*Aspalathus linearis*) iced tea. *Journal of Agricultural and Food Chemistry*, **57**, 4204–4211.

Kotina, E.L., Stepanova, A.V., Tilney, P.M. & Van Wyk, B.-E. (2012). The pharmacognostic value of leaf and stem anatomy in rooibos tea (*Aspalathus linearis*). *South African Journal of Botany*, **82**, 129–133.

Kunle, O.F., Egharevba, H.O. & Ahmadu, P.O. (2012). Standardization of herbal medicines — a review. *International Journal of Biodiversity and Conservation*, **4**, 101–112.

Lattanzio, V., Kroon, P.A., Quideau, S. & Treutter, D. (2008). Plant phenolics – secondary metabolites with diverse functions. In: *Recent Advances in Polyphenol Research, Vol. 1* (edited by F. Daayf & V. Lattanzio). Pp. 1–35. New Jersey: Wiley-Blackwell.

Lavelli, V., Vantaggi, C., Corey, M. & Kerr, W. (2010). Formulation of a dry green tea-apple product: study on antioxidant and color Stability. *Journal of Food Science*, **75**, C184–C190.

Manley, M., Joubert, E. & Botha, M. (2006). Quantification of the major phenolic compounds, soluble solid content and total antioxidant activity of green rooibos (*Aspalathus linearis*) by means of near infrared spectroscopy. *Journal of Near Infrared Spectroscopy*, **14**, 213–222.

Mauer, L.J. & Taylor, L.S. (2010). Water-solids interactions: deliquescence. *Annual Review of Food Science and Technology*, **1**, 41–63.

Ng, M., Fleming, T., Robinson, M., Thomson, B., Graetz, N., *et al.* (2014). Global, regional, and national prevalence of overweight and obesity in children and adults during 1980–2013: a systematic analysis for the global burden of disease study 2013. *The Lancet*, **384**, 766–781.

Pasrija, D., Ezhilarasi, P.N., Indrani, D. & Anandharamkrishnan, C. (2015). Microencapsulation of green tea polyphenols and its effect on incorporated bread quality. *LWT – Food Science and Technology*, **64**, 289–296.

Petrussa, E., Braidot, E., Zancani, M., Peresson, C., Bertolini, A., Patui, S. & Vianello, A. (2013). Plant flavonoids — biosynthesis, transport and involvement in stress responses. *International Journal of Molecular Science*, **14**, 14950–14973.

Salameh, A.K., Mauer, L.J. and Taylor, L.S. (2006). Deliquescence lowering in food ingredient mixtures. *Journal of Food Science*, **71**, E10–E16.

Schulz, H., Joubert, E. & Schütze, W. (2003). Quantification of quality parameters for reliable evaluation of green rooibos (*Aspalathus linearis*). *European Food Research and Technology*, **216**, 539–543.

Senanayake, S.N. (2013). Green tea extract: chemistry, antioxidant properties and food applications — a review. *Journal of Functional Foods*, **5**, 1529–1541.

Shimshoni, J.A., Duebecke, A., Mulder, P.P., Cuneah, O. & Barel, S. (2015). Pyrrolizidine and tropane alkaloids in teas and the herbal teas peppermint, rooibos and chamomile in the Israeli market. *Food Additives & Contaminants: Part A*, **32**, 2058–2067.

Snijman, P.W., Joubert, E., Ferreira, D., Li, X.C., Ding, Y., Green, I.R. & Gelderblom, W.C.A. (2009). Antioxidant activity of the dihydrochalcones aspalathin and nothofagin and their corresponding flavones in relation to other rooibos (*Aspalathus linearis*) flavonoids, epigallocatechin gallate, and trolox. *Journal of Agricultural and Food Chemistry*, **57**, 6678–6684.

Staniforth, J.N. (1993). The design and use of tableting excipients. *Drug Development and Industrial Pharmacy*, **19**, 2273–2308.

Thakur, L., Ghodasra, U., Patel, N. & Dabhi, M. (2011). Novel approaches for stability improvement in natural medicines. *Pharmacognosy Reviews*, **5**, 48–54.

Von Gadow, A., Joubert, E. & Hansmann, C.F. (1997). Comparison of the antioxidant activity of rooibos tea (*Aspalathus linearis*) with green, oolong and black tea. *Food Chemistry*, **60**, 73–77.

Wang, R., Zhou, W. & Isabelle, M. (2007). Comparison study of the effect of green tea extract (GTE) on the quality of bread by instrumental analysis and sensory evaluation. *Food Research International*, **40**, 470–479.

WHO (1992). Quality control methods for medicinal plant materials. World Health Organization, Geneva.

Winkel-Shirley, B. (2002). Biosynthesis of flavonoids and effects of stress. *Current Opinion in Plant Biology*, **5**, 218–223.

6. Addendum A: Supplementary data pertaining to Chapter 3

6.1. Validation of practical optimum hot water extraction parameters

Table 6.1 Yields of major rooibos flavonoids[1] and soluble solids (SS) in optimised hot water extracts (n = 47) and their content in corresponding freeze-dried extracts (FDEs) and plant material production batches.

Batch	Content in plant material[2]				Yields[2]					Extraction efficiency (%)[3]				Content in extract (%)[4]			
	Asp	Iso	Ori	Not	Asp	Iso	Ori	Not	SS	Asp	Iso	Ori	Not	Asp	Iso	Ori	Not
A1	3.788	0.429	0.415	0.287	2.498	0.280	0.215	0.189	20.840	65.941	65.270	51.936	65.876	11.987	1.343	1.032	0.909
A2	3.661	0.434	0.438	0.254	2.378	0.269	0.204	0.170	22.051	64.944	61.821	46.585	67.004	10.782	1.218	0.923	0.772
A3	4.246	0.448	0.447	0.324	2.650	0.274	0.214	0.198	21.783	62.420	61.190	47.783	61.357	12.156	1.258	0.979	0.911
A4	3.711	0.443	0.445	0.286	2.428	0.283	0.217	0.192	21.145	65.419	63.747	48.816	67.292	11.488	1.337	1.026	0.910
A5	3.473	0.414	0.420	0.311	2.298	0.277	0.216	0.204	21.408	66.184	66.946	51.461	65.471	10.727	1.293	1.009	0.950
A6	3.417	0.396	0.384	0.284	2.470	0.293	0.237	0.200	21.554	72.295	74.135	61.696	70.254	11.460	1.361	1.099	0.926
A7	2.800	0.361	0.363	0.280	1.457	0.199	0.166	0.159	16.337	52.044	55.289	45.656	56.765	8.944	1.222	1.016	0.973
A8	2.504	0.356	0.356	0.264	1.250	0.178	0.147	0.145	15.411	49.916	50.074	41.418	54.736	8.108	1.157	0.957	0.938
A9	3.502	0.399	0.400	0.338	1.890	0.211	0.176	0.154	17.594	53.967	52.826	44.045	45.612	10.743	1.197	1.001	0.875
A10	3.484	0.370	0.366	0.266	1.831	0.206	0.171	0.147	17.536	52.557	55.707	46.743	55.347	10.439	1.175	0.975	0.840
A11	2.838	0.331	0.329	0.262	1.479	0.173	0.144	0.128	15.070	52.112	52.267	43.844	48.653	9.810	1.148	0.957	0.847
A12	3.111	0.349	0.348	0.269	1.552	0.177	0.147	0.140	15.779	49.886	50.659	42.303	52.083	9.841	1.120	0.934	0.888
A13	3.210	0.337	0.328	0.314	1.744	0.182	0.151	0.165	17.237	54.332	53.997	45.955	52.659	10.108	1.057	0.874	0.956
A14	2.920	0.344	0.346	0.275	1.938	0.217	0.178	0.162	19.944	66.390	63.124	51.532	58.797	9.713	1.090	0.895	0.810
A15	3.418	0.391	0.390	0.287	1.735	0.202	0.171	0.163	17.236	50.750	51.551	43.819	56.747	10.068	1.170	0.992	0.946
A16	3.845	0.435	0.439	0.303	1.567	0.182	0.153	0.148	17.115	40.758	41.828	34.713	48.831	9.157	1.063	0.890	0.865
A17	2.722	0.330	0.324	0.322	1.511	0.180	0.145	0.142	17.072	55.496	54.535	44.789	44.086	8.843	1.055	0.852	0.831
A18	3.734	0.409	0.406	0.417	1.798	0.207	0.168	0.204	16.468	48.154	50.554	41.433	48.961	10.915	1.255	1.021	1.239
A19	3.020	0.379	0.375	0.315	1.594	0.182	0.154	0.173	17.513	52.774	48.138	41.092	54.760	9.108	1.042	0.880	0.988
A20	3.598	0.390	0.388	0.364	1.974	0.223	0.183	0.202	16.667	54.877	57.309	47.106	55.505	11.560	1.308	1.069	1.182
A21	3.265	0.369	0.367	0.359	1.563	0.182	0.150	0.161	16.231	47.866	49.212	40.828	44.951	9.751	1.134	0.936	1.007
A22	4.488	0.455	0.448	0.508	2.178	0.231	0.189	0.227	18.195	48.530	50.775	42.287	44.755	11.879	1.260	1.033	1.239

A23	4.095	0.454	0.449	0.465	1.912	0.217	0.181	0.200	18.125	46.686	47.744	40.247	42.936	10.595	1.203	1.003	1.108
A24	3.906	0.393	0.391	0.422	2.399	0.251	0.210	0.239	20.594	61.416	63.892	53.733	56.687	11.409	1.195	0.999	1.139
A25	3.389	0.388	0.383	0.354	1.938	0.226	0.183	0.195	19.551	57.175	58.356	47.795	55.212	9.708	1.135	0.918	0.979
A26	3.870	0.396	0.391	0.460	2.485	0.264	0.209	0.275	19.901	64.205	66.543	53.376	59.800	12.053	1.280	1.013	1.333
A27	3.945	0.424	0.422	0.468	2.402	0.261	0.211	0.260	20.425	60.890	61.653	50.101	55.553	11.695	1.272	1.029	1.265
A28	3.813	0.382	0.380	0.446	2.140	0.230	0.189	0.219	18.918	56.127	60.104	49.749	49.043	11.200	1.203	0.989	1.146
A29	3.695	0.388	0.384	0.428	2.046	0.230	0.186	0.230	19.260	55.386	59.325	48.404	53.793	10.698	1.203	0.970	1.203
A30	3.946	0.391	0.386	0.450	2.262	0.238	0.191	0.247	19.600	57.334	60.892	49.354	54.796	11.659	1.227	0.982	1.271
A31	4.007	0.422	0.418	0.474	2.107	0.231	0.190	0.232	19.764	52.589	54.762	45.314	48.972	10.932	1.200	0.984	1.205
A32	3.907	0.412	0.415	0.381	2.150	0.237	0.199	0.170	22.069	55.039	57.634	47.871	44.598	10.125	1.116	0.934	0.801
A33	3.744	0.428	0.434	0.323	2.200	0.242	0.206	0.179	22.109	58.742	56.499	47.417	55.220	10.126	1.113	0.949	0.823
A34	4.337	0.455	0.464	0.359	2.420	0.282	0.229	0.195	22.892	55.784	61.912	49.509	54.344	10.569	1.230	1.003	0.852
A35	3.667	0.420	0.424	0.309	2.510	0.284	0.234	0.218	20.392	68.446	67.796	55.154	70.407	12.330	1.398	1.148	1.069
A36	3.563	0.410	0.412	0.346	2.064	0.239	0.196	0.186	21.218	57.928	58.424	47.577	53.678	9.742	1.130	0.924	0.876
A37	3.820	0.451	0.458	0.339	2.168	0.245	0.202	0.187	21.184	56.739	54.308	44.114	55.085	10.220	1.154	0.954	0.879
A38	3.539	0.427	0.434	0.316	2.089	0.244	0.202	0.178	20.962	59.034	57.202	46.616	56.270	9.951	1.164	0.964	0.846
A39	3.891	0.441	0.443	0.353	2.289	0.252	0.208	0.190	21.310	58.836	57.127	46.911	53.709	10.737	1.183	0.975	0.890
A40	3.781	0.421	0.429	0.293	2.142	0.236	0.194	0.160	20.759	56.654	56.080	45.339	54.513	10.322	1.138	0.937	0.770
A41	3.616	0.421	0.428	0.278	2.170	0.242	0.206	0.154	20.946	60.019	57.515	48.090	55.202	10.362	1.156	0.982	0.733
A42	3.040	0.373	0.382	0.218	2.098	0.250	0.209	0.150	21.978	69.032	67.045	54.825	68.779	9.552	1.137	0.953	0.682
A43	3.624	0.400	0.419	0.329	2.350	0.256	0.215	0.208	22.043	64.842	63.857	51.332	63.098	10.656	1.159	0.975	0.941
A44	3.290	0.390	0.386	0.362	1.690	0.205	0.168	0.179	16.710	51.376	52.560	43.534	49.433	10.109	1.227	1.004	1.069
A45	3.398	0.397	0.395	0.379	1.671	0.196	0.163	0.170	17.963	49.172	49.425	41.204	44.776	9.293	1.092	0.904	0.944
A46	3.747	0.421	0.425	0.378	1.775	0.207	0.171	0.172	18.017	47.373	49.302	40.348	45.613	9.846	1.151	0.950	0.957
A47	4.119	0.455	0.457	0.390	1.952	0.213	0.178	0.183	18.715	47.403	46.712	38.968	46.830	10.433	1.136	0.951	0.976

[1] Asp = aspalathin, Iso = iso-orientin, Ori = orientin, Not = nothofagin; [2] g.100 g^{-1} plant material; [3] (Extract yield/Content in plant material)*(100); [4] g.100 g^{-1} freeze-dried extract

6.2. One-factor-at-a-time (OFAT) extractions

6.2.1. Effect of extraction time on extraction efficiency

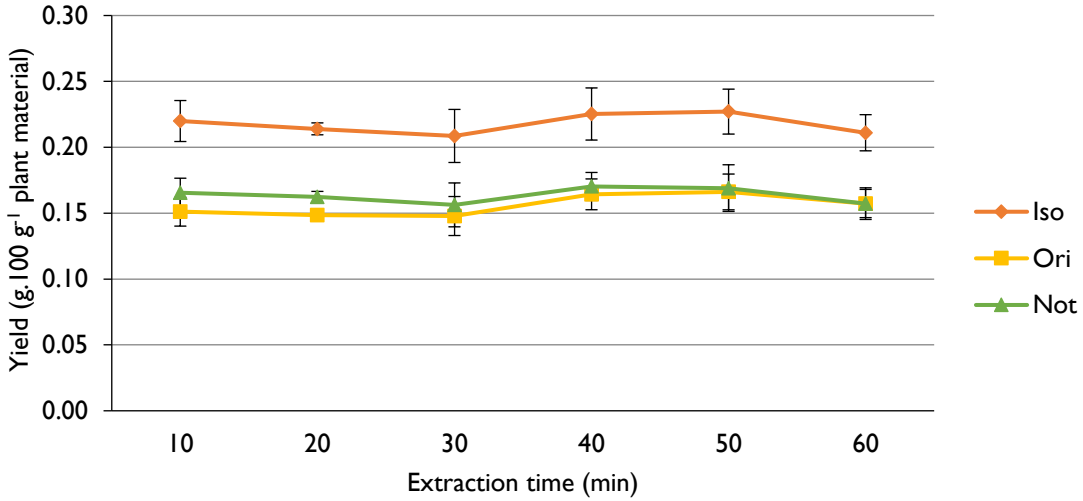

Figure 6.1 Effect of extraction time on yields of iso-orientin (Iso), orientin (Ori) and nothofagin (Not) in green rooibos hot water extract (extraction temperature = 93 °C; water-to-plant material ratio = 10:1, v.m^{-1}).

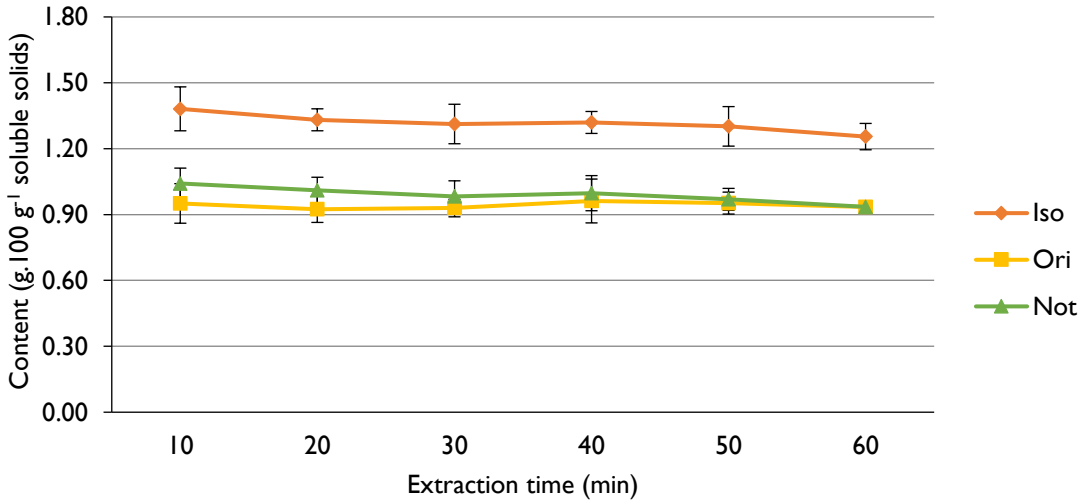

Figure 6.2 Effect of extraction time on contents of iso-orientin (Iso), orientin (Ori) and nothofagin (Not) in green rooibos hot water extract (extraction temperature = 93 °C; water-to-plant material ratio = 10:1, v.m^{-1}).

6.2.2. Effect of extraction temperature on extraction efficiency

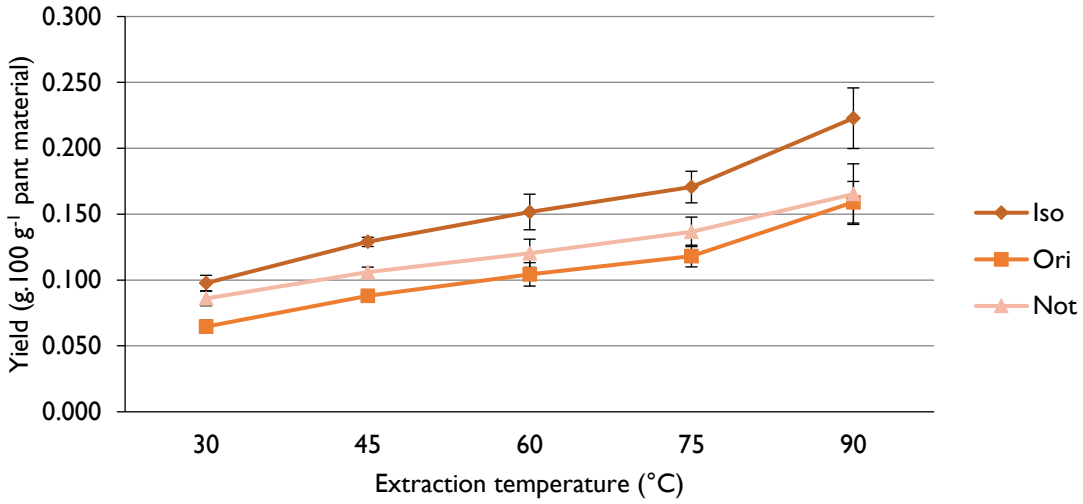

Figure 6.3 Effect of extraction temperature on yields of iso-orientin (Iso), orientin (Ori) and nothofagin (Not) in green rooibos hot water extract (extraction time = 20 min; water-to-plant material ratio = 10:1, v.m^{-1}).

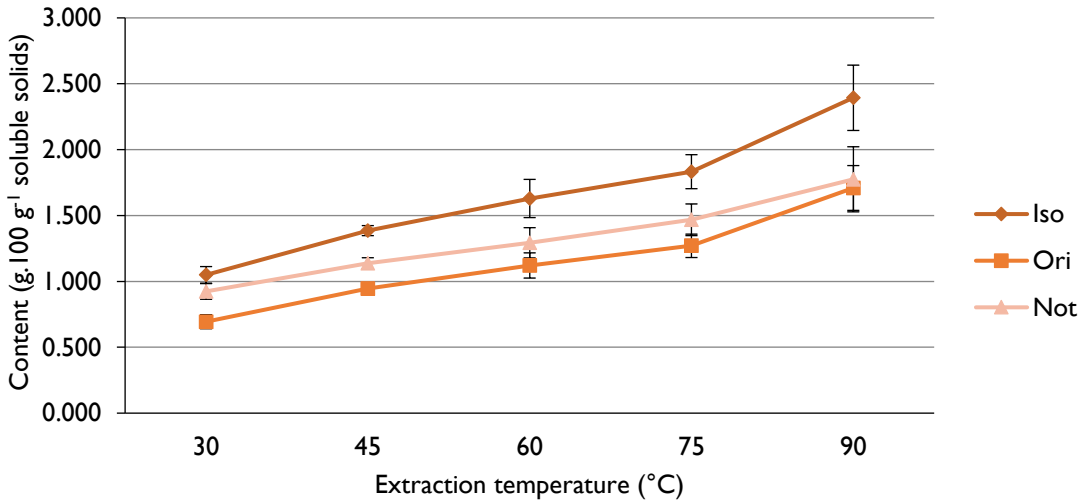

Figure 6.4 Effect of extraction temperature on contents of iso-orientin (Iso), orientin (Ori) and nothofagin (Not) in green rooibos hot water extract (extraction time = 20 min; water-to-plant material ratio = 10:1, v.m^{-1}).

6.2.3. Effect of water-to-plant material ratio on extraction efficiency

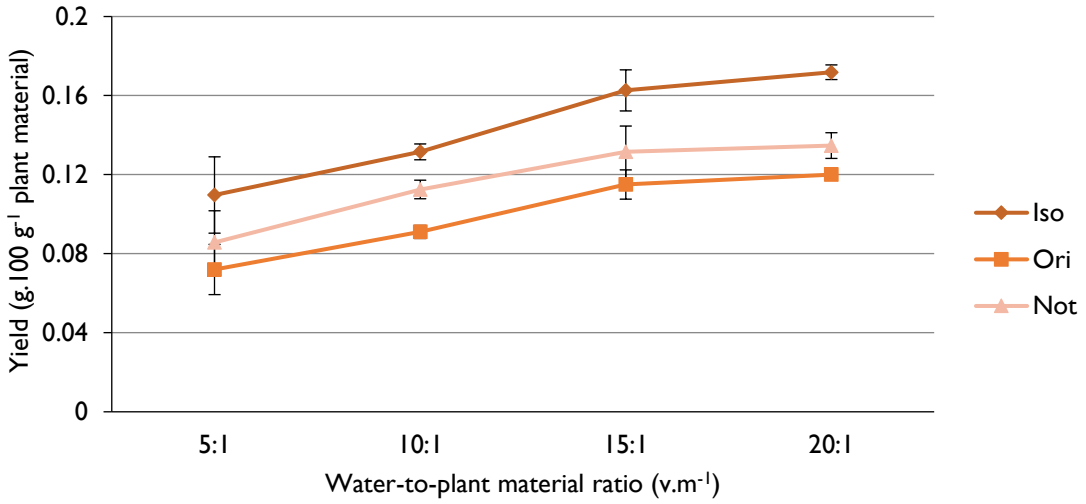

Figure 6.5 Effect of water-to-plant material ratio on yields of iso-orientin (Iso), orientin (Ori) and nothofagin (Not) in green rooibos hot water extract (extraction time = 20 min; extraction temperature = 60 °C).

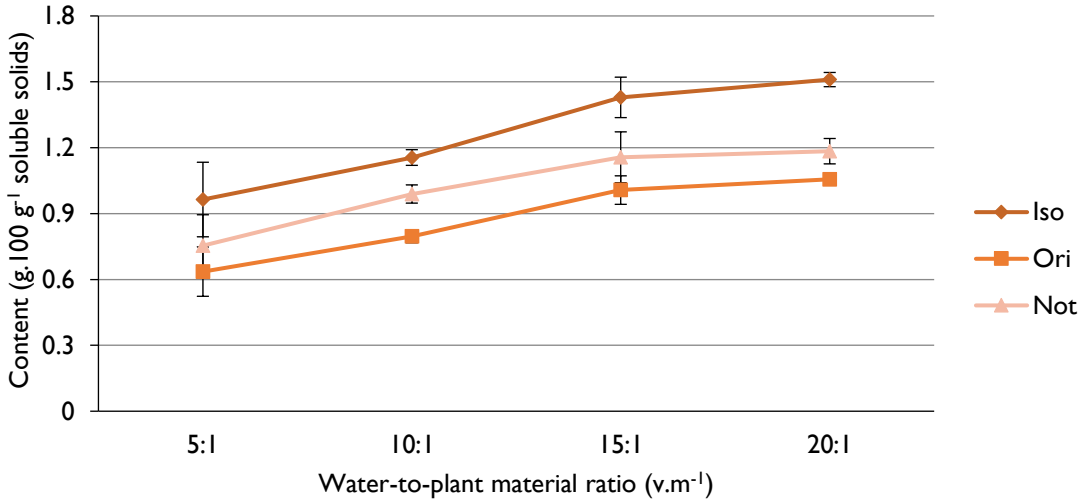

Figure 6.6 Effect of water-to-plant material ratio on contents of iso-orientin (Iso), orientin (Ori) and nothofagin (Not) in green rooibos hot water extract (extraction time = 20 min; extraction temperature = 60 °C).

6.2.4. Effect of particle size fractions on extraction efficiency

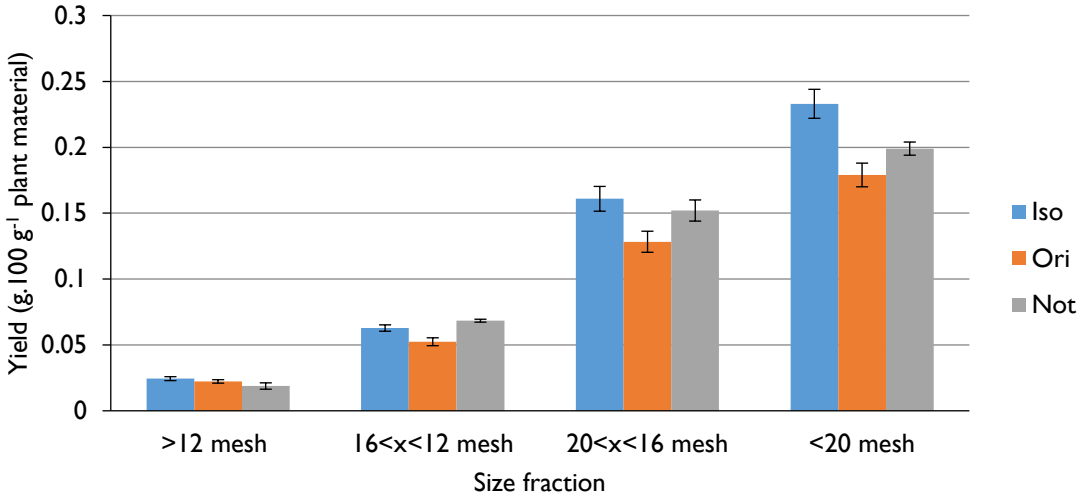

Figure 6.7 Effect of particle size on yields of iso-orientin (Iso), orientin (Ori) and nothofagin (Not) in green rooibos hot water extract (extraction temperature = 60 °C; extraction time = 20 min; water-to-plant material ratio = 15:1; v.m-1).

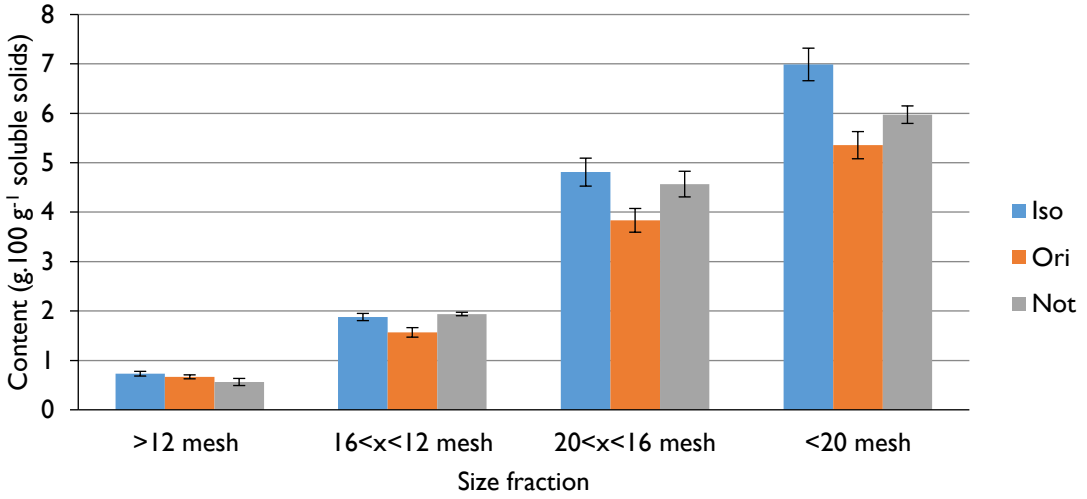

Figure 6.8 Effect of particle size on contents of iso-orientin (Iso), orientin (Ori) and nothofagin (Not) in green rooibos hot water extract (extraction temperature = 60 °C; extraction time = 20 min; water-to-plant material ratio = 15:1; v.m-1).

6.2.5. Effect of various heat treatments on flavonoid contents of green rooibos extract

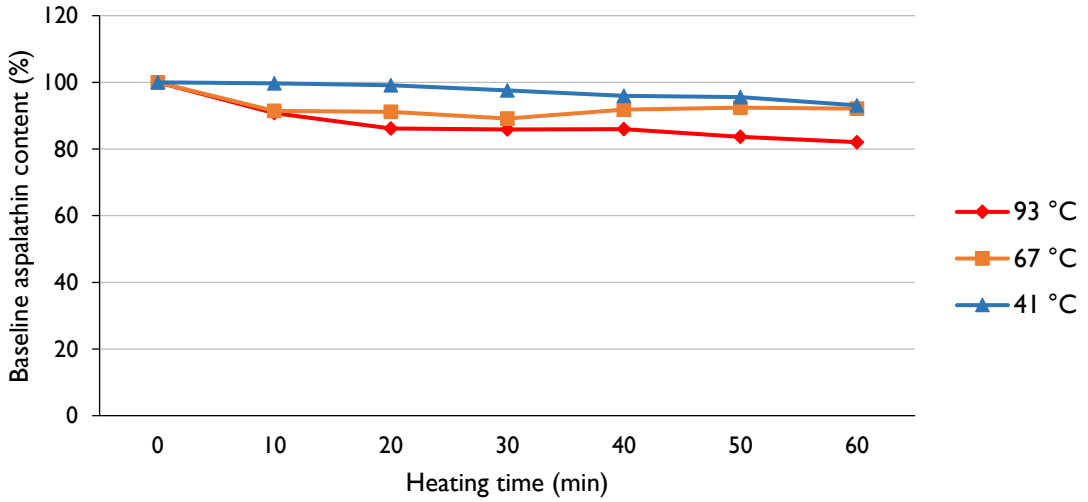

Figure 6.9 Effect of three different heat treatments for 60 min on the aspalathin content of an aqueous green rooibos extract (aspalathin content expressed as percentage of baseline value at time = 0 min).

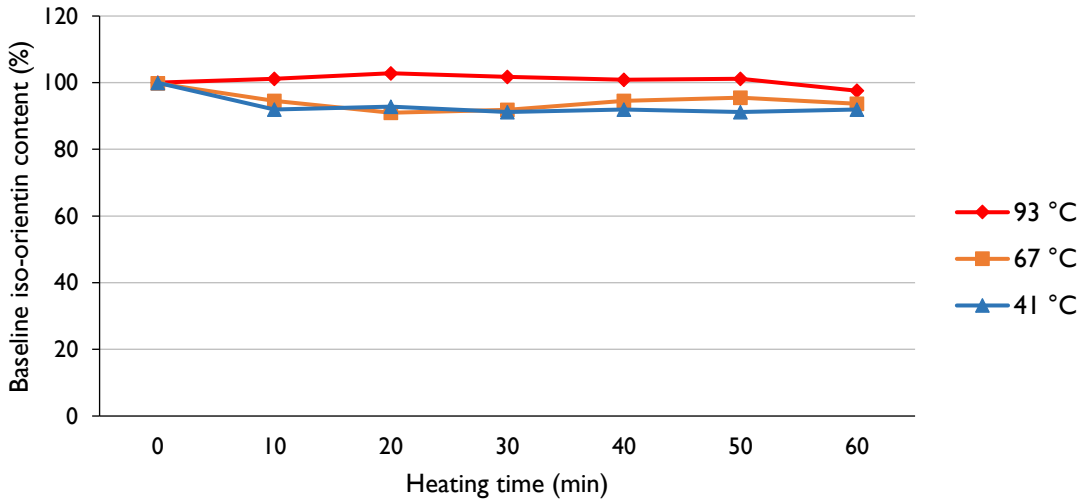

Figure 6.10 Effect of three different heat treatments for 60 min on the iso-orientin content of an aqueous green rooibos extract (iso-orientin content expressed as percentage of baseline value at t = 0 min).

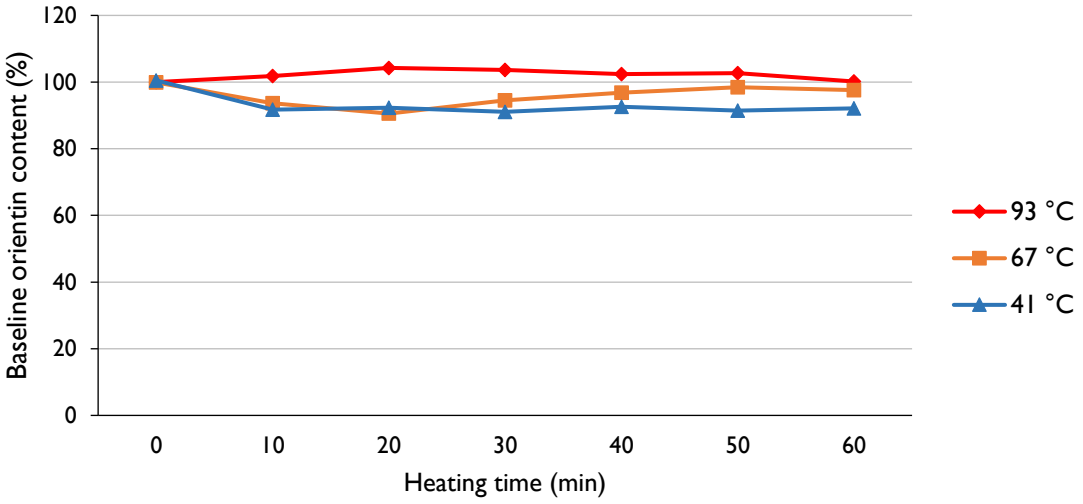

Figure 6.11 Effect of three different heat treatments for 60 min on the orientin content of an aqueous green rooibos extract (orientin content expressed as percentage of baseline value at t = 0 min).

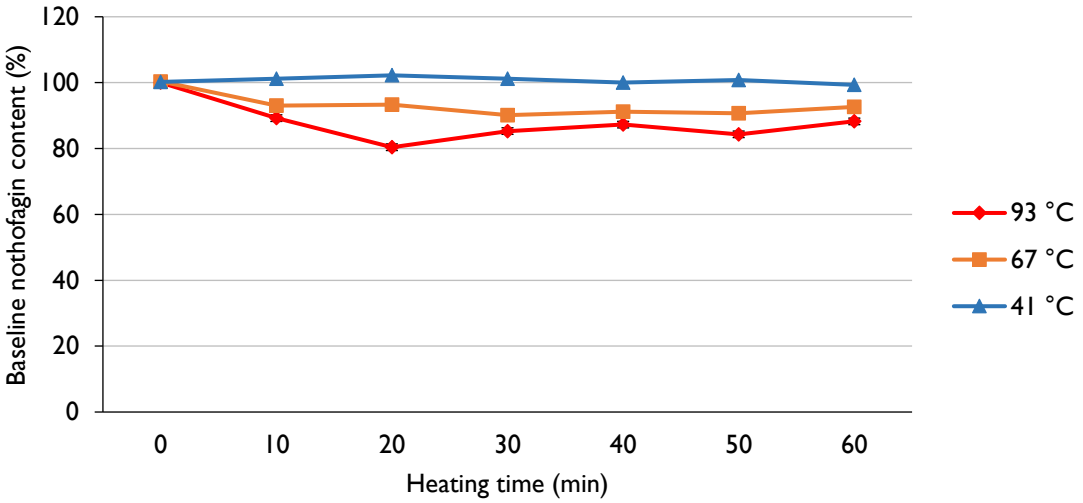

Figure 6.12 Effect of three different heat treatments for 60 min on the nothofagin content of an aqueous green rooibos extract (nothofagin content expressed as percentage of baseline value at t = 0 min).

6.3. UV-spectrophotometric screening of green rooibos extract

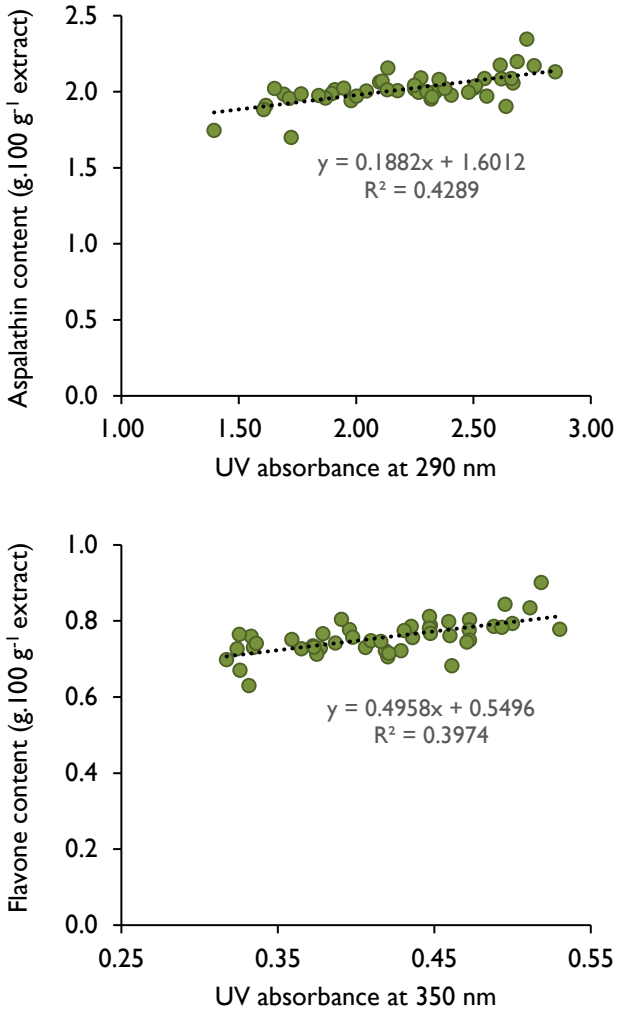

Figure 6.13 Correlation between (a) dihydrochalcone content in green rooibos extract (GRE) and UV absorbance at 290 nm, and (b) flavone content in GRE and UV absorbance at 350 nm.

7. Addendum B: Supplementary data pertaining to Chapter 4

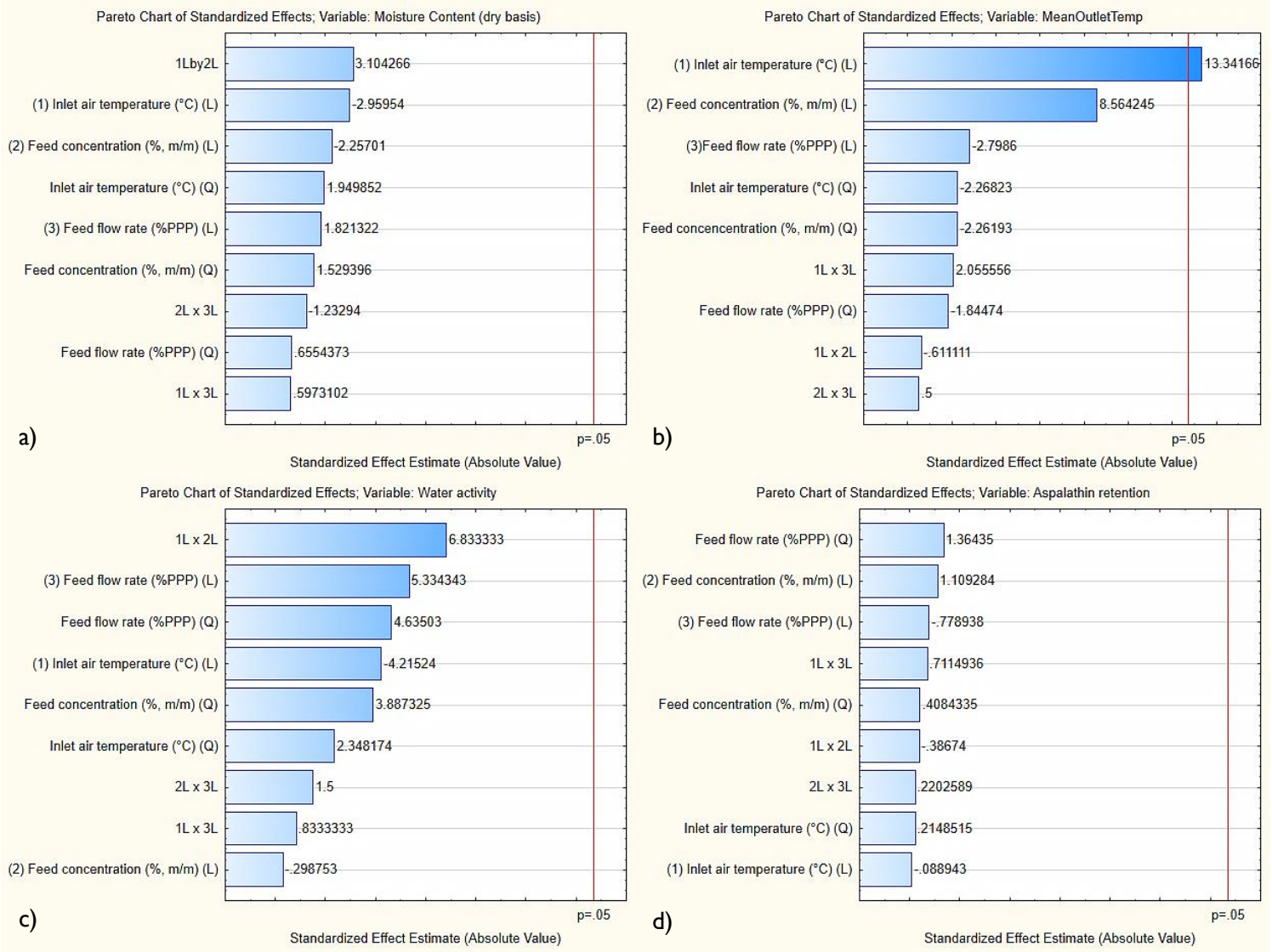

Figure 7.1 Standardised Pareto chart showing linear, quadratic and interaction effects for (a) moisture content (% dry basis), (b) mean outlet air temperature (°C), (c) water activity and (d) aspalathin retention. L = linear effect; Q = quadratic effect; LxL = interaction effect; PPP = peristaltic pump performance).

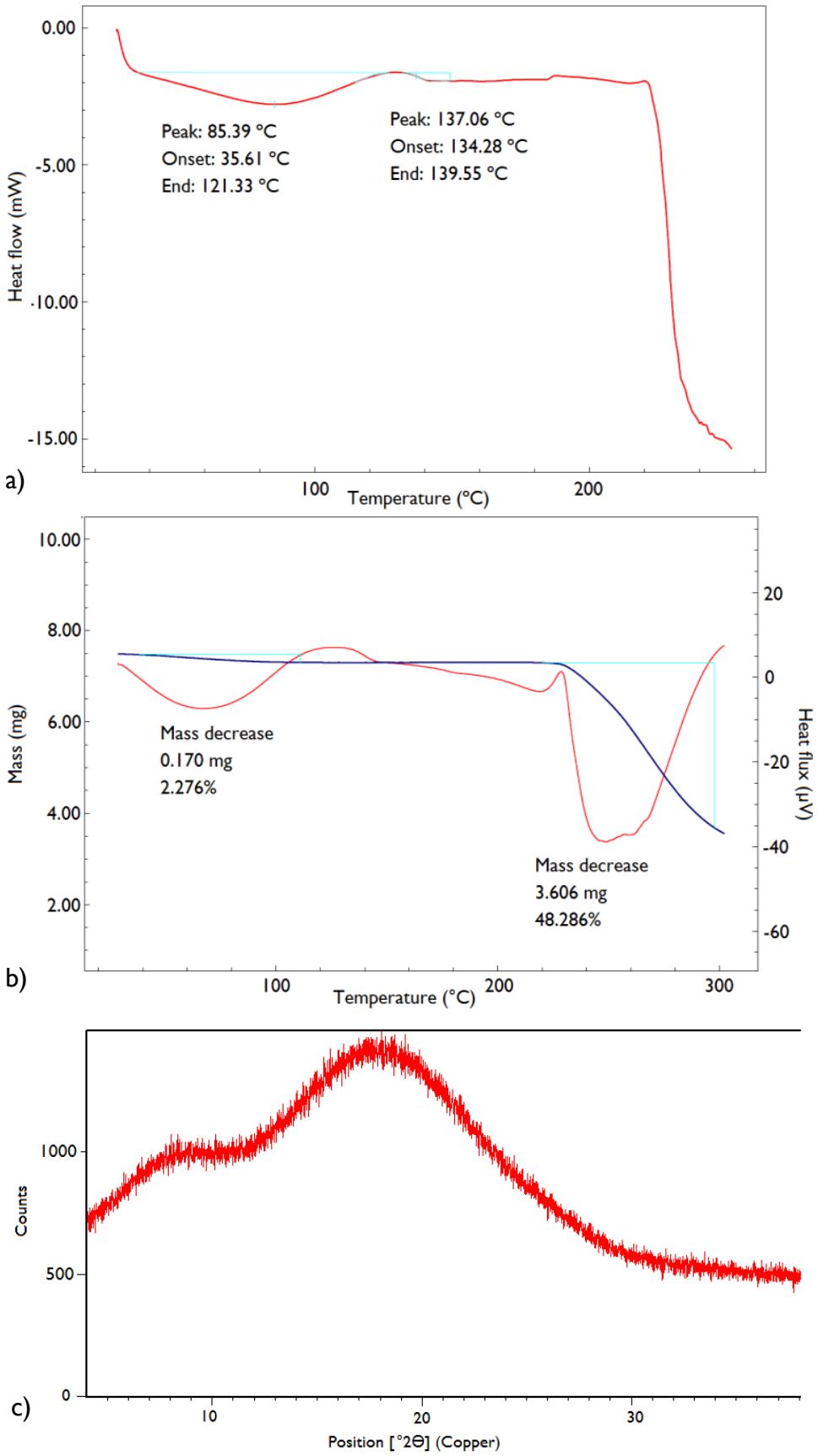

Figure 7.2 (a) Differential scanning calorimetry (DSC) thermogram, (b) thermogravimetric analysis trace (blue) with simultaneous DSC trace (red) and (c) X-ray diffractograms for inulin powder at 25 °C.

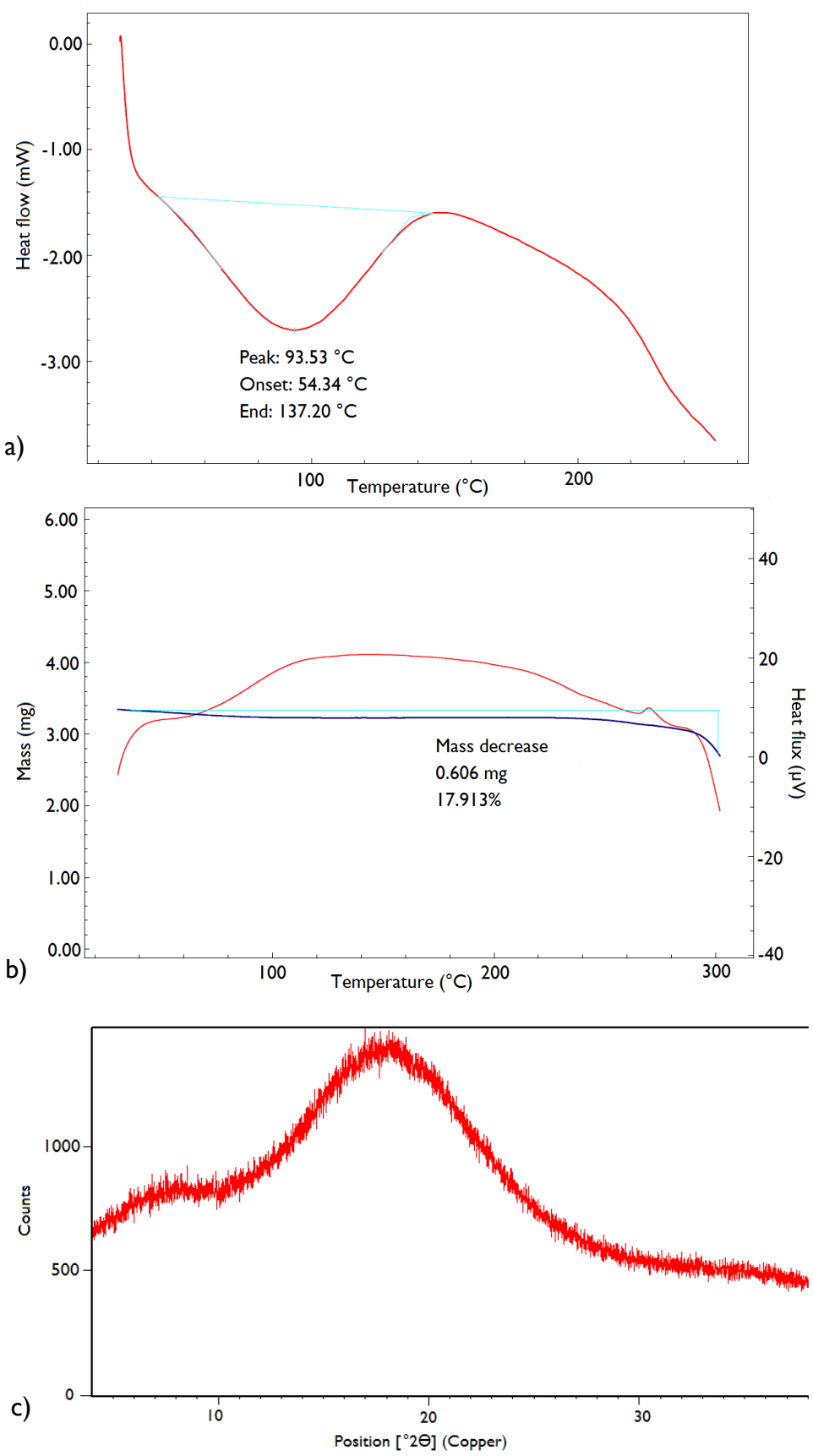

Figure 7.3 (a) Differential scanning calorimetry (DSC) thermogram, (b) thermogravimetric analysis trace (blue) with simultaneous DSC trace (red) and (c) X-ray diffractogram for maltodextrin powder at 25 °C.